Coherent States and Wave Packet Dynamics for the Bogoliubov-de Gennes Equations

Jordan Langham-Lopez, Mphys.

Thesis submitted to the University of Nottingham for the degree of Doctor of Philosophy

July 2016

Abstract

We investigate generalizations of coherent states as a means of representing the dynamics of excitations of the superconducting ground state. We also analyse the propagation of generalized coherent state wave packets under the Bogoliubov-de Gennes Hamiltonian. The excitations of the superconducting ground state are superpositions of electron and hole quasi-particles described by the Bogoliubov-de Gennes equations, that can only exist at energies outside the band gap. A natural generalization relevant to the excitations of the superconducting ground state is the tensor product of canonical and spin coherent states. This state will quickly become de-localized on phase space under evolution by the Bogoliubov-de Gennes Hamiltonian due to the opposite velocities of the quasi-spin components. We therefore define the *electron-hole* coherent states which remain localised on phase space over longer times. We show that the electron-hole coherent states though entangled retain many defining features of coherent states.

We analyse the propagation of both product and electron hole coherent states in a superconductor with a spatially homogeneous superconducting band gap. The dispersion relation indicates that wavepackets defined on the band gap have a zero group velocity, but we will show that interference effects can create states on the band gap that propagate at the Fermi velocity. We also consider the two semiclassical, short wavelength regimes, $\hbar \to 0$ and the large Fermi energy limit $\mu \to \infty$. In general these limits produce behaviour analogous to the canonical coherent states except for isolated cases.

Finally we analyse the dynamics of the Andreev Reflection of a Gaussian wavepacket incident on a discontinuous normal-superconducting interface. We show that restricting the energy bandwidth of the incident state inside the superconducting band gap precludes the wavepacket from fully entering the superconducting region. We again consider the two semiclassical regimes.

Acknowledgements

I am deeply indebted to my parents, their constant support has allowed me to reach this point.

My thanks also go to my supervisor Sven Gnutzmann for his help and advice; and to my long-suffering girlfriend Hannah Somers for putting up with me.

Contents

Chapter 1

Introduction

The Bogoliubov-de Gennes equations describe the excitations of the super-conducting ground state with a spatially inhomogeneous superconducting pair potential [1]. They also have applications in descriptions of superfluid fermions (for example helium-3 at cryogenic temperatures[2]) in the presence of spatially varying external potentials [3]. The microscopic theory of superconductivity developed by Bardeen, Cooper and Schrieffer (BCS) describes the superconducting ground state as a condensate of electron *Cooper-pairs*. The Cooper pairs are formed from electrons with opposite spin and momenta, which then behave like bosons [4]. The same mechanism also occurs in superfluid helium-3 where the Cooper pairs are formed from atoms [5]. The superconducting condensate forms below a critical temperature T_c at which the superconductor undergoes a phase change. The behaviour of *fermionic condensates* (of which superconductors are one example) is closely related to superfluid phenomenon also demonstrated by some Bose-Einstein condensates [6]. The excitations of the BCS ground state are broken Cooper pairs, which consequently demonstrate interesting features [7]. They can only exist above a minimum energy, outside the superconducting energy band gap occupied by Cooper pairs. They are also generally superpositions of electron and hole quasi-particles. The solutions to the coupled Bogoliubov-de Gennes equations are spinors which describe the coupled electron and hole components. The hole component demonstrates a velocity opposite to the momentum of the excitation. This is the source of the interesting quantum dynamics considered in this thesis.

The relationship between classical and quantum phase space trajectories has it's roots in the early development of quantum theory [8]. In this respect canonical coherent states play a unique role as states that best

satisfies quantum-classical correspondence under a quadratic Hamiltonian and for short times under other Hamiltonians [9]. In particular as coherent states are minimum uncertainty states, in semiclassical regimes their evolution can be found using the corresponding classical phase space trajectories. Up to certain times the evolution of coherent states is given by the classical trajectory through the centre of the state and the linearised flow of the nearby trajectories [10–13]. Moreover the additional properties of the canonical coherent states as a continuous, over-complete set allow for their use in the representation of quantum states on classical phase space [8, 14, 15]. The concept of a coherent state has been generalised to other systems and structures [16, 17]. A group theoretic definition of the coherent states allows for the definition of the *spin coherent states* [18–20] which we will associate with the electron-hole degree of freedom of excitations of the superconducting ground state.

A natural representation of the BCS excitations are the *product coherent states* constructed as the tensor product of the canonical coherent states on phase space and the spin coherent states; defined on the corresponding product Hilbert space. Product coherent states are useful tools in the analysis of systems with spin coupling (for example [21]). Under evolution by the Bogoliubov-de Gennes Hamiltonian a product coherent state that is initially well localised on phase space will generally quickly disperse due to the opposite velocities of the two components. We will therefore define the *electron-hole coherent states* on the product space as a superposition of a Gaussian electron component and conjugate Gaussian hole component. The two components will now have the same velocity and thus remain localised on phase space for longer times than product coherent states. Electron-hole coherent states are in general entangled but retain many of the desirable features of scalar canonical coherent states, though they have some analytic disadvantages.

We will analyse the wave packet dynamics of both product and electron-hole states in two settings, also considering the asymptotic short wavelength limits. Firstly in a spatially homogeneous superconductor; as the relevant excitations are superpositions of electron and hole components the dynamics will depend on the coupling between electron and hole components, but also interference between the positive and negative energy stationary solutions of the Bogoliubov-de Gennes equations. Secondly we consider the scattering of quasi-particles at a normal-superconducting boundary. Since

6

excitations cannot exist inside the energy band gap of the superconductor, an electron quasi-particle incident from the normal region with an energy inside the band-gap is retro-reflected as a hole at the boundary (and vice-versa). This scattering process is known as Andreev reflection and is unique as the reflected quasi-particle follows the trajectory of the incident quasi-particle [22–24]. We will analyse the dynamics of a Gaussian wave packet incident on a normal-superconducting boundary showing how it is Andreev reflected without fully penetrating into the superconducting region if the energy bandwidth of the wave packet is restricted to be smaller than the superconducting band gap.

Both semiclassical descriptions of inhomogeneous superconducting systems and wave packets dynamics are well studied fields. The nature of the Bogoliubov-de Gennes equations means that descriptions of spatially inhomogeneous superconductors benefit greatly from the application of semiclassical techniques. In particular a great deal of literature is devoted to WKB style approximations of the stationary solutions [22, 25–27], relying on the slowly varying amplitudes of the electron and hole components. There is also a great deal of literature on wave packet dynamics applied to numerous systems and notable work relating classical phase space trajectories to the evolution of wave packets [10, 28]. It appears though that there are no notable attempts to analyse the dynamics of wave packets constructed from stationary solutions of the Bogoliubov-de Gennes equations.

The structure of this thesis is as follows. Chapter 2 is devoted to the theoretical underpinnings required to arrive at the Bogoliubov-de Gennes equations and the coherent state theory required to define the E-H coherent states. Obviously superconductivity is an extensive field, so we will concentrate on the Bogoliubov-de Gennes equations only giving a brief account of the development of the microscopic theory of superconductivity, concentrating on the parameters that define the Bogoliubov-de Gennes equations. We will go into more detail with the derivation and theoretical features of canonical coherent states and their relation to classical phase space. We will then consider generalizations of the canonical coherent states, and show how a group theoretic definition of coherent states can be used to define the spin coherent states. Finally in this section we will consider classical-quantum correspondence using the framework of the Ehrenfest theorem and the relationship between classical trajectories and the propagation of wave packets.

In Chapter 3 we will first define the product coherent states, the natu-

ral definition for particles with a quasi-spin component, as the product of canonical and product coherent states. We will then define the electron-hole coherent states and analyse their properties. In particular we will devote sub-sections to the group theoretic definition, the representation of superconducting states on phase space using electron-hole coherent states and measuring the entanglement of electron-hole coherent states. This section is based on work produced in collaboration with Marek Kus and Sven Gnutzmann [29].

In Chapter 4 we will derive the stationary solutions for both the spatially homogeneous superconductor and a discontinuous normal-superconducting interface. These results can be found in previous literature [30], but we detail the solutions here as in later chapters they will be used to construct time dependent wave packets. We also consider the representation of the stationary states (and the numerically derived bound eigenstates of a superconducting-normal-superconducting system) on phase space using the E-H coherent states. Finally we give a brief account of an original analysis of limited analytic solutions to the BdG equations when the superconducting band gap varies linearly.

Chapters 5 and 6 present original work analysing the dynamics of wave packets under the Bogoliubov-de Gennes equations for two systems. Chapter 5 and is devoted to wave packet dynamics in a spatially homogeneous superconductor. We will first consider the relationship between the dispersion relation and wave packet dynamics in the scalar case. Applying this approach to the Bogoliubov-de Gennes dispersion relation we shall show how the relative amplitudes of the electron and hole components vary with momentum, and how decomposing a wave packet in the spinor plane wave basis informs the resulting dynamics. Working first in the Heisenberg picture we will consider the difference in the dynamics of the expectation values and variances between the electron-hole and product coherent states. In the case of the homogeneous superconductor we will be able to solve the set of phase space and quasi-spin Heisenberg equations of motion. Using the time dependent operators we will further consider the dynamics of the moments of the two forms of coherent states. In general we will not be able to derive a completely analytic picture, and so will analyse the asymptotic long time behaviour of the moments. The homogeneous superconductor will also allow for a straightforward derivation of the action of the time time evolution operator in the Schrödinger picture. We will show how the electron-hole

and coherent state wave packets relate to each other, and how the contributions from the electron and hole components enter the dynamics. In lieu of simple analytic solutions we will again be required to examine the long-time behaviour of wave packets, but we will also give consideration to the two possible short wavelength limits relevant to the Bogoliubov-de Gennes equations. These are the usual semiclassical limit $\hbar \rightarrow 0$ but also the large Fermi energy limit.

Finally in Chapter 6 we will use the stationary solutions as a basis to derive the scattering of a wave packet incident from a normal region onto a discontinuous normal-superconducting boundary. We will restrict the argument to states inside the superconducting band gap. In this case the wave packet does not fully enter the superconducting region. We will again consider the possible short wavelength regimes, to analyse the propagation of the wave packet in the normal region and the penetration of the wave packet into the superconducting region. The main results of Chapters 5 and 6 will form the basis of two reports we plan to submit in the near future.

Chapter 7 gathers the results of the proceeding chapters, and offers some possible extensions to the work presented. We have omitted several lengthy calculations from the main body of the text so as to better present the main arguments. These can be found in the Appendix, referenced by the chapter and section they refer to. The Appendix also contains notes on some integral solutions and asymptotic techniques used in this thesis.

Chapter 2

Background

2.1 Superconductivity & Andreev Reflection

In this section we will give a brief synopsis of the main features of the microscopic theory of superconductivity which are relevant to the work in this thesis. This thesis will mainly focus on a theoretical analysis of the interesting quantum wave packet dynamics arising from the Bogoliubov-de Gennes (BdG) Hamiltonian, which describes excitations in spatially inhomogeneous superconductors. As such it will be advantageous to have an idea of how the terms in the BdG Hamiltonian arise, and in particular how the variables that describe a superconducting system relate to each other. The BdG Hamiltonian we will investigate is a consequence of the microscopic theory of superconductivity developed by Bardeen, Cooper and Schrieffer (BCS). A full derivation of the theory is somewhat outside the scope of this thesis, so the following is a brief outline which concentrates on the variables that are important in the BdG Hamiltonian and the theoretical steps required to arrive at the BdG Hamiltonian. We roughly follow the prescription as given in Tinkham's 'Introduction to Superconductivity' [31] with elements also from 'Superconductivity of Metals and Alloys' by de-Gennes [1], which are both excellent sources for more detailed derivations of the theory and surrounding topics

2.1.1 BCS Theory

The phenomenon now known as superconductivity was discovered in 1911 by Kamerlingh Onnes [32], evidencing itself as the the disappearance of resistance in mercury below a critical temperature (T_c). Modern experiments have shown a lower bound of around 10^5 years for the characteristic decay

Figure 2.1: Exclusion of a magnetic field from the interior of a superconductor and comparison of flux penetration behaviour of type I and type II superconductors. Adapted from [31].
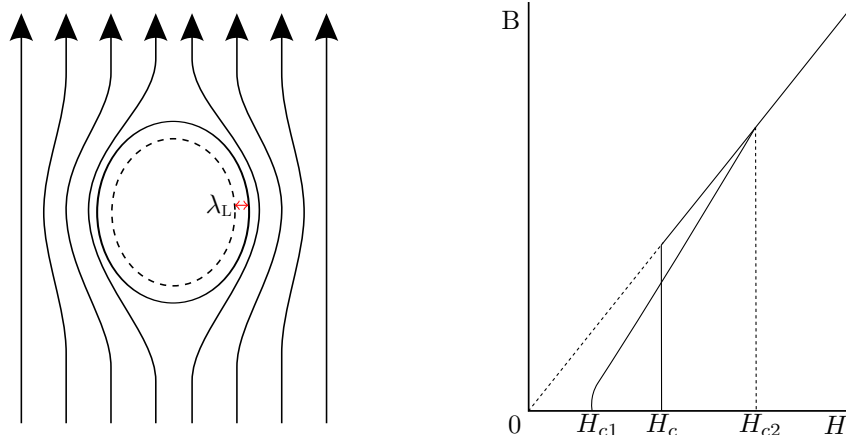
(a) Schematic of the exclusion of a magnetic field from the interior of a superconductor. λ_L is the field penetration depth predicted by London theory. λ_L is typically on the order of nanometres.

(b) Flux penetration (B) of an external field into a type I and type II superconductor with the same critical field strength H_c. Type I superconductors show a discontinuous change in penetration at H_c. Type II superconductors show a continuous increase in flux penetration between H_{c1} and H_{c2}.

time of a current in a superconducting loop [33], implying that superconductors are effectively perfect electrical conductors.

It was later discovered by Meissner and Ochsenfeld in 1933 [34] that a superconductor will also screen an external magnetic field from its interior (now better known as the *Meissner effect*) up to a critical field strength H_c. Moreover a magnetic field will be expelled from the interior of the superconductor as the material is cooled through T_c. This also implies that a superconducting state can be destroyed by a sufficiently strong external magnetic field.

Initial theoretical efforts in superconductivity focused on phenomenological theories describing these two defining macroscopic features of a superconductor, and the relationship between them. London theory (after the brothers F. and H. London) relates the supercurrent inside the superconductor to the Meissner effect [35]. The main result of the theory is an expression for the London penetration depth (λ_L), the distance an external magnetic field penetrates into the superconducting bulk, typically on the order of nanometres (illustrated in Figure 2.1a).

11

Figure 2.2: The intermediate state of a type I superconductor and the vortex core structure on the surface of a type II superconductor.
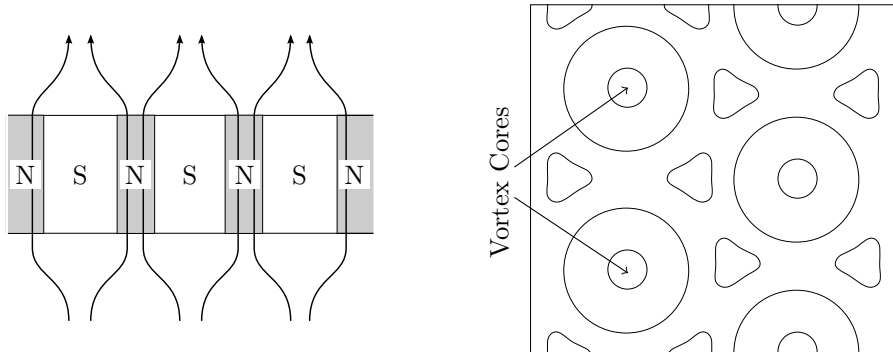
(a) Schematic of the intermediate state of a superconducting slab in a perpendicular magnetic field with intensity $H < H_c$. In this case the intermediate state is a laminar structure of normal and superconducting regions.

(b) Schematic of triangular lattice of vortices on the surface of a type II superconductor. Adapted from [39]. The contours are lines of constant n_s.

Further development of the phenomenological theory by Ginzburg and Landau (GL) [36] introduced a pseudo-wave function $\Psi(q)$ that describes the density of superconducting electrons as $n_s = |\Psi(q)|^2$. This plays the role of a superconducting order parameter. GL theory allows for the description of *intermediate states* of a superconductor, where superconducting and normal states meet at $H \sim H_c$, which London theory could not accommodate. The intermediate states occur when (depending upon the configuration of an external magnetic field and the superconducting sample) the external field may have points that reach sufficient intensity to form normal regions inside the superconductor, even though the external field strength lies below H_c [37, 38]. The example of a superconducting slab in a perpendicular magnetic field is shown in Figure 2.2a. In this case normal bands penetrate through the sample forming a series of laminar superconducting and normal regions.

GL theory also propose an additional superconducting parameter, the coherence length (ξ), characterizing the distance over which $\Psi(q)$ varies. Importantly this gives rise to descriptions of two distinct types of superconductors [36]. Type I superconductors exhibit a discontinuous change in magnetic field penetration at H_c. Type II superconductors (first proposed by Abrikosov [40]) exhibit a continuous increase in flux penetration from H_{c1} up to H_{c2} as shown in Figure 2.1b. The flux penetration between H_{c1} and H_{c2} in type II superconductors is not complete like the intermediate states but takes the form of *flux tubes*, which form magnetic field vortices
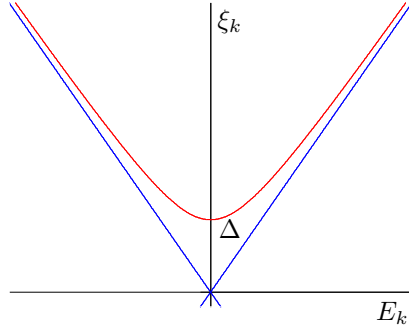
Figure 2.3: The excitation energy spectrum $\xi_k = \sqrt{E_k^2 + |\Delta|^2}$ in a superconductor ($\Delta \neq 0$, red) and normal states ($\Delta = 0$, blue). The minimum excitation energy in the superconductor is Δ which is the origin of the superconducting energy band gap.

on the surface of the superconductor as schematically shown in 2.2b. The magnetic field is maximal at the core of the vortex, decaying over a radius proportional to λ_L and the number of superconducting electrons is reduced in a smaller radius ξ around the core. We will not investigate type II superconductors further in the main body of this thesis, and thus omit further detailed theory here. We should consider though that type II superconductors as well as intermediate states are a key motivating factor for the investigation of spatially inhomogeneous superconductors.

It would take until the 1950's for a detailed microscopic theory to be developed that would propose an explanation of the mechanism behind superconductivity. The background theoretical setting for BCS theory is the *Fermi sea* in a normal conductor consisting of electrons with energies ϵ_k. The normal conductor ground state, if the electrons are non-interacting, consists of all states with energy $\epsilon_k \leq \mu$ occupied (due to their fermionic nature and the Pauli exclusion principle). We will refer to μ as the *Fermi energy* from here on (with the corresponding Fermi momentum $p_{\mathrm{F}} = \sqrt{2m\mu}$). Excitations of the normal ground state are formed by removing an electron with energy $\epsilon_k < \mu$ and raising it to $\epsilon_k > \mu$, creating a quasi-electron with energy $\epsilon_k = \mu + E_k$ and quasi-hole with energy $\epsilon_k = \mu - E_k$. From here on E_k will refer to the energy measured relative to the Fermi energy (i.e. $E_k = \epsilon_k - \mu$).

It was proposed by Cooper that the Fermi sea is unstable against the formation of bound electron states [41], independent of the strength of the attractive force. Cooper demonstrated the possibility of the formation of *Cooper pairs*. These bound states are formed from electrons of opposite spin and momentum which have an energy lower than the Fermi energy, hence the Fermi sea is unstable against the formation of such pairs. The mechanism that generates this attractive force was found to be phonon interactions with the ion cores in the superconductor, first proposed by

Fröhlich [42]. This can be imagined as an electron polarizing the Fermi sea, creating a region of increased positive charge, which in turn attracts another electron, correlating the motion of the pair. We can infer that the process of correlation by phonon interaction is why classical superconductivity requires low temperatures. This is experimentally supported by the finding that T_c is altered by differing isotopes of the superconducting material. Experiments show that T_c decreases with an increase in isotopic mass [43]. This is the mechanism which best explains classical low temperature superconductors, but it is theorized that other mechanisms may contribute to the phenomena in more exotic (high temperature etc. see [44]) superconductors.

BCS theory therefore proposes a superconducting ground state formed from electrons with energies close to the Fermi energy, bound in Cooper pairs. This pairing leads to bosonic behaviour allowing the Cooper pairs to conduct efficiently. The excitations of the superconducting ground state are quasi-particles, which are a superposition of single electron-hole states (effectively split cooper pairs), with excitation energy $\xi_k = \sqrt{E_k^2 + |\Delta|^2}$ as shown in Figure 2.3. The excitations have a minimum energy Δ, and this is the source of the superconducting energy band gap that exists in a superconductor. It's interesting to note that Δ is temperature dependent, and it can be shown that $\Delta(T) \to 0$ as $T \to T_c$ from below, at which point the quasi particle energy spectrum is the same as in a normal conductor. Roughly speaking Δ determines the range of energies of electrons that will contribute to forming Cooper pairs, from within a range $|\Delta|$ of μ. Moreover the order parameter $\Psi(q)$ described by GL theory is proportional to Δ (it was shown in 1959 by Gor'Kov that GL theory is a limiting form of BCS theory [45]) and the minimum energy of the excitations corresponds to the energy required to break a Cooper pair.

The properties of the BCS ground state are best derived using second quantization notation. We define operators $\hat{c}_{\boldsymbol{k}\sigma}^\dagger$ which creates an electron with momentum $\boldsymbol{k}$ and spin σ, and likewise $\hat{c}_{\boldsymbol{k}\sigma}$ the corresponding annihilation operator. For example in this notation the creation of a quasi-electron and hole excitation in the normal state is written as , $\hat{c}_{\boldsymbol{k}'\sigma}^\dagger \hat{c}_{\boldsymbol{k}\sigma}$ and a cooper pair is created by $\hat{c}_{\boldsymbol{k}\uparrow}^\dagger \hat{c}_{-\boldsymbol{k}\downarrow}^\dagger$. These operators obey the standard Fermion anti-commutation relations

$$\{\hat{c}_{\boldsymbol{k}\sigma}, \hat{c}_{\boldsymbol{k}'\sigma'}^\dagger\} = \delta_{\boldsymbol{k}\boldsymbol{k}'}\delta_{\sigma\sigma'} \tag{2.1}$$

$$\{\hat{c}_{\boldsymbol{k}\sigma}, \hat{c}_{\boldsymbol{k}'\sigma'}\} = \{\hat{c}_{\boldsymbol{k}\sigma}^\dagger, \hat{c}_{\boldsymbol{k}'\sigma'}^\dagger\} = 0. \tag{2.2}$$
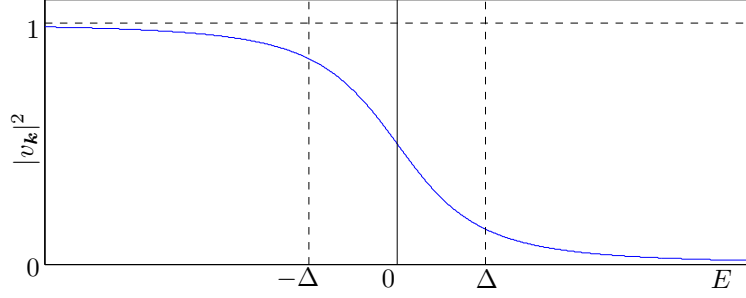
Figure 2.4: The amplitude of Cooper pair occupation, $|v_{\boldsymbol{k}}|^2$, as a function of electron energy relative to the Fermi energy.

We can also naturally define a number operator $\hat{n}_{\boldsymbol{k}\sigma} = \hat{c}^\dagger_{\boldsymbol{k}\sigma}\hat{c}_{\boldsymbol{k}\sigma}$. The form of the superconducting ground state can be derived from the *pairing Hamiltonian* (this variational method is the approach used in the original BCS paper [4], more modern approaches use canonical transformations)

$$\mathcal{H}_{\texttt{pair}} = \sum_{\boldsymbol{k}\sigma} \epsilon_{\boldsymbol{k}} \hat{n}_{\boldsymbol{k}\sigma} + \sum_{\boldsymbol{k}\boldsymbol{k}'} V_{\boldsymbol{k}\boldsymbol{k}'} \hat{c}^\dagger_{\boldsymbol{k}\uparrow} \hat{c}^\dagger_{-\boldsymbol{k}\downarrow} \hat{c}_{\boldsymbol{k}'\uparrow} \hat{c}_{-\boldsymbol{k}'\downarrow}. \tag{2.3}$$

Here the first term is simply the total kinetic energy and the second term the scattering of Cooper pairs, with $V_{\boldsymbol{k}\boldsymbol{k}'}$ the appropriate scattering amplitudes. The attractive binding force arises if $V < 0$. This Hamiltonian omits any other interaction terms, presumed not to be involved in superconductivity such as higher order terms or non Cooper (i.e. opposite momenta and spin) pairings. The BCS ground state is found by minimizing the expected energy of the ground state relative to μ

$$\langle \Psi_G | \left(\mathcal{H}_{\texttt{pair}} - \mu \hat{n}_{\boldsymbol{k}\sigma} \right) | \Psi_G \rangle = 2 \sum_{\boldsymbol{k}} E_{\boldsymbol{k}} v_{\boldsymbol{k}}^2 + \sum_{\boldsymbol{k}} V_{\boldsymbol{k}\boldsymbol{k}'} u_{\boldsymbol{k}} v_{\boldsymbol{k}} u_{\boldsymbol{k}'} v_{\boldsymbol{k}'} \tag{2.4}$$

where $u_{\boldsymbol{k}}$ is the amplitude that a Cooper pair is unoccupied, and $v_{\boldsymbol{k}}$ that it is occupied. $|v_{\boldsymbol{k}}|^2$ as a function of the excitation energy relative to μ is shown in Figure 2.4. It follows that they must satisfy $|u_{\boldsymbol{k}}|^2 + |v_{\boldsymbol{k}}|^2 = 1$. We define the quantities

$$\Delta_{\boldsymbol{k}} = - \sum_{\boldsymbol{k}'} V_{\boldsymbol{k}\boldsymbol{k}'} u_{\boldsymbol{k}'} v_{\boldsymbol{k}'} \quad \text{and} \quad \xi_{\boldsymbol{k}} = \sqrt{\Delta_{\boldsymbol{k}}^2 + E_{\boldsymbol{k}}^2}. \tag{2.5}$$

$\xi_{\boldsymbol{k}}$ turns out to be the aforementioned energy of the quasi-particle excitations of the ground state and $\Delta_{\boldsymbol{k}}$ the minimum excitation energy (which we will also refer to as the *pairing potential*), and also the order parameter derived by the phenomenological theory. The important theoretical step made to make the equations solvable is the approximation that $V_{kk'} = V$ up to a cut off energy away from the Fermi energy. In practice this turns

15

out to be a good approximation indicating that indeed only electrons close to the Fermi level contribute to the cooper pairing.

2.1.2   Bogoliubov-de Gennes Equations

The single electron operators prove cumbersome for the purpose of deriving the form of the excitations of the BCS ground state. A simplification can be made by diagonalizing the pairing Hamiltonian using the Bogoliubov transformations [46]

$$\hat{c}_{\boldsymbol{k}\uparrow} = u_{\boldsymbol{k}}^* \hat{\gamma}_{\boldsymbol{k}0} + v_{\boldsymbol{k}} \hat{\gamma}_{\boldsymbol{k}1}^\dagger \qquad (2.6)$$

$$\hat{c}_{-\boldsymbol{k}\downarrow}^\dagger = u_{\boldsymbol{k}} \hat{\gamma}_{\boldsymbol{k}1}^\dagger - v_{\boldsymbol{k}}^* \hat{\gamma}_{\boldsymbol{k}0} \qquad (2.7)$$

again the cooper pair occupation amplitudes satisfy $|u_{\boldsymbol{k}}|^2 + |v_{\boldsymbol{k}}|^2 = 1$. This choice ensures that the transformations are canonical. The operators $\hat{\gamma}_{\boldsymbol{k},i}$ correspond to coherent mixtures of electron-hole excitations. These effectively broken Cooper pairs are commonly referred to as *Bogolons*. Inverting (2.6) we obtain the operators

$$\hat{\gamma}_{\boldsymbol{k}0}^\dagger = u_{\boldsymbol{k}}^* \hat{c}_{\boldsymbol{k}\uparrow}^\dagger - v_{\boldsymbol{k}}^* \hat{c}_{-\boldsymbol{k}\downarrow} \qquad (2.8)$$

$$\hat{\gamma}_{\boldsymbol{k}1}^\dagger = u_{\boldsymbol{k}}^* \hat{c}_{-\boldsymbol{k}\downarrow}^\dagger + v_{\boldsymbol{k}}^* \hat{c}_{\boldsymbol{k}\uparrow} \qquad (2.9)$$

which create quasi particle excitations in the two spin directions when applied to the BCS ground state. Both operators also have the net effect of increasing the system momentum by $\boldsymbol{k}$. The superconducting ground state is defined as the vacuum state of the annihilation operator

$$\hat{\gamma}_{\boldsymbol{k}0}|\Psi_G\rangle = \hat{\gamma}_{\boldsymbol{k}1}|\Psi_G\rangle = 0. \qquad (2.10)$$

The excited states $\hat{\gamma}_{\boldsymbol{k}0}^\dagger|\Psi_G\rangle$ and $\hat{\gamma}_{\boldsymbol{k}1}^\dagger|\Psi_G\rangle$ correspond to placing with certainty a single electron into one of the states which form a Cooper pair ($\boldsymbol{k}\uparrow$ or $-\boldsymbol{k}\downarrow$), raising the ground state energy accordingly.

Analysing spatially inhomogeneous potentials, and especially of interest for this thesis an inhomogeneous pairing potential $\Delta(q)$, this approach must be altered. This requires the utilization of a generalization of the Bogoliubov transforms

$$\hat{\Psi}(\boldsymbol{r}, \uparrow) = \sum_n \left[\hat{\gamma}_{n\uparrow} u_n(\boldsymbol{r}) - \hat{\gamma}_{n\downarrow}^\dagger v_n^*(\boldsymbol{r}) \right] \qquad (2.11)$$

$$\hat{\Psi}(\boldsymbol{r}, \downarrow) = \sum_n \left[\hat{\gamma}_{n\downarrow} u_n(\boldsymbol{r}) + \hat{\gamma}_{n\uparrow}^\dagger v_n^*(\boldsymbol{r}) \right]. \qquad (2.12)$$

These are annihilation operators in the position representation, as opposed to the momentum representations $\hat{c}_{\boldsymbol{k}}\sigma$'s. The functions $u_n(\boldsymbol{r})$ and $v_n(\boldsymbol{r})$ are position dependent eigenfunctions which diagonalize the effective Hamiltonian

$$\hat{\mathcal{H}}_{\texttt{eff}} = \int \left\{ \sum_\sigma \hat{\Psi}^*(\boldsymbol{r}, \sigma) \left[\frac{1}{2m} \left(i\hbar\nabla + \frac{e}{c}\boldsymbol{A} \right)^2 + U(\boldsymbol{r}) - \mu \right] \hat{\Psi}(\boldsymbol{r}, \sigma) \right.$$
$$\left. + \Delta(\boldsymbol{r})\hat{\Psi}^*(\boldsymbol{r}, \uparrow)\hat{\Psi}^*(\boldsymbol{r}, \downarrow) + \Delta^*(\boldsymbol{r})\hat{\Psi}(\boldsymbol{r}, \uparrow)\hat{\Psi}(\boldsymbol{r}, \downarrow) \right\} dr. \tag{2.13}$$

This requires that $u(\boldsymbol{r})$ and $v(\boldsymbol{r})$ satisfy the coupled BdG equations

$$\hat{\mathcal{H}}_0 u(\boldsymbol{r}) + \Delta(\boldsymbol{r})v(\boldsymbol{r}) = Eu(\boldsymbol{r}) \tag{2.14}$$
$$-\hat{\mathcal{H}}_0^* v(\boldsymbol{r}) + \Delta^*(\boldsymbol{r})u(\boldsymbol{r}) = Ev(\boldsymbol{r}). \tag{2.15}$$

Here

$$\hat{\mathcal{H}}_0 = \frac{1}{2m} \left(i\hbar\nabla + \frac{e}{c}\boldsymbol{A} \right)^2 + U(\boldsymbol{r}) - \mu \tag{2.16}$$

is the standard Hamiltonian for an electron in a magnetic potential $\boldsymbol{A}$ and potential $U(\boldsymbol{r})$ with energy measured relative to μ.

It is straightforward to see that if $\Delta = 0$, the equations decouple, leaving

$$\mathcal{H}_0 u(\boldsymbol{r}) = Eu(\boldsymbol{r}) \tag{2.17}$$
$$\mathcal{H}_0^* v(\boldsymbol{r}) = -Ev(\boldsymbol{r}) \tag{2.18}$$

then $u(\boldsymbol{r})$ corresponds to an electron wave function with energy $\epsilon = \mu + E$ of the normal state. $v(\boldsymbol{r})$ is in effect a time reversed electron, which behaves like a hole with energy $\epsilon = \mu - E$, and they will referred to as such from here on, denoting their respective wave functions $\psi^e(\boldsymbol{r})$ and $\psi^h(\boldsymbol{r})$. A large part of this thesis focuses on the analysis of the dynamics of coherent state wave packets when $\Delta \neq 0$, where interactions between the hole and electron states are introduced. In later chapters we will also consider the generalized time dependent BdG equations

$$\mathcal{H}_0 u(\boldsymbol{r}, t) + \Delta(\boldsymbol{r})v(\boldsymbol{r}, t) = i\hbar\frac{\partial}{\partial t}u(\boldsymbol{r}, t) \tag{2.19}$$
$$-\mathcal{H}_0^* v(\boldsymbol{r}, t) + \Delta^*(\boldsymbol{r})u(\boldsymbol{r}, t) = i\hbar\frac{\partial}{\partial t}v(\boldsymbol{r}, t) \tag{2.20}$$

2.1.3 Andreev Reflection

Boundaries between superconducting and normal regions of superconductors have been an area of rich study. Clearly a complete theory of superconductivity requires description of both superconductors in the intermediate

Figure 2.5: Andreev reflection at a normal-superconductor boundary: An electron incident on the boundary with energy $E < \Delta$ from the normal region is retro-reflected as a hole, with opposite spin, and to first order the same momentum. The incident electron is absorbed into a superconducting Cooper pair inside the superconductor.
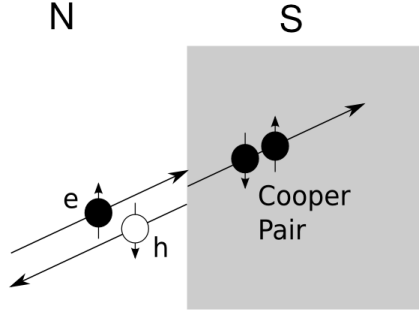
state, and vortex cores present on the surface of type II superconductors (see sub-section 2.1.4 for specific examples). Phenomena such as the Josephson effect [47] can occur in a superconducting wire with a thin insulating region over which not only normal electrons, but also Cooper pairs tunnel across the insulating gap. This has many useful real world applications including extremely sensitive magnetometers and superconducting transistors.

Let us consider a normal-superconducting (N-S) interface. *Andreev reflection* can occur when an electron incident from the normal conductor, meets the N-S interface. If the electron has an energy lower than the minimum excitation energy Δ, we've seen that due to the superconducting energy band gap, it cannot exist alone inside the superconducting bulk. Instead it is absorbed into a superconducting Cooper pair. Conservation of charge and momentum (the cooper pair having a charge $2e$) requires that a hole state is retro-reflected into the normal region with opposite spin, and to first order the same momentum, albeit with the opposite velocity to the incoming electron. This process is shown schematically in Figure 2.5. We can also consider the same process in reverse i.e. a hole incident on the N-S interface, with an electron injected into the normal region. In the asymptotic limit $E \ll \Delta \ll \mu$, the incident state is completely Andreev reflected with a phase shift of $e^{-i\pi/2}$ and the momentum of the Andreev reflected state is exactly that of the incident state, the reflected hole following the path of the incident electron. Andreev reflection was derived concurrently by Andreev [22] and St. James [48] and has been used to explain how a normal conductor can carry a superconducting current between two superconducting regions by Kulik [49] and by Andreev to explain why the thermal resistance of the intermediate state is greater than that of a purely superconducting state [22].

For larger energies but still in the regime $E < \Delta$ we must also consider specular reflection with a finite amplitude. We will also see that the incident

particle penetrates a finite distance into the superconducting region, before being absorbed into a superconducting pair. For a 1-dimensional interface the possible processes can be described in terms of the scattering matrix

$$\boldsymbol{S} = \begin{pmatrix} S_{ee} & S_{eh} \\ S_{he} & S_{hh} \end{pmatrix} \tag{2.21}$$

where S_{he} is the amplitude for an incident electron to be reflected as a hole etc. In chapter 4 we will give a detailed account of the analytic solutions for a discontinuous N-S interface, and generalise to numeric solutions for a continuous transition between normal and superconducting regions, described by $\Delta(q)$. We will apply the scattering matrix to the time dependent Andreev reflection of coherent states in Chapter 6. In the asymptotic limit $|E| \ll \Delta \ll \mu$ the scattering matrix reduces to

$$\boldsymbol{S} = \begin{pmatrix} 0 & -i \\ -i & 0 \end{pmatrix} \tag{2.22}$$

corresponding to complete Andreev reflection. Although this thesis investigates the reflection of states with energy below Δ we can in principle also consider incident quasi-particles with $|E| > \Delta$. We would then need to consider 4 scattering processes, the incident particle still has a probability to be specularly or Andreev reflected, but may also be transmitted into the superconductor as a quasi-particle with energy $\mu + \sqrt{E^2 - \Delta^2}$, which travels freely into the superconducting region. These possible processes are demonstrated in the energy momentum diagram Figure 2.6 for an incident electron with $|E| > \Delta$.
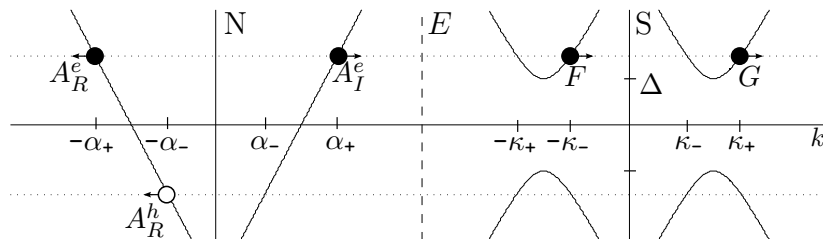
Figure 2.6: Schematic of energy v momentum at an N-S interface showing the possible excitation energies in the normal and superconducting regions. For an incident electron (A_I^e) with $E > \Delta_0$ there is a probability for it to specularly reflected as an electron (A_R^e), or retro-reflected as a hole (A_R^h). It may also be transmitted into the superconductor as an electron or hole-like Bogolon with probability F or G. Adapted from [31].

2.1.4 Semiclassical Approaches to the Bogoliubov-de Gennes Equations

The BdG equations have been previously employed by a number of authors as a means of investigating inhomogeneous superconductors and associated phenomena. We've seen in sub-section 2.1.1 that inhomogeneous superconductors arise both in the case of the intermediate state and the penetrating state of type II superconductors. In both cases the transition from normal to superconducting regions requires semi-classical techniques. Only in the simplified case of a discontinuous normal-superconducting interface (which we will analyse) will we be able to find analytic solutions without approximation. Like the standard scalar Schrödinger equation there are two semi-classical approaches.

The first approach we consider utilizes the WKB wave function as a form of solution. Andreev used this approach in 1964 [22] to calculate the thermal resistance at a N-S interface, and in 1966 [25] to derive the energy spectrum of the intermediate state of the superconductor. Also see Bardeen, Kümmel, Jacobs and Tewordt, 1969 [26]. They apply the WKB method to calculate the energy spectrum and scattering states of a vortex line in a type II superconductor. This approximation takes advantage of the slowly varying amplitudes of $u(\boldsymbol{r})$ and $v(\boldsymbol{r})$ to reduce the second order BdG equations. In the prescription given in Bardeen, Kümmel, Jacobs and Tewordt the solution of the BdG equations may be written in the form

$$\begin{pmatrix} u \\ v \end{pmatrix} = \begin{pmatrix} e^{i\eta/2} \\ e^{-i\eta/2} \end{pmatrix} e^{iS} \tag{2.23}$$

assuming that η is slowly varying over atomic distances and ∇S is a wave-vector close to the Fermi surface (and in general both S and η are complex). They retain terms of order $(\nabla S)^2$, $\nabla S \cdot \boldsymbol{A}$ and $\nabla S \cdot \nabla \eta$, but neglect terms of order $(\nabla \eta)^2$ and $(\nabla \boldsymbol{A})^2$.

The second approach developed by Azbel [50] uses effective classical Hamiltonians and Bohr quantization to study the wave functions and energy spectrum of superconducting quasi-particles. Duncan and Györffy [27] build on this approach to extend the WKB approximation to take account of higher order terms of $\hbar$ in the solution.

They take as the WKB ansatz

$$\begin{pmatrix} u(\boldsymbol{r}) \\ v(\boldsymbol{r}) \end{pmatrix} = \begin{pmatrix} \tilde{u}(\boldsymbol{r}) \\ \tilde{v}(\boldsymbol{r}) \end{pmatrix} e^{\frac{i}{\hbar}S_0(\boldsymbol{r})}(1 + \mathcal{O}(\hbar)) \tag{2.24}$$

Figure 2.7: The S-N-S junction and the corresponding phase space trajectories derived by Duncan and Györffy. Images reproduced from [27].
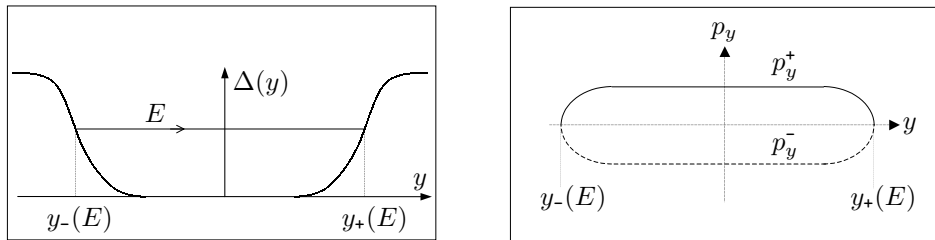
(a) The profile $|\Delta(y)|$ of the S-N-S junction. The classical turning points $y_\pm(E)$ are also indicated.

(b) $p_y^\pm(y)$ as $|\Delta(y)| \to E$. $p_y^\pm(y)$ are constant in the normal region. $P_y^+(E) = P_y^-(E)$ are the classical turning points at which an incident electron (solid) converts into a hole (dashed).

where $\tilde{u}(\boldsymbol{r})$ and $\tilde{v}(\boldsymbol{r})$ are slowly varying amplitudes. Inserting this ansatz into the BdG equations the lowest order approximation is then found by neglecting terms containing $\hbar$ (i.e. $\hat{p} = -i\hbar\nabla$ whose action on the amplitude terms is small). In this regime the differential matrix BdG equations are reduced to a pair of Hamilton-Jacobi equations. The quasi particle described by these equations also have an internal structure describing the complex spinor components at each point along the trajectory. This can be represented by a vector which represents the electron-hole degree of freedom which varies as it travels along the phase space trajectory. The vortex cores present in type II superconductors enter as topological phase contributions to the Hamiltonian.

They show that the extension to include contributions of order $\hbar^2$ is necessary for a derivation of the wave function at the vortex core. This is achieved by using $\hat{p}$ as the ordering parameter instead of $\hbar$, the result being $\hbar$ dependent Hamilton-Jacobi equations and a corresponding $\hbar$ dependent action. This dependence also carries over to the spinor amplitudes. They apply this technique to two inhomogeneous systems, a smoothly varying S-N-S junction (as shown in Figure 2.7a) and a type II vortex core. In section 4.3 we will use numerical techniques to derive the allowed wave functions for a similar S-N-S junction, and show how we can use coherent states to represent them on classical phase space. Their approach predicts that the phase space trajectories are straight lines in the normal region as might be expected for the free motion in this region. At the classical turning points (denoted $y_\pm(E)$) the particle and hole momenta are equal. In contrast the classical orbits are characterised by stationary points satisfying $p_y(y) = 0$.

The velocity, $\boldsymbol{v}^+ > 0$, of a particle travelling along p_y^+ towards y_+ decreases until it reaches zero at the turning point. At this point $p_y^+(y_+) = p_y^-(y_+)$ and the particle converts into a hole as shown in Figure 2.7b. It moves away from the interface with velocity $\boldsymbol{v}^- < 0$. This is consistent with Andreev reflection at the boundary, giving a clear picture of the particle-hole conversion at the interface. One of the benefits of this technique is that Andreev reflection arises naturally from the classical Hamiltonian, rather than requiring wavefunction matching.

2.2 Coherent States & their Semiclassical Applications

Coherent states were first described by Schrödinger in 1926 [9], as a result of seeking a form of quantum state that best satisfies quantum-classical correspondence (a key issue in the interpretation and acceptance of quantum theory during it's early development). Coherent states arise naturally from the study of the quantum harmonic oscillator, and the coherent state wave function was derived by Schrödinger. However further refinement of the theory would wait until the 1960's for developments made by Glauber and Sudarshan motivated by a quantum description of the electromagnetic field, alongside group theoretic developments by Klauder. Coherent states have since become a key feature of quantum mechanics and quantum field theory, and the concept of a coherent state has been generalised to other fields and mathematical structures.

Coherent states have many useful properties for the study of classical-quantum correspondence. In the special case of the quantum harmonic oscillator the canonical expectation values of the coherent states coincide exactly with the phase space trajectory of the corresponding classical harmonic oscillator. This property also holds for short times with other systems. Coherent states are also states of minimum uncertainty on phase space, best satisfying the minimum bound set by the Heisenberg uncertainty principle. As such they also represent the smallest possible deviation of a quantum state from the corresponding classical trajectory.

2.2.1 Canonical Coherent States

Although Schrödinger derived the form of the coherent state wave function there was little further theoretical progress made until the development of the recognisable modern formulation of coherent states through work by Glauber and Sudarshan, and concurrently Klauder. Glauber [51–53] and Surdashan's [54] contributions were motivated by a desire to provide a quantum mechanical description of optical coherence effects. The term coherent states was coined by Glauber, who would provide the definition of coherent states as eigenstates of the annihilation operator. Klauder [14, 55] (at approximately the same time) would contribute a set of continuous states, which contained the basic concept of generalising coherent states to arbitrary Lie groups. This would define what we will refer to as the *Schrödinger-Glauber-Sudarshan* (SGS) *coherent states* of the quantum harmonic oscillator (though other naming conventions include *canonical coherent states* or *field coherent states*).

Coherent states arise naturally from the study of the quantum harmonic oscillator, the quantum analogue of a classical particle in a quadratic potential well. The quantum Hamiltonian is given in terms of phase space observables $\hat{q}$ and $\hat{p}$ as

$$\hat{\mathcal{H}}_{\mathsf{osc}} = \frac{1}{2m}\hat{p}^2 + \frac{1}{2}m\omega^2\hat{q}^2 \tag{2.25}$$

where ω is the angular frequency of the oscillator. It is useful to define the operators $\hat{a}$ and $\hat{a}^\dagger$, referred to as the *annihilation* and *creation* (or *raising* and *lowering*) operators respectively. They are defined in terms of the phase space observables as

$$\hat{a} = \sqrt{\frac{m\omega}{2\hbar}}\left(\hat{q} + \frac{i}{m\omega}\hat{p}\right) \quad \text{and} \quad \hat{a}^\dagger = \sqrt{\frac{m\omega}{2\hbar}}\left(\hat{q} - \frac{i}{m\omega}\hat{p}\right). \tag{2.26}$$

They are aptly named due to their action on the quantized energy eigenstates (or *number states*) of $\hat{\mathcal{H}}_{\mathsf{osc}}$,

$$\hat{a}^\dagger|n\rangle = \sqrt{n+1}|n+1\rangle \quad \text{and} \quad \hat{a}|n\rangle = \sqrt{n}|n-1\rangle. \tag{2.27}$$

With these definitions in hand we can also define the number operator $\hat{N} = \hat{a}^\dagger\hat{a}$, with the action on the number states $\hat{N}|n\rangle = n|n\rangle$.

These operators are closed under the commutation relations $[\hat{a}, \hat{a}^\dagger] = \mathbb{I}$, $[\hat{N}, \hat{a}^\dagger] = \hat{a}^\dagger$ and $[\hat{N}, \hat{a}] = -\hat{a}$. We also define the *ground state* of the harmonic oscillator, defined by the action of the annihilation operator as

$$\hat{a}|0\rangle = 0. \tag{2.28}$$

The harmonic oscillator Hamiltonian can then be re-written in diagonal form as

$$\hat{\mathcal{H}}_{\text{osc}} = \hbar\omega\left(\hat{N} + \frac{1}{2}\right). \tag{2.29}$$

The SGS coherent states, denoted from here on by $|z\rangle$, are defined as eigenstates of the annihilation operator

$$\hat{a}|z\rangle = z|z\rangle \tag{2.30}$$

where $z \in \mathbb{C}$. It can be seen from the action of the annihilation operator that the SGS coherent states are necessarily superpositions of the energy eigenstates of $\mathcal{H}_{\text{osc}}$ written as

$$|z\rangle = e^{-\frac{1}{2}|z|^2}\sum_{n=0}^{\infty}\frac{z^n}{\sqrt{n!}}|n\rangle. \tag{2.31}$$

It will also prove useful to define the non-normalized variant of the coherent states, which we will denote $|z)$, as

$$|z) = e^{\frac{1}{2}|z|^2}|z\rangle = \sum_{n=0}^{\infty}\frac{z^n}{\sqrt{n!}}|n\rangle. \tag{2.32}$$

Although non-normalized they are useful by virtue of being analytic function of z over the entire complex plane. It should be noted that there is no defined eigenstate of the creation operator $a^\dagger$, but the action of $a^\dagger$ on a coherent state

$$a^\dagger|z) = \left(\frac{\partial}{\partial z} + \frac{z^*}{2}\right)|z). \tag{2.33}$$

can be of use in some analytic situations. SGS states are parametrized by the complex number z. It is straight forward to show that the overlap of two distinct coherent states parametrized by w and z respectively is

$$\langle w|z\rangle = \exp\left[-\frac{1}{2}|z|^2 - \frac{1}{2}|w|^2 + w^*z\right] \neq 0 \tag{2.34}$$

and thus coherent states cannot be used to construct an orthonormal basis. The set of coherent states is over-complete though, and allows for a resolution of identity

$$\mathbb{I} = \frac{1}{\pi}\int d^2z\,|z\rangle\langle z|. \tag{2.35}$$

Here the integration is taken over the entire complex plane with $d^2z = d\,\text{Re}(z)\,\text{Im}(z)$. This allows for the representation of a state $|\psi\rangle \in \mathcal{H}_\infty$ in terms of coherent states as $\psi(z^*) \equiv \langle z|\psi\rangle$. This is not an analytic function in z but the non-normalized variant

$$f(z^*) = \psi(z)e^{\frac{1}{2}|z|^2} \tag{2.36}$$

24

is, and generally referred to as the *Bargmann representation* [56].

We can see that the set of coherent states may be mapped one-to-one to classical phase space given that the expectation values of the phase space observables $\hat{p}$ and $\hat{q}$ are

$$\langle z|\hat{q}|z\rangle = \sqrt{\frac{2\hbar}{m\omega}}\,\mathrm{Re}(z) \quad \text{and} \quad \langle z|\hat{p}|z\rangle = \sqrt{2m\hbar\omega}\,\mathrm{Im}(z). \qquad (2.37)$$

We can therefore derive the coherent states wave function in the position basis

$$\langle q|z\rangle = \left(\frac{m\omega}{\pi\hbar}\right)^{\frac{1}{4}}\exp\left[-\frac{m\omega}{2\hbar}(q-\langle\hat{q}\rangle)^2 + \frac{i}{\hbar}\langle\hat{p}\rangle q - \frac{i}{2\hbar}\langle\hat{p}\rangle\langle\hat{q}\rangle\right] \qquad (2.38)$$

noting for later use that $\langle q|z^*\rangle = \langle q|z\rangle^*$. Transforming into the momentum basis we have the representation

$$\langle p|z\rangle = \frac{1}{(\pi m\hbar\omega)^{\frac{1}{4}}}\exp\left[-\frac{1}{2\hbar m\omega}(p-\langle\hat{p}\rangle)^2 - \frac{i}{\hbar}\langle\hat{q}\rangle p - \frac{i}{2\hbar}\langle\hat{p}\rangle\langle\hat{q}\rangle\right] \qquad (2.39)$$

and it will be again important to note that for conjugate z the relevant transformation is

$$\langle p|z^*\rangle = \frac{1}{(\pi m\hbar\omega)^{\frac{1}{4}}}\exp\left[-\frac{1}{2\hbar m\omega}(p+\langle\hat{p}\rangle)^2 - \frac{i}{\hbar}\langle\hat{q}\rangle p - \frac{i}{2\hbar}\langle\hat{p}\rangle\langle\hat{q}\rangle\right] \qquad (2.40)$$

corresponding as we might expect to inverting the complex axis of the complex parametrization of phase space. We will define for later convenience the scaled momentum-width parameter $\lambda = 1/m\hbar\omega$. By inspection it can be seen that the coherent states are Gaussian distributions centred at $\langle z|\hat{q}|z\rangle$ and $\langle z|\hat{p}|z\rangle$.

The SGS coherent states remain coherent states under time evolution by the quantum harmonic oscillator Hamiltonian. This can be shown if we act with the time development operator, $\exp(-it\hat{\mathcal{H}}_{\mathsf{osc}}/\hbar)$, on the coherent state in the number basis

$$\exp\left(-\frac{it}{\hbar}\hat{\mathcal{H}}_{\mathsf{osc}}\right)|z\rangle = e^{-i\omega t/2}e^{-i\omega t\hat{N}}e^{-\frac{1}{2}|z|^2}\sum_{n=0}^{\infty}\frac{z^n}{\sqrt{n!}}|n\rangle. \qquad (2.41)$$

Since the number states are eigenstates of $\hat{N}$ we can rewrite this as

$$e^{-i\omega t/2}e^{-\frac{1}{2}|z|^2}\sum_{n=0}^{\infty}\frac{z^n e^{-i\omega tn}}{\sqrt{n!}}|n\rangle = e^{-i\omega t/2}|ze^{-i\omega t}\rangle. \qquad (2.42)$$

The result, up to an overall phase, is the same coherent state distribution, but parametrized by a new $z' = ze^{-i\omega t}$. $ze^{-i\omega t}$ corresponds to a rotation

Figure 2.8: Contour plots of the Q-function, $|\langle z|w(t)\rangle|^2$ of a coherent states at various times, evolved under the harmonic oscillator Hamiltonian. The corresponding classical trajectory of a single particle is shown in red. The centre of the coherent state follows the classical trajectory without dispersion.

(a) $t = 0$ **(b)** $t = 0.5$ **(c)** $t = 1$
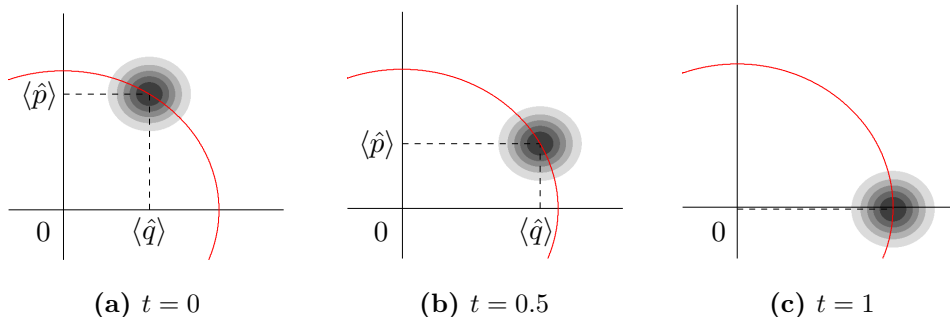
of the location of the coherent state about the origin in the complex plane, with frequency ω as demonstrated in Figure 2.8.

The classical solutions of the harmonic oscillator follows the phase space trajectory $x(t) = x_0 \cos(\omega t + \phi)$ and $p(t) = -m\omega x_0 \sin(\omega t + \phi)$ where ϕ is a phase determined by the initial state of the system. We can see that the centre of the coherent state follows the corresponding classical trajectory whilst also retaining its form. The coherent state in a quadratic potential is a special case where the relationship between the classical and quantum dynamics is exact and non-dispersive. In general this correspondence does not remain exact for other Hamiltonians, but does remain true for short times.

As a simple but enlightening example, the free time dependent (i.e. under the Hamiltonian $\hat{p}^2/2m$) coherent state is in the position basis

$$\Psi(q,t) = \exp\left[-\frac{m\omega}{2\hbar} \frac{1}{\lambda(t)}(q - tv)^2 + \frac{i}{h}p_0\left(q - \frac{1}{2}tv \right) \right] \tag{2.43}$$

where $\lambda(t) = 1 + i\omega t$. The form of the wave packet overall remains Gaussian, with the centre propagating along the path of a free particle with velocity $v = p_0/m$. The width of the wave packet is now linearly dependent on time, and also proportional to ω. We will see analogous wave packets several times in this thesis under the BdG Hamiltonian. We can imagine that the spreading of the state is proportional to ω as contributions to the wave packet propagate at different velocities, thus a larger spread of momenta will cause the state to spread more quickly (see the following section for more discussion).

The uncertainty of a state $|\psi\rangle$, with respect to an observable can be derived from the variance with respect to the corresponding quantum operator

defined as

$$\text{Var}(\hat{A})_{|\psi\rangle} = \langle\psi|\hat{A}^2|\psi\rangle - \langle\psi|\hat{A}|\psi\rangle^2. \tag{2.44}$$

For the phase space observables $\hat{q}$ and $\hat{p}$ with respect to the SGS coherent states the respective variance are $\text{Var}(\hat{q})_{|z\rangle} = \hbar/2m\omega$ and $\text{Var}(\hat{p})_{|z\rangle} = \hbar m\omega/2$. As such their product

$$\text{Var}(\hat{q})_{|z\rangle}\,\text{Var}(\hat{p})_{|z\rangle} = \frac{\hbar^2}{4} \tag{2.45}$$

minimizes the possible uncertainty as bounded by the Heisenberg uncertainty principle. The dependence of the uncertainty on $\hbar$ also means that in the semiclassical limit $\hbar \to 0$ the Gaussian distribution tends towards a δ-function that traces the corresponding classical trajectory. For finite $\hbar$ the minimum uncertainty property of SGS coherent states still minimizes the deviation from the classical trajectory.

The variable ω, as well as being the frequency of the oscillations of the classical harmonic oscillator, also parametrizes the *squeezed states* on phase space. They are deformations of the coherent state distribution in phase space, in either the position or momentum direction whilst retaining the minimum uncertainty relation. When $\omega = 1$, the width is equal in both directions. Since the width of the state in position space is inversely proportional to ω and we must maintain the minimum uncertainty relationship it follows that the width in momentum space is proportional to ω as shown in Figure 2.9. In this thesis ω will often prove useful as a free parameter independent of the system parameters (energy scales etc.) that we can use to control the spatial width or energy/momentum bandwidth of the coherent state wave packet as required.

The resolution of identity in terms of SGS coherent states allows the representation of general quantum states in a coherent state basis

$$|\Psi\rangle = \frac{1}{\pi}\int d^2z\,|z\rangle\langle z|\Psi\rangle. \tag{2.46}$$

Due to the one-to-one correspondence between the parameter z and points $\langle\hat{q}\rangle$ and $\langle\hat{p}\rangle$ on classical phase space coherent states can be used to generate a representation of quantum states on classical phase space.

There are several possible means of representing the probability distributions on phase space (see [57, 58]). We will consider the *Q-function* (or *Husimi distribution*, after its introduction by Husimi in 1940 [59]) $Q(q,p) = |\langle z(q,p)|\Psi\rangle|^2$, where the phase space variables are defined by $q = \langle z|\hat{q}|z\rangle$ and $p = \langle z|\hat{p}|z\rangle$ with respect to the reference coherent state. As the density

Figure 2.9: Contour plots of the Q-function, $Q(q, p) = |\langle z|w \rangle|^2$, of a coherent states with various squeezing parameters. The centre of the state lies at $q_0 = \langle w|\hat{q}|w \rangle$ and $p_0 = \langle w|\hat{p}|w \rangle$. When $\omega = 1$ the width of the state is the same in q and p, varying w 'squeezes' the state in one of the phase space variables, but maintains the overall minimum uncertainty relationship.

(a) $\omega = 1$ **(b)** $\omega = 0.4$ **(c)** $\omega = 2.5$
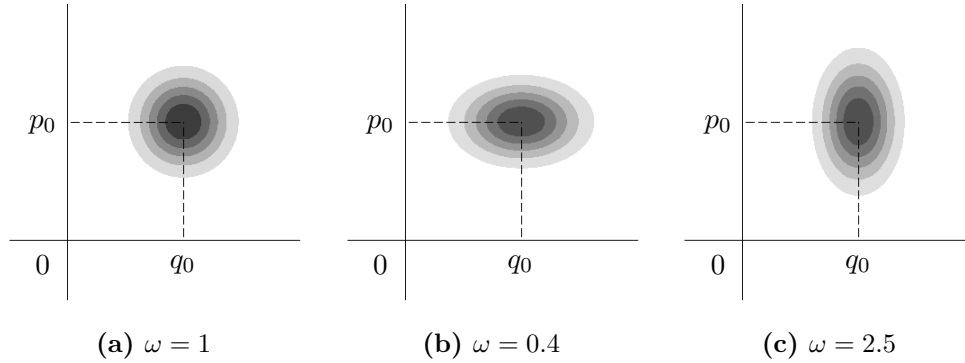
operator is defined by $\hat{\rho} = |\Psi\rangle\langle\Psi|$ we can equivalently define the Q-function as $Q(q, p) = \langle z|\hat{\rho}|z \rangle$. As an example the Husimi distribution of a coherent state, $|w\rangle$ centred at $q_0 = \langle w|\hat{q}|w \rangle$ and $p_0 = \langle w|\hat{p}|w \rangle$ is

$$Q(q, p) = |\langle z|w \rangle|^2 \tag{2.47}$$

$$= \left(\frac{2\sqrt{\omega}}{1+\omega} \right)^{\frac{1}{2}} \exp\left[-\frac{1}{2\hbar m(1+\omega)}(p - p_0)^2 - \frac{m}{2\hbar}\frac{\omega}{(1+\omega)}(q - q_0)^2 \right] \tag{2.48}$$

as shown in Figure 2.9 for various squeezing values of ω_w. Here we've set $\omega_z = 1$ for the reference state $|z\rangle$, which effectively means scaling the position and momentum axis equally.

An operator $\hat{A}$ can then also be represented by its symbol

$$\mathcal{A}(z, z^*) = \langle z|\hat{A}|z \rangle. \tag{2.49}$$

There is a one-to-one correspondence between states and their Q-function, and operators and their symbol.

2.2.2 Ehrenfest's Theorem

We have shown that for the quantum harmonic oscillator the time evolution of the phase space distribution exactly follows the corresponding classical phase space trajectories with no dispersion. This notion of correspondence between quantum expectation values and classical trajectories has been an important area of research and this thesis will partly ask the question; can we in some sense derive *classical* trajectories for BCS excitations despite

their quantum nature? We will examine this and related questions in greater detail in chapter 5.

Ehrenfest's theorem provides a framework for the study of the relationship between quantum expectation values and the corresponding classical equations of motion [60]. Although not an exact relation, we will derive conditions under which the relationship is best satisfied. The starting point is the differential equation for the time dependence of an operator in the Heisenberg picture

$$\frac{d}{dt}\langle \hat{A}(t) \rangle = \frac{i}{\hbar}\langle [\hat{\mathcal{H}}, \hat{A}(t)] \rangle \tag{2.50}$$

for some general Hamiltonian $\mathcal{H}$ and time dependent operator $\hat{A}(t)$. We consider the phase space operators with the canonical commutation relation

$$[\hat{q}, \hat{p}] = i\hbar \tag{2.51}$$

and Hamiltonian operator $\hat{\mathcal{H}}$ defined as

$$\hat{\mathcal{H}} = \frac{\hat{p}^2}{2m} + U(\hat{q}) \tag{2.52}$$

describing a particle in some potential $U(q)$. The expectation values of the phase space operators have the time dependence

$$\frac{d}{dt}\langle \hat{q} \rangle = \frac{1}{m}\langle \hat{p} \rangle \tag{2.53}$$

$$\frac{d}{dt}\langle \hat{p} \rangle = -\left\langle \frac{d}{d\hat{q}}\hat{U}(\hat{q}) \right\rangle. \tag{2.54}$$

These are recognisable as analogous to the classical equations of motion

$$\dot{x} = \frac{p}{m} \qquad \text{and} \qquad \dot{p} = -U'(x) \tag{2.55}$$

for a classical particle in a potential $U(x)$. Essentially this is a statement that the dynamics of the expectation values follow the classical equations of motion. This is only approximately true for equation (2.54), as the right hand side would only correspond exactly to the classical equations if it could instead be written as

$$-\frac{d}{d\langle q \rangle}U(\langle \hat{q} \rangle). \tag{2.56}$$

In general this is not possible for an arbitrary function of $\hat{q}$ as generally $\langle \hat{q}^n \rangle \neq \langle \hat{q} \rangle^n$. This means the quantum dynamics will generally deviate from the classical trajectories. If we suppose that the potential $U(\hat{q})$ is slowly varying then we can expand $dU(\hat{q})/d\hat{q}$ around $\langle \hat{q} \rangle$ to find deviation from classical trajectory as

$$\frac{d}{d\hat{q}}U(\hat{q}) = \frac{d}{d\langle \hat{q} \rangle}U(\langle \hat{q} \rangle) + \frac{d^2}{d\langle \hat{q} \rangle^2}U(\langle \hat{q} \rangle)(q - \langle \hat{q} \rangle) + \frac{1}{2}\frac{d^3}{d\langle \hat{q} \rangle^3}U(\langle \hat{q} \rangle)(q - \langle \hat{q} \rangle)^2 \dots. \tag{2.57}$$

Inserting the expansion back into the Ehrenfest relationship gives

$$\frac{d}{dt}\langle\hat{p}\rangle \approx -\frac{d}{d\langle\hat{q}\rangle}U(\langle\hat{q}\rangle) - \frac{1}{2}\text{Var}(\hat{q})\frac{d^3}{d\langle\hat{q}\rangle^3}U(\langle\hat{q}\rangle). \qquad (2.58)$$

From this result it can be conclude that the accuracy of the Ehrenfest relationship is dependent on the initial width of the state. This also implies a requirement that the Ehrenfest relationship only applies if the state is δ-function like in the sense that is is localised and has a peak value. The solution is trivial in harmonic oscillator case when $U'(q) = m\omega^2 q$, and it is true for any general state under a quadratic potential. The property of the distribution remaining invariant under time development is a special property of SGS coherent states under a quadratic potential.

As the SGS coherent states are minimum uncertainty states, their evolution has a simplified description in semiclassical regimes. As they are strongly localised on phase space, their propagation can be derived from the corresponding classical phase space trajectories. The location of the wave packet then follows the classical trajectory as shown by Ehrenfest's theorem, and the spreading of phase space distribution is described by the linearised flow of nearby classical trajectories. The basic principle behind this approximation allows the Hamiltonian to be approximated by its quadratic Taylor expansion close to the peak of the coherent state's distribution. The exact origin of this method of is hard to locate, but a great deal of the modern development is due to work by Heller [13], Heller & Davis [11] and [12] (this is limited selection of a broad literature on this subject, see [10] for an overview of the subject).

For the free particle example given by Equation (2.43) the spreading of the wave packet is analogous to the spreading shown by an ensemble of freely evolving (and non-interacting) classical particles (see [10]). The lower and higher velocities or the trajectories above and below $\langle\hat{p}\rangle$ create the shearing and spreading of the wave packet in phase space. The time dependent spreading evidenced by (2.43) disappears as $\hbar \to 0$, this is because the width of the wavepacket also scales as $\text{Var}(\hat{p}) \to 0$ meaning the velocity differential across the wave packet disappears.

This approximation only holds up to certain time scales, known as the *Ehrenfest time*. After such times the dispersion of wave packet means the Ehrenfest relation, as applied to localised wave packets, no longer holds and wave packets can no longer be approximated using a single trajectory. As such the Ehrenfest time depends upon the system under consideration.

Schubert *et al* provide a means of describing the evolution of wave packets at and beyond Ehrenfest time scales, describing the transition of a state from localised state to a extended state, in a uniform manner [61].

It is not immediately clear that coherent states evolved under the BdG Hamiltonian allow for the application of this approximation. Firstly as we will show the hole component has a velocity opposite to it's momentum and meaning an initially localised wave packet will generally quickly disperse, motivating the definition of electron-hole coherent states. Secondly when analysing the propagation of wave packets in a spatially homogeneous superconductor; we will show that in certain cases interference between contributions from the positive and negative energy solution of the BdG equations play a strong role in the dynamics in addition to the propagation of the components.

2.2.3 SU(2) Coherent States

The concept and application of coherent states defined on phase space has very much spread from this original motivation and definition. Like BCS theory, the generalisation of coherent states is a broad topic which due to our requirements we will only give a brief overview of. An extensive review can be found in [17] and [16].

The concept of a coherent state can been generalised by first considering the defining features of the SGS coherent states. According to Glauber there are three defining features of the coherent states of the harmonic oscillator (see [53]). They are:

1. The coherent states are eigenstates of the lowering operator, defined by

$$\hat{a}|z\rangle = z|z\rangle \tag{2.59}$$

   for a complex number z.

2. The SGS coherent states can be generated by the action of the displacement operator on the ground state. The displacement operator $\hat{D}(z)$ is defined as

$$\hat{D}(z) = \exp\left(z\hat{a}^\dagger - z^*\hat{a}\right). \tag{2.60}$$

   The SGS coherent states are then defined as the action of the displacement operator on the ground state

$$\hat{D}(z)|0\rangle = |z\rangle. \tag{2.61}$$

3. The SGS coherent states are minimum uncertainty states satisfying

$$\text{Var}(\hat{q})_{|z\rangle}\,\text{Var}(\hat{p})_{|z\rangle} = \frac{\hbar^2}{4}. \qquad (2.62)$$

The first and third definition have been observed in the previous section, the second definition arises naturally when considering the Group-theoretic structure of coherent states. The set of operators $\hat{a}$, $\hat{a}^\dagger$ and $\hat{\mathbb{I}}$ are the generators of an irreducible unitary representation of the Heisenberg-Weyl group $H_3(\mathbb{R})$. The unitary representation is given by the exponent of a anti-hermitian linear combination of the generators

$$\hat{D}(z, \phi) = \exp\left(z\hat{a}^\dagger - z^*\hat{a} + i\phi\right). \qquad (2.63)$$

The action of the displacement operator can be resolved using the Baker-Campbell-Hausdorff formula

$$\exp\left(z\hat{a}^\dagger - z^*\hat{a} + i\phi\right) = e^{z\hat{a}^\dagger}e^{-z^*\hat{a}}e^{-|z|^2/2+i\phi}. \qquad (2.64)$$

Since $\hat{D}(\alpha, \phi)|0\rangle = e^{i\phi}|0\rangle$ setting $\phi = 0$ fixes a phase convention (and we often omit the phase term). $\hat{D}(z)$ effectively translates the Gaussian distribution in phase space to a new centre located at z. Thus the action of $\hat{D}(z)$ on a coherent state $|w\rangle$ is

$$\hat{D}(z)|w\rangle = \exp\left(\text{Im}[zw^*]\right)|z + w\rangle \qquad (2.65)$$

another coherent state translated in the complex plane, up to an overall phase.

Generalizations of the coherent states attempt to apply one of these definitions to other mathematical structures and with the appropriate choices, also generate analogues of other desirable properties of coherent states (which may also include over-completeness, a resolution of identity etc.). The first and third definitions prove less useful as definitions for generalisation, but it proves effective to build on the group theoretic definition.

One such generalisation developed mainly by Perelemov [20, 62] and Gilmore [19] replaces the Heisenberg-Weyl group, from which we generated the SGS states, with another group G with generators that are observables of the quantum system of interest. Taking an irreducible representation of G on the Hilbert space, and a choice of reference state $|\alpha\rangle$ the coherent states are defined by the action of an element of the group $g \in G$ as $g|\alpha\rangle = |g\rangle$. An appropriate choice of reference state will generate analogues of the properties of the SGS states.

The construction we will make use of in conjunction with the SGS states when defining coherent states relevant to the superconducting system, will be the $SU(2)$ coherent states also known as *spin coherent states*. The infinitesimal generators of this group are the angular momentum operators J_x, J_y and J_z with the commutation relations

$$[J_x, J_y] = iJ_z, \quad [J_y, J_z] = iJ_x, \quad [J_z, J_x] = iJ_y \tag{2.66}$$

The irreducible representations are characterised by the half integer j. The total angular momentum is then $J_x^2 + J_y^2 + J_z^2 = j(j+1/2)$ and the Hilbert space has dimensions $2j + 1$. For our purposes we will only be required to consider the simplest case $j = 1/2$ (in anticipation of the two levels describing the electron-hole degree of freedom) on the space $\mathbb{C}^2$. The Hilbert space is spanned by the orthogonal states

$$|+\rangle = \begin{pmatrix} 1 \\ 0 \end{pmatrix} \quad \text{and} \quad |-\rangle = \begin{pmatrix} 0 \\ 1 \end{pmatrix} \tag{2.67}$$

and the generators of $SU(2)$ will be represented using the hermitian Pauli spin operators as

$$J_1 \equiv \frac{1}{2}\sigma_1 = \frac{1}{2}\begin{pmatrix} 0 & 1 \\ 1 & 0 \end{pmatrix}, \quad J_2 \equiv \frac{1}{2}\sigma_2 = \frac{1}{2}\begin{pmatrix} 0 & -i \\ i & 0 \end{pmatrix}, \quad J_3 \equiv \frac{1}{2}\sigma_3 = \frac{1}{2}\begin{pmatrix} 1 & 0 \\ 0 & -1 \end{pmatrix}. \tag{2.68}$$

It will also prove useful to define the non-Hermitian two-level raising and lowering operators

$$J_+ = J_1 + iJ_2 \equiv \sigma_+ = \begin{pmatrix} 0 & 1 \\ 0 & 0 \end{pmatrix} \quad J_- = J_1 - iJ_2 \equiv \sigma_- = \begin{pmatrix} 0 & 0 \\ 1 & 0 \end{pmatrix} \tag{2.69}$$

which are closed under the commutation relations with J_3, $[J_3, J_\pm] = \pm J_\pm$ and $[J_+, J_-] = 2J_3$. The elements of of $SU(2)$ are covered by the parametrization

$$\hat{U}(\beta, \phi) = \begin{pmatrix} \dfrac{e^{i\theta}}{\sqrt{1+|\beta|^2}} & \dfrac{-\beta^* e^{-i\theta}}{\sqrt{1+|\beta|^2}} \\ \dfrac{\beta e^{i\theta}}{\sqrt{1+|\beta|^2}} & \dfrac{e^{-i\theta}}{\sqrt{1+|\beta|^2}} \end{pmatrix} \equiv e^{\beta J_-} e^{-\log(1+|\beta|^2)J_3} e^{-\beta^* J_+} e^{2i\phi J_3} \tag{2.70}$$

where $\beta \in \mathbb{C}$ and $0 \leq \phi \leq 2\pi$. The spin coherent states are then defined by the action of $\hat{U}(\beta, \phi)$ (fixing the phase at $\phi = 0$) on the reference state $|+\rangle$ as

$$|\beta\rangle = \hat{U}(\beta, 0)|+\rangle = \frac{1}{\sqrt{1+|\beta|^2}}\left(|+\rangle + \beta|-\rangle\right). \tag{2.71}$$

Figure 2.10: The $SU(2)$ coherent states map the two-dimensional sphere S^2 onto the complex plane. This is compact when the point at infinity is included.
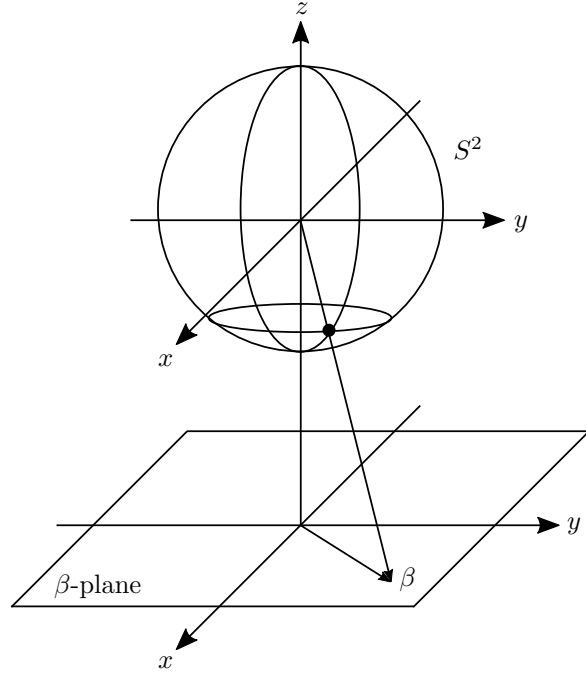
It will also be useful to again define an un-normalized variant that is analytic in β as

$$|\beta) = |+\rangle + \beta|-\rangle. \tag{2.72}$$

The spin coherent states map the two dimensional-sphere S^2 onto the complex plane as illustrated in Figure 2.10. With the inclusion of the coherent state $|\beta = \infty\rangle \equiv |-\rangle$ we can show that the SU(2) coherent states span a manifold equivalent to the unit sphere $S^2 = SU(2)/U(1)$. If we calculate the expectation values with respect to the spin operators they are

$$\langle\beta|\sigma_1|\beta\rangle = \frac{2\,\mathrm{Re}(\beta)}{1+|\beta|^2} \qquad \langle\beta|\sigma_2|\beta\rangle = \frac{2\,\mathrm{Im}(\beta)}{1+|\beta|^2} \qquad \langle\beta|\sigma_3|\beta\rangle = \frac{1-|\beta|^2}{1+|\beta|^2}. \tag{2.73}$$

They build a vector in $\mathbb{R}^3$ of length 1

$$\sum_{j=1}^{3}\langle\beta|\sigma_j|\beta\rangle^2 = 1. \tag{2.74}$$

Like the SGS coherent states the spin coherent states form an overcomplete basis. The overlap of distinct (normalized and un-normalized) spin coherent states is given by

$$(\beta_1|\beta_2) = 1 + \beta_1\beta_2^* \qquad \langle\beta_1|\beta_2\rangle = \frac{1 + \beta_1\beta_2^*}{\sqrt{(1+|\beta_1|^2)(1+|\beta_2|^2)}}. \tag{2.75}$$

A resolution of unity is then found to be

$$\mathbb{I} = \frac{2}{\pi}\int d^2\beta\,\frac{1}{(1+|\beta|^2)^2}|\beta\rangle\langle\beta| = \frac{2}{\pi}\int d^2\beta\,\frac{1}{(1+|\beta|^2)^3}|\beta)(\beta| \tag{2.76}$$

34

where the integration is taken over the unit sphere. Like the SGS coherent states this then also allows for the representation of states on $\mathbb{C}^2$.

Chapter 3

Electron-Hole Coherent States

Using the SGS and $SU(2)$ coherent states, defined on $\mathcal{L}^2$ and $\mathbb{C}^2$ respectively, there is a natural coherent state definition on the product space that can encapsulate the properties of spin or quasi-spin particles.

In this chapter we will define a different set of coherent states on the product space $\mathcal{L}^2 \otimes \mathbb{C}^2$ that may have added relevance for descriptions of superconducting states and the BdG equations. Due to the time reversed nature of the hole component of the BdG equation, an initially well localised product coherent state on the product space will quickly separate. As such it will be beneficial to define what will be termed the electron-hole coherent states, which account for this and remain localised over longer times. An analysis of the advantages of these states over the more natural product definition will form the basis of the following chapter.

3.1 Product Coherent States

With the definition of the SGS and $SU(2)$ coherent states in hand it is straightforward to define coherent states on the tensor Hilbert space $\mathcal{H}_\otimes = \mathcal{L}^2 \otimes \mathbb{C}^2$. If the SGS coherent states parametrized by z occupy $|z\rangle \in \mathcal{L}^2$ and the spin coherent states $|\beta\rangle \in \mathbb{C}^2$, then the *product coherent states* (as we will refer to them from now on) are defined as

$$|z \otimes \beta\rangle = |z\rangle \otimes |\beta\rangle = \left[\hat{D}(z) \otimes \hat{U}(\beta) \right] |0\rangle \otimes |+\rangle. \tag{3.1}$$

A non-normalized variant can again be defined

$$|z \otimes \beta) = |z\rangle \otimes |\beta). \tag{3.2}$$

The product coherent states have been defined as generated by the action of an element of the group $H_3(\mathbb{R}) \times SU(2)$, such that the action of this

36
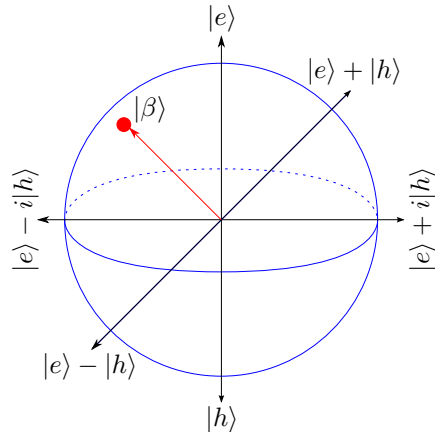
Figure 3.1: The Bloch sphere as used for the purpose of product coherent states. The poles (designated by $\beta = 0$ and the addition of $\beta = \infty$) represent states that only consist of electron or hole components. The equal superpositions of electron and hole components, eigenstates of σ_1 and σ_2, sit on the equator.

group on a product coherent state will be another product state up to an additional phase factor.

For the purposes of describing superconducting states we will therefore associate $|+\rangle = |e\rangle$ with the electron component and $|-\rangle = |h\rangle$ with the hole components of a quasi-particle as

$$|z \otimes \beta\rangle = |z\rangle \otimes \left[\frac{1}{\sqrt{1 + |\beta|^2}}|e\rangle + \frac{\beta}{\sqrt{1 + |\beta|^2}}|h\rangle \right]. \qquad (3.3)$$

In line with the definition of the $SU(2)$ coherent states complex β parametrizes points on the Bloch sphere as shown in Figure 3.1. The pole $\beta = 0$ corresponds to an electron (only) state and $\beta = \infty$ a hole state. β could be parametrized as

$$\beta = e^{i\theta} \tan(\phi) \qquad (3.4)$$

with ϕ the weight of electron and hole components and θ their relative phase. This would parametrize the sphere as

$$|\beta\rangle = \cos(\phi)|e\rangle + \sin(\phi)e^{i\theta}|h\rangle \qquad (3.5)$$

though we will usually consider complex β alone.

The product state construction proves useful when considering systems that occupy tensor product structures, for example Pauli equations where dynamics are coupled to spin variables via the magnetic field. As an example we can look at Bolte and Glaser [21]. They use a product coherent state construction to investigate the propagation of coherent states with spin orbit interaction in semiclassical regimes.

If we consider the dynamics of a product coherent state with central momentum p_0 and a superposition of electron and hole components (i.e. $\beta \neq 0, \infty$); ignoring any oscillations between components, the contributions from

Figure 3.2: Density plot of the Q-function of a product coherent state (i.e. $Q(q,p) = |\langle w|z \otimes \beta \rangle|^2$) with $|\beta|^2 = 1$, in a normal conductor. Plotted both at $t = 0$, when the two contributions from the electron and hole overlap, and after a short time interval. Due to the negative velocity of the hole, the contributions from the two components wave packet quickly separates.

(a) $t = 0$ **(b)** $t > 0$
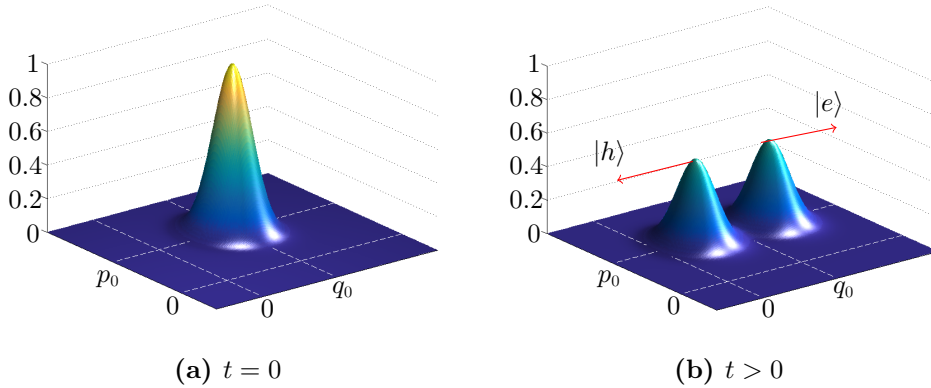
the electron component will have an initial expected velocity $v_e \sim p_0/m$. Due to their time reversed nature the hole will have an expected velocity $v_h \sim -p_0/m$ (this is most obvious for the single particle states in a normal region, though we can consider the same for short times in a superconducting region before rotations between the electron and hole components come into effect. This will be made more concrete in the following chapter). This means an initial product coherent state with non-zero momentum will quickly spread into two components and separate in phase space, losing any desirable semiclassical properties as the components move in opposite directions along the classical trajectories (as illustrated in 3.2). In particular were we to try and consider an analogue of the scalar Ehrenfest relation under the BdG Hamiltonian we will see expectation values that correspond to the relative position of the two components and their relative amplitudes rather than the unique trajectory of a well-localised wave-packet.

3.2 Electron-Hole Coherent States

We will therefore define the *electron-hole* (E-H) *coherent states* on the Hilbert space $\mathcal{H}_\otimes = \mathcal{L}^2 \otimes \mathbb{C}^2$ as

$$|z \bowtie \beta\rangle = \frac{1}{\sqrt{1 + |\beta|^2}}|z\rangle \otimes |e\rangle + \frac{\beta^*}{\sqrt{1 + |\beta|^2}}|z^*\rangle \otimes |h\rangle \tag{3.6}$$

as well as the un-normalized variant

$$|z \bowtie \beta) = |z\rangle \otimes |e\rangle + \beta^*|z^*\rangle \otimes |h\rangle. \tag{3.7}$$

Our analysis will show that the E-H coherent states have theoretical properties as a complete set that are strongly analogous to the SGS coherent states. Although the dynamics are more complicated for E-H coherent states, the localisation properties are closer to SGS coherent states than those shown by product coherent states. Note that the E-H coherent states are no-longer product states yet we will show that we can still define a resolution of identity.

3.2.1 Expectation Values of Electron-Hole Coherent States

The expectation values of the phase space operators with respect to the E-H and for comparison the product coherent states are

$$\langle \hat{q} \rangle_{\bowtie} = q_0 \qquad\qquad \langle \hat{q} \rangle_{\otimes} = q_0 \qquad\qquad (3.8)$$

$$\langle \hat{p} \rangle_{\bowtie} = \frac{1 - |\beta|^2}{1 + |\beta|^2}\, p_0 \qquad \langle \hat{p} \rangle_{\otimes} = p_0. \qquad\qquad (3.9)$$

The expected values of the spin operators are

$$\langle \sigma_1 \rangle_{\bowtie} = \frac{2\,\mathrm{Re}(\beta)}{1 + |\beta|^2} \qquad \langle \sigma_1 \rangle_{\otimes} = \frac{2\,\mathrm{Re}(\beta \langle z | z^* \rangle)}{1 + |\beta|^2} \qquad\qquad (3.10)$$

$$\langle \sigma_2 \rangle_{\bowtie} = \frac{2\,\mathrm{Im}(\beta)}{1 + |\beta|^2} \qquad \langle \sigma_2 \rangle_{\otimes} = \frac{2\,\mathrm{Im}(\beta \langle z | z^* \rangle)}{1 + |\beta|^2} \qquad\qquad (3.11)$$

$$\langle \sigma_3 \rangle_{\bowtie} = \frac{1 - |\beta|^2}{1 + |\beta|^2} \qquad \langle \sigma_3 \rangle_{\otimes} = \frac{1 - |\beta|^2}{1 + |\beta|^2}. \qquad\qquad (3.12)$$

Though the values of $\langle \hat{q} \rangle$ and $\langle \sigma_3 \rangle$ are invariant, the form of $\langle \hat{p} \rangle_{\bowtie}$ suggests that for the E-H states we should instead consider what we will term the *pseudo-velocity* operator defined by $\hat{V} = \sigma_3 \hat{p}$. This operator takes into account the time reversed nature of the hole component and thus has the expectation value with respect to the E-H states

$$\langle \hat{V} \rangle_{\bowtie} = p_0. \qquad\qquad (3.13)$$

Thus the E-H states will be defined on a phase space spanned by position and pseudo-velocity rather than position and momentum. The E-H coherent states will also be parametrized by their central velocity V_0 (to avoid confusion when later also discussing physical velocities given by $v = p/m$, we will reserve the use of upper case V for the pseudo-velocity operator and expectation values, and lower case when referring to physical velocities).

The relative amplitudes of the components described by σ_3 remains unchanged between the states, as might be expected from its diagonal nature.

The expectation values of the off diagonal operators σ_1 and σ_2 mean that where as the product states sit on the Bloch sphere of radius 1, the same value with respect to the E-H states is

$$R^2 = \sum_{i=1}^{3} \langle z \bowtie \beta | \sigma_i | z \bowtie \beta \rangle^2 \leq 1. \tag{3.14}$$

Except in the case that $V_0 = 0$, the E-H coherent states no longer remain on the unit sphere. We can deform the sphere into an ellipsis of unit length in the σ_3 direction and radius $e^{-\lambda V_0^2}$ on the equator then

$$e^{\lambda V_0^2} \left[\langle \sigma_1 \rangle_{\bowtie}^2 + \langle \sigma_2 \rangle_{\bowtie}^2 \right] + \langle \sigma_3 \rangle_{\bowtie}^2 = 1. \tag{3.15}$$

Altogether the phase space on which the E-H coherent states will be set is the complex plane spanned by position and pseudo-velocity expectation values with the described ellipsoid attached at each point.

3.2.2 Minimum Uncertainty

It can also be shown that the E-H coherent states are minimum uncertainty states with respect to the operators $\hat{q}$ and the newly defined pseudo-velocity operator $\hat{V}$. The general standard uncertainty relation for two operators $\hat{A}$ and $\hat{B}$ with respect to a state $|\psi\rangle$ is given by the inequality

$$\text{Var}(\hat{A})_{|\psi\rangle} \, \text{Var}(\hat{B})_{|\psi\rangle} \geq \frac{1}{4} |\langle \psi | [\hat{A}, \hat{B}] | \psi \rangle|^2 \tag{3.16}$$

In the case of the operators $\hat{q}$ and $\hat{V}$ it is a simple calculation to show that with respect to the E-H coherent states the terms on the left are given by

$$\text{Var}(\hat{q})_{\bowtie} \equiv \text{Var}(\hat{q})_{|z\rangle} = \frac{\hbar}{2m\omega} \quad \text{and} \quad \text{Var}(\hat{V})_{\bowtie} \equiv \text{Var}(\hat{p})_{|z\rangle} = \frac{\hbar m\omega}{2} \tag{3.17}$$

analogous to the scalar SGS coherent states. But a direct calculation of the right hand side of equation (3.16), since $\langle [\hat{q}, \hat{V}] \rangle = i\hbar \langle \sigma_3 \rangle$, indicates that there is lower bound with respect to the E-H state of 0. This suggests we should modify the standard derivation. For this to work we write the variances as

$$\text{Var}(\hat{V}) \, \text{Var}(\hat{q}) = \langle (\hat{V} - V)^2 \rangle \langle (\hat{q} - Q)^2 \rangle = \langle (\hat{p} - \sigma_3 V)^2 \rangle \langle (\hat{q} - Q)^2 \rangle \tag{3.18}$$

where $Q = \langle \hat{q} \rangle$ and $V = \langle \hat{V} \rangle$. If we define the operators $\Delta P = \hat{p} - \sigma_3 V$ and $\Delta Q = \hat{q} - Q$ then

$$\langle \Delta P^2 \rangle \langle \Delta Q^2 \rangle = \langle \Delta P \psi | \Delta P \psi \rangle \langle \Delta Q \psi | \Delta Q \psi \rangle \geq |\langle \psi | \Delta P \Delta Q | \psi \rangle|^2. \tag{3.19}$$

For any complex number z we have $|z|^2 \geq (\text{Im}(z))^2$ and

$$\text{Im}[\langle \Delta P \Delta Q \rangle] = \frac{1}{2i} \langle [\Delta P, \Delta Q] \rangle = \frac{\hbar}{2} \tag{3.20}$$

from which the stricter uncertainty relation

$$\text{Var}(\hat{V})_{\bowtie} \text{Var}(\hat{q})_{\bowtie} \geq \frac{\hbar^2}{4} \tag{3.21}$$

follows.

Whilst the electron-hole coherent states satisfy the the uncertainty relationship on position-momentum phase space, they do not obey any analogous relation for the quasi-spin variables. Defining the analogous operator $\Delta \sigma_j = \sigma_j - \langle \sigma_j \rangle$ the uncertainty relation is given by $\sum_{j=1}^{3} \langle \Delta \sigma_j^2 \rangle \geq 2$. This lower bound is equivalent to the upper bound $\sum_{j=1}^{3} \langle \sigma_j \rangle^2 \leq 1$.

3.2.3 Overcompleteness & Resolution of Unity

It is straightforward to calculate the overlap of the permutations of the un-normalized E-H and product coherent states as follows

$$(z \otimes \beta | z' \otimes \beta') = (1 + \beta^* \beta') e^{z^* z'} \tag{3.22}$$

$$(z \bowtie \beta | z' \bowtie \beta') = e^{z^* z'} + \beta \beta'^* e^{zz'^*} \tag{3.23}$$

$$(z \bowtie \beta | z' \otimes \beta') = e^{z^* z'} + \beta \beta' e^{zz'} \tag{3.24}$$

$$(z \otimes \beta | z' \bowtie \beta') = e^{z^* z'} + \beta^* \beta'^* e^{z^* z'^*}. \tag{3.25}$$

This allows for various definitions of a resolution of unity. In terms of the normalized and un-normalized product coherent state basis

$$\mathbb{I} = \frac{2}{\pi^2} \int d^2 z \, d^2 \beta \, \frac{1}{(1 + |\beta|^2)^2} |z \otimes \beta\rangle \langle z \otimes \beta| \tag{3.26}$$

$$= \frac{2}{\pi^2} \int d^2 z \, d^2 \beta \, \frac{e^{-|z|^2}}{(1 + |\beta|^2)^3} |z \otimes \beta)(z \otimes \beta| \tag{3.27}$$

which follows from the correspond resolutions in terms of $SU(2)$ and SGS coherent states. For the E-H coherent states, similar normalized and un-normalized forms of resolution exists

$$\mathbb{I} = \frac{2}{\pi^2} \int d^2 z \, d^2 \beta \, \frac{1}{(1 + |\beta|^2)^2} |z \bowtie \beta\rangle \langle z \bowtie \beta| \tag{3.28}$$

$$= \frac{2}{\pi^2} \int d^2 z \, d^2 \beta \, \frac{e^{-|z|^2}}{(1 + |\beta|^2)^3} |z \bowtie \beta)(z \bowtie \beta| \tag{3.29}$$

which can be seen by first integrating over β, leaving the standard resolution in terms of SGS coherent states.

3.2.4 Electron-Hole Coherent State Representation

Using the resolution of unity we can represent a state $|\Psi\rangle \in \mathcal{H}_\otimes$ as the function

$$\langle z \bowtie \beta | \Psi \rangle = \Psi(z, z^*, \beta, \beta^*). \tag{3.30}$$

The electron and hole components of $|\Psi\rangle$ then map to the functions

$$\Psi(z, z^*, \beta, \beta^*) = \frac{e^{-|z|^2/2}}{1 + |\beta|^2} \left(u_{|\Psi\rangle}(z^*) + \beta v_{|\Psi\rangle}(z) \right) \tag{3.31}$$

where $u_{|\Psi\rangle}(z^*)$ is analytic in z^* and $v_{|\Psi\rangle}(z)$ is analytic in z. For the purposes of representing the action of operators in this representation it will be convenient to instead use the function

$$f_{|\Psi\rangle}(z, z^*, \beta) = u_{|\Psi\rangle}(z^*) + \beta v_{|\Psi\rangle}(z). \tag{3.32}$$

Acting on the un-normalized variant of the E-H coherent states the quasi-spin, raising and lowering operators can be represented in terms of differential operators by

$$\hat{a}|z \bowtie \beta) = \left[z \left(1 - \beta^* \frac{\partial}{\partial \beta^*} \right) + z^* \beta^* \frac{\partial}{\partial \beta^*} \right] |z \bowtie \beta) \tag{3.33}$$

$$\hat{a}^\dagger |z \bowtie \beta) = \left[\frac{\partial}{\partial z} + \frac{\partial}{\partial z^*} \right] |z \bowtie \beta) \tag{3.34}$$

$$\sigma_1 |z \bowtie \beta) = \left[\beta^* \left(1 - \beta^* \frac{\partial}{\partial \beta^*} \right) + \frac{\partial}{\partial \beta^*} \right] |z^* \bowtie \beta) \tag{3.35}$$

$$= \left[\beta^* \left(1 - \beta \frac{\partial}{\partial \beta} \right) + \frac{\partial}{\partial \beta} \right] |z^* \bowtie \beta^*) \tag{3.36}$$

$$\sigma_2 |z \bowtie \beta) = \left[-i\beta^* \left(1 - \beta^* \frac{\partial}{\partial \beta^*} \right) + i \frac{\partial}{\partial \beta^*} \right] |z^* \bowtie \beta) \tag{3.37}$$

$$= \left[-i\beta^* \left(1 - \beta \frac{\partial}{\partial \beta} \right) + i \frac{\partial}{\partial \beta} \right] |z^* \bowtie \beta^*) \tag{3.38}$$

$$\sigma_3 |z \bowtie \beta) = \left[\left(1 - \beta^* \frac{\partial}{\partial \beta^*} \right) - \beta^* \frac{\partial}{\partial \beta^*} \right] |z \bowtie \beta). \tag{3.39}$$

where complex parameters and their conjugates behave as independent variables. The differential operators $(1 - \beta^* \partial / \partial \beta^*)$ and $\beta^* \partial / \partial \beta^*$ are effectively projectors onto the electron and hole components respectively. We can then readily extend these definitions to functions of the raising and lowering operators using

$$\hat{a}^n |z \bowtie \beta) = \left[z^n \left(1 - \beta^* \frac{\partial}{\partial \beta^*} \right) + z^{*n} \beta^* \frac{\partial}{\partial \beta^*} \right] |z \bowtie \beta) \tag{3.40}$$

and similarly

$$\hat{a}^{\dagger n}|z \bowtie \beta) = \left[\frac{\partial^n}{\partial z^n} + \frac{\partial^n}{\partial z^{*n}}\right]|z \bowtie \beta). \tag{3.41}$$

If we consider a scalar state, represented using the Bargmann representation as $f(z^*) = \langle z|\psi\rangle e^{|z|^2/2}$ (see Equation (2.36)) the time-dependent Schrödinger equation can be written as

$$i\frac{\partial}{\partial t}f(z^*) = \left[\mathcal{V}(z^*) - \frac{\omega\hbar}{4}\left(z^{*2} + \frac{\partial^2}{\partial z^{*2}} - 1 - 2z^*\frac{\partial}{\partial z^*}\right)\right]f(z^*) \tag{3.42}$$

where $\mathcal{V}(z^*)$ is a differential operator dependent on the form of the potential $V(q)$.

In a similar manner using the E-H coherent state representation; the time dependent BdG equations may then be written as non-local partial differential equations

$$
\begin{aligned}
i\frac{\partial}{\partial t}f_{|\Psi\rangle}(z, z^*, \beta) = &-\frac{\omega\hbar}{4}\left(1 - \beta^*\frac{\partial}{\partial\beta^*}\right)\left(z^{*2} + \frac{\partial^2}{\partial z^{*2}} - 1 - 2z^*\frac{\partial}{\partial z^*}\right)f_{|\Psi\rangle}(z, z^*, \beta) \\
&+ \frac{\omega\hbar}{4}\beta\frac{\partial}{\partial\beta}\left(z^2 + \frac{\partial^2}{\partial z^2} - 1 - 2z\frac{\partial}{\partial z}\right)f_{|\Psi\rangle}(z, z^*, \beta) \\
&- \mu\left(1 - 2\beta\frac{\partial}{\partial\beta}\right)f_{|\Psi\rangle}(z, z^*, \beta) \\
&+ \Delta_0\left(\beta\left(1 - \beta\frac{\partial}{\partial\beta}\right) + \frac{\partial}{\partial\beta}\right)f_{|\Psi\rangle}(z^*, z, \beta) \tag{3.43}
\end{aligned}
$$

when $\Delta(q) = \Delta_0$ is real and constant. The non-local nature can be seen from the exchange of the arguments $z \to z^*$ in the last term. This representation has similarities to the analytic Bargmann representation, $f_{|\Psi\rangle}(z, z^*, \beta)$ is not analytic in z though.

3.3 The Group Theoretic Approach to Electron-Hole Coherent States

In section 3.1 it was shown that the product coherent states can be produced by the action of a group element of $H_3(\mathbb{R}) \times SU(2)$ acting on the reference state $|0\rangle \otimes |+\rangle \in \mathcal{L}^2 \otimes \mathbb{C}^2$. The repeated application of the group element produces additional product coherent states up to a phase factor. There is no obvious group which has an action on the E-H coherent states that produces the analogous transformations via a linear representation in Hilbert space. It can be shown though that there is a (what will we term)

quasi-linear action of the product group that will lead to the same behaviour for E-H coherent states.

We first define the anti-unitary time-reversal operator $\hat{\tau}$ with the action on an arbitrary state in $\mathcal{H}_\otimes$, represented in the number basis as

$$\hat{\tau}\left(\sum_{n=0}^{\infty} A_{n,+}|n\rangle \otimes |+\rangle + A_{n,-}|n\rangle \otimes |-\rangle\right) = \sum_{n=0}^{\infty} A_{n,+}^*|n\rangle \otimes |+\rangle + A_{n,-}^*|n\rangle \otimes |-\rangle. \tag{3.44}$$

It follows that acting with $\hat{\tau}$ on a product coherent state produces

$$\hat{\tau}|z \otimes \beta\rangle = |z^* \otimes \beta^*\rangle. \tag{3.45}$$

We will therefore define the operator

$$\hat{\mathcal{Z}} = \hat{\mathbb{I}}_\infty \otimes |+\rangle\langle+| + \hat{\tau}(\hat{\mathbb{I}}_\infty \otimes |-\rangle\langle-|) \equiv \begin{pmatrix} 1 & 0 \\ 0 & \hat{\tau} \end{pmatrix} \tag{3.46}$$

where $\hat{\mathbb{I}}$ is the identity operator. This operator is neither linear or anti-linear as it behaves linearly on one subspace but anti-linearly on the other. From the definition it is also clear that $\hat{\mathcal{Z}}$ is its own inverse

$$\hat{\mathcal{Z}}^2 = \hat{\mathbb{I}} \quad \Rightarrow \quad \hat{\mathcal{Z}}^{-1} = \hat{\mathcal{Z}}. \tag{3.47}$$

The norm of a general product state $|\psi\rangle \in \mathcal{L}^2 \otimes \mathbb{C}^2$ is invariant under the action of $\hat{\mathcal{Z}}$

$$\langle \mathcal{Z}\psi|\mathcal{Z}\psi\rangle = \langle\psi|\psi\rangle. \tag{3.48}$$

This is generally not true for the inner product

$$\langle \mathcal{Z}\psi_1|\mathcal{Z}\psi_2\rangle \neq \langle\psi_1|\psi_2\rangle. \tag{3.49}$$

so $\hat{\mathcal{Z}}$ cannot be considered a unitary operator. There is also no way to define a general adjoint of $\hat{\mathcal{Z}}$. Such an adjoint would need to satisfy the condition

$$|\langle\psi_1|\mathcal{Z}\psi_2\rangle| = |\langle\mathcal{Z}^\dagger\psi_1|\psi_2\rangle|. \tag{3.50}$$

This means the use of $\hat{\mathcal{Z}}$ for further analytic purposes is limited.

We can then use $\hat{\mathcal{Z}}$ to transform product coherent states to E-H coherent states and vice-versa

$$\hat{\mathcal{Z}}|z \otimes \beta\rangle = |z \bowtie \beta\rangle \quad \Leftrightarrow \quad \hat{\mathcal{Z}}|z \bowtie \beta\rangle = |z \otimes \beta\rangle. \tag{3.51}$$

This implies that the correct group operation that produces and translates E-H coherent states is given by

$$|z \bowtie \beta\rangle = \hat{\mathcal{Z}}[D(z,0) \otimes U(\beta)]\hat{\mathcal{Z}}(|0\rangle \otimes |+\rangle). \tag{3.52}$$

44

3.4 Electron-Hole Q-Function

The definition of the scalar Q-function given in section 2.2 can be extended to the product coherent states as simply the expectation with respect to the product coherent

$$Q_\otimes(z, \beta) = \langle z \otimes \beta | \hat{\rho} | z \otimes \beta \rangle \tag{3.53}$$

where the density operator now describes a state with electron and hole components $|\psi\rangle \otimes |e\rangle + |\phi\rangle \otimes |h\rangle$. The analogous symbol of an operator $\hat{A}$ is

$$\mathcal{A}_\otimes(z, z^*, \beta, \beta^*) = \langle z \otimes \beta | \hat{A} | z \otimes \beta \rangle. \tag{3.54}$$

A natural definition then also carries over to the E-H states

$$Q_\bowtie(z, \beta) = \langle z \bowtie \beta | \hat{\rho} | z \bowtie \beta \rangle \tag{3.55}$$

but we will show that this Q-function does not retain all the information about the original density matrix. This can be shown if the density operator is expanded in the Fock basis. Considering a general two level state $|\Psi\rangle = |e\rangle \otimes |\psi\rangle + |h\rangle \otimes |\phi\rangle$ and product coherent state $|z \otimes \beta\rangle = (|e\rangle + \beta |h\rangle) \otimes |z\rangle$ (we omit the normalization without any loss to the argument) the components of the state can be expanded in the Fock basis as

$$|\psi\rangle = \sum_n a_n |n\rangle \qquad \text{and} \qquad |\phi\rangle = \sum_m a_m |m\rangle. \tag{3.56}$$

Then the expanded product Q-function is in this basis contains the terms

$$(z \otimes \beta |\Psi\rangle\langle\Psi| z \otimes \beta) = \sum_{m,n} \frac{z^{*m} z^n}{\sqrt{n! m!}} \left[a_m a_n^* + \beta a_n b_m^* + \beta^* b_m a_n^* + |\beta|^2 b_m b_n^* \right]. \tag{3.57}$$

Assigning the numbers n and m to elements of a density matrix the original state can be reliably reproduced.

Now considering the Q-function formed from the electron-hole coherent state in the same basis gives

$$\begin{aligned}
(z \bowtie \beta |\psi\rangle\langle\psi| z \bowtie \beta) = &\sum_{m,n} \frac{a_m a_n^* z^{*m} z^n}{\sqrt{m! n!}} + \beta^* \sum_{m,n} \frac{a_m b_n^* z^{*(m+n)}}{\sqrt{m! n!}} \\
&+ \beta \sum_{m,n} \frac{b_m a_n^* z^{(m+n)}}{\sqrt{m! n!}} + |\beta|^2 \sum_{m,n} \frac{b_m b_n^* z^m z^{*n}}{\sqrt{m! n!}}. \tag{3.58}
\end{aligned}$$

Each term cannot then be discretely assigned to a position in the density matrix due to the $z^{(m+n)}$ terms information is lost about the original state.

In general the E-H symbol for an operator $\hat{A}$

$$\mathcal{A}_\bowtie(z, z^*, \beta, \beta^*) = \langle z \bowtie \beta | \hat{A} | z \bowtie \beta \rangle \tag{3.59}$$

does not have a one-to-one correspondence between the symbol and operators. As a simple example of how this fails consider the expectation value with respect to the operator $\sigma_1 \hat{a}^\dagger \hat{a}$

$$\langle \sigma_1 \hat{a}^\dagger \hat{a} \rangle_\bowtie = \frac{1}{N_+} \left[\beta^* z^{*2} \langle z | z^* \rangle + \beta z^2 \langle z^* | z \rangle \right] \equiv \langle \sigma_1 \hat{a}^2 \rangle_\bowtie \equiv \langle \sigma_1 \hat{a}^{\dagger 2} \rangle_\bowtie. \tag{3.60}$$

Whether some properties of the density matrix can be used to reliably recreate the original state requires further study.

In the dynamical case, given that the initial $(t = 0)$ product state Q-function consists of the terms

$$Q_\otimes(z, \beta) = |\langle z | \psi \rangle|^2 + \beta^* \langle z | \phi \rangle \langle \psi | z \rangle + \beta \langle z | \psi \rangle \langle \phi | z \rangle + |\beta|^2 |\langle z | \phi \rangle|^2. \tag{3.61}$$

The infinitesimal time dependence of the Q-function can be found using the density operator form of the Heisenberg equation

$$\frac{d}{dt} Q_\otimes(z, \beta) = \langle z \otimes \beta | \frac{i}{\hbar} [\hat{\rho}, \hat{\mathcal{H}}] | z \otimes \beta \rangle. \tag{3.62}$$

If we consider a BdG Hamiltonian for a real and constant $\Delta(\hat{q}) = \Delta_0$,

$$\hat{\mathcal{H}}_{\text{BdG}} = \sigma_3 \left(\frac{\hat{p}^2}{2m} - \mu \right) + \sigma_1 \Delta_0 \tag{3.63}$$

this gives

$$\begin{aligned}
\frac{d}{dt} Q_\otimes(z, \beta) = \frac{i}{\hbar} \Big\{ & \left[\mathcal{H}_0(z) - \mathcal{H}_0^*(z) + \Delta_0(\beta - \beta^*) \right] \langle z | \psi \rangle \langle \psi | z \rangle \\
& - \left[(\mathcal{H}_0(z) - \mathcal{H}_0^*(z)) |\beta|^2 + \Delta_0(\beta - \beta^*) \right] \langle z | \phi \rangle \langle \phi | z \rangle \\
& - \left[(\mathcal{H}_0(z) + \mathcal{H}_0^*(z)) \beta - \Delta_0(1 - |\beta|^2) \right] \langle z | \psi \rangle \langle \phi | z \rangle \\
& + \left[(\mathcal{H}_0(z) + \mathcal{H}_0^*(z)) \beta^* - \Delta_0(1 - |\beta|^2) \right] \langle z | \phi \rangle \langle \psi | z \rangle \Big\} \tag{3.64}
\end{aligned}$$

where $\mathcal{H}_0(z)$ is the differential form of the Hamiltonian

$$\mathcal{H}_0(z) = -\frac{\hbar \omega}{4} \left(\frac{\partial^2}{\partial z^2} - 2z \frac{\partial}{\partial z} + z^2 - 1 \right) - \mu. \tag{3.65}$$

Using the differential projection operators onto the terms in the Q-function the time dependence can then be expressed in the form of a Fokker-Planck transport equation; as a differential operator D acting on the original Q-function

$$\frac{d}{dt} Q_\otimes(z, \beta) = D(z, z^*, \beta, \beta^*) Q_\otimes(z, \beta). \tag{3.66}$$

This property does not hold for Q-functions formed from the E-H coherent states. The terms produced by the Q-function with respect to the E-H coherent states are

$$Q_{\bowtie}(z, \beta) = |\langle z|\psi\rangle|^2 + \beta^*\langle z|\psi\rangle\langle\phi|z^*\rangle + \beta\langle z^*|\phi\rangle\langle\psi|z\rangle + |\beta|^2|\langle z^*|\phi\rangle|^2. \quad (3.67)$$

Deriving the infinitesimal time dependence the terms generated by the free motion under $\hat{\mathcal{H}}_0$ are contained in the original Q-function

$$2i\,\mathrm{Im}\left\{\langle z|\psi\rangle\langle\psi|\mathcal{H}_0|z\rangle - \beta^*\langle z|\psi\rangle\langle\phi|\mathcal{H}_0|z^*\rangle + \beta\langle z^*|\phi\rangle\langle\psi|\mathcal{H}_0|z\rangle - |\beta|^2\langle z^*|\phi\rangle\langle\phi|\mathcal{H}_0|z^*\rangle\right\}. \quad (3.68)$$

But the off-diagonal terms in the BdG Hamiltonian related to superconducting states produces additional terms

$$2i\,\mathrm{Im}\left\{\beta^*\langle z|\psi\rangle\langle\psi|\Delta(\hat{q})|z^*\rangle + \langle z|\psi\rangle\langle\phi|\Delta(\hat{q})|z\rangle \right.$$
$$\left. + \beta\langle z^*|\phi\rangle\langle\phi|\Delta(\hat{q})|z\rangle + |\beta|^2\langle z^*|\phi\rangle\langle\psi|\Delta(\hat{q})|z^*\rangle\right\}. \quad (3.69)$$

The time evolution cannot therefore be expressed as an operator acting on the original Q-function.

For practical purposes these limitations of the E-H Q-function can be somewhat overcome by utilizing the projection operators defined as

$$\hat{\mathcal{P}}_e = \begin{pmatrix} 1 & 0 \\ 0 & 0 \end{pmatrix} \equiv |e\rangle\langle e| \quad \text{and} \quad \hat{\mathcal{P}}_h = \begin{pmatrix} 0 & 0 \\ 0 & 1 \end{pmatrix} \equiv |h\rangle\langle h| \quad (3.70)$$

which project onto the electron or hole components of the spinor. The full Q-function contains terms of the form (product or E-H)

$$Q(z) = Q^{ee}(z) + |\beta|^2 Q^{hh}(z) + \beta Q^{eh}(z) + \beta^* Q^{he}(z) \quad (3.71)$$

labelled by the contributing components. The projection onto the elements of the Q-function using the projection operators as

$$Q^{ee}(z) = \langle\hat{\mathcal{P}}_e\hat{\rho}\hat{\mathcal{P}}_e\rangle/\langle\hat{\mathcal{P}}_e\rangle \quad (3.72)$$

and

$$Q^{hh}(z) = \langle\hat{\mathcal{P}}_h\rho\hat{\mathcal{P}}_h\rangle/\langle\hat{\mathcal{P}}_h\rangle. \quad (3.73)$$

Consideration can be given to the meaning of the diagonal terms Q_{eh} and Q_{he} which describe the interactions between electron and hole components. These additional terms are responsible for the inability to reconstruct the time dependent Q-function. We only consider the projection onto the quasi-spin components. Any β dependence can also be traced out of $Q_{\bowtie}(z)$ and

$Q_\otimes(z)$ by integrating over β, arriving at what we will refer to as the reduced Q-function

$$Q^{\texttt{red}}(z) = \int d\beta\, Q(z,\beta) = Q^{ee}(z) + Q^{hh}(z). \tag{3.74}$$

This isolates the non-interfering sum of the electron and hole contributions.

Overall Husimi functions based on E-H coherent states do not have the same mathematical properties shared by SGS and product coherent states. This means they are less useful for analytic purposes, but will be useful for representing the details of the trajectories of the electron and hole components on phase space. The use of E-H and product Q-functions will be demonstrated in chapter 4.

3.5 Entanglement Measure for Electron-Hole Coherent States

It was noted earlier in this chapter that the E-H coherent states are (except for specific cases) entangled i.e. not product states. Here we consider a measure of the entanglement of an E-H coherent state. In general a pure state on $|\Psi\rangle \in \mathcal{H}_\otimes$ is called separable if it can be written as $|\Psi\rangle = |\phi\rangle \otimes |\theta\rangle$ where $|\phi\rangle \in \mathcal{L}^2$ and $|\theta\rangle \in \mathbb{C}^2$, and otherwise entangled. By definition the product coherent states are separable. The E-H coherent states are clearly separable in the special cases of $\beta = 0, \infty$ (as noted these values define states consisting of only an electron or hole component), and also in the case that $V_0 = 0$ where the electron component and conjugate hole component completely overlap independent of the value of β. Otherwise the E-H coherent states are entangled and we would like a measure of this entanglement in terms of the amplitude of the electron and hole components

We first consider how the expectation values of the spin operators can measure the amount of mixing of states in $\mathbb{C}^2$. Pure states $|\theta\rangle \in \mathbb{C}^2$ satisfy $\sum_{i=1}^{3} \langle\theta|\sigma_i|\theta\rangle = 1$ and mixed states are described by the density matrix

$$\hat{\rho} = p_1|\theta_1\rangle\langle\theta_1| + p_2|\theta_2\rangle\langle\theta_2| \tag{3.75}$$

where $p_1, p_2 \geq 0$ and satisfy $p_1 + p_2 = 1$. The expectation values of the quasi-spin operators σ_i are

$$\mathrm{tr}(\hat{\rho}\sigma_i) = \sum_{j=1}^{2} p_j \langle\theta_j|\sigma_i|\theta_j\rangle. \tag{3.76}$$

Assuming that the components $|\theta_1\rangle$ and $|\theta_2\rangle$ are orthogonal as $\hat{\rho}$ is hermitian, then the state is pure if $\hat{\rho}^2 = \hat{\rho}$, either when $p_1 = 1$ or $p_1 = 0$. Defining the quantity

$$R^2 = \sum_{i=1}^{3} \mathrm{tr}(\hat{\rho}\sigma_i)^2, \tag{3.77}$$

since R^2 is rotation invariant it can be assumed that $|\theta_1\rangle = |+\rangle$ and $|\theta_2\rangle = |-\rangle$ and thus R^2 takes the values

$$R^2 = (p_1 - p_2)^2 = (1 - 2p_1)^2. \tag{3.78}$$

This means that $R^2 = 1$ only when the state is pure. Note that $R^2 < 1$ for the values of $0 < p_1 < 1$. The value of R^2 is also minimized at 0 when $p_1 = 1/2$. This measure of entanglement can be used for states on the product space $\mathcal{H}_\otimes$ using the reduced density matrix

$$\hat{\rho}_{\mathbf{red}} = \mathrm{tr}_{\mathcal{L}^2}(|\Psi\rangle\langle\Psi|) \tag{3.79}$$

the trace taken over $\mathcal{L}^2$ such that $\hat{\rho}_{\mathbf{red}}$ is an operator in $\mathbb{C}^2$. $|\Psi\rangle$ is considered separable if and only if $\hat{\rho}_{\mathbf{red}} = \hat{\rho}_{\mathbf{red}}^2$ describes a pure state. R^2 applied to $\hat{\rho}_{\mathbf{red}}$ can be used as a measure of entanglement with the same measure, zero entanglement at $R^2 = 1$ and maximal entanglement when $R^2 = 0$. E-H coherent states can take values in the range $e^{-V_0^2} \leq R^2 \leq 1$. For a state with non zero momentum the lower bound is only satisfied for equal superpositions of electron and hole components ($|\beta|^2 = 1$) and the upper bounds when the state has only an electron or hole component when $\beta = 0, \infty$.

Chapter 4

Andreev Reflection & Stationary States of a Homogeneous Superconductors

In later chapters we will analyse the dynamics of wave packets in both a homogeneous superconductor, and at a discontinuous normal-superconducting boundary. In both situations the wave packets can be constructed from a superposition of the stationary solutions of the BdG equations. In this chapter we will give a detailed account of these stationary solutions.

The stationary solutions at an N-S boundary are the *scattering state* wave functions, the wave functions generated by the various scattering processes of an electron or hole incident on the boundary. We will later use the scattering states derived here as an orthogonal basis with which to find the time dependence of Andreev reflected states from a discontinuous boundary in chapter 6. We will also derive the stationary states of the homogeneous superconductor from which we will construct Gaussian wave packets inside a homogeneous superconductor in chapter 5.

Using the E-H Q-function derived in section 3.4 we will also consider the phase space representation of both the scattering states and the *Andreev States*, the excitation eigenstates that occupy the normal region in continuous S-N-S system as one might find in the intermediate state of a superconductor.

4.1 Stationary States of a Homogeneous Superconductor

We will first, as the simplest example, consider the stationary states of a 1-dimensional homogeneous superconductor. This is described by a spatially independent band gap labelled $\Delta(q) = \Delta_0$, which is also set as both positive and real. We also consider a system with no external potentials or magnetic fields (such that $U(q) = 0$ and $\boldsymbol{A}(q) = 0$). In this case the coupled time independent BdG equations 2.14 and 2.15 can be compactly written in terms of operators acting on a spinor as

$$\hat{\mathcal{H}}_{\text{BdG}}\boldsymbol{\Psi}(q) = \left[\sigma_3\hat{\mathcal{H}}_0 + \sigma_1\Delta(q)\right]\boldsymbol{\Psi}(q) = E\boldsymbol{\Psi}(q) \tag{4.1}$$

where $\boldsymbol{\Psi}(q)$ is a two component spinor wave function (spinors will be denoted from here on in bold-type) which in the position representation has electron and hole quasi-particle wave functions as components

$$\boldsymbol{\Psi}(q) = \begin{pmatrix} \psi^e(q) \\ \psi^h(q) \end{pmatrix} \tag{4.2}$$

(upper indices from here on will refer to the spinor component). The σ_i are the standard Pauli matrices

$$\sigma_1 = \begin{pmatrix} 0 & 1 \\ 1 & 0 \end{pmatrix} \quad \sigma_2 = \begin{pmatrix} 0 & -i \\ i & 0 \end{pmatrix} \quad \sigma_3 = \begin{pmatrix} 1 & 0 \\ 0 & -1 \end{pmatrix} \tag{4.3}$$

and $\hat{\mathcal{H}}_0$ is the free particle Hamiltonian, given in the position basis as

$$\hat{\mathcal{H}}_0 = -\frac{\hbar^2}{2m}\frac{d^2}{dq^2} - \mu \tag{4.4}$$

which measures energies relative to μ. We've seen in section 2.1.3 that in the normal conductor ($\Delta_0 = 0$), the BdG equations decouple. If we take as an ansatz the spinor

$$\boldsymbol{\Psi}(q) = \begin{pmatrix} \tilde{u} \\ \tilde{v} \end{pmatrix} \exp\left(\frac{i}{\hbar}q\alpha\right) \tag{4.5}$$

which inserted into 4.1 (with $\Delta_0 = 0$) gives us the stationary solutions

$$\begin{pmatrix} 1 \\ 0 \end{pmatrix} \exp\left(\pm\frac{i}{\hbar}q\alpha_+(E)\right) \quad \text{and} \quad \begin{pmatrix} 0 \\ 1 \end{pmatrix} \exp\left(\pm\frac{i}{\hbar}q\alpha_-(E)\right). \tag{4.6}$$

Here

$$\alpha_\pm(E) = \sqrt{2m(\mu \pm E)}. \tag{4.7}$$

The solutions $\pm\alpha_+(E)$ represent electron quasi particles with energy $+E$ relative to μ, travelling in the positive/negative q direction respectively.

The $\pm\alpha_-(E)$ solutions represent the hole quasi-particles with energy $-E$ relative to μ, but travelling with velocity anti-parallel to their momenta, hence propagating in the negative/positive direction respectively.

In a superconducting region (i.e. $\Delta_0 > 0$) the solutions to the coupled equations require a little more work, but as long as $\Delta(q)$ is homogeneous the same ansatz can be used. Firstly considering states with positive energies above the band gap ($E > \Delta_0$) the four stationary solutions are

$$\begin{pmatrix} \tilde{u}(E) \\ \tilde{v}(E) \end{pmatrix} \exp\left[\pm\frac{i}{\hbar}q\kappa_+(E)\right] \quad \text{and} \quad \begin{pmatrix} \tilde{v}(E) \\ \tilde{u}(E) \end{pmatrix} \exp\left[\pm\frac{i}{\hbar}q\kappa_-(E)\right]. \tag{4.8}$$

The energy dependent spinor amplitudes are given by

$$\tilde{u}(E) = \left[\frac{1}{2}\left(1 + \frac{1}{E}\sqrt{E^2 - \Delta_0^2}\right)\right]^{\frac{1}{2}} \tag{4.9}$$

and

$$\tilde{v}(E) = \left[\frac{1}{2}\left(1 - \frac{1}{E}\sqrt{E^2 - \Delta_0^2}\right)\right]^{\frac{1}{2}} \tag{4.10}$$

with momenta

$$\kappa_\pm(E) = \left[2m(\mu \pm \sqrt{E^2 - \Delta_0^2})\right]^{1/2}. \tag{4.11}$$

These solutions are position representations of the Bogoliubov quasi-particle operators $\hat{\gamma}_{k0}^\dagger = u_k^*\hat{c}_{k\uparrow}^\dagger - v_k^*\hat{c}_{-k\downarrow}$ where $\hat{c}_{k\uparrow}^\dagger$ creates an electron at $\boldsymbol{k}$ and $\hat{c}_{-k\downarrow}$ destroys an electron below μ, creating a hole at $\boldsymbol{k}$.

For positive energies, the relative amplitudes of $\tilde{u}$ and $\tilde{v}$ mean that the $\pm\kappa_+$ solutions are predominantly *electron-like* superpositions and similarly $\pm\kappa_-$ are predominantly *hole-like*. Only for states on the band gap ($|E| = \Delta_0$) are the states equal superpositions of electron and hole components.

The BdG equations also require solutions for negative energies relative to μ ($E < -\Delta_0$), for which the solutions are given by

$$\begin{pmatrix} \tilde{v}(E) \\ -\tilde{u}(E) \end{pmatrix} \exp\left[\pm\frac{i}{\hbar}q\kappa_+(E)\right] \quad \text{and} \quad \begin{pmatrix} \tilde{u}(E) \\ -\tilde{v}(E) \end{pmatrix} \exp\left[\pm\frac{i}{\hbar}q\kappa_-(E)\right]. \tag{4.12}$$

These solutions correspondingly invert the relative amplitudes of the components, with an additional phase shift applied to the hole component.

We will further consider the behaviour of these stationary states in section 5.1 with relation to the BdG dispersion relation.
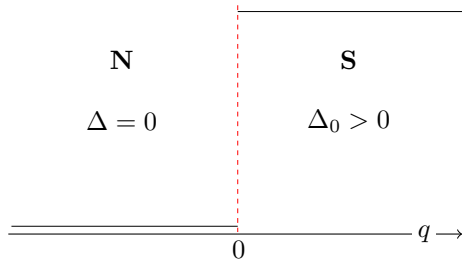
Figure 4.1: The one dimensional Normal-Superconducting boundary model. In the normal region $\Delta(q) = 0$ for $q < 0$ and the superconducting region $\Delta(q) = \Delta_0$ for $q > 0$. We consider electron or holes incident from the normal region on the left.

4.2 Discontinuous Normal-Superconducting Interface Scattering States

We now consider the stationary scattering states created by a electron (or hole) incident on a normal superconducting boundary with energies $|E| < \Delta_0$, which are then both specular and Andreev reflected as well a penetrating a finite distance into the superconducting region. We first consider a discontinuous N-S interface as shown in Figure 4.1, described by the Heaviside step-function $\Delta(q) = \Delta_0 \theta(q)$. μ is also taken as homogeneous across the interface. The form of the coupled BdG equations means that this is one system for which a full set of analytic solutions can be found (without any WKB type approximation as described in section 2.1.4). We will consider more general N-S interfaces in the next section but will be required to utilize numerical techniques.

Many of the solutions found in this section can also be found in work by Blonder, Tinkham and Klapwijk [30] with reference to current across a N-S boundary. We will only be considering the scattering process at energies $|E| < \Delta_0$, but this paper goes into further detail of the additional scattering processes that occur at energies outside the band gap.

The solutions in the normal and superconducting regions either side of the boundary will be considered separately. In the normal region the general solution is a superposition of incident and outgoing electron and hole states as given by equations 4.6. This can be written in spinor notation as

$$\boldsymbol{\Psi}_N(q) = \frac{1}{\sqrt{\alpha_+(E)}} \begin{pmatrix} 1 \\ 0 \end{pmatrix} \left[A_I^e \exp\left(\frac{iq}{\hbar} \alpha_+(E) \right) + A_R^e \exp\left(-\frac{iq}{\hbar} \alpha_+(E) \right) \right]$$
$$+ \frac{1}{\sqrt{\alpha_-(E)}} \begin{pmatrix} 0 \\ 1 \end{pmatrix} \left[A_R^h \exp\left(\frac{iq}{\hbar} \alpha_-(E) \right) + A_I^h \exp\left(-\frac{iq}{\hbar} \alpha_-(E) \right) \right].$$

$$(4.13)$$

In this notation the amplitude superscripts again identify electron or hole spinor components, and the subscript whether the state is incident (I) onto

or reflected (R) from the boundary. Again note that hole states are defined as having negative velocities relative to their momenta (also see the dispersion relation, derived in section 5.1), and if $E = 0$ the incident and reflected states have the same momenta. The difference in momenta between reflected electron and hole components when $E \neq 0$ of the order $2E/\mu$. The leading $1/\sqrt{\alpha_\pm(E)}$ terms normalize the current flux so that

$$j_{e,h} = \frac{\hbar}{m}\left(|A_R^{e,h}|^2 - |A_I^{e,h}|^2\right) \tag{4.14}$$

is the flux carried by the electron/hole component respectively. This choice of normalization also ensures that the scattering matrix will be unitary.

In the superconducting region, although for energies $|E| > \Delta_0$ stationary states can be found as given by equations 4.8 and 4.12, propagating states with energies inside the band-gap cannot exist. Consequently the solutions to the BdG equations inside the band gap are

$$\begin{pmatrix} \nu(E) \\ \nu^*(E) \end{pmatrix} \exp\left(\pm\frac{i}{\hbar}q\kappa_+(E)\right) \quad \text{and} \quad \begin{pmatrix} \nu^*(E) \\ \nu(E) \end{pmatrix} \exp\left(\pm\frac{i}{\hbar}q\kappa_-(E)\right). \tag{4.15}$$

The energy dependent amplitudes are complex continuations of the amplitudes above the band gap given by

$$\nu(E) = \left[\frac{1}{2}\left(1 + \frac{i}{E}\sqrt{\Delta_0^2 - E^2}\right)\right]^{\frac{1}{2}} \tag{4.16}$$

and similarly the momentum term is now also complex

$$\kappa_\pm(E) = \left[2m\left(\mu \pm i\sqrt{\Delta_0^2 - E^2}\right)\right]^{1/2}. \tag{4.17}$$

The (small) imaginary part of $\kappa_\pm$ means that these solutions now correspond to both exponentially decaying ($\pm\kappa_\pm$) and exponentially growing ($\mp\kappa_\pm$) solutions for positive q. For this N-S interface model where the superconducting region is effectively infinitely long only the decaying solutions are physically applicable.

The typical decay length-scale of the decaying solution is given by

$$L(E) = \frac{\hbar v_{\text{F}}}{2\Delta}\left[1 - \left(\frac{E}{\Delta}\right)^2\right]^{\frac{1}{2}} \tag{4.18}$$

although it should be noted that this decay length diverges when $|E| = \Delta_0$, for states on the band gap.

Therefore for energies $|E| < \Delta_0$ the allowed general solution in the superconducting region is

$$\boldsymbol{\Psi}_S(q) = \frac{F}{\sqrt{\kappa_+(E)}} \begin{pmatrix} \nu(E) \\ \nu^*(E) \end{pmatrix} \exp\left(\frac{iq}{\hbar}\kappa_+(E)\right) + \frac{G}{\sqrt{\kappa_-(E)}} \begin{pmatrix} \nu^*(E) \\ \nu(E) \end{pmatrix} \exp\left(-\frac{iq}{\hbar}\kappa_-(E)\right).$$
(4.19)

Were we to consider a superconducting region of finite length, for instance as part of a N-S-N system (i.e. a superconducting region bounded by normal regions) all four terms in the general solution would need to be included to account for reflection at the second S-N boundary, but such systems are not considered in this thesis.

We now consider the possible scattering processes at energies $|E| < \Delta_0$. The possible scattering processes (specular or Andreev reflection) are contained in the scattering matrix $\boldsymbol{S}(E)$, acting on the amplitudes of the incident components as

$$\begin{pmatrix} A_R^e \\ A_R^h \end{pmatrix} = \boldsymbol{S}(E) \begin{pmatrix} A_I^e \\ A_I^h \end{pmatrix} = \begin{pmatrix} S_{ee}(E) & S_{eh}(E) \\ S_{he}(E) & S_{hh}(E) \end{pmatrix} \begin{pmatrix} A_I^e \\ A_I^h \end{pmatrix}.$$
(4.20)

The subscripts denote the possible processes, for example S_{he} is an incident electron Andreev reflected as a hole. This scattering matrix is specific to incident energies inside the superconducting band gap. Were we to consider higher energies we would be required to include the amplitudes for the additional processes that transmit electron-like and hole-like excitations into the superconductor.

The entries of the scattering matrix can be populated, and the corresponding transmission amplitudes in the superconducting region, by first imposing the condition that the component wave functions and their first derivatives are continuous across the N-S boundary (i.e. $\boldsymbol{\Psi}_N(0) = \boldsymbol{\Psi}_S(0)$ and $\boldsymbol{\Psi}'_N(0) = \boldsymbol{\Psi}'_S(0)$). Imposing this condition transfer matrices can be found that relate amplitudes in the normal and superconducting region. The full details of the calculation are omitted here, but the full derivation can be found in Appendix A.1.1 and additional information in [63]. The scattering matrix $\boldsymbol{S}$ can then be populated by setting $A_I^e = 1$ and $A_I^h = 0$ (corresponding to an incident electron with no incident hole component) to find S_{ee} and S_{he}, and then $A_I^e = 0$ and $A_I^h = 1$ (likewise corresponding to an incident hole with no incident electron component) for the other two entries.

We will later use the scattering states to analyse the dynamics of Andreev reflection of a wave packet and so present the details here. In the

normal region they are (the incident component i.e. electron or hole is denoted by the subscript)

$$\boldsymbol{\Psi}_{e,N}(q) = \frac{1}{\sqrt{\alpha_+(E)}}\begin{pmatrix}1\\0\end{pmatrix}\left[e^{iq\alpha_+(E)/\hbar} + S_{ee}(E)e^{-iq\alpha_+(E)/\hbar}\right]$$

$$+ \frac{1}{\sqrt{\alpha_-(E)}}\begin{pmatrix}0\\1\end{pmatrix}S_{he}(E)e^{iq\alpha_-(E)/\hbar} \qquad (4.21)$$

and

$$\boldsymbol{\Psi}_{h,N}(q) = \frac{1}{\sqrt{\alpha_-(E)}}\begin{pmatrix}0\\1\end{pmatrix}\left[e^{-iq\alpha_-(E)/\hbar} + S_{hh}(E)e^{iq\alpha_-(E)/\hbar}\right]$$

$$+ \frac{1}{\sqrt{\alpha_+(E)}}\begin{pmatrix}1\\0\end{pmatrix}S_{eh}(E)e^{-iq\alpha_+(E)/\hbar}. \qquad (4.22)$$

The scattering matrix entries are given by

$$S_{eh}(E) = S_{he}(E) = \gamma^{-1}\sqrt{\alpha_+(E)\alpha_-(E)}\left(\kappa_+(E) + \kappa_-(E)\right) \qquad (4.23)$$

$$S_{ee}(E) = S(E)\gamma^{-1}(E) \qquad S_{hh}(E) = -S^*(E)\gamma^{-1}(E) \qquad (4.24)$$

defining terms for later brevity

$$S(E) = \frac{E}{\Delta_0}\left[\nu^2(\alpha_+ - \kappa_+)(\kappa_- + \alpha_-) + \nu^{*2}(\alpha_+ + \kappa_-)(\kappa_+ - \alpha_-)\right] \qquad (4.25)$$

$$\gamma(E) = \frac{E}{\Delta_0}\left[\nu^2(\alpha_- + \kappa_-)(\alpha_+ + \kappa_+) - \nu^{*2}(\alpha_- - \kappa_+)(\alpha_+ - \kappa_-)\right]. \qquad (4.26)$$

In this thesis we will consider several asymptotic limits. We will first consider the behaviour of the scattering amplitudes in the regime $E \ll \Delta_0 \ll \mu$ (a large Fermi energy limit, and excitation energies close to zero). Expanding the scattering amplitudes in the small parameters E/μ and Δ_0/μ then only retaining terms up to first order leaves

$$S_{ee}(E) \approx -S_{hh}(E) \approx \frac{E}{\mu}\nu^{*2} \quad \text{and} \quad S_{eh}(E) \approx \frac{2E}{\Delta_0}\nu^{*2} \qquad (4.27)$$

where $\nu^{*2} = \frac{1}{2}(1 - i\sqrt{\Delta^2 - E^2}/E)$. We will use these first-order approximations in Section 6.3 where we will also consider expansion of ν^{*2} in E/Δ_0 if $E \ll \Delta_0$.

To lowest order (i.e omitting all terms of order E/μ, Δ_0/μ and E/Δ_0) the scattering matrix simplifies to

$$\boldsymbol{S}(E) \approx \begin{pmatrix}0 & -i\\-i & 0\end{pmatrix} \qquad (4.28)$$

as anticipated in section 2.1.3. This corresponds to incoming electron or hole states being completely Andreev reflected, with no specular reflection and a phase shift of $e^{-i\pi/2}$ between the incident and reflected states.

The corresponding scattering states in the superconducting region are

$$
\boldsymbol{\Psi}_{e,S}(q) = \frac{2E}{\Delta_0} \frac{\sqrt{\alpha_+}}{\gamma} \left[\begin{pmatrix} \nu \\ \nu^* \end{pmatrix} \nu(\kappa_- + \alpha_-) e^{iq\kappa_+/\hbar} + \begin{pmatrix} \nu^* \\ \nu \end{pmatrix} \nu^*(\kappa_+ - \alpha_-) e^{-iq\kappa_-/\hbar} \right]
$$
(4.29)

$$
\boldsymbol{\Psi}_{h,S}(q) = \frac{2E}{\Delta_0} \frac{\sqrt{\alpha_-}}{\gamma} \left[\begin{pmatrix} \nu \\ \nu^* \end{pmatrix} \nu^*(\kappa_- - \alpha_+) e^{iq\kappa_+/\hbar} + \begin{pmatrix} \nu^* \\ \nu \end{pmatrix} \nu(\kappa_+ + \alpha_+) e^{-iq\kappa_-/\hbar} \right]
$$
(4.30)

which describe the penetration of the incident state into the superconducting region before being absorbed into a superconducting pair.

Examples of the electron and hole components of the scattering wave functions $\boldsymbol{\Psi}_e(q)$ created by an incident electron are shown in Figure 4.2 for various values of E, Δ_0 and μ. Oscillations occur due to interference between the incident and reflected electron components. Smaller values of Δ_0/μ mean a smaller amplitude of specular reflection and hence smaller oscillations. It should be noted that the wave functions are normalized by flux when comparing the amplitudes of the components, indicating that the reflected hole is slower than the incident electron. The plots are also scaled by the penetration depth $L(E)$.

We show in Appendix A.3.1 that the scattering states form an orthogonal basis with respect to a measure on E and between electron and hole components, in which we can resolve an incident wave packet, and derive a time dependent picture of the Andreev reflection process for an incident coherent state wave packet.

The Q-function phase space picture of the two components of the scattering states (4.21), (4.22) and (4.29), (4.30), can be found as outlined in section 3.4 either using the projection operators to resolve individual or electron or hole components, or integrating over β to leave the non-interacting sum of the components. After inserting the resolution of identity in the position basis, the electron component from an incident electron requires solutions to the integrals

$$
\langle z | \Psi_e^e \rangle = \int_{-\infty}^{\infty} dq \, \langle z | q \rangle \Psi_e^e(q) = \int_{-\infty}^{0} \langle z | q \rangle \Psi_{e,N}^e(q) \, dq + \int_{0}^{\infty} \langle z | q \rangle \Psi_{e,S}^e(q) \, dq
$$
(4.31)

for the element $Q_{e,\bowtie}^{ee}(z)$ of the E-H Q-function. Here integration is taken over the normal and superconducting regions independently. The hole component has a similar form for $Q_{e,\bowtie}^{hh}(z)$ after the replacement $z \to z^*$. The solutions are given by the error integrals, the full derivation is given in Appendix B.

Figure 4.2: Absolute value squared of the electron (red) and hole (blue) scattering wave functions generated by an incident electron with energy and band gaps as labelled. The oscillations in the electron wave function in the normal region are due to interference between the incident and reflected electron wave functions, thus for smaller values of Δ the smaller specular reflection co-efficient reduces the scale of the oscillations. All other units $m, \hbar = 1$.

(a) $E = 0$, $\Delta_0 = 5$, $\mu = 50$ **(b)** $E = 15$, $\Delta_0 = 20$, $\mu = 50$
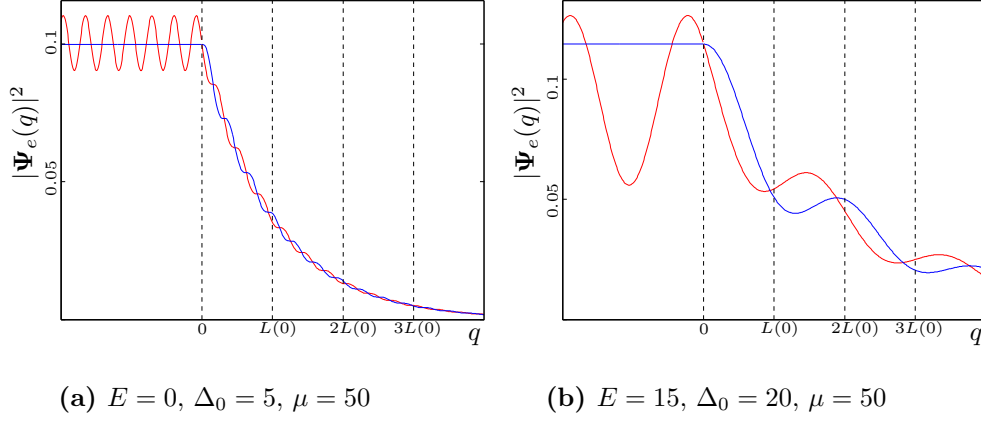
In this specific case of a discontinuous boundary the result in the normal region is

$$
\int_{-\infty}^{0} \langle z|q \rangle \Psi_{e,N}^{e}(q)\, dq =
$$
$$
\left(\frac{\pi \hbar}{m\omega} \right)^{\frac{1}{4}} \frac{1}{\sqrt{2\alpha_+}} \left\{ \operatorname{erfc}\left[\sqrt{\frac{\lambda}{2}} \left(m\omega q - i(p - \alpha_+) \right) \right] e^{-\frac{\lambda}{2}(p-\alpha_+)^2 - \frac{i}{\hbar} q(p-\alpha_+)} \right.
$$
$$
\left. + S_{ee} \operatorname{erfc}\left[\sqrt{\frac{\lambda}{2}} \left(m\omega q - i(p + \alpha_+) \right) \right] e^{-\frac{\lambda}{2}(p+\alpha_+)^2 - \frac{i}{\hbar} q(p+\alpha_+)} \right\}
$$
$$
(4.32)
$$

from which it can be seen that the phase space representation is formed from Gaussian distributions in momentum centred at $\pm \alpha_+(E)$ respectively representing the incident and reflected components. The corresponding result in the superconducting region is

$$
\int_{0}^{\infty} \langle z|q \rangle \Psi_{e,S}^{e}(q)\, dq =
$$
$$
\frac{1}{\sqrt{2}} \left(\frac{\pi \hbar}{m\omega} \right)^{\frac{1}{4}} \left\{ \frac{\nu}{\sqrt{\kappa_+}} F \operatorname{erfc}\left[-\sqrt{\frac{\lambda}{2}} \left(m\omega q - i(p - \kappa_+) \right) \right] e^{-\frac{\lambda}{2}(p-\kappa_+)^2 - \frac{i}{\hbar} q(p-\kappa_+)} \right.
$$
$$
\left. + \frac{\nu^*}{\sqrt{\kappa_-}} G \operatorname{erfc}\left[-\sqrt{\frac{\lambda}{2}} \left(m\omega q - i(p + \kappa_-) \right) \right] e^{-\frac{\lambda}{2}(p+\kappa_-)^2 - \frac{i}{\hbar} q(p+\kappa_-)} \right\}
$$
$$
(4.33)
$$

The projections of the E-H Q-function onto the electron and hole compo-

Figure 4.3: Reduced Q-functions of the scattering state wave functions shown in Figures 4.2a and 4.2b. $Q_\otimes^{\text{red}}(z)$ (top row) and $Q_\bowtie^{\text{red}}(z)$. Energy values as labelled and $\hbar, m = 1$. When $E = 0$ the incident electron and reflected hole coincide along p_{F} for the product Q-function (a). For the E-H Q-function the reflected hole lies at $-p_{\text{F}}$ (c). When $E \neq 0$ the incident electron lies above p_{F} and the reflected hole below p_{F} in the product Q-function picture (b).

(a) $E = 0$, $\Delta_0 = 5$, $\mu = 50$ **(b)** $E = 15$, $\Delta_0 = 20$, $\mu = 50$

(c) $E = 0$, $\Delta_0 = 5$, $\mu = 50$ **(d)** $E = 15$, $\Delta_0 = 20$, $\mu = 50$
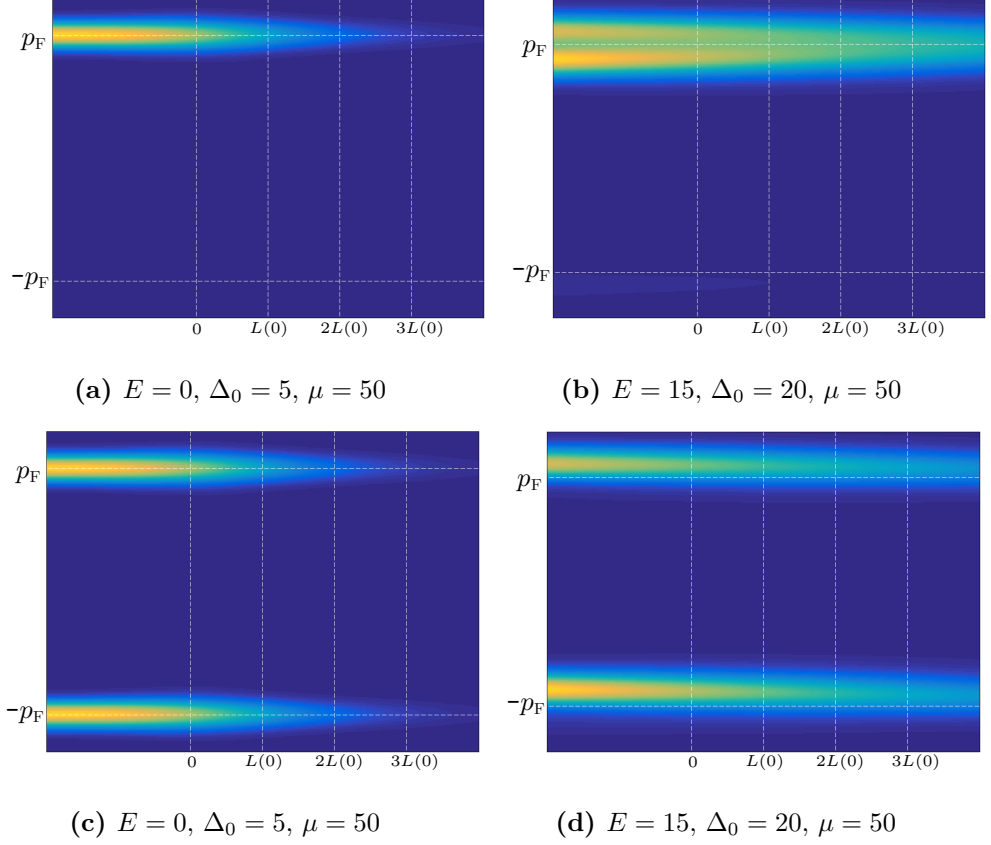
nents are therefore given by

$$Q_\bowtie^{ee}(z) = |\langle z|\Psi_N^e\rangle + \langle z|\Psi_S^e\rangle|^2 \tag{4.34}$$

and

$$Q_\bowtie^{hh}(z) = |\langle z^*|\Psi_N^h\rangle + \langle z^*|\Psi_S^h\rangle|^2. \tag{4.35}$$

Density plots of the E-H and product Q-functions corresponding to the wave functions given in Figure 4.2 are shown in Figure 4.3. The reflection of the hole component in the momentum axis means the E-H Q-function reveals additional details of the components, though care has to be taken if the components overlap as the hole contribution now obscures any reflected electron component shown by the product Q-function.

4.3 Bound Andreev States
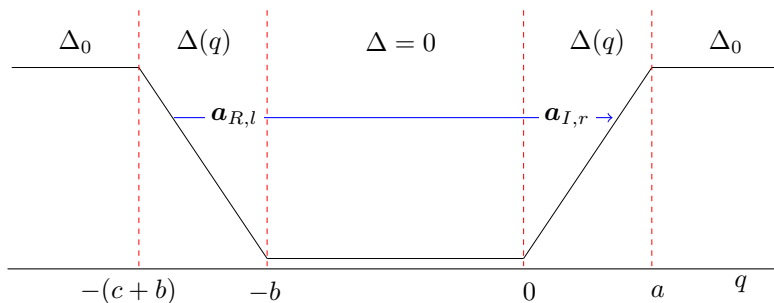
Figure 4.4: The S-N-S system under consideration: We find the allowed eigen-energies where the reflected state on the left becomes the incident state on the right, and similarly on the left.

Andreev states are the eigenstates that occupy the normal region of an S-N-S system as shown in Figure 4.4. The properties and spectrum of S-N-S systems have been studied by a number of authors, see [22, 64, 65]. This one dimensional model consists of a normal region over $-b < q < 0$, bounded by homogeneous superconducting regions extending over $q < -(b+c)$ and $q > a$, with intermediate transitional regions with a spatially dependent $\Delta(q)$ with values $\Delta(0) = \Delta(-b) = 0$ and $\Delta(a) = \Delta(-(b+c)) = \Delta_0$. In the transitional regions, $0 < q < a$ and $-(c+b) < q < -b$, due to the nature of the BdG equations numerical techniques will be required to solve the BdG equations for arbitrary functions of $\Delta(q)$.

Andreev states satisfy the condition that the reflected states outgoing from one boundary are the incident states at the opposite boundary as schematically shown in Figure 4.4. The allowed bound Andreev states can be found by first extending the transfer matrix process, used for the discontinuous boundary, to find the transfer matrices relating electron and hole amplitudes moving from the normal region to the homogeneous superconducting regions through the transitional regions. The full details of the algorithm implemented are omitted here but given in appendix A.1.2.

The bound Andreev state are then found by the process of using the transfer matrix to find the scattering matrix at $q = 0$. Written in terms of the incident and hole amplitudes, on the right (denoted by the subscript)

$$\begin{pmatrix} a_{R,r}^e \\ a_{R,r}^h \end{pmatrix} = \begin{pmatrix} S_{ee,r}(E) & S_{eh,r}(E) \\ S_{he,r}(E) & S_{hh,r}(E) \end{pmatrix} \begin{pmatrix} a_{I,r}^e \\ a_{I,r}^h \end{pmatrix} \tag{4.36}$$

$$\boldsymbol{a}_{R,r} = \boldsymbol{S}_r(E)\boldsymbol{a}_{I,r}. \tag{4.37}$$

Figure 4.5: The real part of, and the logarithm of the eigenvalues of $U(E)$.
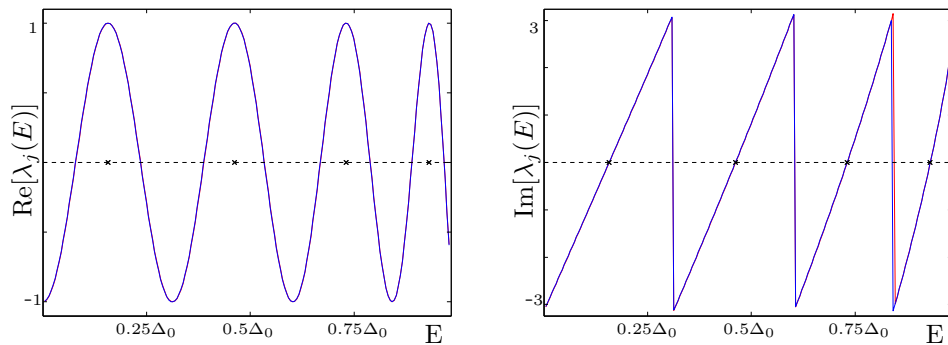
(a) The real part of the eigenvalues $\text{Re}(\lambda_j(E))$ (The two curves overlap due to the symmetry of the system under consideration).

(b) The corresponding logarithm of the two eigenvalues $\log(\lambda_j(E))$. Allowed energies are located where $\log(\lambda_j(E)) = 0$. To find the crossing points the algorithm extrapolates between points of $\log \lambda_j(E)$ on opposite sides of the 0 line.

Similarly on the left we derive the scattering matrix relating the incident and reflected states at $q = -b$ from which we get $\boldsymbol{a}_{R,l} = \boldsymbol{S}_l(E)\boldsymbol{a}_{I,l}$. A transfer matrix that relates reflected states at one boundary to incident states across the normal region is also required. This will be denoted by $\boldsymbol{T}(E)$, with entries that are the phase shifts associated with the election and hole excitations in a normal region

$$\boldsymbol{T}(E) = \begin{pmatrix} \exp(-ib\alpha_+(E)/\hbar) & 0 \\ 0 & \exp(ib\alpha_-(E)/\hbar) \end{pmatrix}. \qquad (4.38)$$

It follows that $\boldsymbol{a}_{I,r} = \boldsymbol{T}(E)\boldsymbol{a}_{R,l}$ relates the reflected states on the left to the incident states on the right. The three matching conditions can then be manipulated to construct an equation that only includes amplitudes on the right

$$\boldsymbol{a}_{R,r} = \boldsymbol{S}_r(E)\boldsymbol{T}(E)\boldsymbol{S}_l(E)\boldsymbol{T}(E)\boldsymbol{a}_{R,r} = \boldsymbol{U}(E)\boldsymbol{a}_{R,r}. \qquad (4.39)$$

For this equality to be satisfied the energies need to be found where

$$\bigl(\mathbb{I} - \boldsymbol{U}(E)\bigr)\boldsymbol{a}_{R,r} = 0. \qquad (4.40)$$

Thus the allowed energies equivalently occur when $\det(\mathbb{I}-\boldsymbol{U}(E)) = 0$. Since $\boldsymbol{U}$ is unitary by construction it can be assumed that the two eigenvalues of $\boldsymbol{U}(E)$ lie on the unit circle and have the form

$$\lambda_j(E) = \exp[i\phi_j(E)] \qquad (4.41)$$

Figure 4.6: Examples of the bound Andreev state wave function and corresponding Q-function density plots. The Q-functions are given for both the and electron and hole components as well as their sum. The system under consideration is shown in figure 4.4, with a linear function of $\Delta(q)$ connecting the normal and homogeneous regions. $\mu = 10$, $\Delta_0 = 3$, $a = c = 5$ and $b = 10$. All other parameters $\hbar, m = 1$
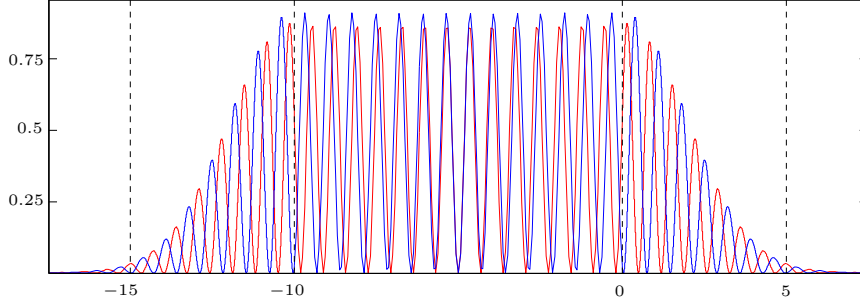
(a) Absolute values of the electron (red) and hole (blue) components of the Andreev state wave functions. $E = 0.16 \times \Delta_0$
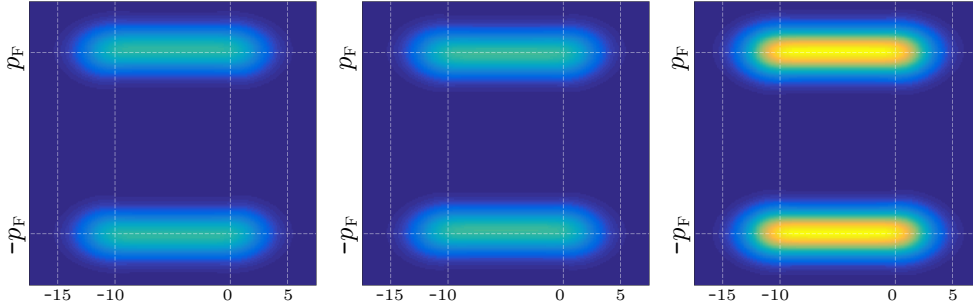
(b) $Q_{\bowtie}^{ee}(q,p)$

(c) $Q_{\bowtie}^{hh}(q,p)$

(d) $Q_{\bowtie}^{\mathtt{red}}(q,p)$
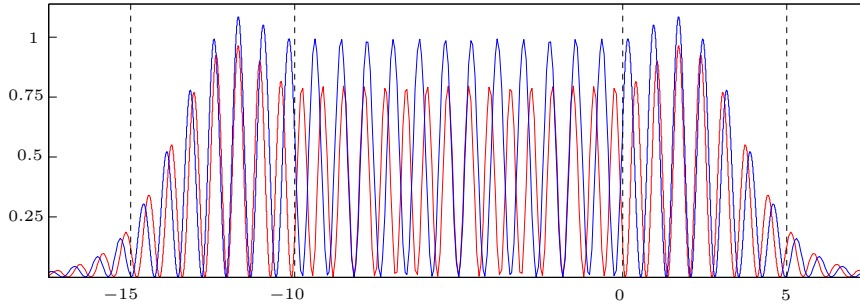
(e) Absolute value squared of the electron (red) and hole (blue) components of the Andreev state wave functions. $E = 0.73 \times \Delta_0$
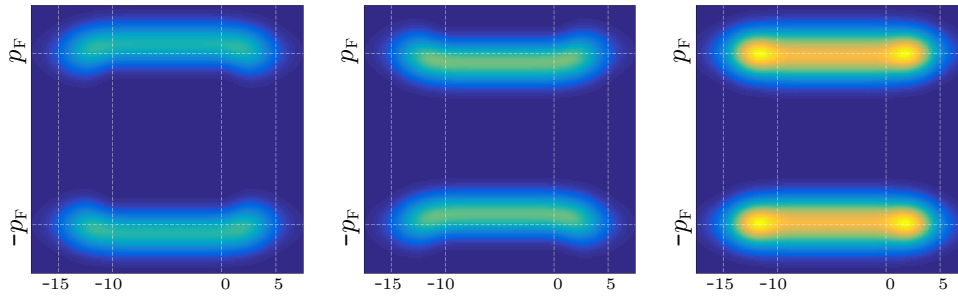
(f) $Q_{\bowtie}^{ee}(q,p)$

(g) $Q_{\bowtie}^{hh}(q,p)$

(h) $Q_{\bowtie}^{\mathtt{red}}(q,p)$

then the allowed energies are found when $\lambda_j(E) = 1$ as shown in Figure 4.5a or equivalently for numerical purposes where $\log \lambda_j(E) = 0$ as shown in Figure 4.5b.

In practice this has been implemented by an algorithm that numerically solves the coupled differential equations given by the BdG equations, to generate $\boldsymbol{U}(E)$ (see section A.1.2 for details) for a range of values of $0 < E < \Delta_0$ (as to not include propagating states at energies $|E| > \Delta_0$ in the superconducting regions). From this list of values the location where $\log \lambda_j(E)$ crosses the origin is found (as shown in Figure 4.5b) and then the location of the eigen-energies extrapolated.

Once the allowed energies are known, it is then straight forward to calculate the Andreev state electron and hole component wave functions, and hence their corresponding Q-function. For the regions of constant Δ_0 and the normal region the solutions are known. For the regions $\Delta(q)$, the wave function are found by numerically solving the differential equations. The Q-function over the intermediate region is then found by numerical integration. Examples are shown in Figure 4.6 where the transitional region is modelled by a linear function of $\Delta(q)$.

4.4 Solutions of the BdG Equations for a Linearly Varying Band Gap

In general it turns out to be difficult to find analytic solutions to the coupled BdG equations for any other superconducting system apart from the homogeneous superconductor or the discontinuous N-S boundary. To generate the Andreev states for varying values of E in the regions with a spatially dependent band gap, $\Delta(q)$, we have relied upon numerical differential equations solvers to generate the corresponding electron and hole wave functions in these regions.

We have found though that we can find limited analytic solutions for a region of linearly varying $\Delta(q)$, described by $\Delta(q) = \delta q$ for a constant δ. By rearranging the BdG equations in the position basis solutions must be found for the matrix differential equation

$$\frac{d^2}{dq^2}\boldsymbol{\psi}(q) = \frac{2m}{\hbar^2}\left[i\delta q\sigma_2 - E\sigma_3 - \mu\right]\boldsymbol{\psi}(q). \tag{4.42}$$

When $E = 0$ (i.e. states on the Fermi energy) a solution ansatz consisting

Figure 4.7: The absolute square of the electron (red) and hole (blue) component wave functions from an incident electron on a linearly varying pair potential $\Delta(q) = q\delta\theta(q)$. The incident electron has energy $E = 0$ and $\delta/\mu = 0.1$, $\hbar =, m = 1$.
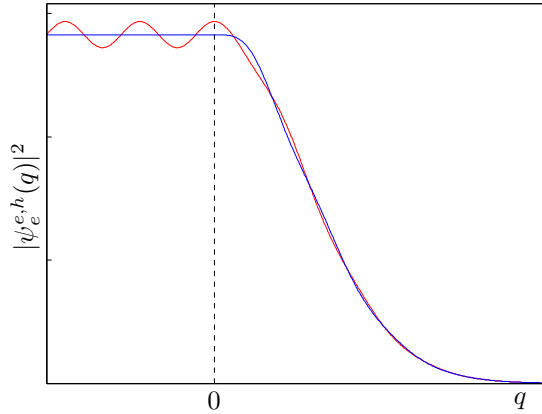
of a constant vector and scalar function in q

$$\boldsymbol{\psi}(q) = \overline{x}f(q) \tag{4.43}$$

can be used. As $E = 0$ the vector is just given by the eigenvector of σ_2. With this condition the solution for $f(q)$ of the resulting differential equation is given by the Airy Functions of the first and second kind (see [66] p.446). The spinor solutions are therefore

$$\boldsymbol{\psi}_{A\pm}(q) = \begin{pmatrix} 1 \\ \pm i \end{pmatrix} \mathrm{Ai}\left[\left(\pm\frac{2im\delta}{\hbar^2}\right)^{\frac{1}{3}}\left(q \pm i\frac{\mu}{\delta}\right)\right] \tag{4.44}$$

and

$$\boldsymbol{\psi}_{B\pm}(q) = \begin{pmatrix} 1 \\ \pm i \end{pmatrix} \mathrm{Bi}\left[\left(\pm\frac{2im\delta}{\hbar^2}\right)^{\frac{1}{3}}\left(q \pm i\frac{\mu}{\delta}\right)\right]. \tag{4.45}$$

For an infinitely long linear potential, starting at $q = 0$ (i.e. $\Delta(q) = q\delta\theta(q)$), the allowed decaying solutions are described by the Airy functions of the first kind. The allowed general solution in the linearly varying region can then be given by the linear sum

$$\boldsymbol{\Psi}_L(q) = F\boldsymbol{\psi}_{A+}(q) + G\boldsymbol{\psi}_{A-}(q). \tag{4.46}$$

If we consider the interface of a normal region and a region of linearly varying $\Delta(q)$ it is straightforward to generalise the transfer matrix technique described in section A.1.1, by again satisfying the corresponding matching conditions at the normal/linear boundary. An example of the component wave functions are shown in Figure 4.7.

Although this is an interesting results in itself, it is of limited use when considering the dynamics of wave packets. For the purpose of wave packet dynamics information is required about the contributions from a range of energies contained under the wave packet. It seems that it is not possible to find a full analytic solutions for an arbitrary non-zero value of E.

We can consider that if it was possible to extend these analytic solutions pertubatively in E close to μ, such a solution could be used to calculate contributions to a Gaussian distribution that is sufficiently sharply peaked around the Fermi momentum as any contributions from energies far from the Fermi energy are suppressed. Although there are well established methods for finding perturbative solutions to matrix differential equations it seems that using a simple pertubative expansion of the form

$$\boldsymbol{\psi}(q) = \boldsymbol{\psi}_0(q) + E\boldsymbol{\psi}_1(q)\dots \tag{4.47}$$

does not provide a simplified analytic form for the higher order terms, although the lowest order term is easily found. In particular it remains to be seen if a small pertubation in the energy produces a small pertubation in the wavefunction.

We might instead consider the same problem in the momentum basis, the BdG equations are rearranged as

$$\frac{d}{dp}\boldsymbol{y}(p) = \frac{1}{\delta\hbar}\left[\left(\frac{p^2}{2m} - \mu\right)\sigma_2 - iE\sigma_1\right]\boldsymbol{y}(p) \tag{4.48}$$

simplifying the required calculation.

Assuming that $\boldsymbol{y}(p)$ can be expanded pertubatively in E as

$$\boldsymbol{y}(p) = \boldsymbol{y}_0(p) + E\boldsymbol{y}_1(p)\dots \tag{4.49}$$

inserting this back into (4.48), the lowest order equation

$$E^0 \Rightarrow \quad \frac{d}{dp}\boldsymbol{y}_0(p) = \frac{1}{\delta\hbar}\left(\frac{p^2}{2m} - \mu\right)\boldsymbol{y}_0(p) \tag{4.50}$$

is easily solved to give

$$\boldsymbol{y}_0(p) = \begin{pmatrix} \cosh(f(p)) \\ i\sinh(f(p)) \end{pmatrix} \quad \text{and} \quad \boldsymbol{y}_0(p) = \begin{pmatrix} -i\sinh(f(p)) \\ \cosh(f(p)) \end{pmatrix} \tag{4.51}$$

where

$$f(p) = \frac{1}{\delta\hbar}\left(\frac{p^3}{6m} - p\mu\right). \tag{4.52}$$

Like the position representation though higher order terms are not easily found.

Chapter 5

Dynamics of Electron-Hole Coherent States in a Spatially Homogeneous Superconductor

In this chapter we will consider the dynamics of Gaussian wave packets which describe quasi-particle excitations inside a spatially homogeneous superconductor, defined by a spatially constant energy band gap $\Delta(q) = \Delta_0$.

We will first analyse the behaviour of the time dependent operators in the Heisenberg picture. We will also consider the difference in behaviour between the E-H and product coherent states, and how both forms of states behave in a semi-classical context. For a region with a constant band gap we can find exact analytic solutions to the set of time dependent operators in the Heisenberg picture, and so we will look at the moments of Gaussian wave packets and again compare the behaviour of the moments with respect to the product or electron-hole states. In lieu of full analytic solutions for the moments we will be required to utilize asymptotic techniques to investigate the time dependence of the moments, in particular we will consider the long time behaviour of E-H and product coherent states.

The second half of this chapter will be dedicated to further investigation into the behaviour of wave packets in a homogeneous superconductor in the Schrödinger picture. In particular we will focus on wave packets centred on the Fermi momentum, where examination of the dispersion relation relevant to the BdG Hamiltonian would suggest that wave packets have the property of a zero group velocity despite the large momentum value. We will again be required to employ asymptotic analysis techniques to examine the long-time behaviour of Gaussian wave packets. Finally we will consider the two short

wavelength limits appropriate to the BdG equations, both the standard semiclassical limit $\hbar \to 0$ and the large Fermi energy limit $\mu \to \infty$.

5.1 Bogoliubov-de Gennes Dispersion Relation

Here we give a brief overview of the dispersion relation and its relations to the dynamics of a scalar wave packet. We will then extend this concept to wave packets with a spin component under the BdG Hamiltonian for an indication of how we should expect wave packets to behave inside a superconductor.

The representation of localised particles by groups of plane waves has roots in the development of quantum theory, and concepts used here are detailed in most quantum mechanics textbooks (for example [67]). When applied to the plane wave solutions of the BdG equations, we will show that the relative amplitudes of the spinor components informs not only how they propagate but how the positive and negative energy solutions interfere.

Let us first consider a free scalar wave packet, many features of which will have analogues when we consider spinor wave packets under the BdG Hamiltonian later in this section. A general time-dependent wave packet defined on position space can be decomposed into travelling plane waves in k-space using the relationship

$$\Psi(q,t) = \int dk\, A(k)\, \exp\left[i(kq - E(k)t/\hbar)\right]. \qquad (5.1)$$

The function $A(k)$ is the amplitude of the plane waves from which $\Psi(q,t)$ is constructed. The plane waves as defined here have an associated flow travelling in the positive direction. For the standard free scalar Schrödinger equation k and $E(k)$ are related by the dispersion relation $E(k) = \hbar^2 k^2/2m$ (though much of what follows still remains valid for different forms of Hamiltonian). If the distribution of wave vectors $A(k)$ is strongly peaked around a mean wave vector k_0 then $E(k)$ can be expanded about k_0, as only information about plane waves with values of k close to the peak k_0 is required. Expanding up to second order around k_0 gives the terms

$$E(k) \approx E(k_0) + E'(k_0)(k - k_0) + \frac{1}{2}E''(k_0)(k - k_0)^2. \qquad (5.2)$$

Firstly only considering terms up to first order in $(k - k_0)$, inserting the expansion back into (5.1) and shifting the origin to the peak of the distribution

$k \rightarrow k_0$ gives

$$\Psi(q,t) \approx \exp\left[i(k_0 q - E(k_0)t)\right] \int dk \ A(k+k_0) \exp\left[i(q - E'(k_0)t)k\right] \quad (5.3)$$

$$= \exp\left[ik_0(q - v_{\mathrm{p}}(k_0)t)\right] \int dk \ A(k+k_0) \exp\left[i(q - v_{\mathrm{g}}(k_0)t)k\right]. \quad (5.4)$$

In the second line we have identified the phase velocity defined as $v_{\mathrm{p}}(k) = E(k)/k$ and the group velocity $v_{\mathrm{g}}(k) = E'(k)$. The phase velocity corresponds to the propagation of the phases and the group velocity to the velocity of the wave packet. This can be made analytically explicit for a Gaussian distribution of k values, parametrized in a manner analogous to previous sections by a central wave vector k_0 and a width parameter λ as

$$A(k) = \sqrt{\frac{\lambda}{\pi}} \exp\left[-\lambda(k - k_0)^2\right] \quad (5.5)$$

with a corresponding Gaussian wave packet defined in the position basis. The propagation of this wave packet in space is therefore approximately described by the function

$$\Psi(q,t) \approx \exp\left[-\frac{1}{4\lambda}\left(q - v_{\mathrm{g}}(k_0)t\right)^2 + ik_0\left(q - v_{\mathrm{p}}(k_0)t\right)\right] \quad (5.6)$$

the original Gaussian wave packet translated to a new peak position located at $v_{\mathrm{g}}(k_0)t$, confirming that the group velocity indeed describes the velocity of the wave packet.

Further considering the next second order term in the expansion (5.2), inserting this into the plane wave resolution gives

$$\Psi(q,t) \approx \exp\left(ik_0(q - v_{\mathrm{p}}(k_0)t)\right) \int dk A(k+k_0) \exp\left(i(q - v_{\mathrm{g}}(v_0)t)k - \frac{it}{2}E''(k_0)k^2\right). \quad (5.7)$$

This indicates that for a Gaussian wave packet, the second order term in the expansion enters the solution as a time dependence in the width of the wave packet

$$\Psi(q,t) \approx \sqrt{\frac{\lambda}{\lambda(t)}} \exp\left[-\frac{1}{4\lambda(t)}\left(q - v_{\mathrm{g}}(k_0)t/\hbar\right)^2 + ik_0\left(q - v_{\mathrm{p}}(k_0)t/\hbar\right)\right] \quad (5.8)$$

where $\lambda(t) = \lambda + itE''(k_0)/2\hbar$. The spreading of the initial Gaussian state is approximately linear in time, and for long times the major contribution to broadening is proportional to $E''(k)$, but also inversely proportional to the initial width. This again shows that spatially narrower wave packets spread more quickly due to consequently being broader in k-space. This can be
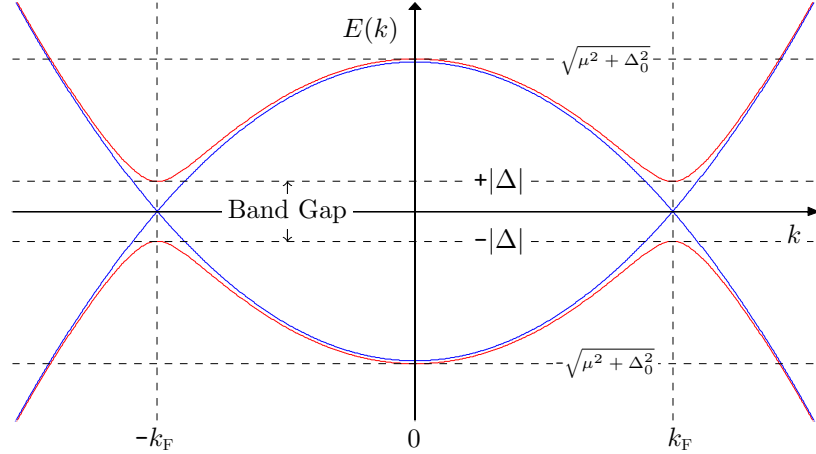
Figure 5.1: The dispersion relation, $E(k) = \pm\sqrt{(\hbar^2 k^2/2m - \mu)^2 + \Delta_0^2}$, relevant to the BdG equations. The positive and negative branches are shown for states both inside a homogeneous superconducting region where $\Delta_0 > 0$ (red) and a normal conductor where $\Delta_0 = 0$ (blue). In the normal case the two branches correspond to electron and hole quasi-particles, who intersect at $\pm k_F$ the Fermi wavenumber $k_F = p_F/\hbar$. In a superconductor the corresponding plane waves are superpositions of electron and hole components.

imagined as being due to the contributions to the wave packet moving at differing velocities. Higher order terms (cubic and above) in the expansion of $E(k)$ are then responsible for non-Gaussian dynamics of the wave packet.

For the time dependent BdG equations the spinor ansatz

$$\begin{pmatrix} u(q,t) \\ v(q,t) \end{pmatrix} = \begin{pmatrix} \tilde{u} \\ \tilde{v} \end{pmatrix} \exp\left[i\left(kq - \frac{t}{\hbar}E(k)\right)\right] \tag{5.9}$$

shows that the BdG dispersion relation has positive and negative energy branches

$$\pm E(k) = \pm\sqrt{\left(\frac{\hbar^2 k^2}{2m} - \mu\right)^2 + \Delta_0^2}. \tag{5.10}$$

These branches are plotted in Figure 5.1 for both states in a normal conductor ($\Delta = 0$) and superconducting ($\Delta > 0$) system. Note again the energy band gap of width $2\Delta_0$ at energies $|E| < |\Delta_0|$ from μ, where single excitations cannot persist in a superconductor.

For a set energy in the range $\Delta_0 < E < \sqrt{\mu^2 + \Delta_0^2}$ the 4 possible stationary states are given by equation (4.8). Likewise in the range $-\Delta_0 > E > -\sqrt{\mu^2 + \Delta_0^2}$ the stationary solutions are given by equation (4.12). Each of the solutions ($\pm\kappa_+$ and $\pm\kappa_-$) are applicable in a limited range of k.

In a normal conductor the scalar dispersion relation

$$\pm E(k) = \pm\left(\frac{\hbar^2 k^2}{2m} - \mu\right) \tag{5.11}$$

Figure 5.2: The spinor component amplitudes as a function of k and their relation to balance of components along the dispersion relation.
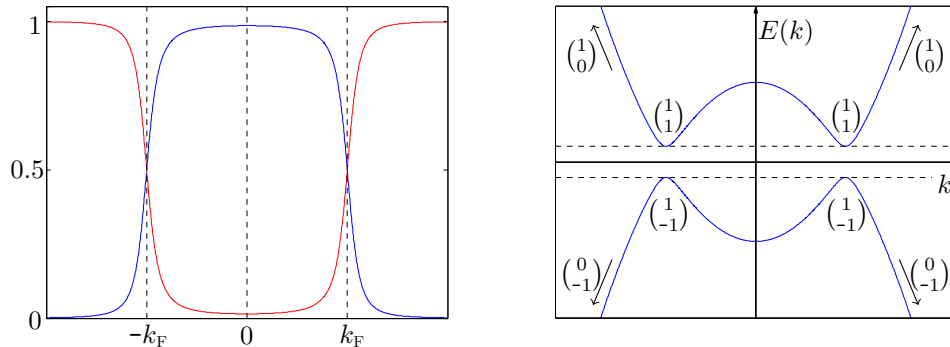
(a) The spinor component amplitudes $|A_+(k)|^2$ (red) and $|A_-(k)|^2$ (blue) as a function of k. $\Delta_0/\mu = 0.25$.

(b) At large values of k the plane waves are predominantly electron/hole-like on the positive/negative energy branches respectively. On $\pm k_{\mathrm{F}}$ they are equal superpositions of components.

is regained as shown in blue in Figure 5.1. The positive branch corresponds to the electron-like quasi-particle. This is equivalent to the free scalar case, albeit with a shift in energies measured relative to μ. The negative energy branch is the corresponding hole excitation, this is the reflection of the electron relation in the energy axis about μ. This is due to the time reversed nature of the hole component. It follows that the group velocity and momenta of a hole quasi-particle have opposite signs.

To examine how the magnitude of the spinor components behave in the superconducting case the dispersion relation can be used to rewrite the amplitudes $\tilde{u}(E)$ and $\tilde{v}(E)$ in terms of k as

$$\tilde{u}(E(k)) \equiv A_+(k) = \left[\frac{1}{2} \left(1 + \frac{\mathcal{H}_0(k)}{\sqrt{\mathcal{H}_0^2(k) + \Delta_0^2}} \right) \right]^{\frac{1}{2}} \tag{5.12}$$

and

$$\tilde{v}(E(k)) \equiv A_-(k) = \left[\frac{1}{2} \left(1 - \frac{\mathcal{H}_0(k)}{\sqrt{\mathcal{H}_0^2(k) + \Delta_0^2}} \right) \right]^{\frac{1}{2}}. \tag{5.13}$$

Here $\mathcal{H}_0(k) = \hbar^2 k^2/2m - \mu$. The amplitudes of $A_+(k)$ and $A_-(k)$ are shown in Figure 5.2a. From this it can be inferred that along the positive branch the states are predominantly electron-like when $|k| > k_{\mathrm{F}}$ (being almost completely electron when $|k| \gg k_{\mathrm{F}}$) and predominantly hole-like when $|k| < k_{\mathrm{F}}$. At the crossing point k_{F} the stationary states are equal superpositions of electron and hole components. The inverse is true along the negative energy branch, with an additional $e^{i\pi}$ phase applied to the hole component.

70

In particular as shown in Figure 5.2b the spinor amplitudes on the positive and negative Fermi momenta are

$$E(\pm k_{\mathrm{F}}) = \Delta_0 \implies \frac{1}{\sqrt{2}} \begin{pmatrix} 1 \\ 1 \end{pmatrix} \quad \text{and} \quad -E(\pm k_{\mathrm{F}}) = -\Delta_0 \implies \frac{1}{\sqrt{2}} \begin{pmatrix} 1 \\ -1 \end{pmatrix}$$

(5.14)

describing equal superpositions of electron and hole components on the edge of the band gap. For energies far from the band gap

$$E(|k| \gg k_{\mathrm{F}}) \gg \Delta_0 \implies \begin{pmatrix} 1 \\ 0 \end{pmatrix} \quad \text{and} \quad -E(|k| \gg k_{\mathrm{F}}) \ll -\Delta_0 \implies \begin{pmatrix} 0 \\ -1 \end{pmatrix}$$

(5.15)

the states are predominantly electron-like or hole-like. When $k = 0$ such that $E(0) = \sqrt{\mu^2 + \Delta_0^2}$ then

$$A_{\pm}(0) = \left[\frac{1}{2} \left(1 \pm \frac{\mu}{\sqrt{\mu^2 + \Delta_0^2}} \right) \right]^{\frac{1}{2}}$$

(5.16)

in the limit $\Delta_0/\mu \to 0$ this simplifies to $A_{\pm}(0) \approx \sqrt{1/2(1 \pm 1)}$. These states will then consist of predominantly one component in this limit. Also note that the operator $i\sigma_2$ takes states from the positive energy branch to the negative and vice-versa.

It can be inferred from Figure 5.2b that interesting dynamics should especially be seen from wave packets located on and close to the Fermi momentum. The equal superposition of electron and hole components will mean wave packets defined in this region will create strong interference between the positive and negative energy branches. At much larger energies as the positive and negative branches consist of predominantly one of the orthogonal electron or hole components, the energy branches will only interfere weakly.

Like the scalar example given by equation 5.1 we will consider the plane wave decomposition of an initial spinor wave packet using the stationary states of the BdG equation (equations (4.8) and (4.12)). Consideration will have to be given as to how the decomposition models the electron-hole degree of freedom parametrized by β as defined in section 3.2.

To discuss the decomposition we label the positive and negative energy branch momentum eigenstates as (the bold notation again denoting a state with spinor components)

$$|\boldsymbol{k}, +\rangle = \begin{pmatrix} A_+(k) \\ A_-(k) \end{pmatrix} |k\rangle \quad \text{and} \quad |\boldsymbol{k}, -\rangle = \begin{pmatrix} A_-(k) \\ -A_+(k) \end{pmatrix} |k\rangle.$$

(5.17)

from which the resolution of identity can be formed

$$\mathbb{I} = \int dk \left(|\boldsymbol{k}, +\rangle\langle\boldsymbol{k}, +| + |\boldsymbol{k}, -\rangle\langle\boldsymbol{k}, -| \right). \qquad (5.18)$$

First considering a general product spinor wave packet

$$|\psi_0 \otimes \beta\rangle = \big(|e\rangle + \beta|h\rangle \big) \otimes |\psi_0\rangle. \qquad (5.19)$$

then the corresponding time dependent wave function can be resolved as

$$\boldsymbol{\psi}_\otimes(q, t, \beta) = \langle q| \exp\left(-\frac{i}{\hbar} t \hat{\mathcal{H}}_{\text{BdG}} \right) |\psi_0 \otimes \beta\rangle \qquad (5.20)$$

$$= \int dk \, \langle q| \exp\left(-\frac{i}{\hbar} t \hat{\mathcal{H}}_{\text{BdG}} \right) \left(|\boldsymbol{k}, +\rangle\langle\boldsymbol{k}, +| + |\boldsymbol{k}, -\rangle\langle\boldsymbol{k}, -| \right) |\psi_0 \otimes \beta\rangle \qquad (5.21)$$

$$= \int dk \, \langle q| \exp\left(-\frac{i}{\hbar} t \hat{\mathcal{H}}_{\text{BdG}} \right) \left(B_+(k)|\boldsymbol{k}, +\rangle + B_-(k)|\boldsymbol{k}, -\rangle \right) \qquad (5.22)$$

$$= \int dk \quad e^{-\frac{i}{\hbar} t E(k)} B_+(k)\langle q|\boldsymbol{k}, +\rangle + e^{\frac{i}{\hbar} t E(k)} B_-(k)\langle q|\boldsymbol{k}, -\rangle \qquad (5.23)$$

where the plane wave amplitudes are given by

$$B_\pm(k) = \left[A_\pm(k) \pm \beta A_\mp(k) \right] \langle k|\psi_0\rangle. \qquad (5.24)$$

This is the product spinor analogue of the scalar decomposition given by (5.1). For wave packets that are well localised and peaked at some k_0 (like the Gaussian coherent state distribution) information about the dynamics of wave packets can be garnered from the dispersion relation, and the balance of the components.

In the following section we will consider several values of k_0 with respect to the Fermi momentum as illustrated in Figure 5.3a. Firstly a wave packet centred far from the Fermi momentum at $k_0 \gg k_{\text{F}}$ and a distribution that is also sufficiently narrow to isolate a small region in k then $A_+(k) \approx 1$ and $A_-(k) \approx 0$. The resulting decomposition of the time dependent wave function will approximately be

$$\boldsymbol{\psi}_\otimes(q, t, \beta) \approx \int dk \, \langle k|\psi_0\rangle e^{iqk} \left[\begin{pmatrix} 1 \\ 0 \end{pmatrix} e^{-itE(k)/\hbar} + \beta \begin{pmatrix} 0 \\ 1 \end{pmatrix} e^{itE(k)/\hbar} \right]. \qquad (5.25)$$

The electron and hole components of the initial wave packet are resolved in positively and negatively propagating plane waves respectively. It can read directly from the dispersion relation that for states centred at $k_0 \gg k_{\text{F}}$ the electron-like component will have a positive group velocity and the

Figure 5.3: Wave packets and the BdG dispersion relation.
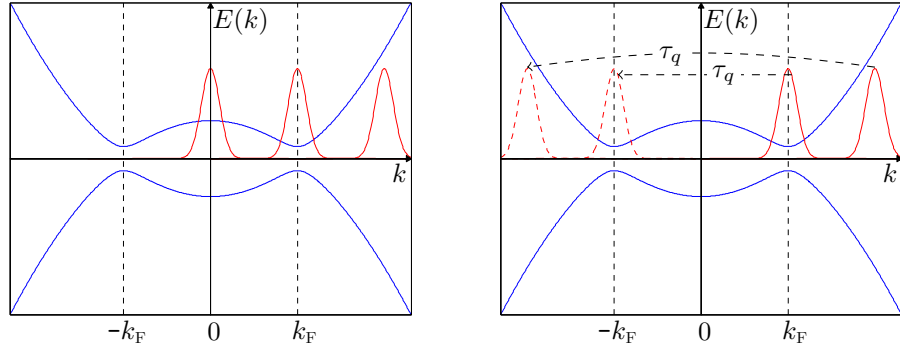
(a) We will consider wave packets located at $k_0 \approx k_F$, $k_0 = 0$ and $k_0 \gg k_F$. Sufficiently narrow Gaussian distributions will isolate contributions from regions of the dispersion relation.

(b) The time reversal operator, τ_q, translates the centre of the initial Gaussian distribution from k_0 to $-k_0$.

hole a negative, confirming that in this case the state initially centred on $k_0 \gg k_F$ will quickly separate. Since the electron and hole components are orthogonal then the wave packet $|\psi_\otimes(q, t, \beta)|^2$ will contain no interference between positive and negative energy branches. Each component will then evolve freely.

When the state is centred on the Fermi momentum $k_0 = k_F$ then $A_+(k_F) \approx A_-(k_F) \approx 1/\sqrt{2}$ and the wave packet decomposes as

$$\psi_\otimes(q, t, \beta) \approx \frac{1}{2} \int dk \langle k|\psi_0\rangle e^{iqk} \left[\begin{pmatrix} 1 \\ 1 \end{pmatrix} (1 + \beta) e^{-itE(k)/\hbar} + \begin{pmatrix} 1 \\ -1 \end{pmatrix} (1 - \beta) e^{itE(k)/\hbar} \right].$$
(5.26)

The electron and hole components of the initial wave packet are resolved in equal superpositions of positive and negative energy contributions. Like the scalar case, expanding the dispersion relation about k_0 the phase velocity of a state centred on k_F is

$$v_{\mathbf{p}}(k_F) = \frac{1}{k_F} E_\pm(k_F) = \pm\frac{\Delta_0}{k_F}$$
(5.27)

but the corresponding group velocity is

$$v_{\mathbf{g}}(k_F) = E'(k_F) = 0.$$
(5.28)

We see that for states centred on the Fermi momentum the group velocity is 0 though the phase velocity remains non zero. This is due to to the two components of the plane wave having the same momentum at k_F, but as they propagate in opposite directions they produce the zero group velocity.

Close to k_{F} the states either side of k_{F} move from electron-like to hole-like and so also move in opposite direction for a given energy. This is only true close to k_{F} though as $E(p)$ is asymmetric about k_{F} at higher energies. This means ignoring any interference effects wave packets on either branch will only disperse as their components move in opposite directions. We will demonstrate in later sections that interesting dynamics can arise due to interference between the energy branches. In particular we will see that although the group velocity as found from the dispersion relation is zero on the band gap, wave packets can in fact be produced that have initial group velocities $\pm v_{\text{F}}$, the Fermi velocity $v_{\text{F}} = p_{\text{F}}/m$.

To create the E-H state the application of the time reversal operator to the hole component inverts the hole component of the wave packet about the origin. This inverts the location of the peak of the wave packet from k_0 to $-k_0$ as shown in Figure 5.3b. As such the action of the $\hat{\mathcal{Z}}$ (see Equation (3.46)) operator means we construct the hole component of our initial state from the negative momentum plane waves. For a general E-H state

$$|\psi_0 \bowtie \beta\rangle = |e\rangle \otimes |\psi_0\rangle + \beta^*|h\rangle \otimes |\psi_0^*\rangle \qquad (5.29)$$

the plane wave amplitudes are replaced by

$$B_{\pm}(k) = A_{\pm}(k)\langle k|\psi_0\rangle \pm \beta^* A_{\mp}(k)\langle k|\psi_0^*\rangle. \qquad (5.30)$$

For the wave packet centred at $k_0 \gg k_{\text{F}}$ since $A(k)_{\pm}$ are symmetric in k their approximate values are unchanged by $\hat{\mathcal{Z}}$ leaving

$$\boldsymbol{\psi}_{\bowtie}(q,t,\beta) \approx \int dk\, e^{iqk} \left[\begin{pmatrix} 1 \\ 0 \end{pmatrix} \langle k|\psi_0\rangle e^{-itE(k)/\hbar} + \begin{pmatrix} 0 \\ 1 \end{pmatrix} \beta^* \langle k|\psi_0^*\rangle e^{itE(k)/\hbar} \right].$$
$$(5.31)$$

As $\langle k|\psi_0^*\rangle$ isolates negative values of k, this now means that the hole component has a positive group velocity, in line with the electron component. Ignoring rotations between the electron and hole components we would expect the components to move together. Due to the lack of interaction between the electron and hole components, apart from the overall time reversal the dynamics of these states will be left mainly unaffected.

For states located on the Fermi momentum the E-H state decomposes as

$$\boldsymbol{\psi}_{\bowtie}(q,t,\beta) \approx \frac{1}{2} \int dk\, e^{iqk} \left[\begin{pmatrix} 1 \\ 1 \end{pmatrix} (\langle k|\psi_0\rangle + \beta^* \langle k|\psi_0^*\rangle) e^{-itE(k)/\hbar} \right.$$
$$\left. + \begin{pmatrix} 1 \\ -1 \end{pmatrix} (\langle k|\psi_0\rangle - \beta^* \langle k|\psi_0^*\rangle) e^{itE(k)/\hbar} \right]. \qquad (5.32)$$

Although the electron and hole component of the initial state are again re-solved in equal superpositions of positive and negative energy contributions, the hole contributions are now located at $-k$.

Here the approximation has been made that the spinor amplitudes are constant over the width of the wave packet. We will show in later sections that this is an appropriate approximation for states at $k_0 = 0$ or $k_0 \gg k_{\mathrm{F}}$, but for states on k_{F} the variation of $E(k)$ across the width of the wave packet will play a strong role in the dynamics.

As with the scalar example, for a Gaussian wave packet the time dependent width of the wave packet in q is given by the second derivative of $E(k)$. On the Fermi momentum this is

$$E''(k_{\mathrm{F}}) = \frac{(\hbar v_{\mathrm{F}})^2}{\Delta_0}. \tag{5.33}$$

The same calculation for the normal conductor dispersion relation (5.11) provides the energy indipendent value $E''(k) = \hbar^2/2m$, the same as the scalar wave packet. This indicates an additional spreading mechanism for wave packets on the band gap. It can be inferred that this is due to the spreading due to opposite velocities of the two components.

5.2   Time Scales & Wave Packet Dimensions

We now consider the time and length scales of interest for Gaussian wave packets under the BdG Hamiltonian. Firstly

$$T_F = \frac{\pi\hbar}{\mu} \tag{5.34}$$

the approximate time for a wave packet with expected momentum $p_{\mathrm{F}} = \sqrt{2m\mu}$ to travel one Fermi wavelength, $\lambda_F = 2\pi\hbar/p_{\mathrm{F}}$, ignoring any rotations between electron-hole components. We also assign

$$T_{\delta q} = \frac{m\delta_q}{p_{\mathrm{F}}} = \delta_q \sqrt{\frac{m}{2\mu}} \propto \sqrt{\frac{\hbar}{\omega\mu}} \tag{5.35}$$

the approximate time required for a wave packet centred on the Fermi momentum p_{F} to travel its own spatial width δ_q. For an initially Gaussian wave packet δ_q is proportional to $\delta_q \propto \sqrt{2\hbar/m\omega}$ which gives the right hand side of (5.35). Finally there is the time-scale

$$T_\sigma(p) = \frac{\pi\hbar}{\sqrt{\langle \mathcal{H}_0(\hat{p}) \rangle^2 + \Delta^2}} \tag{5.36}$$

the approximate time for an initially pure electron state to rotate completely in quasi-spin space through the hole and back to the electron component. For a wave packet centred on p_F this will be $\pi\hbar/\Delta_0$.

We define the length scale $\eta = \delta_q/\lambda_F$ the spatial width of the wave packet measured in units of the Fermi wavelength. Semiclassical constraints require that $\eta \gg 1$ ensuring that the width of the wave packet is much larger than the Fermi wavelength. For a Gaussian wave packet $\eta \propto \sqrt{\mu/\pi^2\omega\hbar}$. The condition $\eta \gg 1$ implies that the time-scales should satisfy $T_{\delta q} \gg T_F$.

These fundamental time-scales also suggest the length scale $d_\sigma(p) = v_F T_\sigma(p_F)$ which we will term the *spin distance*. $d_\sigma(p)$ is the approximate distance the centre of a wavepacket located on the Fermi momentum will travel over one full revolution in quasi-spin. We would like to ensure that the width of the initial wave packet falls in the region between the Fermi wavelength and the spin distance

$$\lambda_F \ll 4\sigma_q \leq d_\sigma(p_F). \tag{5.37}$$

The right hand side of the inequality ensures that the wave packet can travel sufficiently far outside the initial Gaussian envelope before any oscillations between the components set in, otherwise any quasi-spin effects on the dynamics will be contained inside the wave packet envelope.

To this end we assign the parameter x as

$$x = \frac{\delta_q}{d_\sigma(p_F)}. \tag{5.38}$$

x can be used to scale the width of the initial wave packet in terms of $v_F T_\sigma(p_F)$. We will show that x will also provide a means of generating certain dynamic behaviour from Gaussian wave packets under the BdG Hamiltonian located on the Fermi momentum.

For a wave packet centred at $V_0 = p_F$ we set the total spatial width of the initial Gaussian wave packet (i.e. the width of $|\langle q|z\rangle|^2$) as $\delta_q = 4\hbar\sqrt{\lambda/2}$ (where again $\lambda = 1/m\omega\hbar$) this sets the width at 4 standard-deviations, encompassing $\sim 99\%$ of the weight of the Gaussian distribution. We also set the corresponding momentum width at $\delta_p = 4/\sqrt{\lambda}$ (similarly set at 4 standard-deviations of the momentum distribution $\langle p|z\rangle$). We can then rearrange for the spatial and momentum widths for a given value of x

$$\delta_q = \left(\frac{\hbar\pi p_F}{m\Delta_0}\right)x \quad \Rightarrow \quad \delta_p = \left(\frac{16m\Delta_0}{\sqrt{2}\pi p_F}\right)\frac{1}{x}. \tag{5.39}$$

The analysis of the dispersion relation indicates that consideration should also be given to the momentum width of the wave packet relative to the

Figure 5.4: Scaling of the momentum and spatial widths of a wave packet centred at p_{F}. When $x = 1$ the energy of the contributing stationary states fall outside the range Δ_0 of the band gap, but the spin distance $d_\sigma(p_{\mathrm{F}})$ is on the same scale as the spatial width of the wave packet. If $x = 2$ the contributing energies fall inside the range Δ_0 of the band gap but $d_\sigma(p_{\mathrm{F}})$ lies well inside the initial wave packet envelope.

(a) Gaussian envelope in p, $x = 1$

(b) Gaussian envelope in p, $x = 2$

(c) Wave packet at $t = 0$ in q, $x = 1$

(d) Wave packet at $t = 0$ in q, $x = 2$
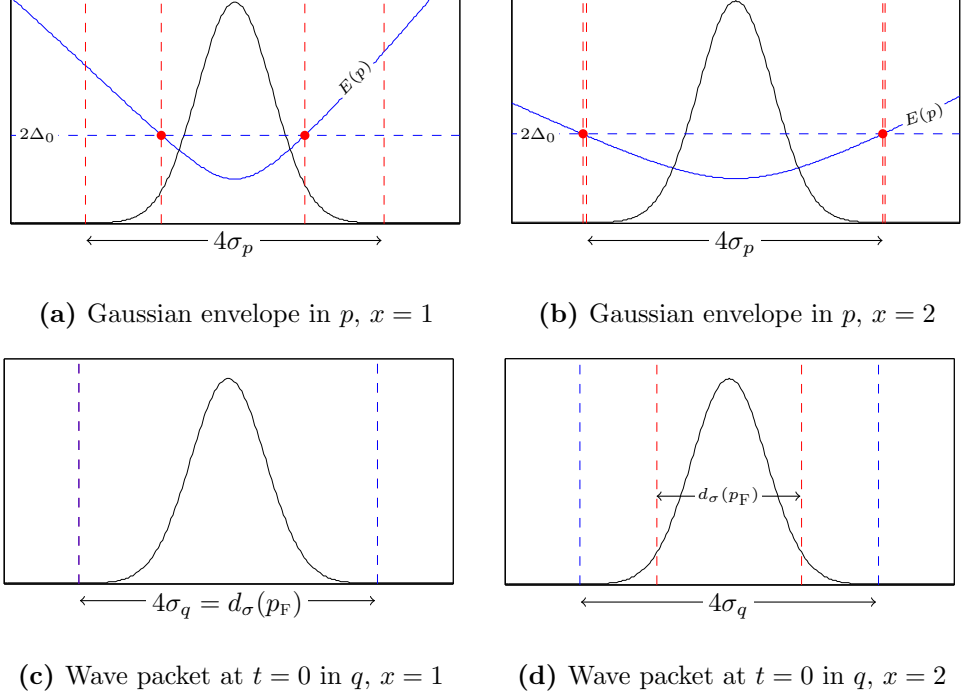
dispersion relation $E(p)$. As shown the shape of the dispersion relation is determined by the ratio Δ_0/μ. The relationship between the dispersion relation and momentum distribution also dictates the range of energies of the plane wave contributions to the wave packet. For a wave packet centred at p_{F} the resultant range of energies is given by

$$\delta_E = E(p_{\mathrm{F}} + \delta_p) - E(p_{\mathrm{F}}). \tag{5.40}$$

If we would like to have the contributing energies lie inside the range $2\Delta_0$ of μ (i.e. within Δ_0 of the band gap) this means $\delta_E \leq \Delta_0$ which for a Gaussian distribution is approximately satisfied when

$$\delta_p \lesssim \frac{\sqrt{3}m\Delta_0}{p_{\mathrm{F}}}. \tag{5.41}$$

Obviously we cannot set δp such that we simultaneously satisfy both of these conditions as shown in Figure 5.4. Scaling x between $1 < x < 2$ means that when $x = 1$, $\langle p|z \rangle$ will include plane wave contributions with $E > 2\Delta_0$ (Figure 5.4a), but $d_\sigma(p_{\mathrm{F}})$ is located in the tails of the initial wave packet (Figure 5.4c). At the other end of the scale when $x \sim 2$ the energies of

the plane wave contributions are well contained inside the range Δ_0 (Figure 5.4b) of the band gap, but $d_\sigma(p_{\mathrm{F}})$ falls inside the spatial width of the wave packet (Figure 5.4d).

The ratio x will prove particularly useful in the analysis of dynamics in the short-wavelength limits $\hbar \to 0$ and $\mu \to \infty$; as it contains all the important features of the wavepacket, and its decomposition, the width of the wave packet, it's central velocity and rate of rotation in quasi-spin.

5.3 Heisenberg Equations of Motion

As shown in section 2.2, under certain conditions we can relate the dynamics of quantum wave packets to classical trajectories generated by the corresponding classical Hamiltonian. In this section we consider the BdG Hamiltonian and the resultant equations of motion. In particular we analyse the difference between the dynamics of product and E-H coherent states. For a scalar particle on phase space the Ehrenfest relations apply to the phase space observables $\langle \hat{q} \rangle$ and $\langle \hat{p} \rangle$. For the BdG Hamiltonian we will also have to consider the observables $\langle \sigma_i \rangle$ that describe the electron-hole degree of freedom. We have also shown in chapter 3 that the E-H coherent states span position-pseudo-velocity phase space and so we will consider the dynamics of the moments of these operators with respect to the E-H coherent states. Where the pseudo-velocity operator is $\hat{V} = \sigma_3 \hat{p}$ we will also confirm that this does in fact describe the initial velocity of the E-H coherent states.

We again utilize the standard Heisenberg time evolution given in general form by

$$\frac{d}{dt}\hat{A}(t) = \frac{i}{\hbar}[\hat{\mathcal{H}}, \hat{A}(t)] \tag{5.42}$$

for a Hamiltonian $\hat{\mathcal{H}}$ and operator $\hat{A}(t)$. For the BdG Hamiltonian this will also require taking into account the commutation relation of the spin operators. We will require the standard canonical commutation relations

$$[\hat{q}, \hat{p}] = i\hbar \tag{5.43}$$

$$[f(\hat{q}), \hat{p}] = i\hbar f'(\hat{q}) \tag{5.44}$$

$$[\hat{q}, \hat{q}] = [\hat{p}, \hat{p}] = 0 \tag{5.45}$$

and the Pauli operator commutator relations

$$[\sigma_i, \sigma_j] = 2i\epsilon_{ijk}\sigma_k \tag{5.46}$$

(where ϵ_{ijk} is the Levi-Cevita symbol). Also note that the spin and canonical operators commute

$$[\hat{p}, \hat{\sigma}_i] = [\hat{q}, \hat{\sigma}_i] = 0. \tag{5.47}$$

Though the spin operator notation has been used here, it will be useful to keep in mind that in bra-ket notation they can be represented in the orthogonal electron-hole basis as

$$\sigma_1 = |e\rangle\langle h| + |h\rangle\langle e| \tag{5.48}$$

$$\sigma_2 = i\left(|h\rangle\langle e| - |e\rangle\langle h|\right) \tag{5.49}$$

$$\sigma_3 = |e\rangle\langle e| - |h\rangle\langle h|. \tag{5.50}$$

It will also be useful to consider the non-hermitian lowering and raising operators defined as $\sigma_\pm = (1/2)[\sigma_1 \pm i\sigma_2]$ with the commutation relations

$$[\sigma_3, \sigma_\pm] = \pm 2\sigma_\pm \tag{5.51}$$

$$[\sigma_+, \sigma_-] = \sigma_3. \tag{5.52}$$

First considering the expectation values of the spin operators, which describe values of complex β on the Bloch sphere as outlined in section 3.1, in switching from product to E-H states the magnitude of β is unaffected

$$\langle z \otimes \beta | \sigma_3(0) | z \otimes \beta \rangle \equiv \langle z \bowtie \beta | \sigma_3(0) | z \bowtie \beta \rangle = \frac{1 - |\beta|^2}{1 + |\beta|^2} \tag{5.53}$$

as we might be expected from the diagonal nature of σ_3. The change in the expectation values of σ_1 and σ_2 is (omitting the normalization)

$$\langle z \otimes \beta | \sigma_1(0) | z \otimes \beta \rangle = 2\operatorname{Re}(\beta) \quad \rightarrow \quad \langle z \bowtie \beta | \sigma_1(0) | z \bowtie \beta \rangle = 2\operatorname{Re}(\beta^* \langle \psi | \psi^* \rangle) \tag{5.54}$$

$$\langle z \otimes \beta | \sigma_2(0) | z \otimes \beta \rangle = 2\operatorname{Im}(\beta) \quad \rightarrow \quad \langle z \bowtie \beta | \sigma_2(0) | z \bowtie \beta \rangle = 2\operatorname{Im}(\beta^* \langle \psi | \psi^* \rangle). \tag{5.55}$$

The most important feature of note is the added dependence on the overlap of the state and its conjugate. If $|z\rangle$ is located at p_0 then the conjugate wave packet is located at $-p_0$. The overlap is given by $\exp(-\lambda V_0^2)$, which can be especially small when $V_0 \geq p_{\mathrm{F}}$.

With these elements in hand; under the BdG Hamiltonian as defined in section 4.2 with no magnetic vector potential ($\boldsymbol{A} = 0$), but for generality an external potential $U(\hat{q})$, the Heisenberg equations of motion on phase space

are

$$\frac{d}{dt}\hat{q}(t) = \frac{1}{m}\hat{V}(t) \tag{5.56}$$

$$\frac{d}{dt}\hat{p}(t) = -U'(\hat{q}(t))\sigma_3(t) - \Delta'(\hat{q}(t))\sigma_1(t) \tag{5.57}$$

$$\frac{d}{dt}\hat{V}(t) = -U'(\hat{q}(t)) + \frac{1}{\hbar}\{\Delta(\hat{q}(t)), \hat{p}(t)\}\sigma_2(t) \tag{5.58}$$

and quasi-spin

$$\frac{d}{dt}\sigma_1(t) = -\frac{2}{\hbar}\hat{\mathcal{H}}_0\sigma_2(t) \tag{5.59}$$

$$\frac{d}{dt}\sigma_2(t) = \frac{2}{\hbar}\left(\hat{\mathcal{H}}_0\sigma_1(t) - \Delta(\hat{q}(t))\sigma_3(t)\right) \tag{5.60}$$

$$\frac{d}{dt}\sigma_3(t) = \frac{2}{\hbar}\Delta(\hat{q}(t))\sigma_2(t). \tag{5.61}$$

Here the anti-commutator $\{\hat{A}, \hat{B}\} = \hat{A}\hat{B} + \hat{B}\hat{A}$ has been used. These equations are somewhat simplified for the raising and lowering operators

$$\frac{d}{dt}\sigma_\pm(t) = \pm\frac{i}{\hbar}\left(2\hat{\mathcal{H}}_0\sigma_\pm(t) + \Delta(\hat{q}(t))\sigma_3(t)\right) \tag{5.62}$$

$$\frac{d}{dt}\sigma_3(t) = \frac{2i}{\hbar}\Delta(\hat{q}(t))\left(\sigma_-(t) - \sigma_+(t)\right). \tag{5.63}$$

In this general case it proves difficult to find a closed set of solutions to the ordered set of equations of motion.

The short time behaviour can be estimated by expanding the time dependent operator as

$$\hat{A}(t) = \hat{A}(0) + \frac{d\hat{A}(0)}{dt}t + \mathcal{O}(t^2). \tag{5.64}$$

Given that in the Heisenberg picture

$$\left\langle\frac{d}{dt}\hat{A}(t)\right\rangle = \frac{d}{dt}\langle\hat{A}(t)\rangle \tag{5.65}$$

the first order term can be evaluated with respect to either a product or E-H state. Firstly for a general product state

$$|\Psi \otimes \beta\rangle = \frac{1}{\sqrt{1 + |\beta|^2}}\left(|e\rangle + \beta|h\rangle\right) \otimes |\Psi\rangle \tag{5.66}$$

(labelling $N_\pm(\beta) = 1 \pm |\beta|^2$ for brevity) the first order terms are for the

phase space operators are

$$\frac{d}{dt}\langle\hat{q}(0)\rangle_\otimes = \frac{1}{m}\left(\frac{N_-(\beta)}{N_+(\beta)}\right)\langle\psi|\hat{p}(0)|\psi\rangle \tag{5.67}$$

$$\frac{d}{dt}\langle\hat{p}(0)\rangle_\otimes = -\frac{1}{N_+(\beta)}\left[N_-(\beta)\langle\psi|U'(\hat{q}(0))|\psi\rangle + 2\operatorname{Re}(\beta)\langle\psi|\Delta'(\hat{q}(0))|\psi\rangle\right]$$
$$\tag{5.68}$$

$$\frac{d}{dt}\langle\hat{V}(0)\rangle_\otimes = -\langle\psi|U'(\hat{q}(0))|\psi\rangle + \frac{2}{\hbar}\left(\frac{\operatorname{Im}(\beta)}{N_+(\beta)}\right)\langle\psi|\{\Delta(\hat{q}(0)),\hat{p}(0)\}|\psi\rangle$$
$$\tag{5.69}$$

and for the quasi-spin operators

$$\frac{d}{dt}\langle\sigma_1(0)\rangle_\otimes = -\frac{4}{\hbar}\frac{\operatorname{Im}(\beta)}{N_+(\beta)}\langle\psi|\hat{\mathcal{H}}_0|\psi\rangle \tag{5.70}$$

$$\frac{d}{dt}\langle\sigma_2(0)\rangle_\otimes = \frac{2}{\hbar}\frac{1}{N_+(\beta)}\left[2\operatorname{Re}(\beta)\langle\psi|\hat{\mathcal{H}}_0|\psi\rangle - N_-(\beta)\langle\psi|\Delta(\hat{q}(0))|\psi\rangle\right] \tag{5.71}$$

$$\frac{d}{dt}\langle\sigma_3(0)\rangle_\otimes = \frac{4}{\hbar}\frac{\operatorname{Im}(\beta)}{N_+(\beta)}\langle\psi|\Delta(\hat{q}(0))|\psi\rangle. \tag{5.72}$$

As might be expected of a product state the phase space and spin operators act independently on their corresponding spaces. This creates a strong dependence on β, this can be seen in particular for the dynamics of the expected position. If $\beta = 0, \infty$ such that that the state only consists of an electron or hole component, it has the form of an Ehrenfest relation. If $|\beta|^2 = 1$ though, the expected position is stationary. The (total) momentum operator can be somewhat misleading. In this case if the initial wave packet is an equal superposition and β is purely imaginary, it would show a constant momentum despite an external potential. The pseudo-velocity operator equation coincides with the Ehrenfest relation if $\operatorname{Im}(\beta) = 0$, suggesting additional dynamics dependent upon complex phase of the of the initial state.

The corresponding general E-H state is given by

$$|\boldsymbol{\psi} \bowtie \beta\rangle = \frac{1}{\sqrt{1+|\beta|^2}}\left(|e\rangle\otimes|\psi\rangle + \beta^*|h\rangle\otimes|\psi^*\rangle\right). \tag{5.73}$$

The respective expectation value equations are

$$\frac{d}{dt}\langle \hat{q}(0)\rangle_\bowtie = \frac{1}{m}\langle \psi|\hat{p}|\psi\rangle \tag{5.74}$$

$$\frac{d}{dt}\langle \hat{p}(0)\rangle_\bowtie = -\frac{1}{N_+(\beta)}\left[\langle \psi|U'(\hat{q}(0))|\psi\rangle - |\beta|^2\langle \psi^*|U'(\hat{q}(0))|\psi^*\rangle\right]$$
$$-\frac{1}{N_+(\beta)}\left[\beta^*\langle \psi|\Delta'(\hat{q}(0))|\psi^*\rangle + \beta\langle \psi^*|\Delta'(\hat{q}(0))|\psi\rangle\right] \tag{5.75}$$

$$\frac{d}{dt}\langle \hat{V}(0)\rangle_\bowtie = -\frac{1}{N_+(\beta)}\left[\langle \psi|U'(\hat{q}(0))|\psi\rangle + |\beta|^2\langle \psi^*|U'(\hat{q}(0))|\psi^*\rangle\right]$$
$$+\frac{i}{\hbar}\frac{1}{N_+(\beta)}\left[\beta\langle \psi^*|\{\Delta(\hat{q}(0)),\hat{p}(0)\}|\psi\rangle - \beta^*\langle \psi|\{\Delta(\hat{q}(0)),\hat{p}(0)\}|\psi^*\rangle\right]$$
$$\tag{5.76}$$

and

$$\frac{d}{dt}\langle \sigma_1(0)\rangle_\bowtie = -\frac{2i}{\hbar}\frac{1}{N_+(\beta)}\left[\beta\langle \psi^*|\hat{\mathcal{H}}_0|\psi\rangle - \beta^*\langle \psi|\hat{\mathcal{H}}_0|\psi^*\rangle\right] \tag{5.77}$$

$$\frac{d}{dt}\langle \sigma_2(0)\rangle_\bowtie = \frac{2}{\hbar}\frac{1}{N_+(\beta)}\left[\beta^*\langle \psi|\hat{\mathcal{H}}_0|\psi^*\rangle + \beta\langle \psi^*|\hat{\mathcal{H}}_0|\psi\rangle\right]$$
$$+\frac{2}{\hbar}\frac{1}{N_+(\beta)}\left[\langle \psi|\Delta(\hat{q}(0))|\psi\rangle - |\beta|^2\langle \psi^*|\Delta(\hat{q}(0))|\psi^*\rangle\right] \tag{5.78}$$

$$\frac{d}{dt}\langle \sigma_3(0)\rangle_\bowtie = \frac{2i}{\hbar}\frac{1}{N_+(\beta)}\left[\beta\langle \psi^*|\Delta(\hat{q}(0))|\psi\rangle - \beta^*\langle \psi|\Delta(\hat{q}(0))|\psi^*\rangle\right]. \tag{5.79}$$

As noted in the transfer from product to E-H states there is an dependence on the overlap of states and their conjugate. But the expected position no longer has any dependence on the electron-hole degree of freedom described by β suggesting that the two components of the wave packet move together. It remains to be seen if this leads to semiclassical trajectories though.

It will also be important to consider the time dependent variance of the operators. It has been shown in section 2.2 that in the scalar case the width of the wave packet grows linearly with time. The infinitesimal time dependence of the variance of an operator is given by

$$\frac{d}{dt}\text{Var}(\hat{A}(t)) = \frac{d}{dt}\langle \hat{A}^2(t)\rangle - 2\langle \hat{A}(t)\rangle\frac{d}{dt}\langle \hat{A}(t)\rangle \tag{5.80}$$

which requires the time dependence of the square of the operators. For the velocity operator this is

$$\frac{d}{dt}(\hat{V}^2(t)) = \frac{d}{dt}(\hat{p}^2(t)) = -\left\{\hat{V}(t),U'(\hat{q}(t))\right\} - \{\Delta'(\hat{q}(t)),\hat{p}(t)\}\sigma_1(t) \tag{5.81}$$

and $\hat{q}(t)$

$$\frac{d}{dt}(\hat{q}^2(t)) = \frac{1}{m}\left\{\hat{V}(t),\hat{q}(t)\right\}. \tag{5.82}$$

82

The time dependence of the spatial variance is then given by

$$\frac{d}{dt}\text{Var}(\hat{q}(t)) = \frac{1}{m}\left[\langle\sigma_3(t)\{\hat{p}(t),\hat{q}(t)\}\rangle - \langle\hat{q}(t)\rangle\langle\sigma_3(t)\hat{p}(t)\rangle\right]. \quad (5.83)$$

Without any further information about the time dependence of the operators additional information about the difference between the E-H and product states cannot be directly found. We therefore look at the short time behaviour of the position operator

$$\hat{q}(t) = \hat{q}(0) + t\frac{d}{dt}\hat{q}(0) + \mathcal{O}(t^2) \quad (5.84)$$

$$= \hat{q}(0) + \frac{t}{m}\hat{V}(0) + \mathcal{O}(t^2) \quad (5.85)$$

for which the variance is then given by

$$\text{Var}(\hat{q}(t)) = \left\langle\left(\hat{q}(0) + \frac{t}{m}\hat{V}(0)\right)^2\right\rangle - \left(\langle\hat{q}(0)\rangle + \frac{t}{m}\langle\hat{V}(0)\rangle\right)^2 + \mathcal{O}(t^2)$$

$$(5.86)$$

$$= \text{Var}(\hat{q}(0)) + t\frac{d}{dt}\text{Var}(\hat{q}(0)) + \left(\frac{t}{m}\right)^2\text{Var}(\hat{V}(0)) + \mathcal{O}(t^2). \quad (5.87)$$

This result can be compared with the variance of the position operator in the scalar (free particle) case, given for short times by $\hat{q}(t) = q(0) + t\hat{p}(0)/m$. With respect to both the E-H and product coherent state the first two terms of Equation (5.87) give equivalent results to the scalar expectation values. There is a discrepancy in the third term though. With respect to the E-H coherent states this term is still equivalent to the scalar operator with respect to the scalar coherent state as

$$\text{Var}(\hat{V}(0))_{\bowtie} \equiv \text{Var}(\hat{p}(0))_{|z\rangle} \quad (5.88)$$

indipendent of the value of β. The same value with respect to the E-H coherent states is

$$\text{Var}(\hat{V}(0))_{\otimes} = \langle z|\hat{p}^2(0)|z\rangle - \left(\frac{1 - |\beta|^2}{1 + |\beta|^2}\right)^2\langle z|\hat{p}(0)|z\rangle^2. \quad (5.89)$$

This will only be equivalent to the scalar case if $|\beta|^2 = 0$. If $|\beta|^2 = 1$, the discrepancy from the scalar example is

$$\text{Var}(\hat{V}(0))_{\otimes} = \text{Var}(\hat{p})_{|z\rangle} + 2\langle z|\hat{p}(0)|z\rangle^2. \quad (5.90)$$

This demonstrates that at least for short times the E-H state grows like a free scalar coherent state. The additional growth shown by the product

state can be especially large if we are considering states close to or above the Fermi momentum. For the rest of this chapter we will only consider superconductors with a spatially homogeneous band-gap, and as such a time indipendent energy spectra. For a spatially dependent band-gap though it may in future work prove useful to consider the *adiabatic approximation.*

Generally speaking the adiabatic theorem states that a system will remain in its instantaneous eigenstate if a perturbation acts slowly enough. Let us as an example first consider the model developed by Born and Oppenheimer [68]. To analyse the behaviour of the electron-nucleus system they noted that that since the ratio of the mass of the electron to the mass of the nucleus, m_e/M is small; it can used as an expansion parameter for the energy spectra of the molecular electron-nucleus system. Without derivation, the physical picture is that the velocity of the nucleus is slow (on the atomic scale) in comparison to that of the electron. The electron therefore quickly adapts to the motion of the nucleus (i.e. adiabatically) remaining at their initial energy level. The dynamics of the nucleus can then be treated semiclassically. This work has proved a key feature of quantum-chemistry greatly simplify atomic problems with a large number of degrees of freedom. The study of Born-Oppenheimer approximations have produced a large body of work with notable work by Hagedorn [69] on the time-dependent Born-Oppenheimer approximation and Spohn and Teufel [70] to name a few.

For the two level electron-hole system we considered in this thesis there is a clear analogue in the model analysed by Landau [71] and Zener [72]. They consider a two-level system with a time-dependent diagonal Hamiltonian $\mathcal{H}_0(t)$ and eigenstates $|1\rangle$ and $|2\rangle$ with degenerate energy levels at a certain value of t (the *diabatic* system). If a (time-indipendent) off-diagonal perturbation is introduced coupling the eigenstates, the energy levels will now repel where they would have crossed for the unperturbed Hamiltonian. This is commonly referred to as *avoided crossing.* If the simplification is made that $\mathcal{H}_0(t)$ varies linearly; the Landau-Zerner formula gives the probability that as the energy gap between the eigenstates varies with time, the state will make a non-adiabatic transition between energy levels. If the energy levels vary slowly the adiabatic approximation indicates that the state will remain at the initial energy level, but faster variations allow for non-adiabatic energy level transitions despite the avoided crossing.

When considering a spatially inhomogeneous superconductor there are

two questions we might consider:

- If the band gap varies slowly for wavepackets propagating at the Fermi velocity can the quasi-spin and phase space dynamics be treated in an indipendent manner in the style of the Born-Oppenheimer approximation. Could one set of dynamics be treated in a semiclassical manner whilst the other behaves adiabatically?

- The BdG has avoided crosses at $\pm p_{\mathrm{F}}$ due to the perturbation of $\sigma_3 \mathcal{H}_0(\hat{p})$ by Δ in the the BdG Hamiltonian. As can be seen from the BdG dispersion relation (Figure 5.1) in a normal conductor the energy curves of the electron and hole quasi-particles intersect at $\pm p_{\mathrm{F}}$ where conversely the dispersion relation has a minimum at $\pm p_{\mathrm{F}}$ in a superconductor. Could we therefore consider a generalization of the Landau-Zerner effect for transitions between electron-like and hole-like energy bands? This could include quantifying an adiabatic condition for the BdG equations.

These are possible directions for future analysis of the BdG equations, though we will not consider them further in this thesis.

5.3.1 Normal Conductor

First as the simplest dynamic example we consider a normally conducting region where $\Delta(\hat{q}) = 0$. Although we know the BdG equations are decoupled, and the dynamics relatively simple, it will serve to illustrate the need for E-H states and their relation to classical trajectories. In this case the phase space Heisenberg equations of motion, 5.56 and 5.57, simplify to

$$\frac{d}{dt}\langle \hat{q}(t) \rangle = \frac{1}{m}\langle \hat{V}(t) \rangle \tag{5.91}$$

$$\frac{d}{dt}\langle \hat{p}(t) \rangle = -\langle U'(\hat{q}(t))\sigma_3(t) \rangle \tag{5.92}$$

which look very much like the Ehrenfest relations for the scalar system the obvious difference being $\sigma_3(t)$ dependence contained in both the expectation values on the right. We will use the projection operators defined in section 3.4 to define the projections of expectation of the electron and hole components as

$$\langle \hat{A} \rangle_e = \frac{\langle \hat{\mathcal{P}}_e \hat{A} \hat{\mathcal{P}}_e \rangle}{\langle \hat{\mathcal{P}}_e \rangle} \quad \text{and} \quad \langle \hat{A} \rangle_h = \frac{\langle \hat{\mathcal{P}}_h \hat{A} \hat{\mathcal{P}}_h \rangle}{\langle \hat{\mathcal{P}}_h \rangle}. \tag{5.93}$$

Then the expected position of each component with respect to a product state is

$$\frac{d}{dt}\langle\hat{q}(t)\rangle_{e,\otimes} = \frac{1}{m}\langle\hat{p}(t)\rangle_{e,\otimes} \qquad \frac{d}{dt}\langle\hat{p}(t)\rangle_{e,\otimes} = -\langle U'(\hat{q}(t))\rangle_{e,\otimes} \qquad (5.94)$$

and

$$\frac{d}{dt}\langle\hat{q}(t)\rangle_{h,\otimes} = -\frac{1}{m}\langle\hat{p}(t)\rangle_{h,\otimes} \qquad \frac{d}{dt}\langle\hat{p}(t)\rangle_{h,\otimes} = \langle U'(\hat{q}(t))\rangle_{h,\otimes}. \qquad (5.95)$$

These are merely the Ehrenfest relations for an independent electron and the corresponding time reversed hole. If we instead consider the pseudo-velocity equation of motion (simplified from equation 5.58)

$$\frac{d}{dt}\langle\hat{V}(t)\rangle = -\langle U'(\hat{q}(t))\rangle \qquad (5.96)$$

pairing this with the expected position they have the form of the Ehrenfest relations for a particle defined by the mean pseudo-velocity. The electron-hole quasi-spin dynamics take the form

$$\frac{d}{dt}\langle\sigma_1(t)\rangle = -\frac{2}{\hbar}\langle\hat{\mathcal{H}}_0\sigma_2(t)\rangle \qquad (5.97)$$

$$\frac{d}{dt}\langle\sigma_2(t)\rangle = \frac{2}{\hbar}\langle\hat{\mathcal{H}}_0\sigma_1(t)\rangle \qquad (5.98)$$

$$\frac{d}{dt}\langle\sigma_3(t)\rangle = 0. \qquad (5.99)$$

The time independence of $\langle\sigma_3(t)\rangle$ should be expected as the lack of interaction between the electron and hole means their relative amplitude remains constant at the initial value $\langle\sigma_3\rangle = (1-|\beta|^2)/(1+|\beta|^2)$ indipendent of the choice of initial product or E-H wave packet. The time dependence of the relative phase components, $\sigma_1(t)$ and $\sigma_2(t)$, can be interpreted as being due to the change in relative phase of the plane wave solutions as they propagate. The time dependent operators are found to be

$$\sigma_2(t) = \sigma_2(0)\cos\left(\frac{2t}{\hbar}\mathcal{H}_0\right) + \sigma_1(0)\sin\left(\frac{2t}{\hbar}\mathcal{H}_0\right) \qquad (5.100)$$

$$\sigma_1(t) = \sigma_1(0)\cos\left(\frac{2t}{\hbar}\mathcal{H}_0\right) - \sigma_2(0)\sin\left(\frac{2t}{\hbar}\mathcal{H}_0\right) \qquad (5.101)$$

or equivalently in terms of the raising and lowering operators

$$\sigma_2(t) = i\left[\sigma_-(0)e^{-2it\mathcal{H}_0/\hbar} - \sigma_+(0)e^{2it\mathcal{H}_0/\hbar}\right] \qquad (5.102)$$

$$\sigma_1(t) = \sigma_+(0)e^{2it\mathcal{H}_0/\hbar} + \sigma_-(0)e^{-2it\mathcal{H}_0/\hbar}. \qquad (5.103)$$

In this form it is clear that these are the contribution from the interference between positive and negative energy branches as they propagate in opposite

directions. Their expected values with respect to a product coherent state is simply

$$\langle \sigma_2(t) \rangle_\otimes = \frac{i}{1 + |\beta|^2} \left[\beta^* \langle z | e^{-2it\mathcal{H}_0/\hbar} | z \rangle - \beta \langle z | e^{2it\mathcal{H}_0/\hbar} | z \rangle \right] \quad (5.104)$$

$$\langle \sigma_1(t) \rangle_\otimes = \frac{1}{1 + |\beta|^2} \left[\beta^* \langle z | e^{-2it\mathcal{H}_0/\hbar} | z \rangle + \beta \langle z | e^{2it\mathcal{H}_0/\hbar} | z \rangle \right] \quad (5.105)$$

where as for the E-H coherent state they are

$$\langle \sigma_2(t) \rangle_\bowtie = \frac{i}{1 + |\beta|^2} \left[\beta \langle z^* | e^{-2it\mathcal{H}_0/\hbar} | z \rangle - \beta^* \langle z | e^{2it\mathcal{H}_0/\hbar} | z^* \rangle \right] \quad (5.106)$$

$$\langle \sigma_1(t) \rangle_\bowtie = \frac{1}{1 + |\beta|^2} \left[\beta \langle z^* | e^{-2it\mathcal{H}_0/\hbar} | z \rangle + \beta^* \langle z | e^{2it\mathcal{H}_0/\hbar} | z^* \rangle \right] . \quad (5.107)$$

The E-H coherent states suppress these interference effects if the overlap of the coherent state and it's conjugate is small.

It is clear then as to why the E-H state definition is required. The two components, although they may have the same initial position in phase space, they will quickly separate as they move in opposite directions. Furthermore if we consider a normal conductor with no external potentials (i.e. $U(\hat{q}) = 0$) such that $d\langle \hat{V} \rangle/dt = 0$ then it is straightforward to solve the differential equation and see that for an initial product coherent state, the components will separate proportional to their initial velocity V_0 as

$$\langle \hat{q}(t) \rangle_\otimes = \frac{t}{m} \left(\frac{1 - |\beta|^2}{1 + |\beta|^2} \right) \langle z | \hat{p} | z \rangle. \quad (5.108)$$

This can be pictured as being due to expected value being located between the two separating states, depending on their relative initial weights. As seen in the general case, for a state with equally weighted electron and hole components (i.e. $|\beta| = 1$) $\langle \hat{q}(t) \rangle_\otimes = 0$, as the motion of the two components cancel each other. If we now calculate the expectation value with respect to the E-H states then

$$\langle \hat{V} \rangle_\bowtie = \frac{1}{1 + |\beta|^2} \left[\langle z | \hat{p} | z \rangle - |\beta|^2 \langle z^* | \hat{p} | z^* \rangle \right] = \langle z | \hat{p} | z \rangle \quad (5.109)$$

as it's straightforward to see that

$$\langle z | \hat{p} | z \rangle \propto \langle z | (\hat{a}^\dagger - a) | z \rangle = -\langle z^* | (\hat{a}^\dagger - a) | z^* \rangle. \quad (5.110)$$

The action of the $\hat{\mathcal{Z}}$ operator inverts the expected momentum such that the projected velocities are

$$\frac{1}{\langle \hat{\mathcal{P}}_e \rangle} \frac{d}{dt} \langle \hat{\mathcal{P}}_e \hat{q} \hat{\mathcal{P}}_e \rangle_\bowtie = \frac{1}{\langle \hat{\mathcal{P}}_h \rangle} \frac{d}{dt} \langle \hat{\mathcal{P}}_h \hat{q} \hat{\mathcal{P}}_h \rangle_\bowtie. \quad (5.111)$$

It follows that

$$\langle \hat{q}(t) \rangle_{\bowtie} = \frac{t}{m} \langle z | \hat{p} | z \rangle \tag{5.112}$$

in this simple case, indicating the E-H coherent state follows the scalar trajectory.

In a normal region the variances of the phase space operators are straightforward to calculate, and found to be

$$\frac{d}{dt} \text{Var}(\hat{q}) = \frac{1}{m} \left[\langle \{\hat{q}, \hat{p}\} \sigma_3 \rangle - 2 \langle \hat{q} \rangle \langle \hat{V} \rangle \right] \tag{5.113}$$

and

$$\frac{d}{dt} \text{Var}(\hat{V}) = 2 \langle \hat{V} \rangle \langle U'(\hat{q}) \rangle \tag{5.114}$$

meaning with no external potentials the variance in pseudo-velocity is constant in a normal region. Since the time dependent operators in this case are simply

$$\hat{V}(t) = \hat{V}_0 \qquad \text{and} \qquad \hat{q}(t) = \frac{t}{m} \hat{V}_0 + \hat{q}(0). \tag{5.115}$$

Inserted back into the time dependent variance of $\hat{q}(t)$ means that

$$\frac{d}{dt} \text{Var}(\hat{q}) = \frac{2t}{m^2} \left[\langle \hat{V}_0^2 \rangle - \langle \hat{V}_0 \rangle^2 \right] = \frac{2t}{m^2} \text{Var}(\hat{V}_0). \tag{5.116}$$

The time dependence of the spatial variance with respect to the product coherent state is

$$\frac{d}{dt} \text{Var}(\hat{q})_{\otimes} = \frac{2t}{m^2} \left[\langle z | \hat{p}^2 | z \rangle - \left(\frac{N_-(\beta)}{N_+(\beta)} \langle z | \hat{p} | z \rangle \right)^2 \right] \tag{5.117}$$

which for a initially only electron or hole state behaves like a single particle but, but not for a general superposition. For a balanced wave packet ($|\beta|^2 = 1$) the variance will contain additional terms dependent on the expected momentum, which can be especially large for a wave packet centred on the Fermi momentum, quickly destroying any localisation.

The same value with respect to the E-H coherent states is given by

$$\frac{d}{dt} \text{Var}(\hat{q})_{\bowtie} = \frac{2t}{m^2} \left[\langle z | \hat{p}^2 | z \rangle - \langle z | \hat{p} | z \rangle^2 \right] = \frac{2t}{m^2} \text{Var}(\hat{p}). \tag{5.118}$$

This is equivalent to a scalar coherent state, with no β dependence evidenced by the product state.

For this simple example at least, E-H coherent states retain localisation in position-velocity phase space, where product states quickly lose localisation in general. This makes them more suitable for classical-quantum

correspondence purposes, having all the advantages of coherent states. As we've seen, and might have expected given the plane wave solutions derived for the time independent case, the dynamics and derived trajectories are somewhat trivial in a normally conducting region (and defining states that remain coherent is also fairly trivial only requiring time reversal of the hole component). The interesting dynamics will arise where coupling between the components is introduced, in particular we are interested in the wave packets concentrated about the Fermi momentum where wave packets consist of equally weighted superpositions of electron and hole components. Far from the Fermi momentum we've shown with the dispersion relation that the components are predominantly electron or hole-like, and thus we would expect to behave much like wave packets in the normal conductor.

5.3.2 Spatially Homogeneous Superconductor

We now consider (and for the rest of this chapter) a spatially homogeneous superconductor defined by the spatially independent band gap $\Delta(q) = \Delta_0 > 0$. The set of Heisenberg equations of motion then simplify to

$$\frac{d}{dt}\hat{q}(t) \;=\; \frac{1}{m}\hat{V}(t) \tag{5.119}$$

$$\frac{d}{dt}\hat{p}(t) \;=\; -U'(\hat{q})\sigma_3(t) \tag{5.120}$$

$$\frac{d}{dt}\hat{V}(t) \;=\; -U'(\hat{q}) + \frac{2}{\hbar}\Delta_0\hat{p}(t)\sigma_2(t) \tag{5.121}$$

$$\frac{d}{dt}\sigma_1(t) \;=\; -\frac{2}{\hbar}\hat{\mathcal{H}}_0\sigma_2(t) \tag{5.122}$$

$$\frac{d}{dt}\sigma_2(t) \;=\; \frac{2}{\hbar}\left[\hat{\mathcal{H}}_0\sigma_1(t) - \Delta_0\sigma_3(t)\right] \tag{5.123}$$

$$\frac{d}{dt}\sigma_3(t) \;=\; \frac{2}{\hbar}\Delta_0\sigma_2(t). \tag{5.124}$$

In the absence of external potentials the total expected momentum is time independent. This will provide a constant of integration which allows analytic solutions to the differential equations. The time derivative of the expected pseudo-velocity now depends on the expectation $\langle\hat{p}\sigma_2(t)\rangle$. The time derivative of the expected position retains the form of an Ehrenfest relation (this is in general true), albeit with the right hand side dependent on the expected pseudo-velocity. We can consider rewriting the equations of motion in terms of the pseudo-velocity operator instead of momentum as a means of representing trajectories on position-pseudo-velocity phase space.

Rewriting the time derivative of the expected velocity as

$$\frac{d}{dt}\langle \hat{V}(t)\rangle = -\frac{2i}{\hbar}\Delta_0 \langle \hat{V}(t)\sigma_1(t)\rangle. \tag{5.125}$$

This can readily also be extended to the Hamiltonian as

$$\hat{\mathcal{H}}_0 = \frac{\hat{p}^2}{2m} - \mu \equiv \frac{\hat{V}^2}{2m} - \mu \tag{5.126}$$

which also implies that $\hat{V}^2(t)$ is time independent in this case. Like the Ehrenfest relation we would like to be able to reformulate the equations of motion in terms of expectation values. This suggests that we seek the separation of the expectation values of the form

$$\langle \hat{V}(t)\sigma_1(t)\rangle \sim \langle \hat{V}(t)\rangle\langle\sigma_1(t)\rangle. \tag{5.127}$$

Presently it is unclear if such an approximation can be made utilizing the E-H coherent states.

Let us now consider solving the ordered differential equations 5.119 - 5.124 for $\Delta_0 > 0$ and $U(q) = 0$. As Δ_0 is indipendent of $\hat{q}(t)$, the time dependent quasi-spin operators form a self contained system, with analytic solutions. A full derivation of the solutions is given A.2.1. From the time dependent spin operators it is then straightforward to also calculate the time dependent pseudo-velocity (given that $\hat{V}(t) = \hat{p}\sigma_3(t)$) and the time dependent position operator as $q(t) = \frac{\hat{p}}{m}\int \sigma_3(t)dt$.

The set of time dependent operators can then be written in terms of the the quasi-spin operators at time 0 and $\hat{p}$ (the position operator doesn't enter explicitly except as a constant of integration in $\hat{q}(t)$). We can write the time dependent quasi-spin operators in general form as the linear sum over contributions of the form

$$\sigma_i(t) = \sum_{j=1}^{3}\sigma_j(0)f_j(\hat{p}, t) + \mathbb{I}g(\hat{p}). \tag{5.128}$$

which will be used in the following section.

5.4 Dynamics of the Moments of Coherent State Wave packets

Though the set of time dependent operators formally contain all the information about the dynamics under the BdG Hamiltonian, it will require

further analysis in order to extract useful information about the moments with respect to E-H and product coherent states. Though a simple example we have shown that the E-H coherent states remain localised in a normal conductor where product states will quickly separate unless they consist of only electron or hole components.

We consider two main questions in this section, firstly how the expectation values and variances differ between E-H and product coherent states in this system. Further consideration will be given as to how the dependence on the initial amplitude of the electron and hole of a initial product wave packet affects the dynamics of the moments. We would expect that a product state that is an equal superposition of electron and hole components will again initially separate. We should also consider how the dependence on the overlap of the coherent states and their conjugate introduced by the E-H wave packet effects their dynamics.

Secondly we will consider both the effect of the parameters that define the superconducting system (in particular the values of Δ_0 and μ that describe the superconducting system), and also the width and central momentum of the initial wave packet.

We have shown in section 5.1 that the dispersion relation indicates that wave packets centred on momenta much larger than the Fermi momentum, or close to zero (as long as $\mu \gg \Delta_0$), will have electron and hole components that very much behave like independent free wave packets. Each component will predominantly consist of superpositions of stationary states from the positive and negative branches respectively. Although we will consider these regimes (mainly as examples) we will mainly focus on wave packets located at $V_0 \approx p_\mathrm{F}$ where the stationary states are balanced superpositions of electron and hole components. The dispersion relation predicts that these wave packets will have zero group velocity, despite the expected values of the velocity having large values.

Given that the time dependent operators can be written in the general form given in equation 5.128, the lack of $\hat{q}$ dependence means it is convenient to resolve the expectation values of each term in the integral form

$$\langle \psi, \beta | \sigma_i(0) f_i(\hat{p}, t) | \psi, \beta \rangle = \int \langle \psi, \beta | \sigma_i(0) f_i(\hat{p}, t) | p \rangle \langle p | \psi, \beta \rangle \, dp \qquad (5.129)$$

$$= \int f_i(p, t) \langle \psi, \beta | p \rangle \sigma_i(0) \langle p | \psi, \beta \rangle \, dp \qquad (5.130)$$

given here for some general 2-component (E-H or product) state $|\psi, \beta\rangle$. In general it has not been possible to find closed analytic solutions for these

integrals. We will therefore consider several approximations, in particular devoting sub-section 5.4.5 to the long time asymptotic behaviour of E-H coherent state wave packets.

Some of the differences between the product and E-H coherent states have been shown in the previous section, and the time dependent operators presented in this form will also allow a clear measure of how these two types of coherent state behave.

The expectation values of the off diagonal components with respect to the product coherent state are given by

$$\langle \sigma_1(0) f_1(\hat{p}, t) \rangle_{\otimes} = \frac{2\,\text{Re}(\beta)}{N_+(\beta)} \langle z| f_1(\hat{p}, t)|z \rangle \tag{5.131}$$

$$= \frac{2\,\text{Re}(\beta)}{N_+(\beta)} \sqrt{\frac{\lambda}{\pi}} \int f_1(p, t) e^{-\lambda(p-V_0)^2} dp \tag{5.132}$$

$$\langle \sigma_2(0) f_2(\hat{p}, t) \rangle_{\otimes} = \frac{2\,\text{Im}(\beta)}{N_+} \langle z| f_2(\hat{p}, t)|z \rangle \tag{5.133}$$

$$= \frac{2\,\text{Im}(\beta)}{N_+(\beta)} \sqrt{\frac{\lambda}{\pi}} \int f_2(p, t) e^{-\lambda(p-V_0)^2} dp \tag{5.134}$$

(where $\lambda = 1/m\hbar\omega$ is the scaled squeezing parameter). As shown previously, quasi-spin operators and $\hat{p}$ dependent terms act on their respective Hilbert spaces independently, the spin operators merely select out the β dependence of each component, and thus show a strong dependence on the initial phase between electron and hole components of the initial wave packet.

The same expectation values with respect to the E-H coherent states are given in integral form as

$$\langle \sigma_1(0) f_1(\hat{p}, t) \rangle_{\bowtie} = \sqrt{\frac{\lambda}{\pi}} \, \langle \sigma_1(0) \rangle_{\bowtie} \int f_1(p, t) e^{-\lambda p^2} \, dp \tag{5.135}$$

$$\langle \sigma_2(0) f_2(\hat{p}, t) \rangle_{\bowtie} = \sqrt{\frac{\lambda}{\pi}} \, \langle \sigma_2(0) \rangle_{\bowtie} \int f_2(p, t) e^{-\lambda p^2} \, dp. \tag{5.136}$$

For brevity we have used

$$\langle \sigma_1(0) \rangle_{\bowtie} = \left(\frac{2\,\text{Re}(\beta)}{N_+(\beta)} \right) e^{-\lambda V_0^2} \qquad \text{and} \qquad \langle \sigma_2(0) \rangle_{\bowtie} = \left(\frac{2\,\text{Im}(\beta)}{N_+(\beta)} \right) e^{-\lambda V_0^2}. \tag{5.137}$$

Like the normal conductor example these off diagonal terms are suppressed by E-H coherent states for large values of λ and V_0. In contrast the dependence on β will always remain for a product state. This can be seen from the location of the distribution as shown in 5.3b. A product state will include interference between components from the same location in k-space. As the $\hat{\mathcal{Z}}$ operator inverts the location of the hole component about the

momentum origin, this now involves interactions at opposite locations on k-space.

The expectation values of the diagonal terms of σ_3 with respect to the E-H and product states are given by

$$\langle \sigma_3(0) f_3(\hat{p}, t)\rangle_\otimes = \frac{N_-(\beta)}{N_+(\beta)} \langle z| f_3(\hat{p}, t)|z\rangle \tag{5.138}$$

and

$$\langle \sigma_3(0) f_3(\hat{p}, t)\rangle_\bowtie = \sqrt{\frac{\lambda}{\pi}}\, N_+^{-1}(\beta) \int f_3(p, t) \left[e^{-\lambda(p-V_0)^2} - |\beta|^2 e^{-\lambda(p+V_0)^2} \right]\, dp. \tag{5.139}$$

Again the product state will always have a dependence on initial balance of components, with theses terms completely disappearing for an equal superposition. The E-H coherent state can in certain cases lose any dependence on the magnitude of β, depending on the form of $f_3(p, t)$. If $f_3(p, t)$ is odd in p then the Gaussian term can be inverted

$$\int f_3(p, t) e^{-\lambda(p+V_0)^2} dp = -\int f_3(p, t) e^{-\lambda(p-V_0)^2} dp \tag{5.140}$$

which allows for the contraction the expectation into the single term

$$N_+(\beta)^{-1} \int f_3(p, t) \left[e^{-\lambda(p-V_0)^2} - |\beta|^2 e^{-\lambda(p+V_0)^2} \right]\, dp = \int f_3(p, t) e^{-\lambda(p-V_0)^2}\, dp \tag{5.141}$$

removing any dependence on the initial amplitude of the quasi-spin.

5.4.1   Expected Pseudo-Velocity

We first analyse the behaviour of the pseudo-velocity operator $\hat{V}(t) = \hat{p}\sigma_3(t)$, this is written in terms of the initial operators as

$$\begin{aligned}
\hat{V}(t) = {}& \frac{\hat{p}\Delta_0}{E(\hat{p})} \left[\sigma_-(0) A_-^2(\hat{p}) - \sigma_+(0) A_+^2(\hat{p}) \right] e^{2itE(\hat{p})/\hbar} \\
& + \frac{\hat{p}\Delta_0}{E(\hat{p})} \left[\sigma_+(0) A_-^2(\hat{p}) - \sigma_-(0) A_+^2(\hat{p}) \right] e^{-2itE(\hat{p})/\hbar} \\
& + \hat{p} \left[1 - \frac{\Delta_0^2}{E^2(\hat{p})} 2\sin^2\left(\frac{t}{\hbar} E(\hat{p}) \right) \right] \sigma_3(0) + \frac{\hat{p}\mathcal{H}_0}{E^2(\hat{p})} \Delta_0 \sigma_1(0). \tag{5.142}
\end{aligned}$$

From this there are some clear key features of the expectation value with respect to the product state. For a state which initially has only electron or hole components ($\beta = 0$ or $\beta = \infty$ respectively) any off diagonal terms will vanish. The expectation value of an initial hole will then be the negative of

an initial electron. If the initial product state is an equal superposition of electron and hole components ($|\beta|^2 = 1$) then (5.142) simplifies to

$$\langle \hat{V}(t) \rangle_\otimes = \langle z| \frac{2\hat{p}\Delta_0}{N_+(\beta)E(\hat{p})} \left[\text{Im}(\beta) \sin\left(\frac{2t}{\hbar}E(\hat{p})\right) - \frac{\mathcal{H}_0}{E(\hat{p})} \text{Re}(\beta) \sin^2\left(\frac{t}{\hbar}E(\hat{p})\right) \right] |z\rangle.$$
(5.143)

This indicates a dependence on the phase of β in the resulting dynamics.

The expectation value with respect to the E-H coherent state is given by the integral

$$\langle \hat{V}(t) \rangle_\bowtie = \left\langle \hat{V}(0) \left\{ 1 + \frac{\Delta_0^2}{E^2(p)} \left[\cos\left(\frac{2t}{\hbar}E(p)\right) - 1 \right] \right\} \right\rangle_\bowtie \qquad (5.144)$$

$$= V_0 - \sqrt{\frac{\lambda}{\pi}} \Delta_0^2 \int \frac{2p}{E^2(p)} \sin^2\left(\frac{t}{\hbar}E(p)\right) e^{-\lambda(p-V_0)^2} dp. \qquad (5.145)$$

The off diagonal terms proportional to $\sigma_1(0)$ and $\sigma_2(0)$ vanish independently of the value β as the integrals generated by theses components have the form

$$\int p f(p) \exp(-\lambda p^2) dp = 0 \qquad (5.146)$$

when $f(p)$ is even. Altogether this means that the expected pseudo-velocity will always be indipendent of the initial electron-hole amplitudes. Also when $\beta = 0$ the E-H and product solutions coincide.

This can clearly then be interpreted as the initial pseudo-velocity $\langle \hat{V}(0) \rangle_\bowtie$, modified by an oscillating term dependent on Δ_0, V_0 and the width of the initial state in δp. The oscillating integral does not have a simple closed solution. In the following sub-section we will analyse the asymptotic behaviour in the long time limit using the stationary phase approximation.

Without further calculation it is also clear that when $V_0 = 0$ the oscillating term vanishes (integrated over odd p) meaning the state remains located at $V_0 = 0$ for all times. The oscillating term is largest when $V_0 = p_{\text{F}}$ (the minimum of $E(p)$) and in a similar manner the oscillations will disappear again when $V_0 \gg p_{\text{F}}$ then the velocity of the wave packet will remain approximately constant.

It is also possible to make some straight forward approximations. Firstly for short times, the sinusoidal term is readily expanded up to second order in t leaving integrals with analytic solutions. This provides the short time approximation

$$\langle \hat{V}(t) \rangle_\bowtie \approx V_0 \left[1 - 2\left(\frac{\Delta_0 t}{\hbar}\right)^2 \right] + \mathcal{O}(t^4) \qquad (5.147)$$

Figure 5.5: $\langle \hat{V}(t) \rangle_{\bowtie}$ for various values of Δ_0/μ and Δ_0/E_0. The are approximate values for a narrow momentum distribution using the Laplace method.
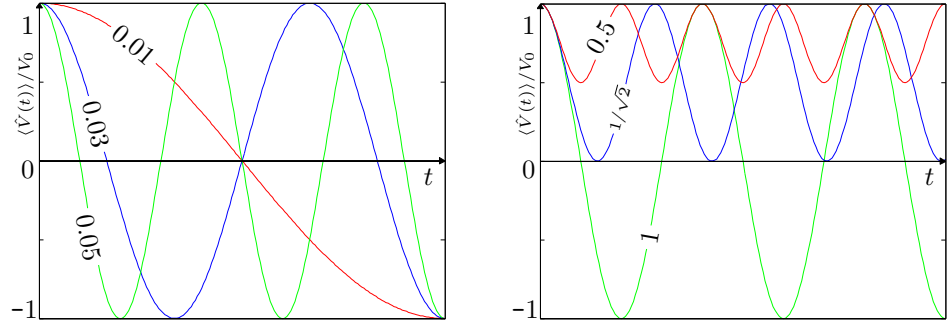
(a) $\langle \hat{V}(t) \rangle_{\bowtie}$ for a state centred on the Fermi momentum such that $\Delta_0/E_0 = 1$. Varying the value of Δ_0/μ, as labelled, increases the rate of oscillation

(b) $\langle \hat{V}(t) \rangle_{\bowtie}$ for a fixed value $\Delta_0/\mu = 0.05$ with values of Δ/E_0 as labelled. Moving to larger momenta increases the rate of oscillations but decreases the amplitude.

(the approximation converges when $2tE(p)/\hbar \ll 1$). For such short times the centre of the wave packet decelerates, retarded by Δ_0 dependent term, the width of state does not come into effect at these short time scales.

Another straight forward approximation is obtained by considering an extremely localised wave packet in momentum space such that the scaled squeezing parameter $\lambda = 1/m\omega\hbar \to \infty$. Although we have the freedom to do this by either scaling ω or $\hbar$ (and we will consider the difference between these two scalings in section 5.5.3) scaling $\omega \to 0$ by itself allows the use of the lowest order Laplace approximation by evaluating any other terms at the peak of the Gaussian (equivalent to evaluating the limiting δ-function behaviour of a Gaussian distribution, essentially the plane wave solution). We should also note that this choice is equivalent to scaling $x \to \infty$ (see section 5.2) producing a very narrow energy bandwidth but broad spatial distribution. We should see this evidenced in the dynamics. This also isolates the effects of the width of the wave packet from the dynamics for a clearer picture of how the momentum eigenstates contribute.

For a state centred on $V_0 = p_{\mathrm{F}}$ the oscillating term is simply approximated as

$$\sqrt{\frac{\lambda}{\pi}} \Delta_0^2 \int \frac{2p}{E^2(\hat{p})} \sin^2\left(\frac{t}{\hbar} E(\hat{p})\right) e^{-\lambda(p-p_{\mathrm{F}})^2} dp \approx 2V_0 \sin^2\left(\frac{t}{\hbar}\Delta_0\right) \tag{5.148}$$

meaning the expected pseudo-velocity oscillates as

$$\langle \hat{V}(t) \rangle_{\bowtie} \approx V_0 - 2V_0 \sin^2\left(\frac{t}{\hbar}\Delta_0\right) = V_0 \cos\left(\frac{2t}{\hbar}\Delta_0\right) \tag{5.149}$$

95

between $\pm V_0$ with a frequency $2\Delta_0/\hbar$. The same approximation with respect to the product state is

$$\langle \hat{V}(t) \rangle_\otimes \approx \frac{V_0}{N_+(\beta)} \left[N_-(\beta) \cos\left(\frac{2t}{\hbar} \Delta_0 \right) + 2\,\mathrm{Im}(\beta) \sin\left(\frac{2t}{\hbar} \Delta_0 \right) \right] \qquad (5.150)$$

showing that though the first term disappears when $|\beta|^2 = 1$, oscillations will always remain if $\mathrm{Im}(\beta) \neq 0$.

If the centre of the momentum distribution is moved away from the Fermi momentum, the same approximation for a narrow wave packet is

$$\langle \hat{V}(t) \rangle_\bowtie \approx V_0 - 2V_0 \left(\frac{\Delta_0}{E_0} \right)^2 \sin^2\left(\frac{t}{\hbar} E_0 \right) \qquad (5.151)$$

where $|E_0| > \Delta_0$ is the energy that corresponds to the central momentum V_0 (i.e. $E_0 = E(V_0)$). Moving from the Fermi momentum the frequency of the oscillations increases, but the amplitude of the oscillations decrease. In particular for the value $E_0 = \sqrt{2}\Delta_0$ then

$$\langle \hat{V}(t) \rangle \approx \langle \hat{V}(0) \rangle - V_0 \sin^2\left(\frac{t}{\hbar} \sqrt{2}\Delta_0 \right) \qquad (5.152)$$

which oscillates between 0 and V_0. $V(t)$ will therefore always be positive when $E_0 > \sqrt{2}\Delta_0$, though quasi-spin oscillations are still present they are insufficient to hold the wave packet at the origin.

5.4.2 Expected Position

The expected position with respect to the E-H coherent state is given in integral form by

$$\langle \hat{q}(t) \rangle_\bowtie = \langle \hat{q}(0) \rangle_\bowtie + \left\langle \frac{\hbar}{2m} \hat{V}(0) \left\{ \frac{2t}{\hbar} + \frac{\Delta_0^2}{E(\hat{p})^2} \left[\frac{1}{E(\hat{p})} \sin\left(\frac{2t}{\hbar} E(\hat{p}) \right) - \frac{2t}{\hbar} \right] \right\} \right\rangle_\bowtie$$
$$(5.153)$$

$$= \frac{t}{m} V_0 + \frac{\hbar \Delta_0^2}{2m} \sqrt{\frac{\lambda}{\pi}} \int \frac{p}{E^2(\hat{p})} \left[\frac{1}{E(\hat{p})} \sin\left(\frac{2t}{\hbar} E(\hat{p}) \right) - \frac{2t}{\hbar} \right] e^{-\lambda(p-V_0)^2} dp$$
$$(5.154)$$

on the second line $\langle \hat{q}(0) \rangle_\bowtie = 0$ has been set without any loss of generality. Analogous to the expected velocity the first term is just the simple propagation of the wave packet at a fixed initial velocity and the second term an oscillating Δ_0 dependent term. Properties of the expected pseudo-velocity carry over to the position, in particular when $V_0 = 0$ the state then remains centred at $q = 0$, the oscillations are maximal at $V_0 = \pm p_\mathrm{F}$, and they again
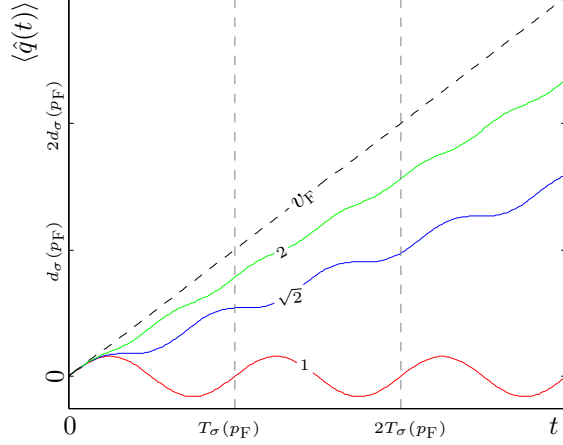
Figure 5.6: The approximate value of $\langle \hat{q}(t) \rangle_{\bowtie}$ as $\lambda \to \infty$ for a fixed value $\Delta_0/\mu = 0.05$ for various values of $E(V_0)/\Delta_0$ as labelled. The dashed line for comparison represents a free wave packet travelling at the Fermi velocity $v_{\mathrm{F}} = p_{\mathrm{F}}/m$.

disappear at larger central momenta past the Fermi momentum, where the wave packet will approximately freely propagate.

An analytic approximation for short times, by expanding the oscillating term up to 3rd order in t, is easily found giving

$$\langle \hat{q}(t) \rangle_{\bowtie} = \frac{t}{m} V_0 \left[1 - \frac{2}{3} \left(\frac{\Delta_0}{\hbar} \right)^2 t^2 \right] + \mathcal{O}(t^5). \tag{5.155}$$

The lowest order Laplace approximation for a localised wave packet in momentum, centred at $V_0 = p_{\mathrm{F}}$ gives

$$\langle \hat{q}(t) \rangle_{\bowtie} \approx \frac{\hbar}{2} \frac{v_{\mathrm{F}}}{\Delta_0} \sin \left(\frac{2t}{\hbar} \Delta_0 \right) \tag{5.156}$$

the centre of the wave packet oscillating about the origin, as the corresponding velocity oscillates between $\pm V_0$. The same approximation for a product state is

$$\langle \hat{q}(t) \rangle_{\otimes} \approx \frac{\hbar}{2} \frac{v_{\mathrm{F}}}{\Delta_0} \left[2 \operatorname{Im}(\beta) \left[1 - \cos \left(\frac{2t}{\hbar} \Delta_0 \right) \right] + N_-(\beta) \sin \left(\frac{2t}{\hbar} \Delta_0 \right) \right] \tag{5.157}$$

showing again that the E-H and product wave packets coincide for when $\beta = 0$, but also that the product state retains oscillations even if the amplitude of the two components is balanced (i.e. $|\beta| = 1$) if $\operatorname{Im}(\beta) > 0$ another feature not present in for E-H states.

Moving away from the Fermi momentum the lowest order Laplace approximation is

$$\langle \hat{q}(t) \rangle_{\bowtie} \approx \frac{t}{m} V_0 \left[1 - \left(\frac{\Delta_0}{E_0} \right)^2 \right] + \frac{\hbar}{2m} \frac{V_0}{E_0} \left(\frac{\Delta_0}{E_0} \right)^2 \sin \left(\frac{2t}{\hbar} E_0 \right). \tag{5.158}$$

As $\Delta_0 < E_0$, this would suggest that for higher energies above the band gap, although the frequency of the oscillations increase, the decrease in the

Figure 5.7: Numerically integrated solutions for $\langle \hat{q}(t) \rangle_{\bowtie}$ and $\langle \sigma_3(t) \rangle_{\bowtie}$ where $\langle \hat{V}(0) \rangle_{\bowtie} = p_{\mathrm{F}}$. For widths of wave packets $x = 1$, $x = 1.5$ and $x = 2$ (as labelled). The centre of a free wave packet travelling at v_{F} is also shown for comparison. $\langle \sigma_3(t) \rangle_{\bowtie}$ is given for a pure electron wave packet $\beta = 0$. The time axis is given in units of $T_\sigma(p_{\mathrm{F}})$.

(a) $\langle \hat{q}(t) \rangle_{\bowtie}$

(b) $\langle \sigma_3(t) \rangle_{\bowtie}$
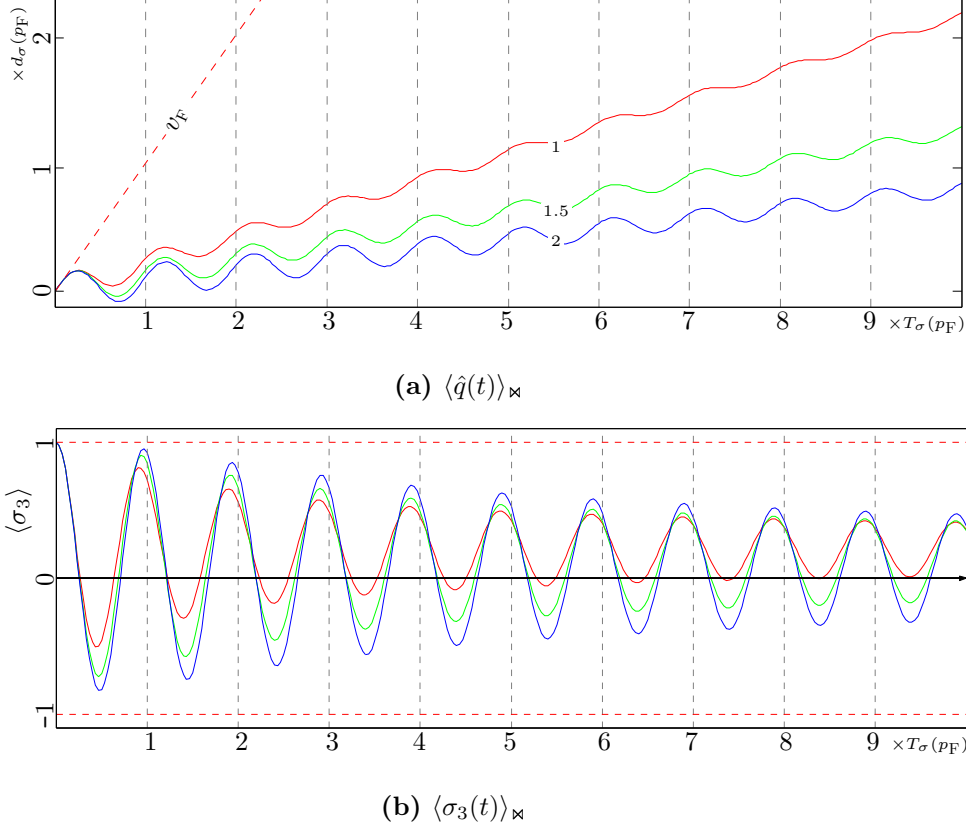
amplitude of the oscillations means the centre of the wave packet begins to behave much like a free state with central momentum p_{F} as shown Figure 5.6.

For a picture of how the width of the wave packet enters the dynamics numerically integrated solutions for $\langle \hat{q}(t) \rangle_{\bowtie}$ and the corresponding $\langle \sigma_3(t) \rangle_{\bowtie}$ are shown in Figures 5.7 and 5.8 for wave packets located on the Fermi momentum, alongside the expected position of a free scalar wave packet propagating at v_{F}. The expectation values are shown for various values of the parameter $x = \delta_q / v_{\mathrm{F}} T_\sigma(p_{\mathrm{F}})$, which as outline in section 5.2 scales the width of the initial Gaussian wave packet in terms of the spin distance $d_\sigma = v_{\mathrm{F}} T_\sigma(p_{\mathrm{F}})$.

Figure 5.7a shows the expected position of an E-H coherent state for various values of x. If the width of the wave packet of the order d_σ (i.e. $x \approx 1$) the wave packet moves quickly from the initial position. For wave packets wider than $d_\sigma(p_{\mathrm{F}})$ (i.e. $x > 1$) the wave packet oscillates closer to it's

initial position. For much larger and smaller values of x as shown in Figure 5.8a, the smaller values of x means the wave packet increasingly propagates like a free wave packet moving at the Fermi velocity, with no interaction between components causing oscillations. Conversely the wave packet that is much larger than d_σ oscillates about the origin without propagating away from the origin.

Plots 5.7b and 5.8b show how the expected position relates the time evolution of $\langle \sigma_3(t) \rangle$, smaller values of x produce smaller oscillations, that decay in amplitude more quickly. They also show a stronger bias towards positive values of $\langle \sigma_3 \rangle$ (i.e. the initial electron component) over time, causing the wave packet to propagate more quickly when averaged over many oscillations. Conversely the larger value of x retains oscillations over longer times, but also the larger amplitude of the oscillations retains a negative (hole) component.

5.4.3 Expected Quasi-Spin

We will now consider the time dependent quasi-spin moments. Applying the same analysis to the time dependent spin operators, firstly $\langle \sigma_1(t) \rangle$ in integral form is

$$
\begin{aligned}
\langle \sigma_1(t) \rangle_\bowtie = {} & \int \frac{\mathcal{H}_0}{E(p)} \left[\langle \sigma_+(0) \rangle_\bowtie A_+^2(p) + \langle \sigma_-(0) \rangle_\bowtie A_-^2(p) \right] e^{-\lambda p^2 + \frac{2i}{\hbar} t E(p)} dp \\
& + \int \frac{\mathcal{H}_0}{E(p)} \left[\langle \sigma_-(0) \rangle_\bowtie A_+^2(p) - \langle \sigma_+(0) \rangle_\bowtie A_-^2(p) \right] e^{-\lambda p^2 - \frac{2i}{\hbar} t E(p)} dp \\
& + \langle \sigma_3(0) \rangle_\bowtie \int \frac{\mathcal{H}_0 \Delta_0}{E^2(p)} \left[1 - \cos\left(\frac{2t}{\hbar} E(p) \right) \right] e^{-\lambda (p - V_0)^2} dp \\
& + \langle \sigma_1(0) \rangle_\bowtie \int \frac{\Delta_0^2}{E^2(p)} e^{-\lambda p^2} dp.
\end{aligned}
\tag{5.159}
$$

The central pseudo-velocity of the initial wave packet has the effect of scaling any terms proportional to $\sigma_1(0)$, $\sigma_+(0)$ or $\sigma_-(0)$ by $\exp(-\lambda V_0^2)$. For wave packets centred at $V_0 \approx 0$ these terms will make larger contributions, but as the wave packet move towards momentum centred close to and above the Fermi momentum (as μ is considered a large parameter) the contributions from these terms will be heavily suppressed by the Gaussian tails, only leaving terms dependent upon the initial balance of electron and hole components.

An analytic short time approximation is readily found up to first order

Figure 5.8: Numerically integrated solutions for $\langle \hat{q}(t) \rangle_\bowtie$ and $\langle \sigma_3(t) \rangle_\bowtie$ where $\langle \hat{V}(0) \rangle = p_F$. For widths of wave packets $x = 0.1$, $x = 1.5$ and $x = 20$ (as labelled). The centre of a free wave packet travelling at v_F is also shown for comparison. $\langle \sigma_3(t) \rangle$ is given for a pure electron wave packet $\beta = 0$. The time axis is given in units of $T_\sigma(p_F)$. For values of $x \gg 2$ the wave packet is confined to oscillate about the origin and for values $x \ll 1$ the position of the wave packet moves towards propagating at the Fermi velocity.

(a) $\langle \hat{q}(t) \rangle_\bowtie$

(b) $\langle \sigma_3(t) \rangle_\bowtie$
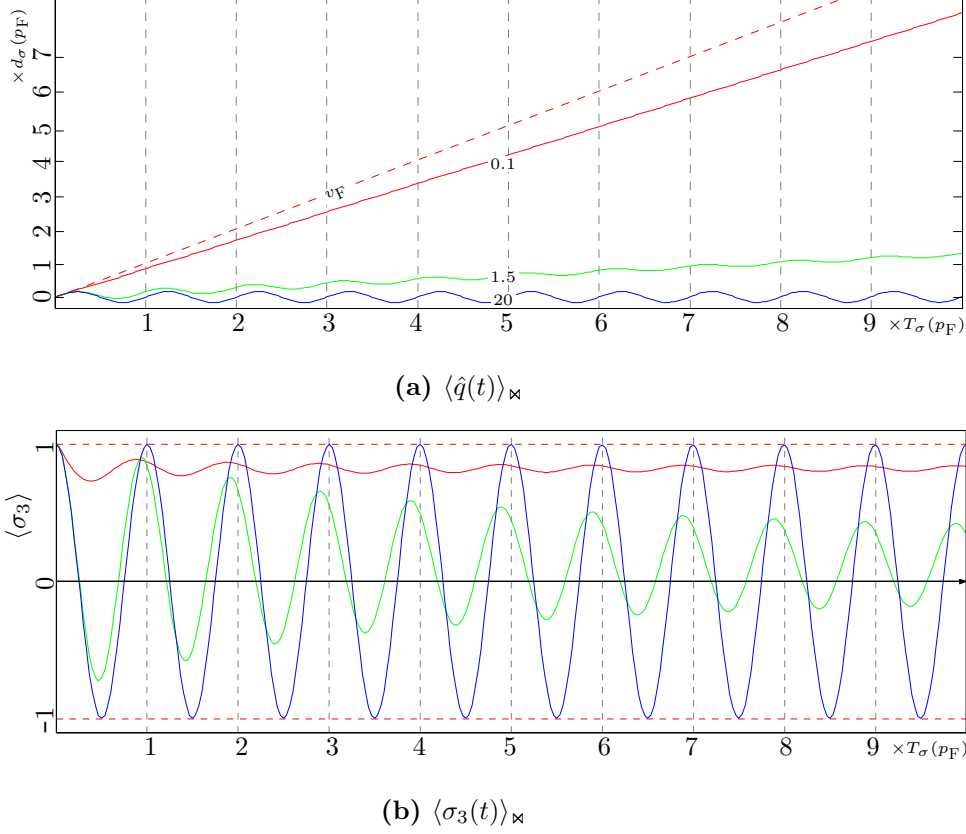
in t given by

$$\langle \sigma_1(t) \rangle_\bowtie \approx \langle \sigma_1(0) \rangle_\bowtie - \frac{2t}{\hbar} \langle \sigma_2(0) \rangle_\bowtie \left[\frac{1}{4m\lambda} - \mu \right] + \mathcal{O}(t^2) \qquad (5.160)$$

If we consider wave packet with $\langle \hat{V}(0) \rangle \approx p_F$ (and $\delta_p \ll p_F$) and only retain terms not suppressed by $\exp\left(-\lambda V_0^2\right)$ leaves

$$\langle \sigma_1(t) \rangle_\bowtie \approx \langle \sigma_1(0) \rangle_\bowtie + \langle \sigma_3(0) \rangle_\bowtie \sqrt{\frac{\lambda}{\pi}} \, 2\Delta_0 \int \frac{\mathcal{H}_0(p)}{E^2(p)} \sin^2\left(\frac{t}{\hbar} E(p)\right) e^{-\lambda(p-V_0)^2}.$$
$$(5.161)$$

We note that in this regime the dependence on $\langle \sigma_3(0) \rangle_\bowtie$ means any large oscillations will therefore vanish when the initial state is an equal superposition of electron and hole components and conversely will be largest when the initial state consists of only an electron or hole component.

100

The expected value of $\sigma_2(t)$ is given by

$$\langle\sigma_2(t)\rangle_\bowtie = i\sqrt{\frac{\lambda}{\pi}}\int \left[\langle\sigma_-(0)\rangle_\bowtie A_-^2(p) - \langle\sigma_+(0)\rangle_\bowtie A_+^2(p)\right] e^{-\lambda p^2 + \frac{2i}{\hbar}tE(p)}dp$$

$$+ i\sqrt{\frac{\lambda}{\pi}}\int \left[\langle\sigma_-(0)\rangle_\bowtie A_+^2(p) - \langle\sigma_+(0)\rangle_\bowtie A_-^2(p)\right] e^{-\lambda p^2 - \frac{2i}{\hbar}tE(p)}dp$$

$$- \langle\sigma_3(0)\rangle_\bowtie\sqrt{\frac{\lambda}{\pi}}\int \frac{\Delta_0}{E(p)}\sin\left(\frac{2t}{\hbar}E(p)\right) e^{-\lambda(p-V_0)^2}dp. \qquad (5.162)$$

The short time approximation up to first order in t is

$$\langle\sigma_2(t)\rangle_\bowtie \approx \langle\sigma_2(0)\rangle_\bowtie - \frac{2t}{\hbar}\Delta_0\langle\sigma_3(0)\rangle_\bowtie + \frac{2t}{\hbar}\langle\sigma_1(0)\rangle_\bowtie\left[\frac{1}{4m\lambda} - \mu\right] + \mathcal{O}(t^2) \qquad (5.163)$$

Again considering $V_0 \geq p_\mathrm{F}$, neglecting terms that are not suppressed by $\exp\left(-\lambda V_0^2\right)$ leaves only an oscillating term

$$\langle\sigma_2(t)\rangle_\bowtie \approx -\langle\sigma_3(0)\rangle_\bowtie\sqrt{\frac{\lambda}{\pi}}\Delta_0\int \frac{1}{E(p)}\sin\left(\frac{2t}{\hbar}E(p)\right) e^{-\lambda(p-V_0)^2}dp. \qquad (5.164)$$

Finally $\langle\sigma_3(t)\rangle_\bowtie$ is

$$\langle\sigma_3(t)\rangle_\bowtie = \sqrt{\frac{\lambda}{\pi}}\int \frac{\Delta_0}{E(p)}\left[\langle\sigma_-(0)\rangle_\bowtie A_-^2(p) - \langle\sigma_+(0)\rangle_\bowtie A_+^2(p)\right] e^{-\lambda p^2 + \frac{2i}{\hbar}tE(p)}dp$$

$$- \sqrt{\frac{\lambda}{\pi}}\int \frac{\Delta_0}{E(p)}\left[\langle\sigma_-(0)\rangle_\bowtie A_+^2(p) - \langle\sigma_+(0)\rangle_\bowtie A_-^2(p)\right] e^{-\lambda p^2 - \frac{2i}{\hbar}tE(p)}dp$$

$$+ \langle\sigma_3(0)\rangle_\bowtie - \langle\sigma_3(0)\rangle_\bowtie\sqrt{\frac{\lambda}{\pi}}2\Delta_0\int \frac{\Delta_0}{E^2(p)}\sin^2\left(\frac{t}{\hbar}E(p)\right) e^{-\lambda(p-V_0)^2}$$

$$+ \langle\sigma_1(0)\rangle_\bowtie\int \frac{\mathcal{H}_0\Delta_0}{E^2(p)}e^{-\lambda p^2}dp \qquad (5.165)$$

which for short times is

$$\langle\sigma_3(t)\rangle_\bowtie \approx \langle\sigma_3(0)\rangle_\bowtie + \frac{2t}{\hbar}\Delta_0\langle\sigma_2(0)\rangle_\bowtie + \mathcal{O}(t^2). \qquad (5.166)$$

When $V_0 \geq p_\mathrm{F}$ the non-suppressed terms leaves

$$\langle\sigma_3(t)\rangle_\bowtie = \langle\sigma_3(0)\rangle_\bowtie - \langle\sigma_3(0)\rangle_\bowtie\sqrt{\frac{\lambda}{\pi}}2\Delta_0\int \frac{\Delta_0}{E^2(p)}\sin^2\left(\frac{t}{\hbar}E(p)\right) e^{-\lambda(p-V_0)^2} \qquad (5.167)$$

again when $|\beta|^2 = 1$ all the spin dynamics will be suppressed. Like the phase space variables, for a sufficiently narrow wave packet in momentum the lowest order Laplace approximation can be made giving

$$\langle\sigma_1(t)\rangle_\bowtie \approx \langle\sigma_1(0)\rangle_\bowtie + \langle\sigma_3(0)\rangle_\bowtie 2\left(\frac{\Delta_0}{E_0}\right)\sqrt{1 - \left(\frac{\Delta_0}{E_0}\right)^2}\sin^2\left(\frac{t}{\hbar}E_0\right) \qquad (5.168)$$

$$\langle\sigma_2(t)\rangle_\bowtie \approx -\langle\sigma_3(0)\rangle_\bowtie\frac{\Delta_0}{E_0}\sin\left(\frac{2t}{\hbar}E_0\right) \qquad (5.169)$$

$$\langle\sigma_3(t)\rangle_\bowtie \approx \langle\sigma_3(0)\rangle_\bowtie - \langle\sigma_3(0)\rangle_\bowtie 2\left(\frac{\Delta_0}{E_0}\right)^2\sin^2\left(\frac{t}{\hbar}E_0\right). \qquad (5.170)$$
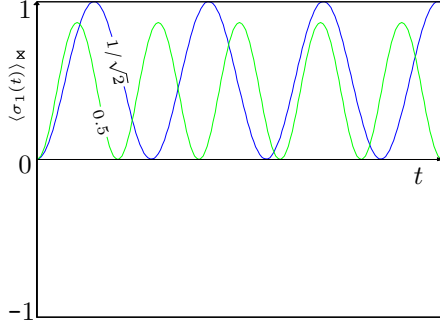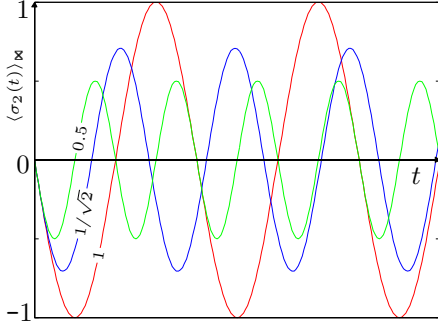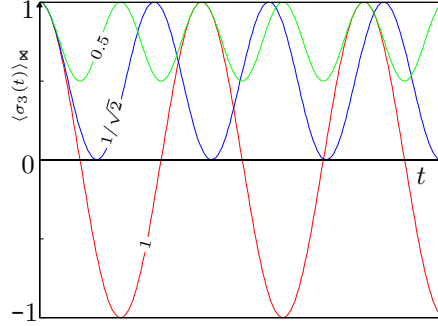
Figure 5.9: The expected values of the time dependent spin operators for a set value of $\Delta_0/\mu = 0.05$ and $|\beta|^2 = 0$, for various values of Δ_0/E_0. The values derived from a lowest order Laplace approximation.

(a) $\langle \sigma_1(t) \rangle_{\bowtie}$

(b) $\langle \sigma_2(t) \rangle_{\bowtie}$

(c) $\langle \sigma_3(t) \rangle_{\bowtie}$

These are shown in Figure 5.9 for various values of Δ_0/E_0 and a state with only an initial electron component. This shows that a wave packet centred on the Fermi momentum will have a (small) constant value for $\langle \sigma_1(t) \rangle_{\bowtie}$ but $\langle \sigma_2(t) \rangle_{\bowtie}$ and $\langle \sigma_3(t) \rangle_{\bowtie}$ will oscillate between $\langle \sigma_3(0) \rangle$. Any oscillations in the quasi-spin basis will be maximal when $E_0 = \Delta_0$ (on the Fermi momentum).

Overall this shows that E-H coherent states that are initially equal superpositions of electron and hole components then only exhibit small oscillations. These terms would not be suppressed when considering a product state as the two components of the initial wave packet overlap in phase space. This coincides with the picture that the quasi-spin dynamics are described on an ellipses of radius $\exp(-\lambda V_0^2)$ in the σ_1 and σ_2 directions.

5.4.4 Variances on Phase Space

Now let us consider the time dependent variances of wave packets on position-pseudo-velocity phase space. This will give us some indication of how the states retain their shape (and thus their usefulness for semiclassical purposes). With the time dependent operators in hand we can consider the time dependent variances directly, for which we require the squares of the time dependent operators.

The time dependent spin operators still satisfy $(\sigma_i(t))^2 = \mathbb{I}$, and it follows

that $(\hat{V}(t))^2 = \hat{p}^2$ is time indipendent. The corresponding expectation value with respect to the E-H state is

$$\langle \hat{V}(t)^2 \rangle_{\bowtie} = V_0^2 + \frac{1}{2\lambda}. \tag{5.171}$$

This means that any time dependence in the variance of the pseudo-velocity operator will be contained in $\langle \hat{V}(t) \rangle^2$. Omitting the full calculation this indicates that the variance of the velocity will both oscillate an increase linearly dependent on the location and width of the initial momentum distribution. If we consider the lowest order order Laplace approximation given by equation (5.151). Inserted into the variance gives

$$\text{Var}(\hat{V}(t))_{\bowtie} \approx \frac{1}{2\lambda} + V_0^2 \left[1 - \left(1 - 2 \left(\frac{\Delta_0}{E_0} \right)^2 \sin^2 \left(\frac{t}{\hbar} E_0 \right) \right)^2 \right] \tag{5.172}$$

and as we've seen, larger central momenta will produce faster, but smaller oscillations in the variance.

For a wave packet located at the Fermi momentum this simplifies to

$$\text{Var}(\hat{V}(t))_{\bowtie} \approx \frac{1}{2\lambda} + V_0^2 \sin^2 \left(\frac{2t}{\hbar} \Delta_0 \right). \tag{5.173}$$

In this case the variance will merely oscillate about $1/2\lambda$ the momentum width of the initial wave packet, though this choice of approximation lacks any information about the influence of the width of the wave packet.

The square of $\hat{q}(t)$ is somewhat cumbersome to calculate, being that if we write $q(t)$ in general form as

$$\hat{q}(t) = \hat{q}(0) + \sum_{i=1}^{3} f_i(\hat{p}, t) \sigma_i(0) \tag{5.174}$$

then the square contains the terms

$$\hat{q}(t)^2 = \hat{q}(0)^2 + \sum_{i=1}^{3} \left[f_i(\hat{p}, t)^2 + \sigma_i(0) \{ \hat{q}(0), f_i(\hat{p}, t) \} \right]. \tag{5.175}$$

For short times it is straightforward to expand $\hat{q}(t)$ up to second order in t as

$$\hat{q}(t) \approx \hat{q}(0) + \frac{t}{m} \hat{V}(0) + \frac{\Delta_0 t^2}{m\hbar} \hat{p} \sigma_2(0) + \mathcal{O}(t^3). \tag{5.176}$$

Calculating the variance using this expression we find the general form without reference to a particular state

$$\text{Var}(\hat{q}) \approx \text{Var}(\hat{q}(0)) + \left(\frac{t}{m} \right)^2 \text{Var}(\hat{V}(0)) + \frac{t}{m} \left(\langle \{ \hat{V}(0), \hat{q}(0) \} \rangle - 2 \langle \hat{V}(0) \rangle \langle \hat{q}(0) \rangle \right)$$

$$+ \frac{\Delta_0 t^2}{m\hbar} \langle \sigma_2(0) \{ \hat{q}(0), \hat{p}(0) \} \rangle + \left(\frac{\Delta_0 t^2}{m\hbar} \right)^2 \text{Var}(\hat{p} \sigma_2(0)). \tag{5.177}$$

We can compare this solution with a scalar wave packet under the free Hamiltonian. In this case the time dependent variance is given by

$$\text{Var}(\hat{q}(t)) = \text{Var}(\hat{q}(t)) + \frac{t^2}{m^2}\,\text{Var}(\hat{p}(0)) + \frac{t}{m}\left[\langle\{\hat{p}(0),\hat{q}(0)\}\rangle - 2\langle\hat{p}(0)\rangle\langle\hat{q}(0)\rangle\right]. \tag{5.178}$$

We can see that there is similar behaviour between the two systems, albeit with the momentum replaced by the pseudo-velocity and two additional terms proportional to Δ_0. Expanding the anti-commutator in the first additional Δ_0 dependent term gives

$$\sigma_2(0)\{\hat{q}(0),\hat{p}(0)\} = i\frac{\hbar}{2}\sigma_2(0)\left(\hat{a}^{\dagger 2} - \hat{a}^2\right). \tag{5.179}$$

It is straight forward to see that the expectation values of this operator disappears with respect to the E-H coherent state. Clearly for a product coherent this does not apply where the additional term will be of the form

$$\langle\sigma_2(0)\{\hat{q}(0),\hat{p}(0)\}\rangle_\otimes = \frac{1}{N_+}\,\text{Im}(\beta z^2). \tag{5.180}$$

This will only disappear where $z = z^*$, or equivalently $p_0 = 0$.

With respect to the E-H coherent state the variance of $\hat{p}\sigma_2(0)$ is simply $1/2\lambda$. This indicates additional dispersion of the wave packet at longer times dependent on the width of the wave packet. With respect to the product state this value if

$$\langle\hat{p}\sigma_2(0)\rangle_\otimes = 2\,\text{Im}(\beta)p_0 \tag{5.181}$$

where this term can be especially large for large central momenta.

Overall the shows that at least for short times the variance of the E-H coherent state behaves in an analogous manner to the free scalar coherent state. The product states though shows additional growth dependent on the location of the wave packet.

5.4.5 Long Time Stationary Phase Approximation

Let us now consider the asymptotic long time behaviour of the expectation values. We will show that for large enough values of t, the time dependent integrals we could not find closed analytic solutions to are dominated by contributions from stationary phase points.

We will use the stationary phase approximation, which applies to oscillatory integrals of the form

$$I(\lambda) = \int f(x)\exp\left[i\lambda\theta(x)\right]dx. \tag{5.182}$$

In the limit $\lambda \to \infty$ (when x is real), the dominant contribution to the integral comes from the region close to the stationary phase point(s) x_{s}. x_{s} satisfies $\theta'(x_{\mathrm{s}}) = 0$. For large values of λ the fast oscillations away from the stationary point cancel and thus suppress any other contributions to the integral (see appendix C.2 for a more detailed derivation and discussion of this approximation).

For our purposes we need to find the asymptotic approximation to integrals of the general form

$$I(t) = \int f(p) \exp\left[\pm\frac{2it}{\hbar}E(p)\right] dp \tag{5.183}$$

as $t \to \infty$. The points of stationary phase, p_{s}, satisfy

$$\left.\frac{d}{dp}E(p)\right|_{p_{\mathrm{S}}} \equiv \frac{p_{\mathrm{s}}\mathcal{H}_0(p_{\mathrm{s}})}{mE(p_{\mathrm{s}})} = 0. \tag{5.184}$$

This equality is clearly satisfied where $p_{\mathrm{s}} = 0$, but also when $\mathcal{H}_0(p_{\mathrm{s}}) = 0$ at both $p_{\mathrm{s}} = \pm p_{\mathrm{F}}$. Altogether the general solution is therefore

$$I(t) \approx \sum_{p_{\mathrm{S}}} f(p_{\mathrm{s}}) \left(\frac{\pi\hbar}{t|E''(p_{\mathrm{s}})|}\right)^{\frac{1}{2}} \exp\left[\pm i\left(\frac{2t}{\hbar}E(p_{\mathrm{s}}) + \frac{\pi c}{4}\right)\right] \tag{5.185}$$

where the summation is performed over the distinct points of stationary phase (it can be safely assumed that they are distinct when p_{F} is a large parameter) and c is the sign of $E''(p_{\mathrm{s}})$. This approximation also requires the values of the phase term evaluated at the stationary phase points $E(\pm p_{\mathrm{F}}) = \Delta_0$, $E(0) = \sqrt{\mu^2 + \Delta_0^2}$ and also the second derivatives evaluated at the stationary phase points

$$\left.\frac{d^2E(p)}{dp^2}\right|_{\pm p_{\mathrm{F}}} = \frac{2\mu}{m\Delta_0} \quad \text{and} \quad \left.\frac{d^2E(p)}{dp^2}\right|_0 = \frac{-\mu}{mE(0)}. \tag{5.186}$$

Inserting these values into Equation (5.185) gives the general solution from which the expectation values will be constructed

$$\int f(p)e^{\pm 2itE(p)/\hbar}dp \approx \left(\frac{\pi}{\omega t\mu\lambda}\right)^{\frac{1}{2}} \left\{ f(0)\sqrt{E(0)}\exp\left[\pm i\left(\frac{2t}{\hbar}E(0) - \frac{\pi}{4}\right)\right] \right.$$
$$\left. + [f(p_{\mathrm{F}}) + f(-p_{\mathrm{F}})]\sqrt{\frac{\Delta_0}{2}}\exp\left[\pm i\left(\frac{2t\Delta_0}{\hbar} + \frac{\pi}{4}\right)\right] \right\}. \tag{5.187}$$

As shown in Appendix C.2, the stationary phase contributions are dominant when the width of stationary phase region is effectively narrower than any

105

Figure 5.10: Comparison of Numerical integration (red-dashed) and stationary phase approximation (blue) of the expected velocity and position of a E-H coherent state wave packet centred at $V_0 = p_F$. The time axis is given in units of $t_{crit} = \Delta_0/4\omega\mu$, the minimum time where the stationary phase approximation width is narrower than the Gaussian envelope. Here $\Delta_0/\mu = 0.05$, $x = 2$.
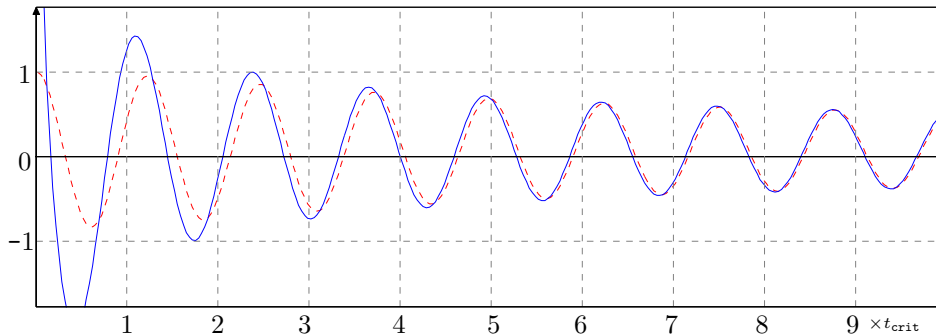
(a) $\langle \hat{V}(t) \rangle_{\bowtie} / \langle \hat{V}(0) \rangle_{\bowtie}$
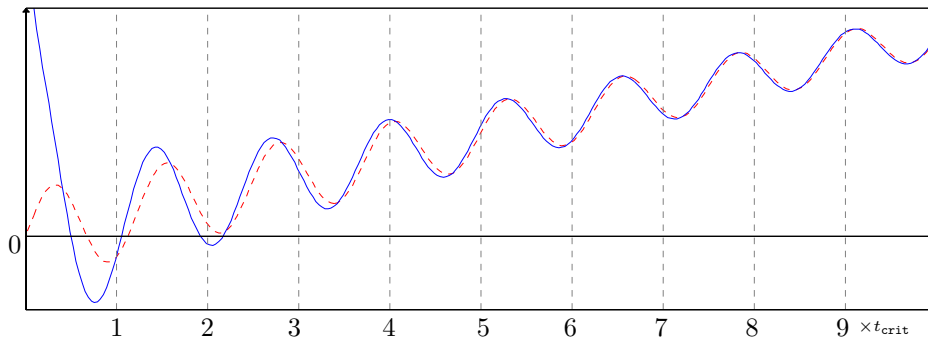
(b) $\langle \hat{q}(t) \rangle_{\bowtie}$

significant changes in the preceding amplitude term. In this particular case this equivalent to the requirement that the width of the stationary phase region is narrower than the width of the Gaussian envelope in momentum-space described by $\exp(-\lambda(p - V_0)^2/2)$. This is satisfied when

$$\frac{2t E''(p_s)}{\hbar} \gg \lambda. \tag{5.188}$$

Therefore the contribution from $p_s = 0$ is dominant at times satisfying

$$t \gg \frac{1}{2\omega\mu} \sqrt{\mu^2 + \Delta_0^2} \approx \frac{1}{2\omega} \tag{5.189}$$

and the contributions from $p_s = \pm p_F$ are dominant for times greater than

$$t \gg \frac{\Delta_0}{4\omega\mu} \tag{5.190}$$

in the regime $\mu \gg \Delta$. This means contributions from the stationary point $p_s = \pm p_F$ are in general dominant long before contributions from $p_s = 0$.

A comparison between numerically integrated solutions to $I(t)$ and the corresponding stationary phase approximation of $\langle \hat{q}(t) \rangle_{\bowtie}$ and $\langle \hat{V}(t) \rangle_{\bowtie}$ are shown in Figure 5.10, the time axis is given in units of $t_{\text{crit}} = \Delta_0/4\omega\mu$, the minimum time at which stationary phase contributions from $p_{\text{S}} = \pm p_{\text{F}}$ become significant.

$\langle \hat{V}(t) \rangle_{\bowtie}$

First considering the expected pseudo-velocity; the stationary phase point at $p = 0$ makes no contributions (due to the leading power of p in $\hat{V}_0$) leaving the sum over the contributions at $\pm p_{\text{F}}$

$$\langle \hat{V}(t) \rangle_{\bowtie} = V_0 - \sqrt{\lambda\pi}\, m\Delta_0 \operatorname{Im}\left[iZ_-(V_0)\right]$$
$$+ \left(\frac{m\Delta_0}{\omega t}\right)^{\frac{1}{2}} \cos\left(\frac{2t}{\hbar}\Delta_0 + \frac{\pi}{4}\right)\left[e^{-\lambda(p_{\text{F}}-V_0)^2} - e^{-\lambda(p_{\text{F}}+V_0)^2}\right]. \quad (5.191)$$

where

$$Z_{\pm}(V_0) = w\left(-\sqrt{\lambda}(V_0 - a)\right) \pm w\left(\sqrt{\lambda}(V_0 + a)\right) \quad (5.192)$$

and $a = \sqrt{2m(\mu + i\Delta_0)}$. The function $w(x)$ is the *Fadeeva function* (or the *plasma dispersion function*[73]) a scaled complementary error functions defined as $w(x) = e^{-x^2}\operatorname{erfc}(-ix)$ (see Appendix B for details). This term arises from separating the integral term in $\langle \hat{V}(t) \rangle_{\bowtie}$ (equation (5.145)) into time dependent oscillating and stationary terms as

$$\sqrt{\frac{\lambda}{\pi}}\Delta_0^2 \int \frac{p}{E^2(p)}\left[1 - \cos\left(\frac{2t}{\hbar}E(p)\right)\right]e^{-\lambda(p-V_0)^2}dp. \quad (5.193)$$

The stationary integral can be solved using

$$\sqrt{\frac{\lambda}{\pi}}\Delta_0^2 \int \frac{p}{E^2(p)}e^{-\lambda(p-V_0)^2}dp = \sqrt{\lambda\pi}\,m\Delta_0 \operatorname{Im}\left[iZ_-(V_0)\right] \quad (5.194)$$

the full details of this calculation are given in Appendix A.2.2.

Due to the lack of contributions from $p = 0$ the time dependent oscillations in the pseudo-velocity are maximal when $V_0 = \pm p_{\text{F}}$. The oscillations completely cancel when the wave packet is located on $V_0 = 0$. The oscillation are also suppressed for wave packets centred at momenta $V_0 \gg p_{\text{F}}$. Moreover the oscillations are scaled by Δ_0 and decay over time.

Though the Faddeeva function is an exact solution to the stationary integral it will be useful to have an approximate picture of the behaviour of this term as a function of V_0. In the regime $\Delta_0 \ll \mu$ it can be shown that

(see Appendix A.2.2) integral 5.194 can be approximated as the convolution of the Gaussian terms $\exp\left(-\lambda(p-V_0)^2\right)$ centred at V_0 and a Lorentz distribution of the form

$$f(p; \mp p_{\mathrm{F}}, \Delta_0/v_{\mathrm{F}}) = \frac{1}{\pi}\left[\frac{\Delta_0/v_{\mathrm{F}}}{(p \pm p_{\mathrm{F}})^2 + (\Delta_0/v_{\mathrm{F}})^2}\right] \tag{5.195}$$

which is peaked at $\pm p_{\mathrm{F}}$ and has a width described by the half-width half-max Δ_0/v_{F}. As such $\mathrm{Im}[iw(-\sqrt{\lambda}(V_0-a))]$ is largest when $V_0 = -p_f$ and inversely $\mathrm{Im}[iw(\sqrt{\lambda}(V_0+a))]$ is largest when $V_0 = p_{\mathrm{F}}$. Away from the the Fermi momenta these terms will quickly disappear if both the Gaussian and Lorentz distribution are suitably narrow (i.e. if λ is large and Δ_0/v_{F} small).

For a wave packet located at $V_0 \approx p_{\mathrm{F}}$ this implies that the dominant contributions to Equation (5.191) are

$$\langle \hat{V}(t)\rangle_{\bowtie} = V_0 - \sqrt{\lambda\pi}\, m\Delta_0 \,\mathrm{Im}\left[iw(-\sqrt{\lambda}(V_0-a))\right] \tag{5.196}$$

$$+ \left(\frac{m\Delta_0}{\omega t}\right)^{\frac{1}{2}} \cos\left(\frac{2t}{\hbar}\Delta_0 + \frac{\pi}{4}\right) e^{-\lambda(p_{\mathrm{F}}-V_0)^2}. \tag{5.197}$$

The expected pseudo-velocity is a constant value described by the first two terms with oscillations that both decrease in time and scale with the width of the initial wave packet. If $\delta p \ll \Delta_0/v_{\mathrm{F}}$ the Faddeeva function term is approximately equal to V_0, which cancels with the first term. This means the expected pseudo-velocity only oscillates about 0.

When $V_0 = 0$, the Faddeeva function terms in equation (5.191) cancel directly with each other. This leaves a wave packet located at a constant $V(t) = V_0 = 0$. At momenta $V_0 \gg p_{\mathrm{F}}$ the expected pseudo-velocity is approximately a constant $\langle \hat{V}(t)\rangle_{\bowtie} = V_0$.

$\langle \hat{q}(t)\rangle_{\bowtie}$

One may calculate $\langle \hat{q}(t)\rangle_{\bowtie}$ in a similar manner. The dominant contributions only come from the stationary points $\pm p_{\mathrm{F}}$ giving

$$\langle \hat{q}(t)\rangle_{\bowtie} = \frac{t}{m}\left\{V_0 - \sqrt{\pi\lambda}\, m\Delta_0 \,\mathrm{Im}\left[iZ_-(V_0)\right]\right\}$$

$$+ \frac{\hbar}{2}\left(\frac{1}{m\Delta_0\omega t}\right)^{\frac{1}{2}} \sin\left(\frac{2t}{\hbar}\Delta_0 + \frac{\pi}{4}\right)\left[e^{-\lambda(p_{\mathrm{F}}-V_0)^2} - e^{-\lambda(p_{\mathrm{F}}+V_0)^2}\right].$$

$$\tag{5.198}$$

As the expected position moves with the expected pseudo-velocity many general features carry over from $\langle \hat{V}(t)\rangle_{\bowtie}$. When the initial wave packet is

located at $V_0 = 0$ it remains on the origin, with no other oscillations. A wave packet located at $V_0 \approx p_{\text{F}}$ has the remaining dominant terms

$$\langle \hat{q}(t) \rangle_{\bowtie} = \frac{t}{m} \left\{ V_0 - \sqrt{\pi \lambda}\, m \Delta_0 \operatorname{Im} \left[iw(-\sqrt{\lambda}(V_0 - a)) \right] \right\}$$

$$+ \frac{\hbar}{2} \left(\frac{1}{m \Delta_0 \omega t} \right)^{\frac{1}{2}} \sin \left(\frac{2t}{\hbar} \Delta_0 + \frac{\pi}{4} \right) e^{-\lambda(p_{\text{F}} - V_0)^2}. \qquad (5.199)$$

Again if $\delta p \ll \Delta_0 / v_{\text{F}}$ the first two terms cancel, leaving only the oscillations about the origin. The amplitude of the oscillations also decrease over time.

$\langle \boldsymbol{\sigma_i(t)} \rangle_{\bowtie}$

Applying the stationary phase approximation to the spin operators firstly for $\sigma_1(t)$

$$\langle \sigma_1 \rangle_{\bowtie} \approx \sqrt{\lambda \pi} \Delta_0 m \left(\langle \sigma_3 \rangle_{\bowtie} \operatorname{Re} \left[\frac{i}{a} Z_+(V_0) \right] + \langle \sigma_1 \rangle_{\bowtie} \operatorname{Im} \left[\frac{i}{a} w(\sqrt{\lambda}a) \right] \right)$$

$$+ \left(\frac{\mu}{\omega t E(0)} \right)^{\frac{1}{2}} \frac{1}{E(0)} \left(\langle \sigma_1 \rangle_{\bowtie} \mu + \Delta_0 \langle \sigma_3 \rangle_{\bowtie} e^{-\lambda V_0^2} \right) \cos \left(\frac{2t}{\hbar} E(0) - \frac{\pi}{4} \right)$$

$$+ \left(\frac{\mu}{\omega t E(0)} \right)^{\frac{1}{2}} \langle \sigma_2 \rangle_{\bowtie} \sin \left(\frac{2t}{\hbar} E(0) - \frac{\pi}{4} \right) \qquad (5.200)$$

The dependence on V_0 of the E-H wave packet is again important here, where the magnitude of $\langle \sigma_3(0) \rangle_{\bowtie}$ is only dependent on the value of β, the overlap between coherent states contained in $\langle \sigma_1(0) \rangle_{\bowtie}$ and $\langle \sigma_2(0) \rangle_{\bowtie}$ means that the oscillating terms and the second Faddeeva function term are maximised when $V_0 = 0$.

Moving to a wave packet initially centred at $V_0 \approx p_{\text{F}}$, when $p_{\text{F}} \gg \delta p$ all the terms are appropriately suppressed except for the constant Faddeeva term

$$\langle \sigma_1(t) \rangle_{\bowtie} \approx \sqrt{\lambda \pi} m \Delta_0 \langle \sigma_3(0) \rangle_{\bowtie} \operatorname{Re} \left[\frac{i}{a} w \left(-\sqrt{\lambda}(V_0 - a) \right) \right]. \qquad (5.201)$$

For $\langle \sigma_2(t) \rangle_{\bowtie}$ there are additional terms evaluated at $\pm p_{\text{F}}$, in total

$$\langle \sigma_2 \rangle_{\bowtie} \approx \left(\frac{E(0)}{\omega t \mu} \right)^{\frac{1}{2}} \left[\langle \sigma_2 \rangle_{\bowtie} \cos \left(\frac{2t}{\hbar} E(0) - \frac{\pi}{4} \right) \right.$$

$$\left. - \frac{1}{E(0)} \left(\langle \sigma_1 \rangle_{\bowtie} \mu + \Delta_0 \langle \sigma_3 \rangle_{\bowtie} e^{-\lambda V_0^2} \right) \sin \left(\frac{2t}{\hbar} E(0) - \frac{\pi}{4} \right) \right]$$

$$+ \left(\frac{\Delta_0}{2 \omega t \mu} \right)^{\frac{1}{2}} \left[\langle \sigma_2 \rangle_{\bowtie} 2 \cos \left(\frac{2t}{\hbar} \Delta_0 + \frac{\pi}{4} \right) e^{-\lambda p_{\text{F}}^2} \right.$$

$$\left. - \langle \sigma_3 \rangle_{\bowtie} \sin \left(\frac{2t}{\hbar} \Delta_0 + \frac{\pi}{4} \right) \left[e^{-\lambda(p_{\text{F}} - V_0)^2} + e^{-\lambda(p_{\text{F}} + V_0)^2} \right] \right].$$

$$(5.202)$$

again there is strong dependence on the momentum location of the wave packet. The wave packet centred at $V_0 \approx p_{\mathrm{F}}$ leaves

$$\langle\sigma_2(t)\rangle_{\bowtie} \approx -\left(\frac{\Delta_0}{2\omega t\mu}\right)^{\frac{1}{2}}\langle\sigma_3(0)\rangle_{\bowtie}\sin\left(\frac{2t\Delta_0}{\hbar}+\frac{\pi}{4}\right)e^{-\lambda(p_{\mathrm{F}}-V_0)^2} \qquad (5.203)$$

retaining oscillations about the origin with amplitude proportional to Δ_0, which decay over time. Finally for σ_3

$$\begin{aligned}
\langle\sigma_3(t)\rangle_{\bowtie} =\ & 2\langle\sigma_1(0)\rangle_{\bowtie}\sqrt{\lambda\pi}m\Delta_0\,\mathrm{Re}\left[\frac{i}{a}w(\sqrt{\lambda}a)\right]\\
& +\langle\sigma_3(0)\rangle_{\bowtie}\left\{1-\sqrt{\lambda\pi}m\Delta_0\,\mathrm{Im}\left[\frac{i}{a}Z_+(V_0)\right]\right\}\\
& +\frac{\Delta_0}{\sqrt{\omega t\mu E(0)}}\left\{\left[\langle\sigma_-(0)\rangle_{\bowtie}A_-^2(0)-\langle\sigma_+(0)\rangle_{\bowtie}A_+^2(0)\right]e^{i(2tE(0)/\hbar-\pi/4)}\right.\\
& \qquad\qquad -\left[\langle\sigma_-(0)\rangle_{\bowtie}A_+^2(0)-\langle\sigma_+(0)\rangle_{\bowtie}A_-^2(0)\right]e^{-i(2tE(0)/\hbar-\pi/4)}\\
& \qquad\qquad +\langle\sigma_3(0)\rangle_{\bowtie}\frac{\Delta_0}{E(0)}e^{-\lambda V_0^2}\bigg\}\\
& +\left(\frac{\Delta_0}{2\omega t\mu}\right)^{\frac{1}{2}}\left\{2\langle\sigma_2(0)\rangle_{\bowtie}\sin\left(\frac{2t\Delta_0}{\hbar}+\frac{\pi}{4}\right)e^{-\lambda p_{\mathrm{F}}^2}\right.\\
& \qquad\qquad +\langle\sigma_3(0)\rangle_{\bowtie}\cos\left(\frac{2t\Delta_0}{\hbar}+\frac{\pi}{4}\right)\left[e^{-\lambda(p_{\mathrm{F}}+V_0)^2}+e^{-\lambda(p_{\mathrm{F}}-V_0)^2}\right]\bigg\}.
\end{aligned}$$
$$(5.204)$$

$$\begin{aligned}
\langle\sigma_3\rangle_{\bowtie} \approx\ & \langle\sigma_3\rangle+\sqrt{\lambda\pi}\Delta_0 m\left(\langle\sigma_1\rangle_{\bowtie}\mathrm{Re}\left[\frac{i}{a}w(\sqrt{\lambda}a)\right]-\langle\sigma_3\rangle_{\bowtie}\mathrm{Im}\left[\frac{i}{a}Z_+(V_0)\right]\right)\\
& +\left(\frac{\mu}{\omega t E(0)}\right)^{\frac{1}{2}}\frac{\Delta_0}{\mu}\left[\langle\sigma_2\rangle_{\bowtie}\sin\left(\frac{2t}{\hbar}E(0)-\frac{\pi}{4}\right)\right.\\
& \qquad\qquad +\frac{1}{E(0)}\left(\langle\sigma_1\rangle_{\bowtie}\mu+\Delta_0\langle\sigma_3\rangle e^{-\lambda V_0^2}\right)\cos\left(\frac{2t}{\hbar}E(0)-\frac{\pi}{4}\right)\bigg]\\
& +\left(\frac{\Delta_0}{2\omega t\mu}\right)^{\frac{1}{2}}\left[\langle\sigma_2\rangle_{\bowtie}2\sin\left(\frac{2t}{\hbar}\Delta_0+\frac{\pi}{4}\right)e^{-\lambda p_{\mathrm{F}}^2}\right.\\
& \qquad\qquad +\langle\sigma_3\rangle_{\bowtie}\cos\left(\frac{2t}{\hbar}\Delta_0+\frac{\pi}{4}\right)\left(e^{-\lambda(p_{\mathrm{F}}-V_0)^2}+e^{-\lambda(p_{\mathrm{F}}+V_0)^2}\right)\bigg]
\end{aligned}$$
$$(5.205)$$

The remaining terms for a wave packet centred at $V_0 = p_{\mathrm{F}}$ are the previously derived constant and an oscillating term

$$\begin{aligned}
\langle\sigma_3(t)\rangle_{\bowtie} \approx\ & \langle\sigma_3(0)\rangle_{\bowtie}\left\{1-\sqrt{\lambda\pi}m\Delta_0\,\mathrm{Im}\left[\frac{i}{a}w\left(-\sqrt{\lambda}(V_0-a)\right)\right]\right\}\\
& +\langle\sigma_3(0)\rangle_{\bowtie}\left(\frac{\Delta_0}{2\omega t\mu}\right)^{\frac{1}{2}}\cos\left(\frac{2t\Delta_0}{\hbar}+\frac{\pi}{4}\right)e^{-\lambda(p_{\mathrm{F}}-V_0)^2} \qquad (5.206)
\end{aligned}$$

Figure 5.11: The time dependent entanglement measure $R(t)^2$ for an initially electron wave packet ($\beta = 0$) centred on the Fermi momentum with various values of $x = \delta_q/v_F T_\sigma(p_F)$ as labelled. The time axis is given in units of $T_\sigma(p_F)$.
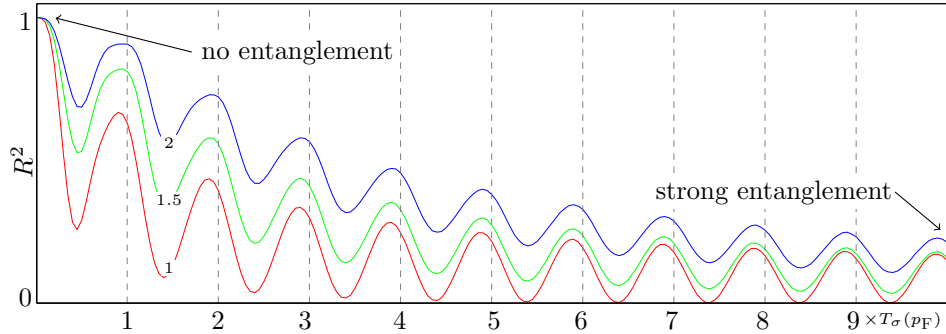
oscillating out of phase with the expectation of $\langle \sigma_2(t) \rangle$.

In all three cases a state that is an equal superposition of electron and hole components will only leave small oscillations of order $\exp(-\lambda V_0^2)$.

5.4.6 Time Dependent Entanglement

As a final note in this section we will briefly consider the time dependent behaviour of the measure of entanglement derived in section 3.5, written in time dependent form as

$$R(t)^2 = \sum_{i=1}^{3} \langle \sigma_i(t) \rangle^2 \tag{5.207}$$

designed such that the state is maximally entangled when $R^2 = 0$ and not entangled when $R^2 = 1$ (though E-H states can only reach the minimum bound $e^{-\lambda V_0^2}$). Although we omit detailed calculation of this parameter, we can derive key features from the preceding analysis of the expected spin values. Of course the product coherent states are not initially entangled by definition but will become strongly entangled after a short time if $\beta \neq 0, \infty$. In the case of E-H states we can consider how the time dependent entanglement depends upon the the dynamics we have derived for the individual quasi-spin components.

The initial entanglement is maximized for initial states that are balanced superpositions defined by $|\beta|^2 = 1$ and $V_0 \neq 0$. Overall the state will remain close to maximum entanglement as any remaining oscillation will be small due to the overlap of coherent states and their conjugate as shown in the previous section.

Oscillations can occur in the entanglement measure by starting with an initial state with only an electron (or hole) component. This will retain

the largest oscillating terms. The oscillations have the largest amplitude for states centred on the Fermi momentum. The rate and amplitude of the oscillations also depend upon the width of the initial wave packet as shown in Figure 5.11, for a state centred on the Fermi momentum with various values of x. This infers that a wave packet with a narrower momentum bandwidth wave packet remains less entangled over more cycles of $T_\sigma(p_{\mathrm{F}})$, though eventually they all become strongly entangled at large times.

5.5 Wave Packet Dynamics of Electron-Hole Coherent States

The Heisenberg picture provided a means of analysing the dynamics of the expectation values, moreover we have considered the connection with phase space trajectories in the spirit of the Ehrenfest relationship. A spatially homogeneous band gap allowed for a complete set of solutions to the operator equations of motion, and the same setting will allow us to find the action of the time evolution operator $\hat{U}(t) = \exp(-it\mathcal{H}_{\mathrm{BdG}}/\hbar)$ on a spinor wave function in the Schrödinger picture, in a fairly simple manner. In this section we will use this fact to derive a clearer picture of the dynamics of E-H and product coherent state wave packets under the BdG Hamiltonian and how they relate to the dispersion relation of the BdG Hamiltonian.

5.5.1 Bogoliubov-de Gennes Time Evolution Operator

For a full description we first need to find the action of the time development operator $\hat{U}(t) = \exp[-it\hat{\mathcal{H}}/\hbar]$, for the BdG Hamiltonian acting on an initial two component state. We will only consider the behaviour in q, as we've seen $\langle \hat{p}(t) \rangle$ is time independent. As $\hat{U}(t)$ is a function of the spin operators and $\hat{p}$ only we use the general method (to find the action of group element of $SU(2)$) of expanding the exponential as $e^x = \sum x^n/n!$. Since

$$[\hat{\mathcal{H}}_0 \sigma_3 - \Delta_0 \sigma_1]^2 = \left[\hat{\mathcal{H}}_0^2 + \Delta_0^2\right] \mathbb{I} \tag{5.208}$$

(as the anti-commutator cancels) then the even terms sum to

$$\sum_n \frac{(-1)^n}{(2n)!} \left[\frac{t^2}{\hbar^2}(\hat{\mathcal{H}}_0^2 + \Delta_0^2)\right]^n = \cos\left(\frac{t}{\hbar}E(\hat{p})\right) \mathbb{I} \tag{5.209}$$

where the definition $E(\hat{p}) = \sqrt{\mathcal{H}_0(\hat{p})^2 + \Delta_0^2}$ has been used. The sum over odd terms is similarly

$$\sum_n \frac{(-1)^n}{(2n+1)!} \left(\frac{t}{\hbar}\right)^{2n+1} [\hat{\mathcal{H}}_0^2 + \Delta_0^2]^n \left[\hat{\mathcal{H}}_0\sigma_3 - \Delta_0\sigma_1\right]$$

$$= -\frac{i}{E(\hat{p})} \sin\left(\frac{t}{\hbar}E(\hat{p})\right) \left[\hat{\mathcal{H}}_0\sigma_3 - \Delta_0\sigma_1\right]. \tag{5.210}$$

Although the solution has been given here in term of sinusoidal terms, it will be better presented using the projection operators in the electron-hole basis as

$$\hat{U}(t) = e^{-itE(\hat{p})/\hbar} \left[\hat{\mathcal{P}}_e A_+^2(\hat{p}) + \hat{\mathcal{P}}_h A_-^2(\hat{p})\right] + e^{itE(\hat{p})/\hbar} \left[\hat{\mathcal{P}}_e A_-^2(\hat{p}) + \hat{\mathcal{P}}_h A_+^2(\hat{p})\right]$$

$$+ \frac{i\Delta_0}{E(\hat{p})} \sin\left(\frac{t}{\hbar}E(\hat{p})\right) \sigma_1 \tag{5.211}$$

where

$$A_\pm(\hat{p}) = \left[\frac{1}{2}\left(1 \pm \frac{\mathcal{H}_0(\hat{p})}{\sqrt{\mathcal{H}_0^2(\hat{p}) + \Delta_0^2}}\right)\right]^{\frac{1}{2}}. \tag{5.212}$$

This expression is equivalent to the action of the time development operator on the momentum eigenstate decomposition given by

$$e^{-it\mathcal{H}(\hat{p})/\hbar}\big(|\boldsymbol{p}, +\rangle\langle\boldsymbol{p}, +| + |\boldsymbol{p}, -\rangle\langle\boldsymbol{p}, -|\big)$$

$$= e^{-itE(p)/\hbar}|\boldsymbol{p}, +\rangle\langle\boldsymbol{p}, +| + e^{itE(p)/\hbar}|\boldsymbol{p}, -\rangle\langle\boldsymbol{p}, -| \tag{5.213}$$

$$= e^{-itE(p)/\hbar}|p\rangle\langle p|\big(A_+(p)|e\rangle + A_-(p)|h\rangle\big)\big(A_+(p)\langle e| + A_-(p)\langle h|\big)$$

$$+ e^{itE(p)/\hbar}|p\rangle\langle p|\big(A_-(p)|e\rangle - A_+(p)|h\rangle\big)\big(A_-(p)\langle e| - A_+(p)\langle h|\big). \tag{5.214}$$

After expanding all the terms we arrive at the form of (5.211) since $\hat{\mathcal{P}}_+ \equiv |e\rangle\langle e|$, $\hat{\mathcal{P}}_- \equiv |h\rangle\langle h|$ and $\sigma_1 \equiv |h\rangle\langle e| + |e\rangle\langle h|$.

Applying $\hat{U}(t)$ to the product coherent state gives

$$\hat{U}(t)\left[|e\rangle + \beta|h\rangle\right]|z\rangle = e^{-itE(\hat{p})/\hbar}\left[A_+^2(\hat{p})|e\rangle + A_-^2(\hat{p})\beta|h\rangle\right]|z\rangle$$

$$+ e^{itE(\hat{p})/\hbar}\left[A_-^2(\hat{p})|e\rangle + A_+^2(\hat{p})\beta|h\rangle\right]|z\rangle$$

$$+ \frac{\Delta_0}{2E(\hat{p})}\left[e^{itE(\hat{p})/\hbar} - e^{-itE(\hat{p})/\hbar}\right] \times (|h\rangle + \beta|e\rangle)|z\rangle. \tag{5.215}$$

Applied to an initial E-H state the action is conversely

$$\hat{U}(t)\left[|e\rangle|z\rangle + \beta^*|h\rangle|z^*\rangle\right] = e^{-itE(\hat{p})/\hbar}\left[A_+^2(\hat{p})|e\rangle|z\rangle + A_-^2(\hat{p})\beta^*|h\rangle|z^*\rangle\right]$$

$$+ e^{itE(\hat{p})/\hbar}\left[A_-^2(\hat{p})|e\rangle|z\rangle + A_+^2(\hat{p})\beta^*|h\rangle|z^*\rangle\right]$$

$$+ \frac{\Delta_0}{2E(\hat{p})}\left[e^{itE(\hat{p})/\hbar} - e^{-itE(\hat{p})/\hbar}\right] \times (|h\rangle|z\rangle + \beta^*|e\rangle|z^*\rangle). \tag{5.216}$$

Let us first consider an initial E-H state that is just an electron component (i.e. $\beta = 0$). Inserting the identity in the momentum basis, gives the wave function in the plane wave decomposition. The full solution will then consist of terms of the general form

$$I(q,t) = \int f(p) e^{\pm it E(p)/\hbar} \langle q|p \rangle \langle p|z \rangle dp. \tag{5.217}$$

The coherent state wave function in terms of momentum eigenstates $\langle q|p \rangle \langle p|z \rangle$ is given by

$$\langle q|p \rangle \langle p|z \rangle = \sqrt{\frac{\lambda}{\pi}} \exp\left[-\frac{\lambda}{2}(p - V_0)^2 - \frac{i}{\hbar} p q_0 \right] \exp\left[\frac{i}{\hbar} pq \right]. \tag{5.218}$$

Here q is the phase space position variable and q_0 the initial location of the wave packet. Without loss of generality this will be set at $q_0 = 0$. We have also dropped the overall phase $iq_0 V_0/\hbar$ from the exponent as it has no effect on the resultant dynamics. The corresponding solution for terms containing the conjugate coherent state $|z^*\rangle$ can easily be found by the translation $V_0 \to -V_0$ in the momentum axis.

We will analyse the time dependent states resulting from an initial E-H coherent state that only has either an electron ($\beta = 0$) or hole ($\beta = \infty$) component independently. Lower indices again indicate the initial component and the upper indices the spinor component. Each initial component has a resulting time dependent spinor wave function with components

$$\boldsymbol{\psi}_e(q,t) = \psi_e^e(q,t)|e\rangle + \psi_e^h(q,t)|h\rangle \tag{5.219}$$

$$\boldsymbol{\psi}_h(q,t) = \psi_h^h(q,t)|h\rangle + \psi_h^e(q,t)|e\rangle \tag{5.220}$$

which in integral form are

$$\psi_e^e(q,t) = \int \left[e^{-it E(p)\hbar} A_+^2(p) + e^{it E(p)\hbar} A_-^2(p) \right] \langle q|p \rangle \langle p|z \rangle \, dp \tag{5.221}$$

and

$$\psi_h^h(q,t) = \int \left[e^{-it E(p)\hbar} A_-^2(p) + e^{it E(p)\hbar} A_+^2(p) \right] \langle q|p \rangle \langle p|z^* \rangle \, dp. \tag{5.222}$$

It is straightforward to show that $\psi_h^h(q,t) = \psi_e^{e*}(q,t)$ from the spectral symmetry of the BdG Hamiltonian. In a similar manner for the terms that mix electron and hole components

$$\psi_e^h(q,t) = \int \frac{\Delta_0}{2E(p)} \left[e^{it E(p)/\hbar} - e^{-it E(p)/\hbar} \right] \langle q|p \rangle \langle p|z \rangle \, dp \tag{5.223}$$

and

$$\psi_h^e(q,t) = \int \frac{\Delta_0}{2E(p)} \left[e^{itE(p)/\hbar} - e^{-itE(p)/\hbar} \right] \langle q|p\rangle \langle p|z^*\rangle \, dp \qquad (5.224)$$

which are related by $\psi_h^e(q,t) = -\psi_e^{h*}(q,t)$. Combining these relations the state resulting from an initial hole only wave packet can be expressed in terms of the initial electron wave function as

$$\boldsymbol{\psi}_h(q,t) = i\sigma_2 \boldsymbol{\psi}_e^*(q,t) \qquad (5.225)$$

where $i\sigma_2 \equiv |h\rangle\langle e| - |e\rangle\langle h|$. We have seen that this is the operator that takes states from the positive to the negative branch of the dispersion relation. We can then construct the time dependent wave function resulting from an arbitrary initial superposition from the linear sum of initial components

$$\langle q|\hat{U}(t)|z \bowtie \beta\rangle \equiv \boldsymbol{\psi}_\bowtie(q,t,\beta) = N_+^{-1/2}(\beta) \left[\boldsymbol{\psi}_e(q,t) + \beta^* \boldsymbol{\psi}_h(q,t) \right] \qquad (5.226)$$

$$= N_+^{-1/2}(\beta) \left[\boldsymbol{\psi}_e(q,t) + \beta^* i\sigma_2 \boldsymbol{\psi}_e^*(q,t) \right]. \qquad (5.227)$$

The electron and hole components of this wave function (after the action of $i\sigma_2$) are given by

$$\boldsymbol{\psi}_\bowtie(q,t,\beta) = N_+^{-1/2}(\beta) \left[\left(\psi_e^e(q,t) - \beta^* \psi_e^{h*}(q,t) \right) |e\rangle + \left(\psi_e^h(q,t) + \beta^* \psi_e^{e*}(q,t) \right) |h\rangle \right].$$
$$(5.228)$$

The absolute value of the wave function will have electron and hole contributions $|\boldsymbol{\psi}_\bowtie(q,t,\beta)|^2 = |\psi^e(q,t,\beta)|^2 + |\psi^h(q,t,\beta)|^2$. These terms are given by

$$|\psi^e(q,t,\beta)|^2 = N_+^{-1}(\beta) \left[|\psi_e^e(q,t)|^2 + |\beta|^2 |\psi_e^h(q,t)|^2 \right.$$
$$\left. - \beta \psi_e^e(q,t)\psi_e^h(q,t) - \beta^* \psi_e^{e*}(q,t)\psi_e^{h*}(q,t) \right] \qquad (5.229)$$

and

$$|\psi^h(q,t,\beta)|^2 = N_+^{-1}(\beta) \left[|\beta|^2 |\psi_e^e(q,t)|^2 + |\psi_e^h(q,t)|^2 \right.$$
$$\left. + \beta \psi_e^e(q,t)\psi_e^h(q,t) + \beta^* \psi_e^{e*}(q,t)\psi_e^{h*}(q,t) \right]. \qquad (5.230)$$

This means that the sum of the first two terms of each component will be the β indipendent term $|\psi_e^e(q,t)|^2 + |\psi_e^h(q,t)|^2$ which is the wave function of an initial electron only wave packet with $\beta = 0$. The final two terms of each component proportional to $\psi_e^e(q,t)\psi_e^h(q,t)$ and $\psi_e^{e*}(q,t)\psi_e^{h*}(q,t)$ corresponding to interference between initial electron and hole components. The sum of theses terms in $|\boldsymbol{\psi}_\bowtie(q,t,\beta)|^2$ will cancel overall. The resulting E-H wave packet has no dependence upon the initial value of β.

In contrast the wave functions produced by an initial electron or hole for a product state are related by

$$\boldsymbol{\psi}_h(q,t) = i\sigma_2\boldsymbol{\psi}_e^*(-q,t) \tag{5.231}$$

which can be used to construct the time dependent wave function from an arbitrary product state superposition

$$\boldsymbol{\psi}_\otimes(q,t,\beta) = N_+^{-1/2}(\beta)\left[\boldsymbol{\psi}_e(q,t) + \beta i\sigma_2\boldsymbol{\psi}_e^*(-q,t)\right]. \tag{5.232}$$

The electron and hole components are given by

$$\boldsymbol{\psi}_\otimes(q,t,\beta) = N_+^{-1/2}\left[\left(\psi_e^e(q,t) - \beta\psi_e^{h*}(-q,t)\right)|e\rangle + \left(\psi_e^h(q,t) + \beta\psi_e^{e*}(-q,t)\right)|h\rangle\right]. \tag{5.233}$$

The electron and hole contributions to the wave packet $|\boldsymbol{\psi}_\otimes(q,t,\beta)|^2$ will be symmetric in q, the relative amplitudes of the two contributions proportional to $|\beta|^2$. $|\boldsymbol{\psi}_\otimes(q,t,\beta)|^2$ will therefore be completely symmetric when the initial wave packet is a balanced superposition of electron and hole components (i.e. $|\beta|^2 = 1$). This again also shows that when $\beta = 0$ (and there are no symmetric contributions to $|\boldsymbol{\psi}_\otimes(q,t,\beta)|^2$) the E-H and product coherent states will coincide.

The full integrals required to find the components of $\boldsymbol{\psi}_e(q,t)$ have the general form

$$I(q,t) = N\int f(p)\exp\left[-\frac{\lambda}{2}(p-V_0)^2 + \frac{i}{\hbar}pq\right]\exp\left[\pm\frac{it}{\hbar}E(p)\right]\,dp. \tag{5.234}$$

with a normalization constant

$$N = \frac{1}{\sqrt{2\pi N_+(\beta)}}\left(\frac{\lambda}{\pi}\right)^{\frac{1}{4}}. \tag{5.235}$$

Due to the form of the integral further analytic insight into the behaviour of the wave packet will again require asymptotic techniques. Numerically integrated solutions are shown in Figures 5.12 to 5.20. They show the evolution of the electron and hole components ($|\psi^e(q,t)|^2$ and $|\psi^h(q,t)|^2$ respectively) and their sum $|\boldsymbol{\psi}(q,t)|^2$ at time steps of $0.25 \times T_\sigma(p_{\mathrm{F}})$. Each set of plots also shows the corresponding q v t density plot, again for each component and their sum. We have placed the analysis of these plots in their corresponding captions.

Figure 5.21 shows the same initial electron density plot, over a longer time period, with the expected position ($\langle\hat{q}(t)\rangle_\Join$) as calculated in section 5.4 overlaid.

Figure 5.12: Figures a - i show snapshots of the propagation of an initial electron ($\beta = 0$) Gaussian wave packet located at $V_0 = p_F$ with parameters $\Delta_0/\mu = 0.05$, $x = 1$ ($x = \delta_q/d_\sigma(p_F)$ the ratio of the initial width of wavepacket to the approximate distance the wavepacket will travel after one revolution in quasi-spin). Red and blue dashed lines denote electron ($|\psi^e(q,t,0)|^2$) and hole ($|\psi^h(q,t,0)|^2$) component wave functions respectively, and green their sum. The dashed vertical lines correspond to the $4\sigma_q$ width of the initial wave packet. Figures j - l are the corresponding q v t density plots, again for each component, and their sum.

As the width of the initial wave packet is of the order $v_F T_\sigma(p_F)$ the wave packet quickly shows oscillations outside the initial envelope. The electron component is biased toward positive q whilst the hole component remains symmetric and centred on the origin (we will comment on this further in the following section on the stationary phase approximation). The spatial oscillations over the Gaussian envelope correspond to wave-fronts of the electron component propagating away from the origin as the whole wave packet oscillates between electron and hole components.

(a) $t = 0$

(b) $t = 0.25 \times T_\sigma(p_F)$

(c) $t = 0.5 \times T_\sigma(p_F)$

(d) $t = 0.75 \times T_\sigma(p_F)$

(e) $t = T_\sigma(p_F)$

(f) $t = 1.25 \times T_\sigma(p_F)$

(g) $t = 1.5 \times T_\sigma(p_F)$

(h) $t = 1.75 \times T_\sigma(p_F)$

(i) $t = 2 \times T_\sigma(p_F)$

(j) $|\psi^e(q,t,0)|^2$

(k) $|\psi^h(q,t,0)|^2$

(l) $|\psi(q,t,0)|^2$
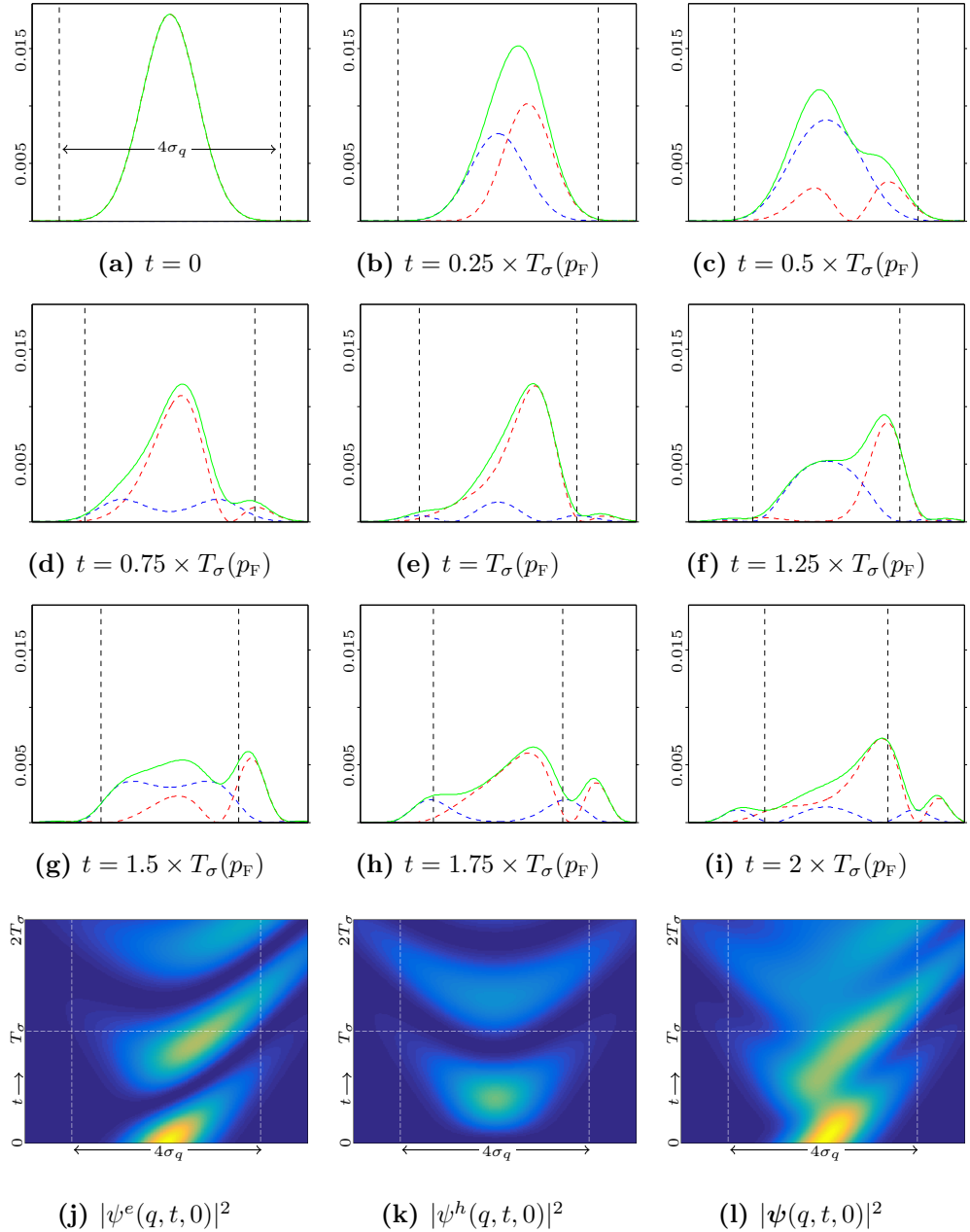
Figure 5.13: Figures a - i show snapshots of the propagation of an initial electron ($\beta = 0$) Gaussian wave packet located at $V_0 = p_{\mathrm{F}}$ with parameters $\Delta_0/\mu = 0.05$, $x = 2$. Red and blue dashed lines denote electron ($|\psi^e(q,t,0)|^2$) and hole ($|\psi^h(q,t,0)|^2$) components respectively and green their sum. The dashed vertical lines correspond to the $4\sigma_q$ width of the initial wave packet. Figures j - l are the corresponding q v t density plots, again for each component, and their sum.

We can see that in comparison to Figure 5.12, since the wave packet has contributions from a narrower energy band, the wave packet though still oscillating between components remains well localised on the origin. Any effects due to the oscillation between components are largely contained under the Gaussian envelope. The amplitudes of the components are also more closely matched where as when $x = 1$, the electron component is generally stronger.

(a) $t = 0$

(b) $t = 0.25 \times T_\sigma(p_{\mathrm{F}})$

(c) $t = 0.5 \times T_\sigma(p_{\mathrm{F}})$

(d) $t = 0.75 \times T_\sigma(p_{\mathrm{F}})$

(e) $t = T_\sigma(p_{\mathrm{F}})$

(f) $t = 1.25 \times T_\sigma(p_{\mathrm{F}})$

(g) $t = 1.5 \times T_\sigma(p_{\mathrm{F}})$

(h) $t = 1.75 \times T_\sigma(p_{\mathrm{F}})$

(i) $t = 2 \times T_\sigma(p_{\mathrm{F}})$

(j) $|\psi^e(q,t,0)|^2$

(k) $|\psi^h(q,t,0)|^2$

(l) $|\boldsymbol{\psi}(q,t,0)|^2$
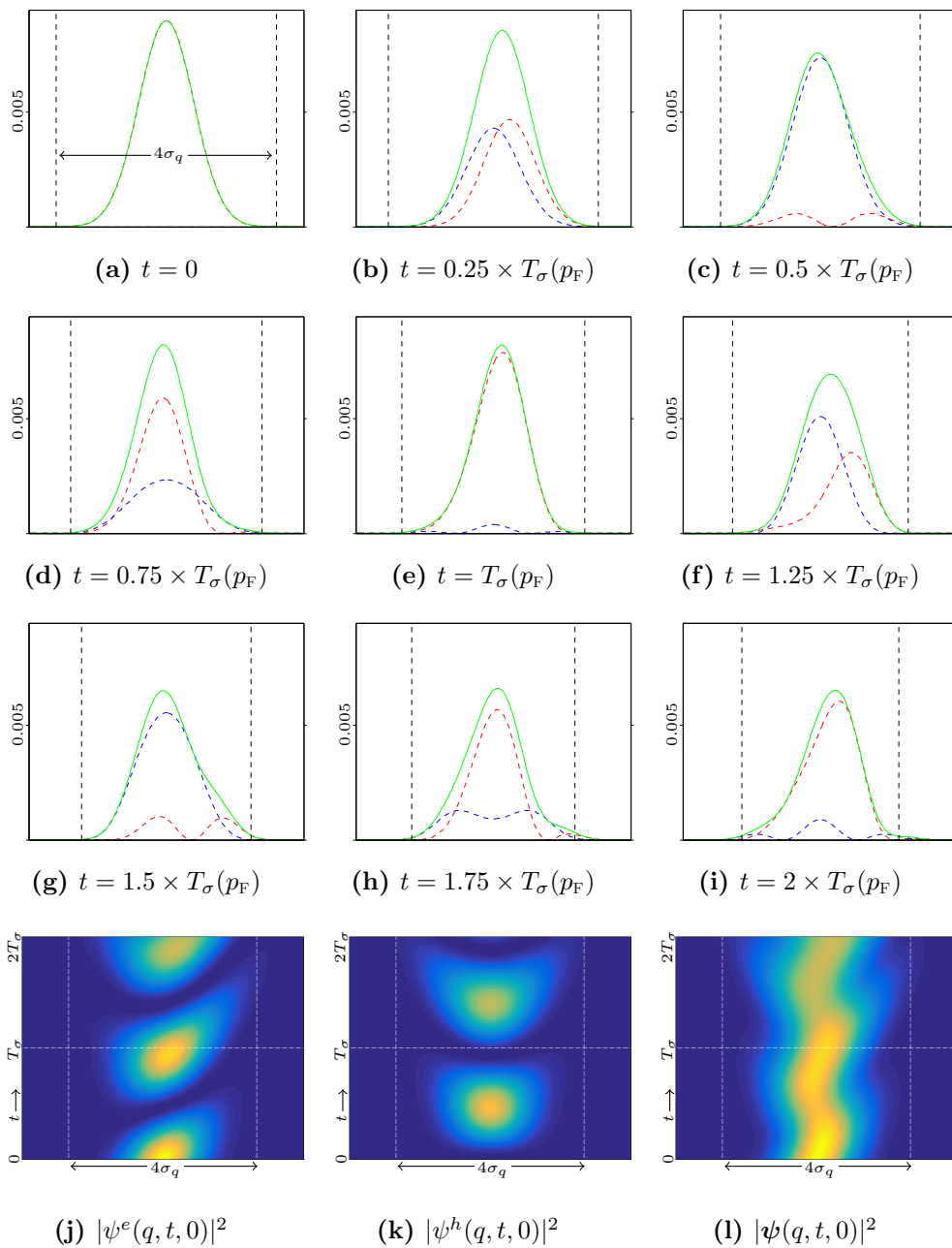
Figure 5.14: Figures a - i show the propagation of a initial electron ($\beta = 0$) coherent state wave packet located at $V_0 = p_{\mathrm{F}}$, with parameters $\Delta_0/\mu = 0.05$ and $x = 0.5$. Red and blue dashed lines denote electron ($|\psi^e(q,t,0)|^2$) and hole ($|\psi^h(q,t,0)|^2$) respectively and green their sum. The dashed vertical lines correspond to the $4\sigma_q$ width of the initial wave packet. Figures j - l are the corresponding q v t density plots, again for each component, and the sum.

As $x < 1$, $v_{\mathrm{F}} T_\sigma(p_{\mathrm{F}})$ is now well outside the width of the initial wave packet the wave packet propagates from under the initial wave packet before the rotation between components takes effect. Consequently the wave packet remains biased towards the electron component, and also quickly dissipates and loses its initial profile. After two full revolutions of the quasi-spin the bulk of the wave packet lies well outside the original width of the wave packet.

(a) $t = 0$ **(b)** $t = 0.25 \times T_\sigma(p_{\mathrm{F}})$ **(c)** $t = 0.5 \times T_\sigma(p_{\mathrm{F}})$

(d) $t = 0.75 \times T_\sigma(p_{\mathrm{F}})$ **(e)** $t = T_\sigma(p_{\mathrm{F}})$ **(f)** $t = 1.25 \times T_\sigma(p_{\mathrm{F}})$

(g) $t = 1.5 \times T_\sigma(p_{\mathrm{F}})$ **(h)** $t = 1.75 \times T_\sigma(p_{\mathrm{F}})$ **(i)** $t = 2 \times T_\sigma(p_{\mathrm{F}})$

(j) $|\psi^e(q,t,0)|^2$ **(k)** $|\psi^h(q,t,0)|^2$ **(l)** $|\psi(q,t,0)|^2$
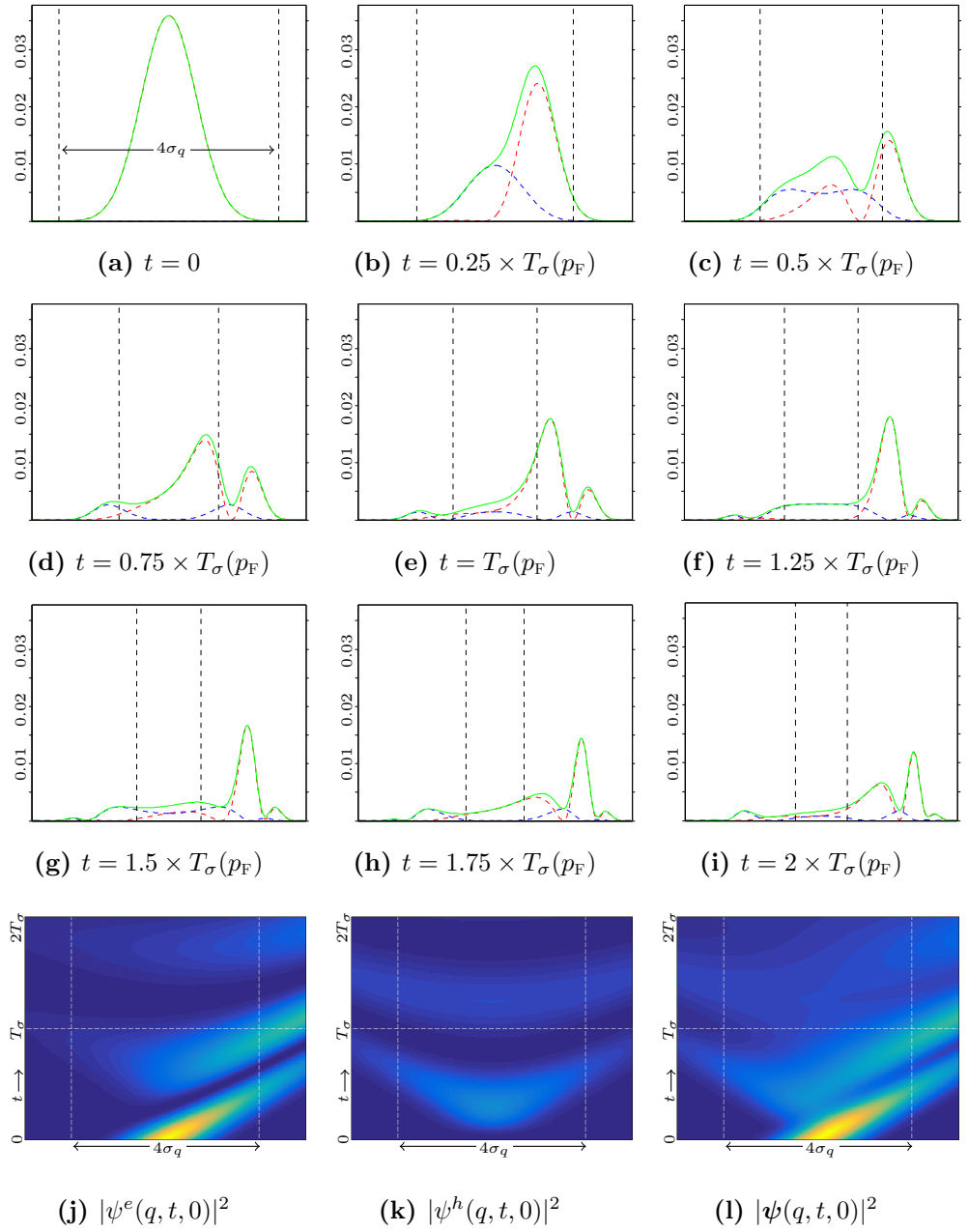
Figure 5.15: Figures a - i show snapshots of the propagation of a initial electron ($\beta = 0$) coherent state wave packet located at $V_0 = p_F$ with parameters $\Delta_0/\mu = 0.05$ and $x = 2.5$. Red and blue dashed lines denote electron ($|\psi^e(q,t,0)|^2$) and hole ($|\psi^h(q,t,0)|^2$) components respectively and green their sum. The dashed vertical lines correspond to the $4\sigma_q$ width of the initial wave packet. Figures j - l are the corresponding q v t density plots, again for each component, and their sum.

The analysis in the Heisenberg picture suggests that as the energy bandwidth becomes narrower the wave packet will only oscillate about the origin without also propagating away from the origin. We can see here that a larger value of x in comparison to the previous plots means the wave packet fully oscillates between the electron and hole components. Any dynamics resulting from the rotation between components are contained under the initial envelope. Consequently the wave packet remains close to its initial profile and also disperses more slowly. The contributions from the two components are also increasingly symmetric.

(a) $t = 0$ **(b)** $t = 0.25 \times T_\sigma(p_F)$ **(c)** $t = 0.5 \times T_\sigma(p_F)$

(d) $t = 0.75 \times T_\sigma(p_F)$ **(e)** $t = T_\sigma(p_F)$ **(f)** $t = 1.25 \times T_\sigma(p_F)$

(g) $t = 1.5 \times T_\sigma(p_F)$ **(h)** $t = 1.75 \times T_\sigma(p_F)$ **(i)** $t = 2 \times T_\sigma(p_F)$

(j) $|\psi^e(q,t,0)|^2$ **(k)** $|\psi^h(q,t,0)|^2$ **(l)** $|\boldsymbol{\psi}(q,t,0)|^2$
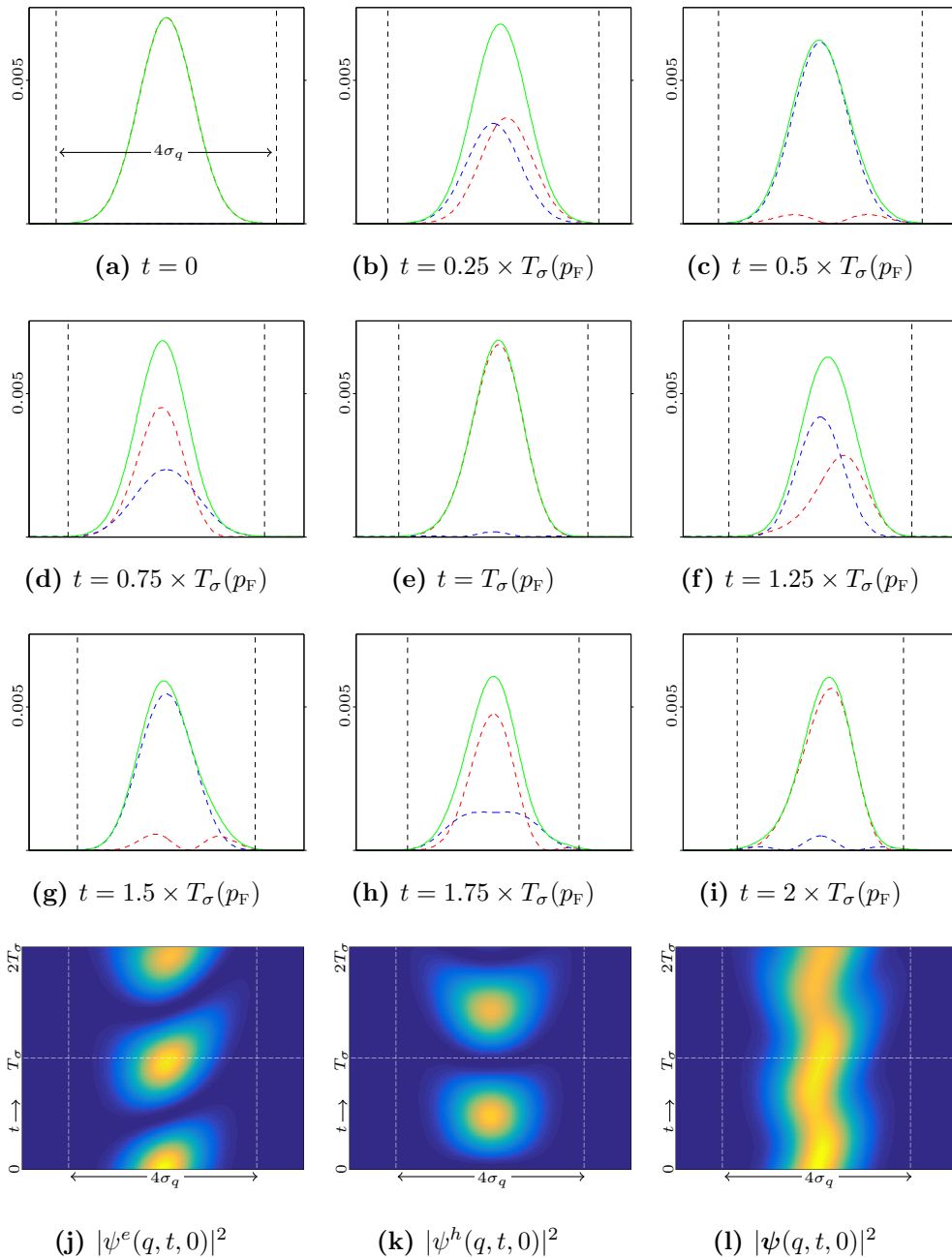
Figure 5.16: Figures a - i now show the propagation of a product coherent state located at $V_0 = p_F$ with an initially equal superposition of electron and hole components ($\beta = 1$) and parameters $\Delta_0/\mu = 0.05$, $x = 1$. Red and blue dashed lines denote electron ($|\psi^e(q,t,1)|^2$) and hole ($|\psi^h(q,t,1)|^2$) respectively and green their sum. The dashed vertical lines correspond to the $4\sigma_q$ width of the initial wave packet. Figures j - l are the corresponding q v t density plots, again for each component, and their sum.

As we have seen from the integral form a product coherent state has a $|\beta|^2$ dependent spatial symmetry between components. It's clear that in this case of an equal superposition the two components propagate in opposite directions. Both components now oscillate in the same manner rather than the out of phase oscillation seen in the previous examples. As the hole component propagates in the opposite direction to the electron, the overall state remains centred on the origin, spreading over time, though the components moving outside the width of the initial wave packet create oscillations in the width of the wave packet. The value of x now dictates how the wave packet spreads, in this case the wave packet quickly dissipates.

(a) $t = 0$

(b) $t = 0.25 \times T_\sigma(p_F)$

(c) $t = 0.5 \times T_\sigma(p_F)$

(d) $t = 0.75 \times T_\sigma(p_F)$

(e) $t = T_\sigma(p_F)$

(f) $t = 1.25 \times T_\sigma(p_F)$

(g) $t = 1.5 \times T_\sigma(p_F)$

(h) $t = 1.75 \times T_\sigma(p_F)$

(i) $t = 2 \times T_\sigma(p_F)$

(j) $|\psi^e(q,t,1)|^2$

(k) $|\psi^h(q,t,1)|^2$

(l) $|\psi_\otimes(q,t,1)|^2$

121
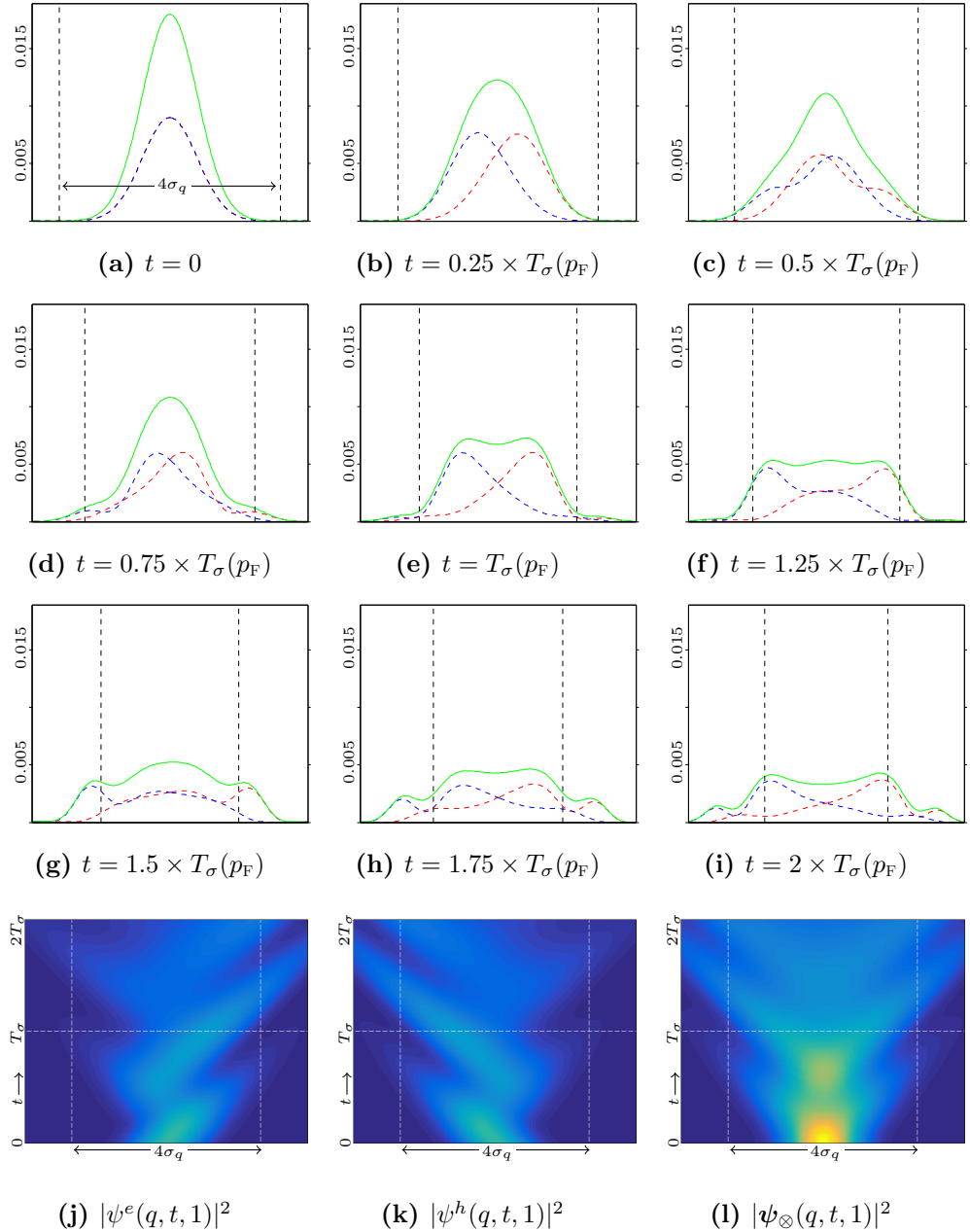
Figure 5.17: Figures a - i show snapshots of the propagation of a product state located at $V_0 = p_{\mathrm{F}}$ consisting of an initially equal superposition of electron and hole components ($\beta = 1$) with parameters $\Delta_0/\mu = 0.05$, $x = 2$. Red and blue dashed lines denote electron ($|\psi^e(q,t,1)|^2$) and ($|\psi^h(q,t,1)|^2$) respectively and green their sum. The dashed vertical lines correspond to the $4\sigma_q$ width of the wave packet. Figures j - l are the corresponding q v t density plots, again for each component, and their sum.

The narrower energy bandwidth for this wave packet in comparison to Figure 5.16 means this wave packet both remains located on the origin and retains its initial form over a large number of oscillations. The oscillations between components are evidenced as oscillations in the width of the wave packet. The wave packet also disperses more slowly, with the bulk of the wave packet still contained inside the initial width of the envelope after two full oscillation of the quasi-spin. As x increases the wave packet becomes increasingly close to the description given by the dispersion relation. We can see how the zero group velocity arises from the opposed velocities of the two components.

(a) $t = 0$

(b) $t = 0.25 \times T_\sigma(p_{\mathrm{F}})$

(c) $t = 0.5 \times T_\sigma(p_{\mathrm{F}})$

(d) $t = 0.75 \times T_\sigma(p_{\mathrm{F}})$

(e) $t = T_\sigma(p_{\mathrm{F}})$

(f) $t = 1.25 \times T_\sigma(p_{\mathrm{F}})$

(g) $t = 1.5 \times T_\sigma(p_{\mathrm{F}})$

(h) $t = 1.75 \times T_\sigma(p_{\mathrm{F}})$

(i) $t = 2 \times T_\sigma(p_{\mathrm{F}})$

(j) $|\psi^e(q,t,1)|^2$

(k) $|\psi^h(q,t,1)|^2$

(l) $|\psi_\otimes(q,t,1)|^2$
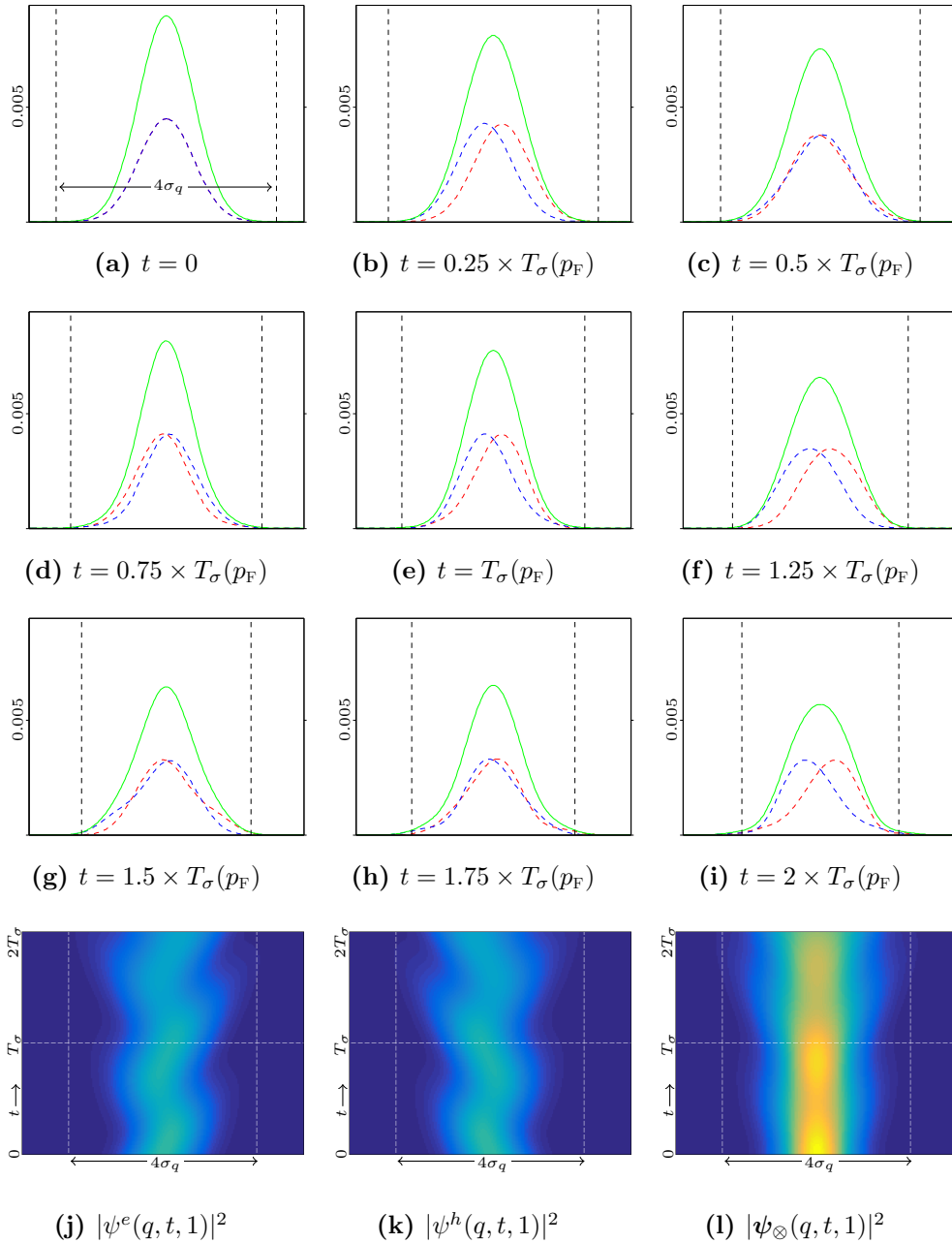
Figure 5.18: Figures a - i show snapshots in the propagation of product state located at $V_0 = p_{\mathrm{F}}$ consisting of an initially equal superposition of electron and hole components, except now with a phase shift between components ($\beta = i$) with parameters $\Delta_0/\mu = 0.05$, $x = 2$. Red and blue dashed lines denote electron ($|\psi^e(q,t,i)|^2$) and ($|\psi^h(q,t,i)|^2$) respectively and green their sum. The dashed vertical lines correspond to the $4\sigma_q$ width of the initial wave packet. Figures j - l are the corresponding q v t density plots, again for each component, and their sum.

The analysis in the Heisenberg picture indicated that the product coherent state wave packet has dynamics dependent on the magnitude of $\mathrm{Im}(\beta)$. Here β is purely imaginary and we can see that these dynamics are due to the oscillations of the two components being out of phase. Although here $x = 2$, in comparison to 5.17 the wave packet still oscillates strongly about the origin, although these oscillations are still spatially symmetric and the wave packet does not dissipate quickly.

(a) $t = 0$ **(b)** $t = 0.25 \times T_\sigma(p_{\mathrm{F}})$ **(c)** $t = 0.5 \times T_\sigma(p_{\mathrm{F}})$

(d) $t = 0.75 \times T_\sigma(p_{\mathrm{F}})$ **(e)** $t = T_\sigma(p_{\mathrm{F}})$ **(f)** $t = 1.25 \times T_\sigma(p_{\mathrm{F}})$

(g) $t = 1.5 \times T_\sigma(p_{\mathrm{F}})$ **(h)** $t = 1.75 \times T_\sigma(p_{\mathrm{F}})$ **(i)** $t = 2 \times T_\sigma(p_{\mathrm{F}})$

(j) $|\psi^e(q,t,i)|^2$ **(k)** $|\psi^h(q,t,i)|^2$ **(l)** $|\psi_\otimes(q,t,i)|^2$
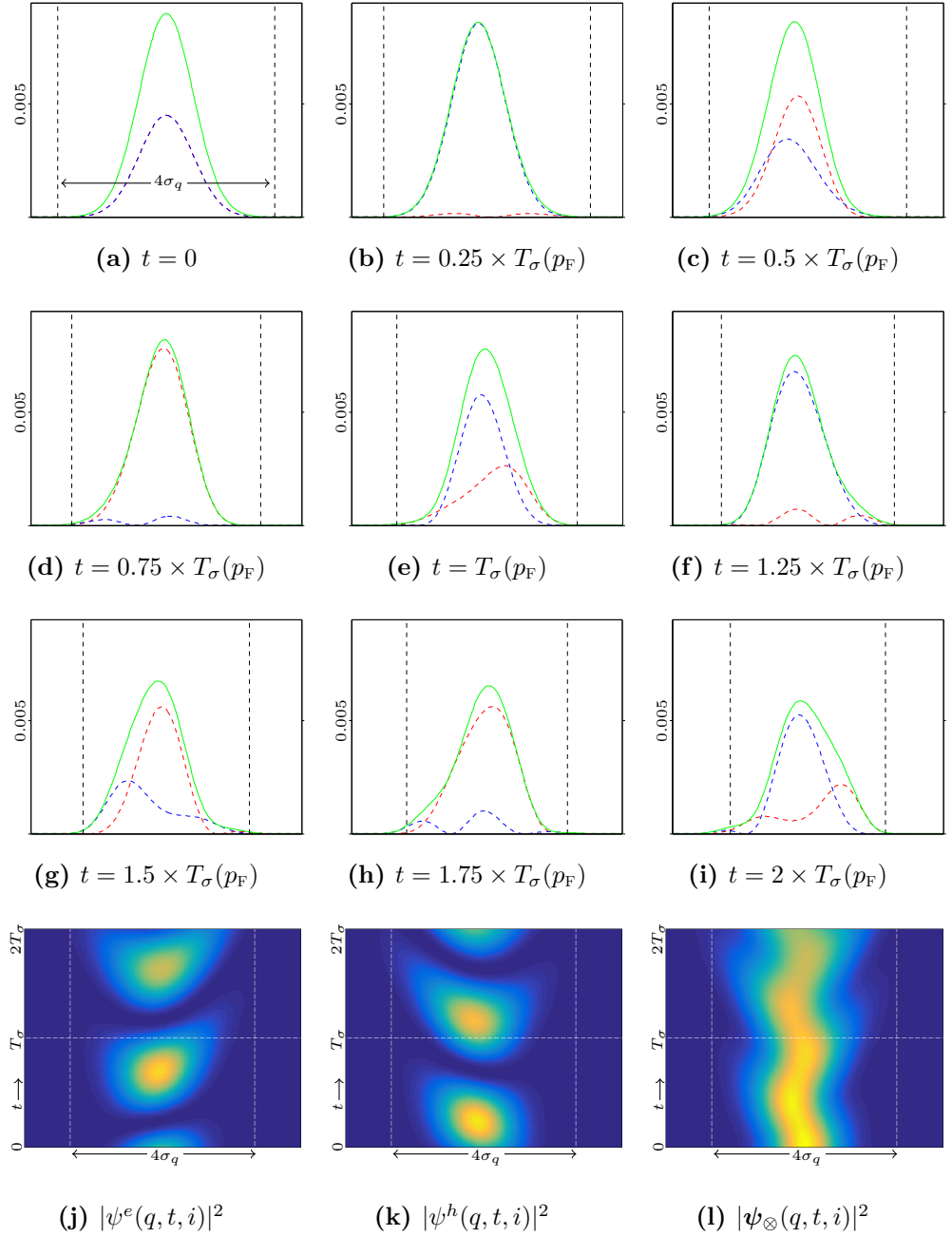
Figure 5.19: Figures a - i now show snapshots in the propagation of a E-H coherent state located at $V_0 = p_{\mathrm{F}}$ with an equal superposition of components initially ($\beta = 1$) with parameters $\Delta_0/\mu = 0.05$ and $x = 1$. Red and blue dashed lines denote electron ($|\psi^e(q,t,1)|^2$) and hole ($|\psi^h(q,t,1)|^2$) components respectively and green their sum. The dashed vertical lines correspond to the $4\sigma_q$ width of the initial wave packet. Figures j - l are the corresponding q v t density plots, again for each component, and their sum. These plots show how the sum of the electron and hole components of the E-H coherent state wave packet is equivalent to the behaviour of a wave packet with initially only an electron component shown in Figure 5.12. The fast oscillations over the individual components are due to interference between the electron and hole contributions, but they cancel overall.

(a) $t = 0$ **(b)** $t = 0.25 \times T_\sigma(p_{\mathrm{F}})$ **(c)** $t = 0.5 \times T_\sigma(p_{\mathrm{F}})$

(d) $t = 0.75 \times T_\sigma(p_{\mathrm{F}})$ **(e)** $t = T_\sigma(p_{\mathrm{F}})$ **(f)** $t = 1.25 \times T_\sigma(p_{\mathrm{F}})$

(g) $t = 1.5 \times T_\sigma(p_{\mathrm{F}})$ **(h)** $t = 1.75 \times T_\sigma(p_{\mathrm{F}})$ **(i)** $t = 2 \times T_\sigma(p_{\mathrm{F}})$

(j) $|\psi^e(q,t,1)|^2$ **(k)** $|\psi^h(q,t,1)|^2$ **(l)** $|\psi_{\bowtie}(q,t,1)|^2$
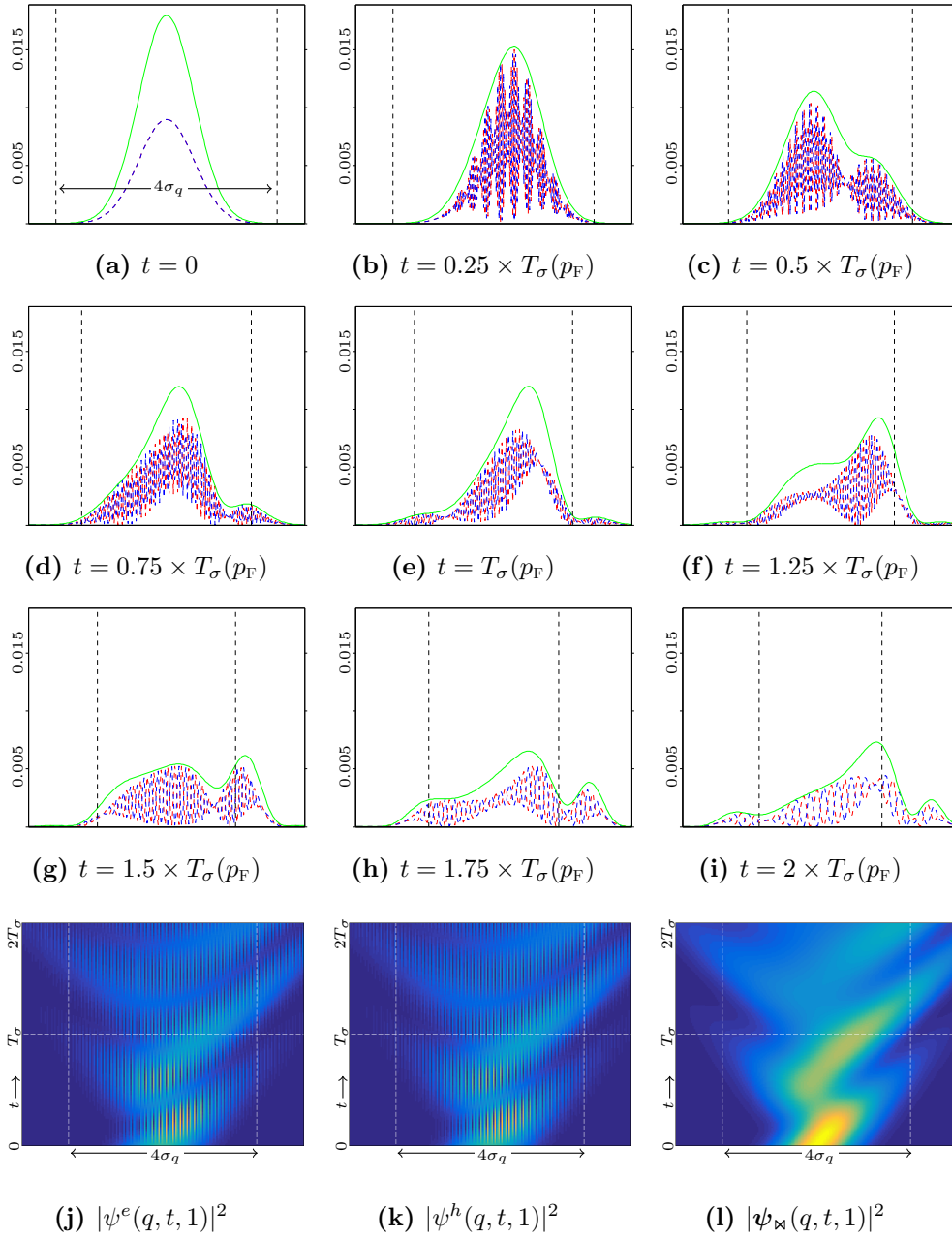
Figure 5.20: Figures a - i show snapshots of the propagation of a E-H coherent state located at $V_0 = p_F$ initially consisting of an equal super position of components ($\beta = 1$) and parameters $\Delta_0/\mu = 0.05$ and $x = 2$. Red and blue dashed lines denote electron ($|\psi^e(q,t,1)|^2$) and hole ($|\psi^h(q,t,1)|^2$) components respectively and green their sum. The dashed vertical lines correspond to the $4\sigma_q$ width of the initial wave packet. Figures j - l are the corresponding q v t density plots, again for each component, and their sum. Again the sum of the electron and hole components produce a wave packet that is equivalent to the behaviour of the initially electron only wave packet as shown in figure 5.13

(a) $t = 0$

(b) $t = 0.25 \times T_\sigma(p_F)$

(c) $t = 0.5 \times T_\sigma(p_F)$

(d) $t = 0.75 \times T_\sigma(p_F)$

(e) $t = T_\sigma(p_F)$

(f) $t = 1.25 \times T_\sigma(p_F)$

(g) $t = 1.5 \times T_\sigma(p_F)$

(h) $t = 1.75 \times T_\sigma(p_F)$

(i) $t = 2 \times T_\sigma(p_F)$

(j) $|\psi^e(q,t,1)|^2$

(k) $|\psi^h(q,t,1)|^2$

(l) $|\boldsymbol{\psi}_\bowtie(q,t,1)|^2$
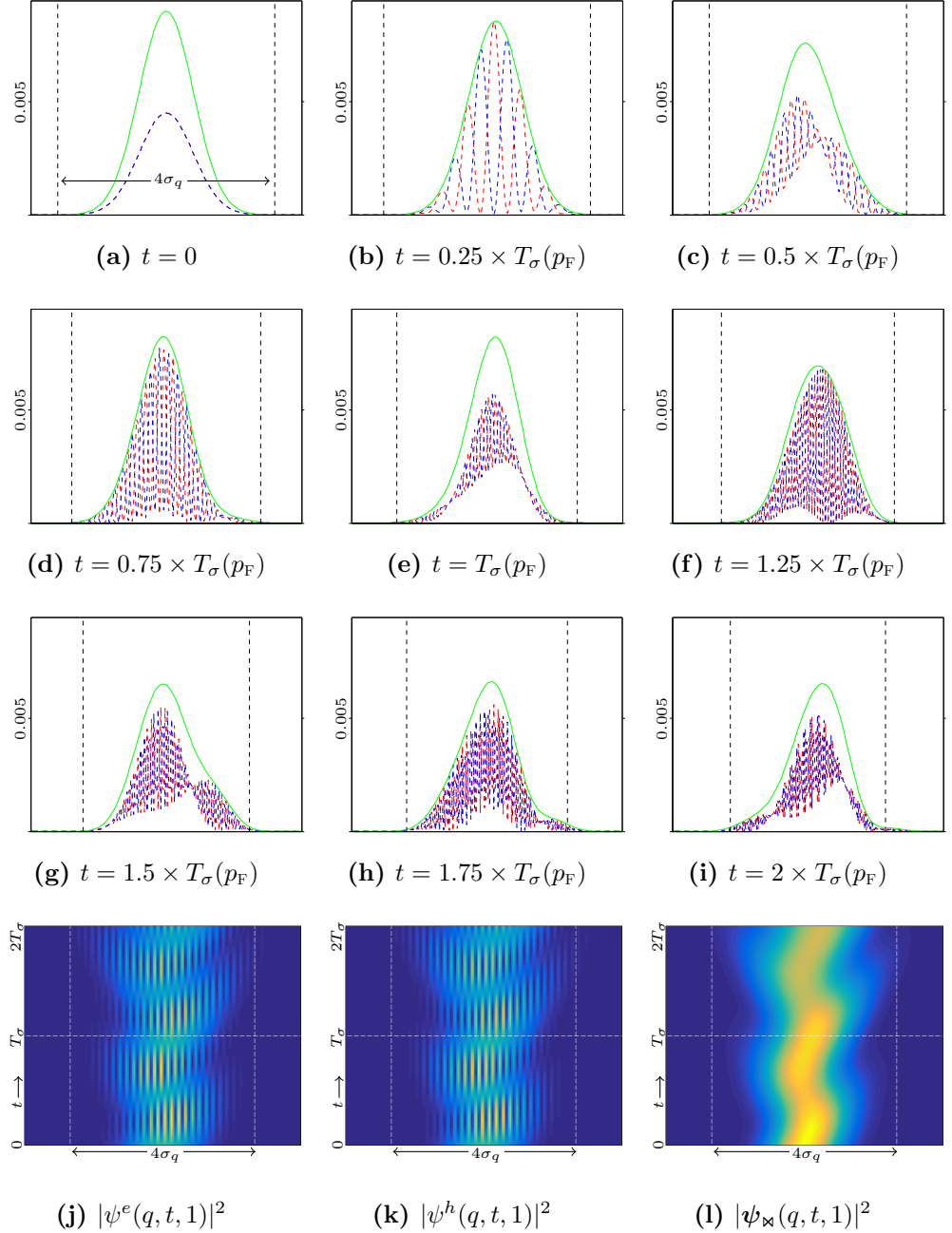
Figure 5.21: q v t density plots of the propagation of an initially electron ($\beta = 0$) E-H coherent state wave packet located at $V_0 = p_F$ with parameters $\Delta_0/\mu = 0.05$, for 10 cycles of $T_\sigma(p_F)$ and varying wave packet widths $x = 1$ and $x = 2$ as labelled. The red dashed line is the expected position of the wave packet as calculated in the Heisenberg picture (see section 5.4).

Over longer time-scales we can see how the smaller value of x causes the wave packet to more quickly dissipate due to the velocity of the individual components. Larger values of x mean the wave packet retains it form over a larger number of rotation cycles. Though the expected position of both wave packets demonstrate a positive velocity the smaller value of x means the expected position quickly propagates away from the origin.
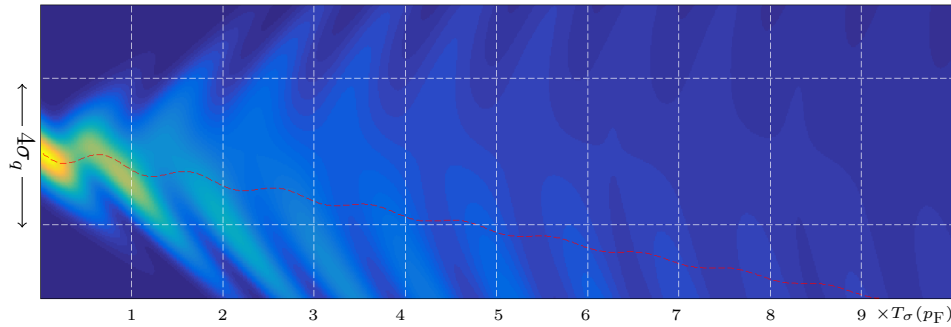
(a) $|\psi_\bowtie(q, t, 0)|^2$, $x = 1$
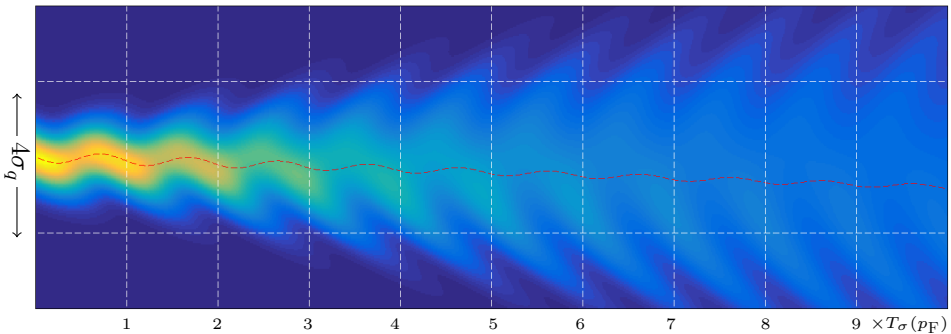
(b) $|\psi_\bowtie(q, t, 0)|^2$, $x = 2$

5.5.2   Asymptotic Long Time Behaviour

We again analyse the long time behaviour of E-H coherent state wave packets using the stationary phase approximation. In this case this will require analysis of stationary phase contributions that also depend on q. For wave packets located on the Fermi momentum we will show how oscillations arise from the electron and hole contributions, and the propagation of the wave packet from the asymmetry of the plane wave contributions described by the dispersion relation.

The integral given by Equation (5.234) must first be put into a form suitable for the application of the stationary phase approximation. Labelling

the overall phase term in the integral

$$\frac{pq}{t} \pm E(p) = \theta_\pm(p) \tag{5.236}$$

then equation (5.234) can be written in a form suitable for the application of the stationary phase approximation as

$$I(q,t) = N \int f(p) \exp\left[-\frac{\lambda}{2}(p - V_0)^2 + \frac{it}{\hbar}\theta_\pm(p)\right] dp \tag{5.237}$$

in the limit $t \to \infty$. As a naive approach to the approximation we might only consider the stationary points of $E(p)$ as we did in the Heisenberg picture, suspecting that the term pq/t only makes small contributions at long times. However it needs to be taken into account that the range of q under consideration is potentially unbounded and at long times the propagation and spread of the wave packet may mean there are significant contributions where pq is of the same order as t. This has a significant effect on the location of the stationary phase points, and is especially important for spatially broad wave packets that are very localised in momentum.

We therefore consider the points of stationary phase p_s, satisfying the condition $\theta'_\pm(p_s) = 0$. When $q = 0$ the solution is straightforward as it requires solving

$$E'(p_s) \equiv \frac{p_s \mathcal{H}_o(p_s)}{mE(p_s)} = 0. \tag{5.238}$$

for p_s. This gives the three stationary phase solutions previously found in Sub-section 5.4.5, $p_s = \{0, \pm p_F\}$. When $q \neq 0$ the solution is more involved, as it then requires solving

$$E'(p_s) = \mp\frac{q}{t} \tag{5.239}$$

for p_s. Analytically this is tricky, requiring finding the roots of a high order polynomial. However this equation can be written as a third order polynomial of $\mathcal{H}_0$. The full set of six solutions are analytic and given in full by

$$\pm p_1(q,t) = \pm\frac{1}{t}\sqrt{\frac{m}{3}}\left[X^{1/3} + Y^2 X^{-1/3} + Z\right]^{\frac{1}{2}} \tag{5.240}$$

$$\pm p_2(q,t) = \pm\frac{1}{t}\sqrt{\frac{m}{6}}\left[-X^{1/3} - Y^2 X^{-1/3} + i\sqrt{3}\left(X^{1/3} - Y^2 X^{-1/3}\right) + 2Z\right]^{\frac{1}{2}} \tag{5.241}$$

$$\pm p_3(q,t) = \pm\frac{1}{t}\sqrt{\frac{m}{6}}\left[-X^{1/3} - Y^2 X^{-1/3} - i\sqrt{3}\left(X^{1/3} - Y^2 X^{-1/3}\right) + 2Z\right]^{\frac{1}{2}}. \tag{5.242}$$
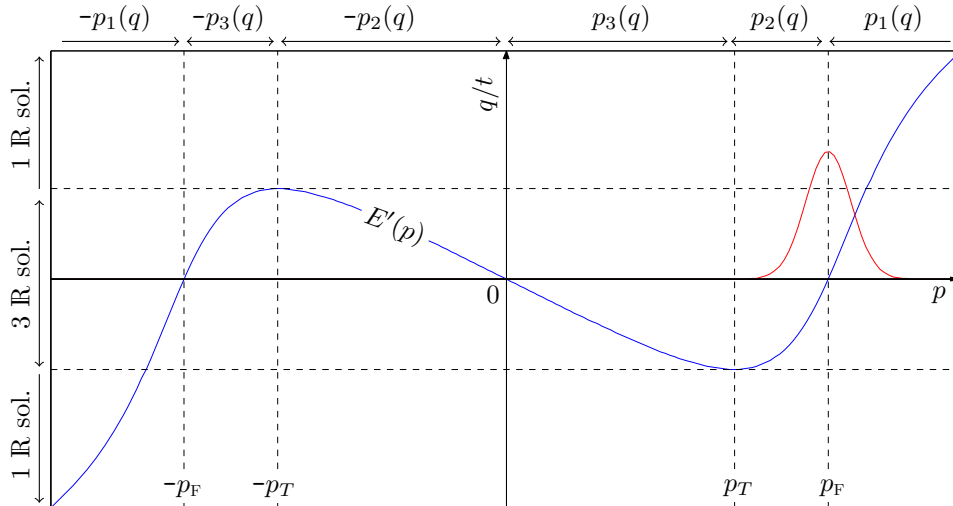
Figure 5.22: Illustration of the regions of $E'(p)$ over which the 3 stationary phase solutions $p_i(q,t)$ are applicable. The number of real solutions (which permit stationary phase approximations) depends upon the value of q/t under consideration. At the points $E'(\pm p_T)$ the stationary phase points $\pm p_2(q)$ and $\pm p_3(q)$ coalesce into a single saddle point. This requires additional corrections to the stationary phase approximation. We will typically consider Gaussian distributions centred at $V_0 = p_F$ as shown in red. A sufficiently narrow distribution will mean that we need only consider contributions from stationary phase point that fall under the Gaussian profile.

The shorthand

$$X = \left[3\sqrt{3m}q\Delta_0 t^2 + \sqrt{Y^3 + (3\sqrt{3m}q\Delta_0 t^2)^2} \right]^2 \tag{5.243}$$

$$Y = mq^2 - 2\mu t^2 \tag{5.244}$$

$$Z = mq^2 + 4\mu t^2 \tag{5.245}$$

has been introduced. The six solutions, $\pm p_i(q,t)$, parametrize sections of the curve $E'(p)$ in terms of q/t. Only contributions to the stationary phase approximation from the real stationary points of $\theta'_\pm(p)$ need to be considered, as contributions from complex stationary points are exponentially suppressed. With this in mind each solution only contributes to the approximation over a limited range of q/t and corresponding values of p as illustrated in Figure 5.22. The ranges of p and q/t over which the $p_i(q,t)$

are real are

$$p_1(q) \implies \quad p > p_{\mathrm{F}} \qquad q/t > 0$$
$$-p_1(q) \implies \quad p < -p_{\mathrm{F}} \qquad q/t < 0$$
$$p_2(q) \implies \quad p_{\mathrm{T}} < p < p_{\mathrm{F}} \qquad q/t < 0$$
$$-p_2(q) \implies \quad 0 < p < -p_{\mathrm{T}} \qquad q/t > 0$$
$$p_3(q) \implies \quad 0 < p < p_{\mathrm{T}} \qquad q/t < 0$$
$$-p_3(q) \implies \quad p_{\mathrm{F}} < p < -p_{\mathrm{T}} \qquad q/t > 0$$

where $\pm p_{\mathrm{T}}$ are the turning points between $\pm p_2(q, t)$ and $\pm p_3(q, t)$ respectively. They satisfy $\theta''(\pm p_{\mathrm{T}}) \equiv E''(\pm p_{\mathrm{T}}) = 0$. The number of real solutions changes with the value of q/t under consideration. There are three real solutions when $E'(-p_{\mathrm{T}}) < q/t < E'(p_{\mathrm{T}})$, and only one real solution $\pm p_1(q, t)$ outside this range, where $p_2(q, t)$ and $p_3(q, t)$ are imaginary. It must also be considered that as q/t approaches $E'(p_{\mathrm{T}})$ from above or $E'(-p_{\mathrm{T}})$ from below, $\pm p_2(q, t)$ and $\pm p_3(q, t)$ will move toward each other before coalescing at $E'(\pm p_{\mathrm{T}})$.

The asymptotic analysis will first be performed under the assumption that the stationary points are well separated in p. The case of coalescing stationary points is discussed below. It will also assist in calculations if we note that the symmetry of $E'(p)$ implies that $p_3(q) = p_2(-q)$ and $p_1(q) = p_1(-q)$.

Applying the stationary phase approximation to integral (5.237) gives

$$I(q, t) \approx N \sum_{p_i \in \Re} f(p_i) \exp\left[-\frac{\lambda}{2}(p_i - V_0)^2 + \frac{it}{\hbar}\theta_\pm(p_i)\right]$$

$$\times \int \exp\left[\pm\frac{it}{2\hbar}E''(p_i)(p - p_i)^2\right] dp \qquad (5.246)$$

$$= N \sum_{p_i \in \Re} f(p_i) \sqrt{\frac{2\pi\hbar}{t|E''(p_i)|}} \exp\left[-\frac{\lambda}{2}(p_i - V_0)^2 + i\left(\frac{t}{\hbar}\theta_\pm(p_i) \pm \frac{c\pi}{4}\right)\right]. \qquad (5.247)$$

Here we will label the contributions by their stationary phase point and energy branch as

$$I(q, t) \approx N \sum_{p_i \in \Re} A(p_i) S_-[p_i, \pm] \qquad (5.248)$$

for later convenience. The subscript S_- here refers to the sign of V_0 in the Gaussian (i.e. this is positive for a hole state). The summation is made over the real stationary phase points p_i, hence the number of terms in the

summation will depend on the value of q/t. Additionally $c = \mathrm{sgn}(E''(p_i))$. This approximation requires that the width of the stationary phase contribution is narrower than the real Gaussian envelope in $I(q,t)$ (see Appendix C.2). This is true for times $t \gg 1/m\omega E''(p_s)$.

At isolated values of q/t the stationary points coalesce. In this case a uniform approximation needs to be performed that generally leads to a Airy-type integral. Though we will in practice not derive the uniform approximation we can show how to treat this case in principal. It has been shown that $\theta_\pm(p)$ has stationary points $\pm p_i(q)$ and that two of the stationary points coalesce at $p_3(q_T) = p_2(q_T) \equiv p_s$. It can then be assumed that at this degenerate stationary point

$$\theta'_\pm(p_s, q_T) = 0, \quad \theta''_\pm(p_s, q_T) = 0, \quad \theta'''_\pm(p_s, q_T) \neq 0, \tag{5.249}$$

at a certain position q_T for a given value of t. It has been shown by Chester, Friedman and Ursell [74] that in a neighbourhood of $(p_s(q), q_T)$ there is change of variables $p = P(q,s)$ and functions $\vartheta(q)$ and $\rho(q)$ such that

$$\theta_\pm(q,p) = \vartheta(q) + \rho(q)s + \frac{1}{3}s^3. \tag{5.250}$$

The new variable satisfies $P(q_T, 0) = p_s$ and the function satisfies $\rho(q_T) = 0$. The stationary points are then located at $s = \pm\sqrt{-\rho(q)}$ where $\rho(q) < 0$ when $q < q_T$. Inserting (5.250) back into the stationary phase integral the approximation is then given in terms of s as

$$I(q) \approx N \int ds \, f(P(q,s))P'(q,s)$$
$$\times \exp\left[-\frac{\lambda}{2}(P(q,s) - V_0)^2 + \frac{i}{\hbar}t\left(\vartheta(q) + \rho(q)s + \frac{1}{3}s^3\right)\right]. \tag{5.251}$$

The largest contributions now come from the new stationary points at $s = \pm\sqrt{-\rho(q)}$ meaning

$$\approx Nf(p_s)P'(q_T, 0)\exp\left[-\frac{\lambda}{2}(p_s - V_0)^2 + \frac{i}{\hbar}t\vartheta(q)\right]\int \exp\left[\frac{i}{\hbar}t\left(\rho(q)s + \frac{1}{3}s^3\right)\right]ds. \tag{5.252}$$

After rescaling the integral the solution is the Airy function

$$\approx N\left(\frac{\hbar}{t}\right)^{\frac{1}{3}}f(p_s)P'(q_T, 0)\exp\left[-\frac{\lambda}{2}(p_s - V_0)^2 + \frac{i}{\hbar}t\vartheta(q)\right]\mathrm{Ai}\left(\frac{\rho(q)}{(\hbar/t)^{2/3}}\right). \tag{5.253}$$

Figure 5.23: $E'(p)$ as a function of Δ_0/μ and the location of the Gaussian momentum distributions.
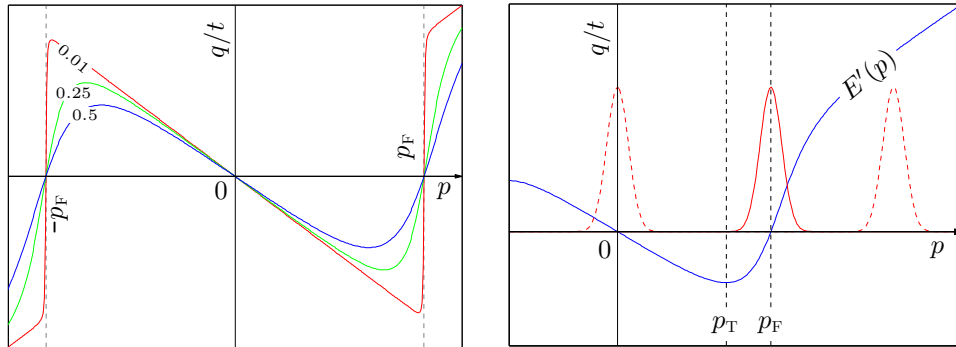
(a) $E'(p)$ for various values of Δ_0/μ: 0.01 (red), 0.25 (green), 0.5 (blue). When $\Delta_0/\mu \to 0$, as $\mu \to \infty$ $E'(p)$ is discontinuous at p_F. This will also dictate which stationary phase points fall within the Gaussian distribution.

(b) We will mainly consider Gaussian distributions centred at $V_0 = p_F$ but also look at larger momenta and $V_0 = 0$. Each location of momentum distribution isolates different stationary phase contributions along $E'(p)$.

The main difficulty in extending the approximation in this case comes from finding an analytic form for the location of the turning points.

In the case of distinct stationary points analysing the full set of contributions from all the stationary phase points would be cumbersome considering the three possible solutions at a given value of q/t for both $\theta_+(p)$ and $\theta_-(p)$. However since we are considering Gaussian momentum distributions; if the momentum distribution is sufficiently narrow any stationary phase contributions sufficiently far from from V_0 will be suppressed in the tails of the Gaussian distribution as illustrated in Figure 5.23b. A single stationary phase point will then generally dominates for a given value of q/t greatly simplifying the calculation. Although our main interest lies in E-H coherent states located close to the Fermi energy, we will also briefly consider electron-hole wave packets centred at $V_0 = 0$ and $V_0 \gg p_f$ as examples of the application of the stationary phase method.

$V_0 \gg p_F$

First we consider a wave packet with central pseudo-velocity $V_0 \gg p_F$. Based on the dispersion relation and the corresponding stationary states we expect that the wave packet will propagate like a free wave packet with little quasi-spin interaction due to the balance of components on each energy branch.

In practice calculating the stationary phase approximation will require

that the positive and negative regions of q are considered independently, as the contributing stationary phase points change across the $q = 0$ line.

We consider an initial electron wave packet ($\beta = 0$). For positive values of q, a wave packet located at $V_0 \gg p_F$ then isolates a single stationary phase point $p_1(q)$. The two other possible stationary points are suppressed by the tails of the Gaussian. The three stationary phase solutions to $\theta'_+(p_S) = 0$ are given by $E'(p) = -q/t$ which are all suppressed for positive values of q and thus we need only consider contributions from the positive energy contributions.

The stationary phase approximation has the simple form for positive values of q

$$\psi(t, q_+)_e \approx N \left[A_+^2(p_1(q))|e\rangle - \frac{\Delta_0}{2} E^{-1}(p_1(q))|h\rangle \right] S_-[p_1(q), -]. \quad (5.254)$$

The absolute value squared for positive q is then

$$|\psi(t, q_+)_e|^2 \approx \left(\frac{\hbar}{\pi m \omega} \right)^{\frac{1}{2}} \frac{\exp\left[-\lambda(p_1(q) - V_0)^2\right]}{t|E''(p_1(q))|} \left\{ A_+^4(p_1(q)) + \frac{\Delta_0^2}{4} E^{-2}(p_1(q)) \right\}. \quad (5.255)$$

A similar calculation for negative q gives the analogous result

$$|\psi(t, q_-)_e|^2 \approx \left(\frac{\hbar}{\pi m \omega} \right)^{\frac{1}{2}} \frac{\exp\left[-\lambda(p_1(-q) - V_0)^2\right]}{t|E''(p_1(-q))|} \left\{ A_-^4(p_1(-q)) + \frac{\Delta_0^2}{4} E^{-2}(p_1(-q)) \right\}. \quad (5.256)$$

The location of $p_1(q, t)$ can be estimated by expanding the derivative of the phase term about V_0 up to first order

$$E'(p) \approx E'(V_0) + E''(V_0)(p - V_0). \quad (5.257)$$

Since $V_0 \gg p_F$ the $\mathcal{H}_0(p)$ term dominates in $E(p)$ and thus $\mathcal{H}_0/E(p) \sim 1$. Therefore a good linear approximation of $E'(p) \approx p/m$ can be made at these large momenta values. Satisfying the stationary phase approximation then means that

$$p_1(q, t) \approx \frac{mq}{t}. \quad (5.258)$$

Since $p_1(q, t)$ is approximately linear in q, the wave packet remains approximately Gaussian. The centre of the wave packet is located at $q = tV_0/m$, consistent with the trajectory of a free particle. This approximation at a large energy also indicates that the wave packet propagating into negative q is suppressed as $A_-(p) \to 0$ as $p \to \infty$, and in a similar manner the amplitude $\Delta_0^2/E^2(p)$ suppresses any contributions to the hole component.

Although it has been shown that in general the E-H wave packet follows the wave packet resulting from an initial electron, in practice the analogous result for an initial hole ($\beta = \infty$) can be obtained from the electron-hole symmetry of the BdG equations. For an E-H coherent state the reflection about $p = 0$ from $V_0 \to -V_0$ means that for positive q the only contributing stationary phase point is from the positive energy branch where $E'(p) = -q/t$, with the solution $-p_1(-q)$. The full approximation is therefore for positive q

$$\psi(t, q_+)_h \approx N \left[A_+^2(p_1(q))|h\rangle + \frac{\Delta_0}{2} E^{-1}(p_1(q))|e\rangle \right] S_+[-p_1(q), +]. \quad (5.259)$$

as the amplitude terms are even in p and the symmetry $p_1(q) = p_1(-q)$. The wave packet generated by an E-H coherent state with only an initial hole component will therefore follow the electron component as anticipated.

This example confirms previous (but somewhat trivial results) for a wave packet centred at large momenta, namely that wave packets propagate in a manner analogous to a freely propagating state.

$V_0 = 0$

We'll now consider a somewhat more involved example of a wave packet centred at $V_0 = 0$. In this case the contributing stationary phase points are $-p_2(q)$ and $p_3(q)$. Again the assumption is made that contributions from other stationary phase points are suppressed by the tails of the Gaussian distribution, especially avoiding any need to consider coalescing saddle points at $p_0 = p_T$ (satisfied if $4\sigma_p \ll p_T$ then any contributions at the coalescing point are suppressed).

For positive values of q the corresponding stationary phase points for positive and negative energy phase terms are

$$\theta_-'(p) \implies -p_2(q) \equiv -p_3(-q)$$
$$\theta_+'(p) \implies p_3(-q) \equiv p_2(q).$$

Considering an initial electron wave packet the contributions to the stationary phase approximation are for positive q

$$\psi(t, q_+)_e \approx N \left[A_+^2(-p_2(q))|e\rangle - \frac{\Delta_0}{2} E^{-1}(-p_2(q))|h\rangle \right] S_-[-p_2(q), -]$$
$$+ N \left[A_-^2(p_2(q))|e\rangle + \frac{\Delta_0}{2} E^{-1}(p_2(q))|h\rangle \right] S_-[p_2(q), +]. \quad (5.260)$$

This can be further simplified as the amplitude terms are even in p and it can also be shown that $S_-[-p_0, \pm] = S_-[p_0, \mp]^*$ which leads to

$$\psi(t, q_+) \approx N \sqrt{\frac{2\pi\hbar}{t|E''(p_2(q))|}} \exp\left[-\frac{\lambda}{2}p_2^2(q)\right] \left\{ \frac{i\Delta_0}{E(p_2(q))} \sin\left(\frac{t}{\hbar}\theta_+(p_2(q)) + \frac{c\pi}{4}\right) |h\rangle \right.$$

$$+ A_+^2(p_2(q)) \exp\left[-i\left(\frac{t}{\hbar}\theta_+(p_2(q)) + \frac{c\pi}{4}\right)\right] |e\rangle$$

$$\left. + A_-^2(p_2(q)) \exp\left[i\left(\frac{t}{\hbar}\theta_+(p_2(q)) + \frac{c\pi}{4}\right)\right] |e\rangle \right\}. \tag{5.261}$$

Similarly for negative q the two contributing stationary phase points are

$$\theta_+'(p) \implies -p_2(-q)$$

$$\theta_-'(p) \implies p_3(q) \equiv p_2(-q).$$

and by a similar process the stationary phase approximation is given by

$$\psi(t, q_-) \approx N\left[A_+^2(p_2(-q))|e\rangle - \frac{\Delta_0}{2}E^{-1}(p_2(-q))|h\rangle\right] S_- [p_2(-q), -]$$

$$+ N\left[A_-^2(p_2(-q))|e\rangle + \frac{\Delta_0}{2}E^{-1}(p_2(-q))|h\rangle\right] S_- [-p_2(-q), +]. \tag{5.262}$$

Using the relation $S_-^*[p_2(q_+), +] = S_-[p_2(-q_-), -]$ the approximation can be written in spinor form for valid all values of q

$$\psi(t, q)_e \approx N \sqrt{\frac{2\pi\hbar}{t|E''(p_2(|q|))|}} \exp\left[-\frac{\lambda}{2}p_2^2(|q|)\right] \left\{ \frac{i\Delta_0}{E(p_2(|q|))} \sin\left(\frac{t}{\hbar}\theta_+(p_2(|q|)) + \frac{c\pi}{4}\right) |h\rangle \right.$$

$$\left. + \cos\left[\frac{t}{\hbar}\theta_+(p_2(|q|)) + \frac{c\pi}{4}\right] |e\rangle - \frac{iH_0(p_2(|q|))}{E(p_2(|q|))} \sin\left[\frac{t}{\hbar}\theta_+(p_2(|q|)) + \frac{c\pi}{4}\right] |e\rangle \right\}. \tag{5.263}$$

A good approximation of $E'(p)$ around $p = 0$ can be made up to the linear term in p giving $E'(p) \approx -p\mu/mE(0)$. The stationary phase point p_2 is then approximately located at

$$p_2(|q|, t) \approx -\frac{m|q|E(0)}{t\mu}. \tag{5.264}$$

Due to the linear dependence on q, the Gaussian term in (5.263) remains approximately a Gaussian profile centred on $q = 0$, with a time dependent width. The absolute value is the wave packet

$$|\psi_e(q, t)|^2 \approx \left(\frac{\hbar}{\pi m\omega}\right)^{\frac{1}{2}} \frac{1}{t|E''(p_2(|q|))|} \exp\left[-\lambda\left(\frac{mE(0)}{t\mu}\right)^2 |q|^2\right] \tag{5.265}$$

134

which merely remains centred on the origin with a linear time dependence in the width of the wave packet in a similar manner to the free scalar coherent state with zero momentum.

These two examples show that we can apply the stationary phase approximation to find the dynamics of an E-H Gaussian wave packet when $V_0 = \pm p_{\text{F}}$ and $V_0 = 0$. In both cases the wave packet behaves as would be expected from the dispersion relation and if $\mu \gg \Delta_0$ the wave packet behaves in an analogous manner to the dynamics of a scalar wavepacket.

$V_0 = p_{\text{F}}$

We now consider the region of interest close to the Fermi momentum where the dispersion relation predicts that wave packets have zero group velocity but non-zero phase velocity. For a wave packet centred on the Fermi momentum (or equivalently where $E_0 \approx \Delta_0$) further consideration needs to be given as to how the stationary phase points are contained in the width of the wave packet. For the previous two examples the stationary phase points that are not suppressed have been far from p_{T} without any additional requirement on the momentum bandwidth apart from $\delta_p \ll p_{\text{F}}$. But in this case, if we are considering the regime $\mu \gg \Delta_0$ this means that $|p_{\text{F}} - p_{\text{T}}|$ is especially small as shown by Figure 5.23a. Moreover $|p_{\text{F}} - p_{\text{T}}| \to 0$ as $\Delta_0/\mu \to 0$.

In order to avoid any complications arising from the inclusion of the coalescing stationary phase points $p_2(q)$ and $p_3(q)$ when $|q/t| = E'(p_{\text{T}})$ the choice can be made to scale the momentum width of the wave packet in proportion to Δ_0/μ. If we scale the wave packet such that the $4\sigma_p$ width of the Gaussian distribution is contained in the distance $|p_{\text{F}} - p_{\text{T}}|$ as

$$\lambda \gg \left(\frac{2}{p_{\text{T}} - p_{\text{F}}} \right)^2 \tag{5.266}$$

any contributions from the coalescing stationary phase points will then be suppressed by the tails of the Gaussian wave packet. This is illustrated in Figure 5.23b.

For an initial electron coherent state ($\beta = 0$) the wave function in integral form is given by

$$\psi(t, q)_e = N \int e^{-itE(p)/\hbar} \left[A_+^2 |e\rangle - \frac{\Delta_0}{2E(p)} |h\rangle \right] \langle q|p\rangle \langle p|z\rangle dp$$

$$+ N \int e^{itE(p)/\hbar} \left[A_-^2 |e\rangle + \frac{\Delta_0}{2E(p)} |h\rangle \right] \langle q|p\rangle \langle p|z\rangle dp. \tag{5.267}$$

Figure 5.24: Comparison of numeric (red) and long time stationary phase approximation (blue) $|\psi_\bowtie(q,t,0)|^2$ as $t \to \infty$. $\Delta_0/\mu = 0.05$, $x = 1$ and the wave packet is centred at $V_0 = p_F$. Dashed lines correspond to the location of the turning points of $E'(p)$ located at $q_T = tE''(p_T)$ where the approximation fails due to the influence of coalescing saddle points. t_{min} is the minimum time at which the stationary phase contributions become dominant. In this case this is given by $t_{min} = (m\omega E''(p_F))^{-1}$
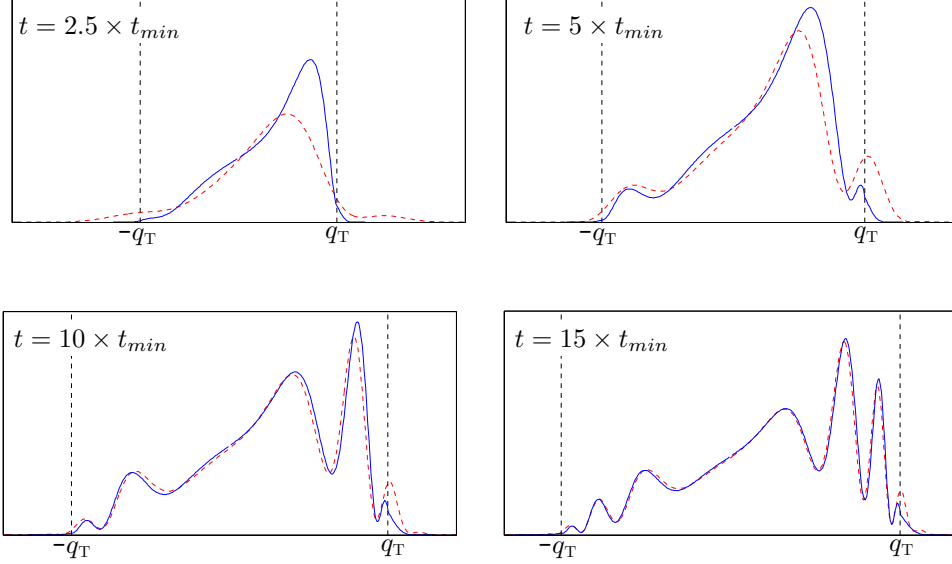
The stationary phase solutions for $q/t > 0$ and $q/t < 0$ are again required to be treated independently. The solutions to the stationary phase condition changes from $p_1(q) > p_F$ for positive values of q/t to $p_2(q) < p_F$ for negative values. For positive q the relevant stationary phase contributions are

$$\begin{aligned}
\theta_+(p) &\implies p_2(-q,t) \\
\theta_-(p) &\implies p_1(q,t)
\end{aligned}$$

as any contributions from $p_3(-q,t)$ are suppressed by design. The stationary phase approximation for positive q is therefore

$$\psi(t,q_+)_e \approx N \left[A_+^2(p_1(q))|e\rangle - \frac{\Delta_0}{2} E^{-1}(p_1(q))|h\rangle \right] S_-[p_1(q),-]$$
$$+ N \left[A_-^2(p_2(-q))|e\rangle + \frac{\Delta_0}{2} E^{-1}(p_2(-q))|h\rangle \right] S_-[p_2(-q),+] \tag{5.268}$$

and for negative q

$$\psi(t, q_-)_e \approx N \left[A_+^2(p_2(q)) |e\rangle - \frac{\Delta_0}{2} E^{-1}(p_2(q)) |h\rangle \right] S_-[p_2(q), -]$$
$$+ N \left[A_-^2(p_1(-q)) |e\rangle + \frac{\Delta_0}{2} E^{-1}(p_1(-q)) |h\rangle \right] S_-[p_1(-q), +].$$
(5.269)

The hole components for positive and negative q are related by $\psi(t, q_-)_e^h = \psi(t, -q_+)_e^{h*}$. Thus the absolute value of the hole component of the wave packet will always remain symmetrically located around the origin, but there is a clearly a spatial asymmetry in the electron component as shown by the numerical plots.

Examining the terms contained in the absolute value of the electron component for positive q, firstly there are two non oscillating terms

$$N^2 \left(A_+(p_1(q))^4 |S_-[p_1(q), -]|^2 + A_-(p_2(-q))^4 |S_-[p_2(-q), +]|^2 \right). \quad (5.270)$$

From the form of S (Equation (5.248)) we can infer that these are Gaussian like terms peaked at $p_i = V_0$. There are also oscillating terms arising from the interference between the two stationary phase points

$$N^2 [A_+(p_1(q)) A_-(p_2(-q))]^2 \left(S_-[p_1(q), -]^* S_-[p_2(-q), +] + \text{C.C.} \right). \quad (5.271)$$

Moreover expanding the right hand bracket of Equation (5.271) it contains both the product of real Gaussian contributions from both stationary points

$$\exp \left[-\frac{\lambda}{2} (p_1(q) - V_0)^2 - \frac{\lambda}{2} (p_2(-q) - V_0)^2 \right] \quad (5.272)$$

which will suppress any oscillations away from the origin. It also contain oscillating terms of the form

$$\exp \left[\frac{i}{\hbar} q [p_1(q) - p_2(-q)] - \frac{i}{\hbar} t [E(p_1(q)) + E(p_2(-q))] \right] + \text{C.C.} \quad (5.273)$$

Numerically integrated results show that the oscillations over the wave packet correspond to wave-fronts propagating from the origin, we can see from these terms that the position of the peaks is dependent on the asymmetry between the behaviour of stationary points either side of p_F. In this case if $p_1(q)$ and $p_2(-q)$ were symmetric in q the resulting oscillations would also be spatially symmetric.

It has been shown that $E'(p)$ is well approximated by a linear function close to $p \gg p_F$ and $p = 0$. In the region close to p_F this approximation

is of limited value as it does not take into account the asymmetry of $p_1(q)$ and $p_2(-q)$ above and below $q/t = 0$. This asymmetry is not present (or is relatively small) for stationary phase points either side of the origin or $V_0 \gg p_\text{F}$.

We can consider a very narrow wave packet in momentum, such that $E'(p)$ can be approximated linearly about p_F (in effect the wave packet will be too narrow to see any asymmetry in $E(p)$ close to p_F). Going back to the phase term $E(p)$ and expanding up to second order around the Fermi momentum

$$E(p) \approx \Delta_0 + \frac{\mu}{m\Delta_0}(p - p_\text{F})^2 \tag{5.274}$$

gives $E''(p) \approx 2\mu/m\Delta_0$. It follows that the stationary phase solutions $p_1(q,t)$ and $p_2(q,t)$ close to p_F are approximately linearly dependent on q/t giving the approximate locations

$$p_1 \approx p_\text{F} + \frac{m\Delta_0 q}{2\mu t} \quad \text{when} \quad q > 0 \tag{5.275}$$

$$p_2 \approx p_\text{F} + \frac{m\Delta_0 q}{2\mu t} \quad \text{when} \quad q < 0. \tag{5.276}$$

Inserting approximations (5.275) and (5.276) into the stationary phase approximation the absolute square of the initial electron spinor wave function can be written in a form that is valid for all q as

$$|\psi(q,t)^e_e|^2 \approx \left(\frac{m\hbar}{\pi\omega}\right)^{\frac{1}{2}} \frac{\Delta_0}{2\mu t} \exp\left[-\lambda \left(\frac{m\Delta_0}{2\mu t}\right)^2 q^2\right]$$
$$\left\{A_+^4 \left(p_\text{F} + \frac{m\Delta_0 q}{2\mu t}\right) + A_-^4 \left(p_\text{F} - \frac{m\Delta_0 q}{2\mu t}\right)\right.$$
$$\left.+4A_+^2 \left(p_\text{F} + \frac{m\Delta_0 q}{2\mu t}\right) A_-^2 \left(p_\text{F} - \frac{m\Delta_0 q}{2\mu t}\right) \cos\left[\frac{t}{\hbar}\Delta_0 \left(1 + \frac{m}{\mu}\left(\frac{q}{2t}\right)^2\right) + \frac{\pi}{4}\right]\right\}.$$
$$\tag{5.277}$$

Overall the wave packet remains symmetric and centred on the origin, with time dependent oscillations between the components.

This symmetry in q arises as this approximation has modelled the stationary phase points contained inside the Gaussian envelope as symmetric across the $q = 0$ line. In effect the wave packet is sufficiently narrow as to suppress any asymmetry effects from higher terms in the expansion. Increasing the momentum bandwidth of the initial wave packet will quickly start to include regions of $E'(p)$ that are no longer symmetric in p, and as such will begin to shift the state from the origin and also deviate the distribution from the initial Gaussian profile. This is consistent with the

numerical plots where the narrower momentum bandwidth is seen to hold the wave packet close to the origin. To get a full picture of the position dependence of the stationary points would require including more terms in the expansion of $E'(p)$, especially up to third order. In terms of complexity extracting more information about the location of the stationary phase points is essentially equivalent to finding the full stationary phase solution so we will only state the full solution in terms of the stationary phase points.

5.5.3 Short Wavelength Behaviour

The short wavelength limit can be achieved both by taking the usual classical limit $\hbar \to 0$ but also the large Fermi energy limit $\mu \to 0$. Considering the time dependent BdG equation

$$\left[-\left(\frac{\hbar^2}{2m} \frac{d^2}{dq^2} + \mu \right) \sigma_3 + \Delta_0 \sigma_1 \right] \psi(q,t) = i\hbar \frac{d}{dt} \psi(q,t) \qquad (5.278)$$

rescaling the time $t \to \tau$ gives

$$\left[-\left(\frac{d^2}{dq^2} + \frac{2m\mu}{\hbar^2} \right) \sigma_3 + \frac{2m\Delta_0}{\hbar^2} \sigma_1 \right] \psi(q,\tau) = i \frac{d}{d\tau} \psi(q,\tau). \qquad (5.279)$$

The two parameters $2m\mu/\hbar^2$ and $2m\Delta_0/\hbar^2$ both grow in the limit $\hbar \to \infty$, but in the limit $\mu \to \infty$ only $2m\mu/\hbar^2$ grows. In general we may consider asymptotic limits where both parameters grow at different rates. This allows $\hbar$ and m to remain fixed, and then consider the energy parameters μ and Δ_0 as quantities that define the short wavelength asymptotics here.

We should also consider the relationship between the fundamental length and time-scales, and the shape of the initial wave packet in these two short wavelength regimes. The dynamics of the wave packet are dictated by the energy parameters $2m\mu/\hbar$, $2m\Delta_0/\hbar$ and the expected energy of the initial wave packet. The shape of the initial wave packet depends on the squeezing parameter ω and $\hbar$.

We have also introduced the spin distance length scale (for a wave packet with $V_0 = p_\mathrm{F}$)

$$d_\sigma(p_\mathrm{F}) = v_\mathrm{F} T_\sigma(p_\mathrm{F}) = \frac{p_\mathrm{F}}{m} \frac{\pi \hbar}{\Delta_0} \qquad (5.280)$$

in section 5.2 as the distance the centre of the wave packet will travel in the time it takes for a full revolution in electron-hole quasi-spin space. We also introduced the ratio x in section 5.2 as

$$x = \frac{\delta_q}{d_\sigma(p_\mathrm{F})} = \frac{1}{\sqrt{\hbar\omega\mu}} \frac{2\Delta_0}{\pi}. \qquad (5.281)$$

The analysis in previous sections has shown that the value of x has a strong effect on the resulting dynamics on the Fermi momentum. If ω does not scale like μ or $\hbar$, this will mean that x will scale as $1/\sqrt{\mu\hbar}$. Their are two possible asymptotic cases, $x \to 0$ as $\mu \to \infty$ meaning that the wave packet moves quickly well outside the initial envelope (see the numerically integrated example Figure 5.14) and $x \to \infty$ as $\hbar \to 0$ meaning the wave packet remains well localised and stationary as any oscillations will be contained inside the initial envelope (see the numerically integrated example Figure 5.15).

These two asymptotic values of x indicate behaviour analogous with a free particle. To see any oscillatory dynamics in these short wavelength regimes will require a fixed value of x. This can be achieved by scaling ω like μ or $\hbar$. Considering the inverse of Equation (5.281)

$$\omega = \frac{1}{\hbar\mu}\left(\frac{2\Delta_0}{x\pi}\right)^2 \tag{5.282}$$

gives the wave packet squeezing necessary to retain finite values of x. We will show that except for a small number of specific cases, in the short wavelength regime one cannot generally define a wave packet that retains a finite width, and has a finite non-zero value of x.

$\boldsymbol{\mu \to \infty}$

We first consider the simplest case of scaling $\mu \to \infty$ whilst holding all other system parameters constant. This means that $d_\sigma(p_{\mathrm{F}}) \to \infty$ as v_{F} scales like $\sqrt{\mu}$. If we first consider scaling the width of the wave packet so that x remains finite then the wave packet will have the parameters

$$\omega \to 0 \quad \implies \quad \sigma_q \to \infty \qquad \sigma_p \to 0.$$

This wave packet loses any spatial information, and the resultant solutions are simply plane waves.

If instead the value of ω is fixed by scaling x as $x \sim 1/\mu$, in this case as $x \to 0$ the wave packet will quickly move away from under the initial envelope. This can be shown analytically by considering that since Δ_0 is fixed, the ratio $\Delta_0/\mu \to 0$. In this limit $E'(p)$ shows a discontinuity at $\pm p_{\mathrm{F}}$ (see Figure 5.23a). This discontinuity occurs due to the curves $\pm E(p)$ approaching the intersecting dispersion relations that describe free electron and hole particle in a normal conductor as both shown in Figure

5.1. Expanding $E(p)$ around $\pm p_\text{F}$, where $E'(p)$ changes sign, as

$$E(p) = \mathcal{H}_0 \sqrt{1 + \left(\frac{\Delta_0}{\mathcal{H}_0}\right)^2} = \mathcal{H}_0 \left[1 + \frac{1}{2}\left(\frac{\Delta_0}{\mathcal{H}_0}\right)^2 \dots\right] \tag{5.283}$$

then the expansion on the right converges towards $\mathcal{H}_0$ very quickly as $\mu \to \infty$ except at $p = p_\text{F}$. In this regime the expansion either side of p_F is

$$E(p) \approx \begin{cases} \mathcal{H}_0, & \text{if } p < -p_\text{F} \text{ and } p > p_\text{F} \\ -\mathcal{H}_0, & \text{if } -p_\text{F} < p < p_\text{F} \end{cases}. \tag{5.284}$$

As the width of the momentum distribution is fixed independent of μ, we might attempt to apply the the stationary phase approximation. The discontinuities at $E'(p)$ would require a method of evaluating stationary phase contributions on the discontinuity. If instead the discontinuous approximation of $E(p)$ is inserted into the electron component of the wave function, the amplitude term $\mathcal{H}_0/E(p)$ in the regions either side of $\pm p_\text{F}$ will behave like

$$\frac{\mathcal{H}_0}{E(p)} \to \begin{cases} 1, & \text{if } p < -p_\text{F}, \ p > p_\text{F} \\ -1, & \text{if } -p_\text{F} < p < p_\text{F} \end{cases}. \tag{5.285}$$

In total the time dependent terms in Equation (5.267) for the electron component then tend to the simplified form

$$\left[A_+^2(p)e^{-itE(p)/\hbar} + A_-^2(p)e^{itE(p)/\hbar}\right] \to \begin{cases} e^{-it\mathcal{H}_0(\hat{p})/\hbar}, & \text{if } p < -p_\text{F}, \ p > p_\text{F} \\ e^{it\text{-}\mathcal{H}_0(\hat{p})/\hbar}, & \text{if } -p_\text{F} < p < p_\text{F} \end{cases}. \tag{5.286}$$

Even though previously the regions either side of p_F had to be treated independently, in the large μ limit the time development function can be written as a single continuous function over the full range of p (excluding p_F) as

$$\hat{U}(t) \approx \exp\left(-\frac{it}{\hbar}\mathcal{H}_0(\hat{p})\right). \tag{5.287}$$

This is of course recognisable as the time evolution operator for free motion of the electron with no interaction (i.e. in a normally conducting region). The solution is easily found with no further approximation as the exponent is now quadratic in p. The resulting wave function is simply

$$\psi(q,t)_e \approx N \int \exp\left[-\frac{\lambda}{2}(p - V_0)^2 + \frac{i}{\hbar}pq - \frac{it}{\hbar}\mathcal{H}_0(p)\right] dp \tag{5.288}$$

$$= N\sqrt{\frac{2\pi}{a(t)}} \exp\left[-\frac{1}{2a(t)\hbar^2}(q - v_\text{F}t)^2 + \frac{iV_0}{\hbar}\left(q - \frac{tV_0}{2m}\right) + \frac{it\mu}{\hbar}\right] \tag{5.289}$$

Figure 5.25: Comparison of numerically integrated (red) and asymptotic approximations (blue) of an initial electron component E-H wave packet $|\psi_{\bowtie}(q, t, 0)|^2$ when $\mu \to \infty$. The other system parameters (Δ and ω) held constant at a fixed time.
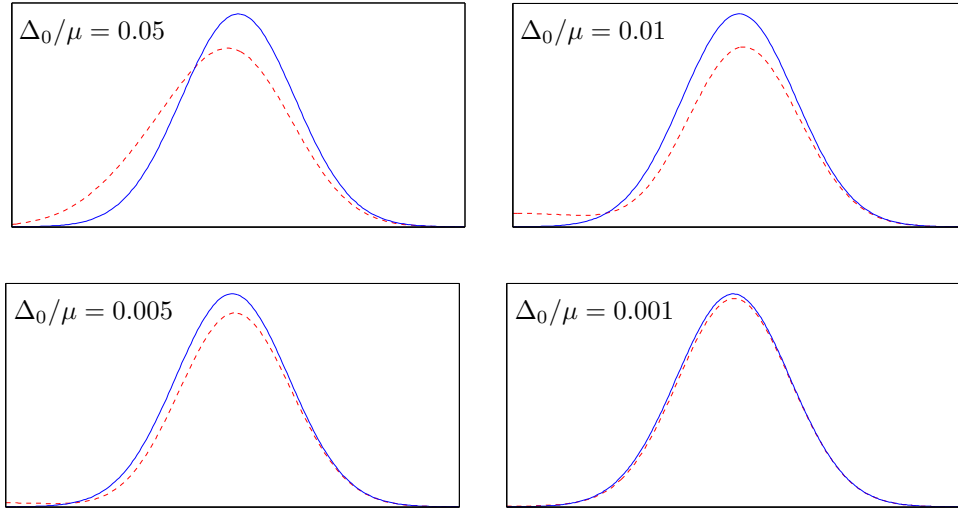
where $a(t) = \lambda + it/\hbar m$. The resultant position wave packet is simply

$$|\psi(q, t)_e|^2 \approx \left(\frac{\lambda}{\pi}\right)^{\frac{1}{2}} \frac{1}{|a(t)|} \exp\left[-\frac{\lambda}{|a(t)|^2 \hbar^2} (q - v_{\mathrm{F}} t)^2\right] \quad (5.290)$$

describing a Gaussian wave packet moving at the Fermi velocity as predicted by the behaviour of x in this limit. Comparison of the numerically integrated solution and this approximation are shown in Figure 5.25 demonstrating convergence for increasingly small values of Δ_0/μ.

To summarise scaling μ alone does not generate a wave packet that is both localised and demonstrates oscillations about the origin. The more interesting regime is when Δ_0 scales alongside μ, parametrizing the scaling of Δ_0 as $\Delta_0 = \delta\mu^\alpha$ where $0 < \alpha \leq 1$. This choice of scaling also has the consequence that both v_{F} and $T_\sigma(P_F)$ now scale like μ. v_{F} is proportional to $\sqrt{\mu}$ and $T_\sigma(P_F)$ scales in the inverse manner $\sim 1/\mu^\alpha$.

There is still a free choice in the scaling of x and ω. For fixed finite values of x it can be seen from Equation (5.282) that there are three cases to consider as $\mu \to \infty$

$$0 < \alpha < 1/2 \implies \omega \to 0$$
$$\alpha = 1/2 \implies \omega \text{ remains at a fixed value}$$
$$1/2 < \alpha < 1 \implies \omega \to \infty.$$

The first case scales like the previous example (albeit more slowly) and the resultant solutions will again be plane wave solutions with no resolution in

Figure 5.26: Comparison of numerically integrated (red) and stationary phase approximation (blue) of $|\psi_\bowtie(q,t,0)|^2$ as $\mu \to \infty$, with Δ_0 also scaled as $\Delta_0 = \delta\mu^{1/2}$ at a fixed time $t = 1$, $\delta = 0.05$. $\mu_{crit} = (\lambda\hbar/t\theta''(0))^2$ is the approximate value at which the stationary phase contributions become dominant. Dashed lines indicate the origin and $|q| = tv_F$ where the approximation fails.
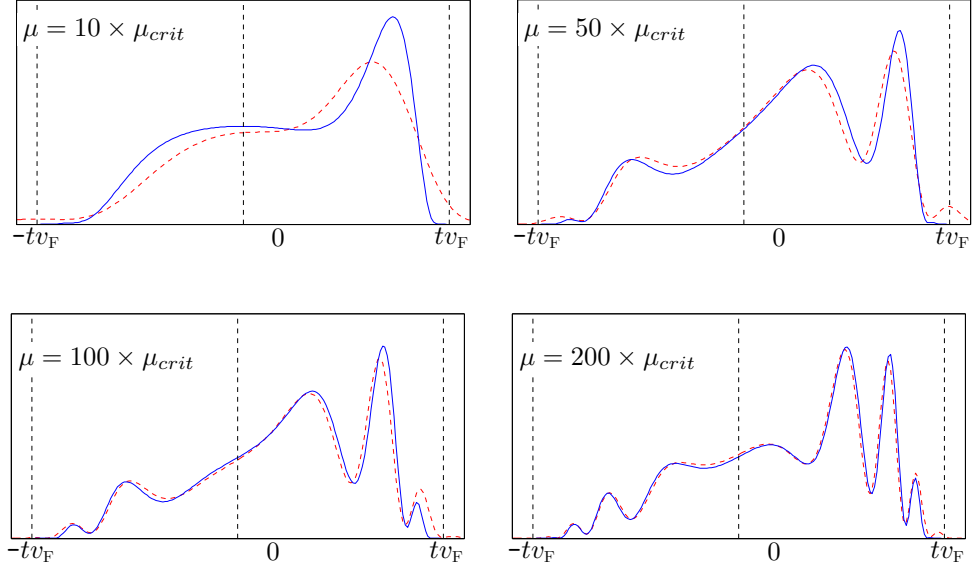
q, albeit with the new scaling applied to $E(p)$. The third case scales in the inverse manner, the wave packet becoming increasingly narrow in q and no definition in p.

Considering instead finite values of ω, the same regimes of α apply

$$0 < \alpha < 1/2 \quad \implies \quad x \to 0$$
$$\alpha = 1/2 \quad \implies \quad x \text{ remains at a fixed value}$$
$$1/2 < \alpha < 1 \quad \implies \quad x \to \infty.$$

The behaviour of x indicates that the first and third case will behave like the free particle. The first case will move away from the origin and the third case will be a stationary wave packet remaining on the origin.

In both cases their is a balanced regime $\alpha = 1/2$, which retains finite values of both x and ω. These wave packets will have both finite dimensions and will be sufficiently narrow as to exhibit oscillations that move outside the Gaussian envelope. For the wave packet located on the Fermi momentum this asymptotic approximation can be derived using the stationary phase approximation with μ as the large parameter. Details of of the calculation can be found in Appendix A.2.3. The resulting stationary

phase approximation of the electron wave function is given by

$$\psi_e^e(q, t) \approx N \sqrt{\frac{2\pi\hbar}{t\mu^{1/2}|\varphi''(p_{\mathrm{S}}(q))|}} \exp\left[-\frac{\lambda}{2}p_{\mathrm{S}}^2(q) + \frac{i}{\hbar}qp_{\mathrm{F}}\right]$$
$$\times \left\{ A_+^2(p_{\mathrm{F}} + p_{\mathrm{S}}(q))e^{-\frac{i}{\hbar}\sqrt{\mu}\,\theta_+(-p_{\mathrm{S}}(q)) - \frac{i\pi c}{4}} + A_-^2(p_{\mathrm{F}} - p_{\mathrm{S}}(q))e^{\frac{i}{\hbar}\sqrt{\mu}\,\theta_+(-p_{\mathrm{S}}(q)) + \frac{i\pi c}{4}} \right\}$$

$$(5.291)$$

and the corresponding hole

$$\psi_e^h(q, t) \approx N \sqrt{\frac{2\pi\hbar}{t\mu^{1/2}|\varphi''(p_{\mathrm{S}}(q))|}} \frac{\Delta_0}{2} \exp\left[-\frac{\lambda}{2}p_{\mathrm{S}}^2(q) + \frac{i}{\hbar}qp_{\mathrm{F}}\right]$$
$$\times \left\{ E^{-1}(p_{\mathrm{F}} - p_{\mathrm{S}}(q))e^{\frac{i}{\hbar}\sqrt{\mu}\,\theta_+(-p_{\mathrm{S}}(q)) + \frac{i\pi c}{4}} - E^{-1}(p_{\mathrm{F}} + p_{\mathrm{S}}(q))e^{-\frac{i}{\hbar}\sqrt{\mu}\,\theta_+(-p_{\mathrm{S}}(q)) - \frac{i\pi c}{4}} \right\}.$$

$$(5.292)$$

The stationary point $p_{\mathrm{S}}(q)$ in this case is located at

$$p_{\mathrm{S}}(q) = \sqrt{\frac{m}{2}}\, q\delta \left[(tv_{\mathrm{F}})^2 - q^2\right]^{-1/2} \tag{5.293}$$

and the phase term is given by

$$\theta_\pm(p) = \frac{pq}{\sqrt{\mu}} \pm t \left[\frac{2}{m}p^2 + \delta^2\right]^{1/2}. \tag{5.294}$$

This approximation is valid for values of μ satisfying

$$\mu \gg \left(\frac{\lambda\hbar}{t\theta_+''(0)}\right)^2. \tag{5.295}$$

A comparison between the numerically integrated solution and this approximation are shown in Figure 5.26 for increasing values of $\mu_{crit} = (\lambda\hbar/t\theta''(p_{\mathrm{S}}(0)))^2$, the approximate minimum value of μ at which the stationary phase contributions become dominant.

It should also be noted that this approximation breaks down for $|q| \geq tv_{\mathrm{F}}$ (as marked on the plots). Indeed $p_{\mathrm{S}}(q)$ is singular when the equality is satisfied, and complex for larger values. The singularity could have been removed by including the slowly varying Gaussian term in the approximation (rather than evaluating it at $p_{\mathrm{S}}(q)$). This example is more suitable for a clear picture of the dynamics though.

Since $p_{\mathrm{S}}(q)$ is not exactly linear in q, the envelope $\exp(-\lambda p_{\mathrm{S}}^2/2)$ does not exactly describe a Gaussian profile. It is still peaked at the origin at the minimum of $p_{\mathrm{S}}(q)$. The strength of the peak is also described by the parameter $(tv_{\mathrm{F}})^2 - q^2$. This implies that the width of the wave packet

144

is approximately tV_F as can be seen in Figure 5.26. This envelope is also symmetric in q, locating the bulk of the wave packet about the origin, but as $p_0(q)$ is approximately linear in q a spatial asymmetry occurs due to the amplitude terms $E(p_{\mathrm{F}} \pm p_{\mathrm{s}})$.

$\hbar \to 0$

Now let us consider the short wavelength limit $\hbar \to 0$ for fixed values of μ and Δ_0. We need to consider that $\hbar$ dependence appears both in the time-scale $T_\sigma(p_{\mathrm{F}})$ and (in the case of the minimum uncertainty coherent state) the spatial and momentum widths in both q and p given by

$$\delta q = \sqrt{\frac{\hbar}{2m\omega}} \qquad \text{and} \qquad \delta p = \sqrt{\frac{\hbar m\omega}{2}}. \qquad (5.296)$$

The squeezing operator ω as therefore scaled as $\omega = \Omega\hbar^\gamma$ over the range $-1 \leq \gamma \leq 1$. The two ends of the range correspond to fixing the widths of the wave packet in p and q respectively. The standard semiclassical approximation is found at $\gamma = 1/2$.

Applying this choice of scaling to x gives

$$x = \left(\frac{2\Delta_0}{\pi\sqrt{\mu\Omega}}\right)\hbar^{-\frac{1}{2}(1+\gamma)}. \qquad (5.297)$$

There are then three cases to be considered, $\gamma = \pm 1$ and intermediate values.

Firstly when δp is held constant indipendent of $\hbar$ (i.e. $\gamma = -1$), the resultant value of x is also indipendent of $\hbar$. Ω can then be scaled such that oscillations will be seen that move outside the initial wave packet (though both the width of the wave packet and $d_\sigma(p_{\mathrm{F}})$ tend to 0 identically). For any other values $-1 < \gamma \leq 1$, x will always tend to ∞, and the wave packet will remain located on the origin. The value of ω is fixed when $x \sim 1/\sqrt{\hbar}$, and in this case the wave packet shrinks in both p and q identically as $\sim \sqrt{\hbar}$.

This scaling is consistent with the previous assertion that $\hbar \to 0$ is equivalent to scaling Δ_0 and μ in an identical manner. In both cases there is a choice to either fix the value of ω or x. Fixing x means $\omega \to \infty$, the width of the wave packet tending to 0. Fixing the the value of ω means $x \to \infty$ and the wave packet will remain centred on the origin.

We omit the full details of calculations of these three asymptotic approximations here, but details can again be found in section A.2.3. We arrive at each approximation by noting that each term in the exponent of the integral

$$I(q,t) = N \int f(p) \exp\left[-\frac{\lambda}{2}(p - V_0)^2 + \frac{i}{\hbar}pq\right] \exp\left[\pm\frac{it}{\hbar}E(p)\right] dp \qquad (5.298)$$

Figure 5.27: Comparison of Numeric (red) and asymptotic approximations (blue) when $\hbar \to 0$. $\Delta_0/\mu = 0.05$ at a fixed time. $\hbar_{min}$ is defined by the minimum value of $\hbar$ at which the appropriate approximation becomes significant.
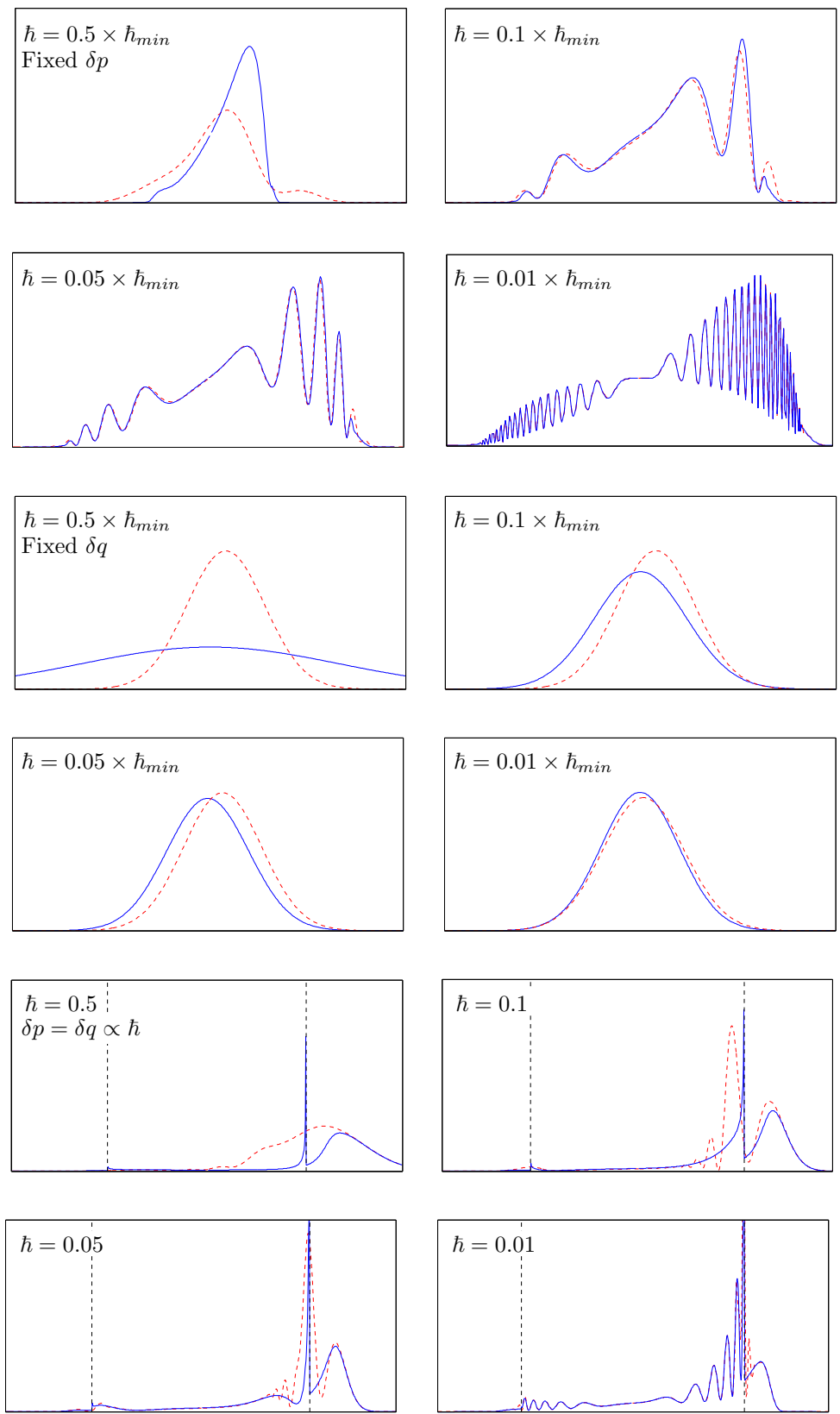
scales in some manner by $\hbar$. The choice of scaling for ω will change the weight of contributions from either the real Gaussian term or complex phase term.

$\gamma = -1$: We will first consider holding the momentum width of the wave packet fixed (corresponding to $\gamma = -1$). The phase term in the exponent scales like $1/\hbar$. The resulting approximation is functional identical to the stationary phase solutions for long times derived in sub-section 5.5.2, though now the stationary phase are found for

$$\theta_\pm(p) = pq \pm tE(p) \tag{5.299}$$

as $\hbar \to 0$. The stationary phase solutions are the same as the long time case. We will again label the general solution in the same manner

$$I(q,t) \approx N \sum_{p_i} A(p_i) \sqrt{\frac{2\pi\hbar}{t|E''(p_i)|}} \exp\left[-\frac{1}{2m\Omega}(p_i - V_0)^2 + \frac{i}{\hbar}\theta_\pm(p_i) \pm \frac{ic\pi}{4}\right] \tag{5.300}$$

$$= N \sum_{p_i \in \Re} A(p_i) S_-[p_i, \pm]. \tag{5.301}$$

This still allows for a choice of fixed value of x using the scaling $\Omega = (2\Delta_0/x\pi\sqrt{\mu})^2$ as δ_p is indipendent of $\hbar$. For a wave packet centred on the Fermi momentum the stationary phase contributions are given by the spinor, for positive q

$$\psi_\bowtie(q_+, t, 0) \approx N\left[A_+^2(p_1(q))|e\rangle - \frac{\Delta_0}{2}E^{-1}(p_1(q))|h\rangle\right] S_-[p_1(q), -]$$
$$+ N\left[A_-^2(p_2(-q))|e\rangle + \frac{\Delta_0}{2}E^{-1}(p_2(-q))|h\rangle\right] S_-[p_2(-q), +] \tag{5.302}$$

and for negative values of q

$$\psi_\bowtie(q_-, t, 0) \approx N\left[A_+^2(p_2(q))|e\rangle - \frac{\Delta_0}{2}E^{-1}(p_2(q))|h\rangle\right] S_-[p_2(q), -]$$
$$+ N\left[A_-^2(p_1(-q))|e\rangle + \frac{\Delta_0}{2}E^{-1}(p_1(-q))|h\rangle\right] S_-[p_1(-q), +]. \tag{5.303}$$

This is essentially equivalent to the the long time behaviour, the only difference being the time scales, as anticipated at the start of this sub-section. Although the spatial width of the wave packet scales like $\hbar$ the time-scale

$T_\sigma(p_\mathrm{F})$ shrinks at the same rate. The above approximation applies for values of $\hbar$ satisfying

$$\hbar \ll tm\Omega E''(p_i) \tag{5.304}$$

thus it improves over longer times. The approximation breaks down for coalescing stationary points at the turning points located at p_T satisfying $E''(p_\mathrm{T}) = 0$ (see section 5.5.2 for details).

$\gamma = 1$: Considering the case $\gamma = 1$ (corresponding to fixing the spatial width of the wave packet). The momentum width of the wave packet scales like $1/\hbar^2$. Therefore the real Gaussian term in the integral (5.234) is dominant (i.e. narrower than) over the stationary phase contributions from the phase term. The Laplace method may then be employed (see Appendix C.1) to evaluate the integral at the peak of the Gaussian. The asymptotic solution in spinor form is given by

$$\psi_{\bowtie}(q,t,0) \approx \frac{N\hbar}{2}\sqrt{\frac{2\pi}{a(t)}}\left(|e\rangle - |h\rangle\right)\exp\left[-\frac{1}{2a(t)}q^2 + \frac{i}{\hbar}(qp_\mathrm{F} - t\Delta_0)\right]$$
$$+ \frac{N\hbar}{2}\sqrt{\frac{2\pi}{a^*(t)}}\left(|e\rangle + |h\rangle\right)\exp\left[-\frac{1}{2a^*(t)}q^2 + \frac{i}{\hbar}(qp_\mathrm{F} + t\Delta_0)\right].$$
$$\tag{5.305}$$

where $a(t) = 1/m\Omega + it\hbar E''(V_0))$. This describes a wave packet that remains located on the origin with the envelope of the wave packet described by

$$\exp\left[-\frac{q^2}{2m\Omega|a(t)|^2}\right]. \tag{5.306}$$

as anticipated by the value of x. This approximation is valid when $\hbar$ satisfies the condition

$$\hbar \ll \frac{1}{m\Omega t E''(V_0)} \tag{5.307}$$

and thus is increasingly accurate at shorter times.

$\gamma = 0$: At the central value $\gamma = 0$, the width in both p and q scale identically by $\sqrt{\hbar}$. Since both the width of the stationary phase contribution and the Gaussian contribution shrink at the same rate we should consider an asymptotic solution that takes into account contributions from both. We can therefore arrive at an approximation by considering the convolution of the contributions from the Gaussian envelope and stationery phase

contribution. The general solution is given by

$$I(q,t) \approx NA\left(z_{\mp}\right)\sqrt{\frac{2\pi}{\lambda\gamma_{\mp}}}\exp\left[\pm\frac{itE''(p_i)}{2\hbar\gamma_{\mp}}(p_i - V_0)^2 + \frac{i}{\hbar}\theta_{\pm}(V_0)\right] \quad (5.308)$$

where the width of the resultant distribution is described by

$$\gamma_{\pm} = 1 \pm itm\omega E''(p_i) \quad (5.309)$$

and the complex parameter $z_{\pm}$ is given by

$$z_{\pm} = \gamma_{\pm}^{-1}\left(V_0 \pm itm\omega E''(p_i)p_i\right). \quad (5.310)$$

The solution is again constructed from the same stationary phase point contributions as found in the long time case. Though the value of x tends to ∞ more slowly at $1/\sqrt{\hbar}$ as both δ_q and $T_\sigma(p_{\text{F}})$ tend to zero. The resulting non-oscillating envelope of the wave packet is described by

$$\exp\left[-\frac{m\omega}{2\hbar}\frac{E''(p_i)}{|\gamma_{\mp}|^2}t^2(p_i - V_0)^2\right]. \quad (5.311)$$

Although there is an influence from the oscillating terms, the wave packet still remains restricted about the origin as predicated by the value of x.

Chapter 6

Time Dependent Andreev Reflection of Coherent States

In this chapter we will analyse the dynamics of a Gaussian wave packet incident from the normal region onto a discontinuous N-S interface. The wave packets are superpositions of the stationary state scattering solutions derived in Section 4.2. We will show how the state with central pseudo-velocity close to the Fermi momentum is mainly Andreev reflected and partially specularly reflected at the N-S interface. Part of the wave packet will also penetrate into the superconducting region, although in this case the wave packet will not fully penetrate into the superconducting region.

As in the previous chapter, we will also consider the short wavelength limits $\hbar \to 0$ and $\mu \to \infty$ using asymptotic techniques to compare the dynamics in these regimes.

6.1   Time Dependent Andreev Reflection

The ultimate goal of this chapter is a derivation of the time dependent Andreev reflection of an initially Gaussian wave packet. This will be done using the known stationary scattering states derived in section 4.2. In principle this will allow for an analysis of arbitrary initial states (under certain conditions we will discuss below). The time dependent spinor state will be denoted as

$$|\mathbf{\Phi}(t)\rangle = \exp\left(-\frac{it}{\hbar}\hat{\mathcal{H}}_{\text{BdG}}\right)|\mathbf{\Phi}(0)\rangle \qquad (6.1)$$

for an initial state of the wave packet $|\mathbf{\Phi}(0)\rangle$. This is written in terms of the electron-like and hole-like components

$$|\mathbf{\Phi}(t)\rangle = |\Phi^e(t)\rangle \otimes |e\rangle + |\Phi^h(t)\rangle \otimes |h\rangle \qquad (6.2)$$

labelled by the superscript. The time dependent spinor wave function is then

$$\mathbf{\Phi}(q,t) = \langle q| \exp\left(-\frac{it}{\hbar}\hat{\mathcal{H}}_{\mathrm{BdG}}\right)|\mathbf{\Phi}(0)\rangle. \qquad (6.3)$$

The action of the time development operator on the initial wave packet can be found by decomposing the initial state in the scattering basis. The scattering states are eigenstates of the BdG Hamiltonian with eigenvalue

$$\hat{\mathcal{H}}_{\mathrm{BdG}}|E,\sigma\rangle = E|E,\sigma\rangle. \qquad (6.4)$$

The scattering states have been denoted in bra-ket notation with incident energy E and $\sigma = \{e,h\}$ indicating the incident component. The corresponding spinor wave functions are given in section 4.2. We only consider scattering states for incident particles with energies inside the superconducting band gap, this will ensure that only the decaying states inside the superconducting region contribute. This will also limit the allowed momentum bandwidth of the initial incident wave packet. If like the Gaussian wavepacket, the momentum distribution of the wave packet is non-zero along the real line then the momentum bandwidth of the initial wave packet will be chosen so that the contributions from scattering states that propagate into the superconductor (i.e. $E > \Delta_0$) can be neglected (clearly this will restrict the possible distributions under consideration).

The scattering states are orthogonal both with respect to energy and E' and between spin components, i.e.

$$\langle E', \sigma'|E,\sigma\rangle = \delta(E'-E)\delta_{\sigma'\sigma}. \qquad (6.5)$$

This result is derived in detail in appendix A.3.1 for scattering states with energies $|E| < \Delta_0$. Since contributions from states $|E| > \Delta_0$ are neglected we will introduce the projection onto the subspace of states with energy $|E| < \Delta_0$ labelled $\mathcal{P}_{|E|<\Delta_0}$. This can be resolved in the scattering basis as

$$\mathcal{P}_{|E|<\Delta_0} = \sum_{\sigma} \int_{-\Delta_0}^{\Delta_0} dE\, |E,\sigma\rangle\langle E,\sigma|. \qquad (6.6)$$

The summation is performed over the incident electron and hole states as well as integrating over energy contributions across the superconducting band gap.

Using (6.6) the time dependent wave functions are therefore resolved as

$$\boldsymbol{\Phi}(q,t) = \sum_\sigma \int_{-\Delta_0}^{\Delta_0} dE \, \langle q | \exp\left[-\frac{it\mathcal{H}_{\mathrm{BdG}}}{\hbar}\right] |E,\sigma\rangle \langle E,\sigma|\boldsymbol{\Phi}(0)\rangle \qquad (6.7)$$

$$= \sum_\sigma \int_{-\Delta_0}^{\Delta_0} dE \, \exp\left[-\frac{itE}{\hbar}\right] \boldsymbol{\Psi}_\sigma(q,E)\langle E,\sigma|\boldsymbol{\Phi}(0)\rangle. \qquad (6.8)$$

The functions $\boldsymbol{\Psi}_\sigma(q,E)$ are just the spinor scattering wave functions. $\langle E,\sigma|\boldsymbol{\Phi}(0)\rangle$ resolves the initial state in the scattering basis and can be calculated using the known solutions in the position basis using

$$\langle E,\sigma|\boldsymbol{\Phi}(0)\rangle = \int dq \, \boldsymbol{\Psi}_\sigma^\dagger(q,E)\boldsymbol{\Phi}(q,0). \qquad (6.9)$$

It needs to be taken into consideration that since the scattering states inside the superconducting region are restricted to the decaying wave functions; it is not generally possible to fully resolve any part of the initial wavepacket that lies in the superconducting region in this restricted scattering basis on $\mathcal{P}_{|E|<\Delta_0}$. In practice the approximation used will be

$$\langle E,\sigma|\boldsymbol{\Phi}(0)\rangle \approx \int_{-\infty}^{0} dq \, \boldsymbol{\Psi}_\sigma^\dagger(q,E)\boldsymbol{\Phi}(q,0) \qquad (6.10)$$

by ensuring the bulk of the initial wave packet lies in the normal region. This will ensure that any errors introduced from neglecting the components of the initial state in the superconducting region are negligible. We will later apply this to an initial Gaussian wave packet.

As a simple example we can consider an initial electron wave function supported on a finite range of energies inside the band gap, centred in space at some q_0 in the normal region. This is described by a box function in the energy basis, producing a spatial wave packet of the form $\mathrm{sinc}(q - q_0)$ at $t = 0$. If the initial wave packet is defined sufficiently far from the N-S boundary (such that it is interacting weakly with the boundary) the coefficients for a initial pure electron wave packet are defined by

$$\langle E,\sigma|\Phi_N,0\rangle = \begin{cases} \exp\left[-\frac{iq_0}{\hbar}\alpha_+(E)\right] & a \leq E \leq b \quad \text{and} \quad \sigma = e \\ 0 & \text{otherwise} \end{cases} \qquad (6.11)$$

where $|a|, |b| < \Delta_0$. The wave function spinor in the normal region is then given by

$$\boldsymbol{\Phi}_N(q,t) = \sum_\sigma \int_a^b dE \, \exp\left[-\frac{i}{\hbar}\left(tE + q_0\alpha_+(E)\right)\right] \boldsymbol{\Psi}_{e,N}(q,E) \qquad (6.12)$$

152

Figure 6.1: Time steps in the Andreev reflection of a box function distribution of energies, centred on $E = 0$, with $\delta_E = 0.5 \times \Delta_0$. The time steps are fractions of $T = |q_0|/v_F$ the approximate time taken for the centre of the wave packet to meet the boundary. $\Delta_0/\mu = 0.01$. Electron component is shown in red and the hole in blue.

(a) $t = 0 \times T$ **(b)** $t = 0.5 \times T$ **(c)** $t = 1 \times T$

(d) $t = 1.5 \times T$ **(e)** $t = 2 \times T$ **(f)** $t = 2.5 \times T$
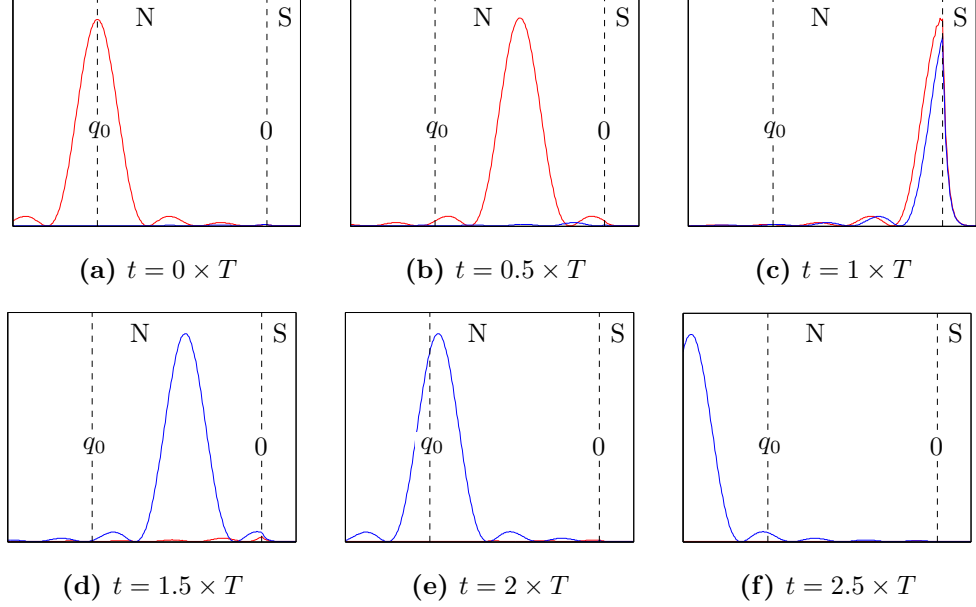
and in the superconducting region

$$\mathbf{\Phi}_S(q,t) = \sum_\sigma \int_a^b dE \, \exp\left[-\frac{i}{\hbar}\left(tE + q_0\alpha_+(E)\right)\right] \mathbf{\Psi}_{e,S}(q,E). \qquad (6.13)$$

Time steps for the Andreev reflection of this wave packet are shown in Figure 6.1, generated using numerical integration. The initial wave packet is a pure electron state, with central energy $E_0 = 0$ and the energy bandwidth set at half the value of Δ_0 so as to ensure that contributions from states propagating into the superconducting region are not introduced.

6.2 Andreev Reflection of a Gaussian Wave packet

We now look at the time evolution of a Gaussian wave packet that is initially an electron component incident from the normal region. First the Gaussian wave packet is resolved in the scattering basis. The coefficients have terms of the general integral form

$$\int_{-\infty}^0 dq \mathbf{\Psi}_{\sigma,N}^\dagger(q,E)\mathbf{\Phi}(q,0) \propto NA(E)\int_{-\infty}^0 \exp\left[-\frac{\lambda}{2}(q-q_0)^2 + \frac{i}{\hbar}q\big(V_o \pm \alpha_+(E)\big)\right] dq \qquad (6.14)$$

Figure 6.2: Detail at the N-S boundary of the Andreev reflection of the wave packet shown in Figure 6.1. The initial wave packet centred on $E = 0$, with $x = 0.1$, $y = 2$, $\Delta_0 = 0.05$. The time steps are in units $T = m|q_0|/p_\mathrm{F}$. Electron component is shown in red and the hole in blue. $L(0)$ is the typical decay length given by Equation (4.18).

(a) $t = 0.9 \times T$

(b) $t = 0.95 \times T$

(c) $t = 1 \times T$

(d) $t = 1.05 \times T$

(e) $t = 1.1 \times T$

(f) $t = 1.15 \times T$
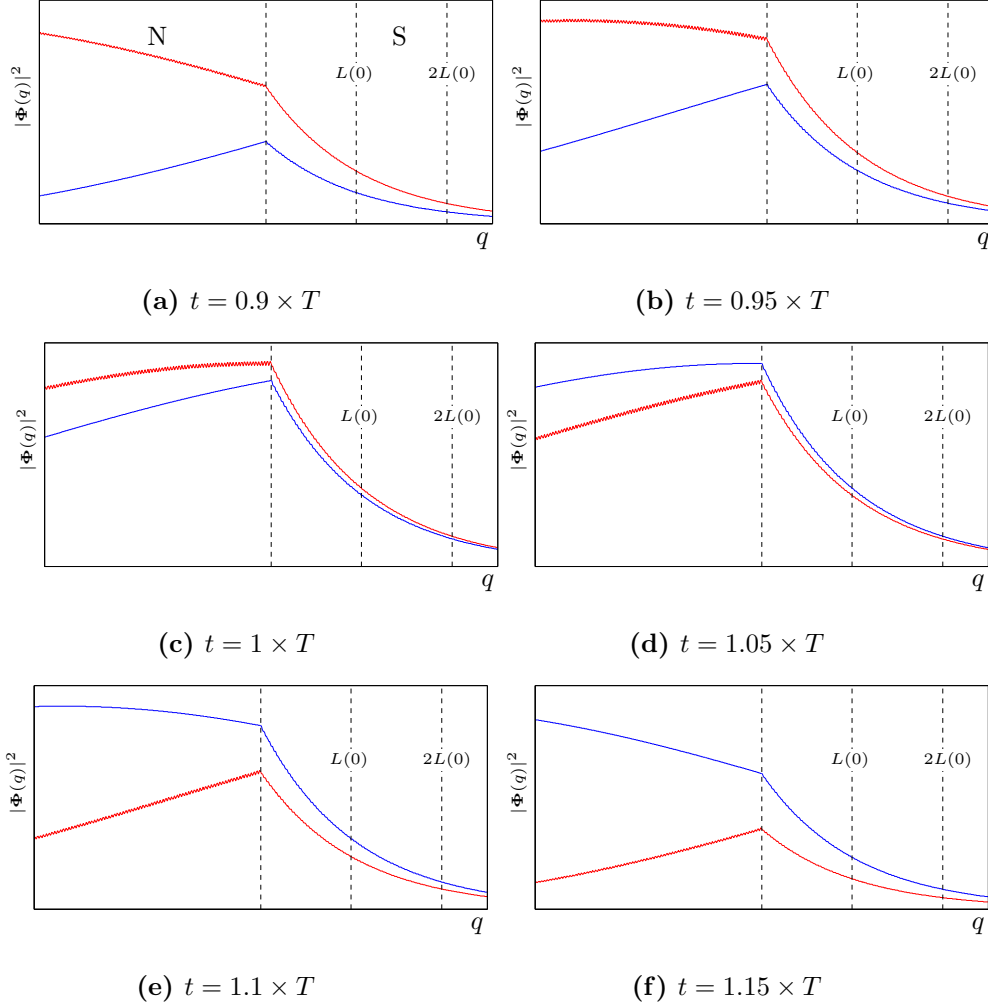
where $\lambda = m\omega/\hbar$ and $N = (\lambda/\pi)^{1/4}$ and $A(E)$ is a scattering amplitude term. The solution to integral (6.14) is analytic and can be written in terms of the Faddeeva function $w(z)$ (see Appendix B) as

$$\int dq = \frac{N^{-1}}{\sqrt{2}} A(E) \exp\left(-\frac{m\omega}{2\hbar} q_0^2\right) w\big(z(\pm\alpha_+(E))\big) \qquad (6.15)$$

where

$$z\big(\pm\alpha_+(E)\big) = \sqrt{\frac{\lambda}{2}} \big(im\omega q_0 - (V_0 \pm \alpha_+(E))\big). \qquad (6.16)$$

Applying this solution to the scattering states in the normal region the coefficients are, indexed by the incident component appropriately,

$$A_e(E) = \langle E, e | \mathbf{\Phi}_N(0) \rangle$$
$$= \frac{N^{-1}}{\sqrt{2\alpha_+(E)}} \exp\left(-\frac{m\omega}{2\hbar} q_0^2\right) [w(z(-\alpha_+(E))) + S_{ee}^* w(z(\alpha_+(E)))]$$

(6.17)

$$A_h(E) = \langle E, h | \mathbf{\Phi}_N(0) \rangle$$
$$= \frac{N^{-1}}{\sqrt{2\alpha_+(E)}} \exp\left(-\frac{m\omega}{2\hbar} q_0^2\right) S_{eh}^*(E) w[z(\alpha_+(E))].$$

(6.18)

These are the most general analytic solutions, which will resolve the wave packet at any value of q_0 in the normal region and generate the corresponding decaying continuation the superconducting region. However it includes Faddeeva terms that are difficult to work with.

The value of q_0 has been chosen so that errors from not including the propagating superconducting states are negligible, this will mean that only the very tails of the initial Gaussian wave packet enter the superconducting region. This will also mean that the Faddeeva functions can be removed, with any errors in the coefficients being negligible. In effect the approximation made for an arbitrary

$$\int_{-\infty}^{0} dq \, \mathbf{\Psi}_{\sigma,N}^\dagger(q, E)\mathbf{\Phi}(q, 0) \approx \int_{-\infty}^{\infty} dq \, \mathbf{\Psi}_{\sigma,N}^\dagger(q, E)\mathbf{\Phi}(q, 0).$$

(6.19)

If q_0 is sufficiently far from the boundary the extension to the limit $q = \infty$ only introduces additional small terms into the integration over the tails of the Gaussian.

If the width of the initial wave packet is again assigned (at four standard deviations) as $\delta_q = 4\sqrt{\hbar/m\omega}$. The approximation is considered valid when q_0 is greater than δ_q and the bulk of the Gaussian is contained in the normal region. This can be done by ensuring that q_0 satisfies

$$|q_0| \gg 4\sqrt{\frac{\hbar}{m\omega}}$$

(6.20)

to minimize any errors arising from omitting the energy contributions outside the band width.

Using this approximation the scattering coefficients of the initial electron

155

Figure 6.3: Time steps in the Andreev reflection of an electron Gaussian wave packet, centred on $E = 0$, with $x = 0.1$, $y = 2$, $\Delta_0 = 0.05$. The time steps are scaled by $T = m|q_0|/p_F$ (the approximate time taken for the centre of the wave packet to meet the boundary). Electron component is shown in red and the hole in blue.

(a) $t = 0 \times T$

(b) $t = 0.5 \times T$

(c) $t = 0.9 \times T$

(d) $t = 1 \times T$

(e) $t = 1.1 \times T$

(f) $t = 1.5 \times T$
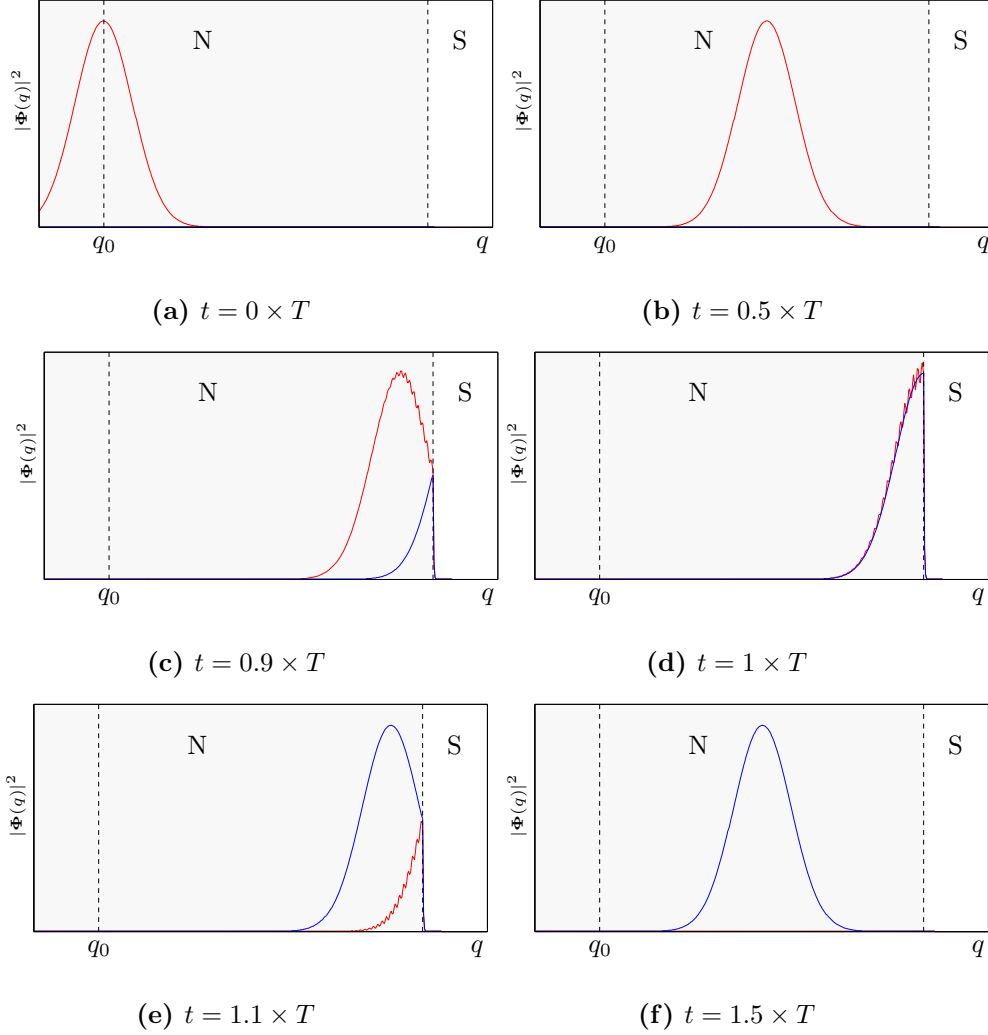
Gaussian wave packet are then simplified to

$$A_e(E) = N^{-1}\sqrt{\frac{2}{\alpha_+(E)}}\left[G(-\alpha_+(E)) + S_{ee}^*(E)G(\alpha_+(E))\right] \tag{6.21}$$

$$A_h(E) = N^{-1}\sqrt{\frac{2}{\alpha_+(E)}}\,S_{eh}^*(E)G(\alpha_+(E)) \tag{6.22}$$

where $G(\pm\alpha_+(E))$ labels the Gaussian distribution in momentum space

$$G(\pm\alpha_+(E)) = \exp\left[-\frac{\lambda}{2}\big(V_0 \pm \alpha_+(E)\big)^2 + \frac{i}{\hbar}q_0\big(V_0 \pm \alpha_+(E)\big)\right]. \tag{6.23}$$

The electron and hole components of the time dependent spinor wave func-

156

tion resulting from an incident electron wave packet are therefore

$$\Phi_N^e(q,t) = \int \frac{dE}{\sqrt{\alpha_+(E)}} \left[A_e(E) \left(e^{\frac{iq}{\hbar}\alpha_+(E)} + S_{ee}(E)e^{-\frac{iq}{\hbar}\alpha_+(E)} \right) + A_h(E)S_{eh}(E)e^{-\frac{iq}{\hbar}\alpha_+(E)} \right] e^{-\frac{it}{\hbar}E}$$

(6.24)

$$\Phi_N^h(q,t) = \int \frac{dE}{\sqrt{\alpha_-^{1/2}(E)}} \left[A_e(E)S_{he}(E)e^{\frac{iq}{\hbar}\alpha_-(E)} + A_h(E) \left(e^{-\frac{iq}{\hbar}\alpha_-(E)} + S_{hh}(E)e^{\frac{iq}{\hbar}\alpha_-(E)} \right) \right] e^{-\frac{it}{\hbar}E}$$

(6.25)

in the normal region, and in the superconducting region

$$\mathbf{\Phi}_S(q,t) = \int dE \left[A_e(E)\mathbf{\Psi}_{e,S} + A_h(E)\mathbf{\Psi}_{h,S} \right] e^{-\frac{it}{\hbar}E}.$$

(6.26)

If we assume that for a state centred at p_F contributions to the integral lie in the regime $E < \Delta \ll \mu$, then the non-oscillating term in the decomposition $G(\pm\alpha_+(E))$ can be approximate as

$$\exp\left[-\frac{\lambda}{2}\left(p_\mathrm{F} \pm \alpha_+(E)\right)^2 \right] \approx \exp\left[-\frac{\lambda}{2}p_\mathrm{F}^2 \left(1 \pm 1 \pm \frac{E}{2\mu}\right)^2 \right].$$

(6.27)

This implies that contributions from $G(+\alpha_+)$ are in general suppressed and $G(-\alpha_+)$ is approximately Gaussian. The energy bandwidth is then approximately $\delta_E \approx 4(2\hbar\omega\mu)^{1/2}$. To ensure that the energy width lies inside the require range ω is set at

$$\omega = \frac{1}{2\hbar\mu}\left(\frac{x\Delta_0}{4}\right)^2$$

(6.28)

where x sets the bandwidth as a ratio of Δ_0 and thus must satisfy $x \ll 1$. Scaling the energy bandwidth in such a manner clearly has the adverse effect of broadening the wave packet in space. The value of q_0 we then be chosen as

$$q_o = y \times \delta_q = y \left(\frac{16\hbar}{x\Delta_0}\sqrt{\frac{2\mu}{m}}\right).$$

(6.29)

When $y \gg 1$ this ensures the initial wave packet is sufficiently far from the boundary to minimize any contributions from the boundary. Although there will be contributions from stationary points of the oscillating terms under the integral, they will be time dependent, this choice of ω ensures the required energy bandwidth at all times.

Numerically integrated examples are shown in Figure 6.3 for a wave packet with $\delta_E = 0.1 \times \Delta_0$ where $\Delta/\mu = 0.05$. Restricting the energy bandwidth means the the initial wave packet is much broader in space than

the depth that the wave packet penetrates into the superconducting region. With this choice the wave packet is completely Andreev reflected, the reflected hole wave packet demonstrating little dispersion. Although the wave packet fully meets the boundary, the Gaussian envelope does not move into the superconducting region, as only the exponentially decaying solution contribute in the superconducting region. Details of the penetration of the wave packet at the boundary are shown in Figure 6.4. Additional oscillations can also be seen over the electron component wave packet due to the interaction with the reflected electron component.

6.3   Short Wavelength Approximations

The short wavelength approximation can be applied in a manner analogous to sub-section 5.5.3. We will consider the short wavelength behaviour in both the limits $\mu \to \infty$ (with various scalings of Δ_0) and $\hbar \to 0$.

The scaling parameter α is again assigned as

$$\Delta_0 = \delta \mu^\alpha \tag{6.30}$$

where $0 \leq \alpha \leq 1$. Using this scaling consideration also needs to be given to the requirement that $\delta_E < \Delta_0$ in this regime. For an initial coherent state the energy bandwidth is approximately $\delta_E \sim 4(2\hbar\omega\mu)^{1/2}$. When $0 \leq \alpha < 1/2$, as $\mu \to \infty$ the energy bandwidth is then naturally wider than Δ_0 unless the state is squeezed to satisfy $\delta_E < \Delta_0$ by setting

$$\omega = \frac{1}{2\hbar}\left(\frac{x\delta}{4}\right)^2 \mu^{2\alpha-1}. \tag{6.31}$$

This scaling means $\omega \to 0$ and therefore $\delta_q \to \infty$ also. If we consider the case $\alpha = 1/2$, where the energy bandwidth is of the same order of Δ_0. This consequently also fixes the value of ω, and the width in q remains constant. It is not required that $\delta_E/\Delta_0 \to 0$ as $\mu \to \infty$, but it is required that $\delta_E < \Delta_0$ so that the errors from omitting contributions from states at $|E| > \Delta_0$ are still negligible.

When $1/2 < \alpha \leq 1$, the energy bandwidth, is naturally smaller than Δ_0 without requiring any additional squeezing. This means that $\delta_E < \Delta_0$ is satisfied for values of ω

$$\omega < \frac{1}{2\hbar}\left(\frac{\delta}{4}\right)^2 \mu^{2\alpha-1}. \tag{6.32}$$

In all the cases $0 \leq \alpha < 1$ the terms inside the integral can consistently be expanded in powers of Δ_0/μ and E/μ (albeit with slower convergence for larger values of α). Depending on the value of α we can also consider whether higher powers in E/Δ_0 can be neglected. When $0 \leq \alpha \leq 1/2$ these terms will need to be retained as contributing energies may be on the same order as Δ_0. Conversely when $1/2 < \alpha < 1$, the contributing energies and Δ_0 can be ordered by magnitude

$$\delta_E \sim \sqrt{\mu} \quad \implies \quad \delta_E < \Delta_0 < \mu \tag{6.33}$$

we can then consider additionally truncating an expansion in terms of order E/Δ_0.

The choice of scaling effects the decay length $L(E)$, given by (Equation (4.18))

$$L(E) = \frac{1}{\sqrt{2m}} \left(\frac{\hbar}{\delta} \right) \mu^{\frac{1}{2} - \alpha} \left(1 - \left(\frac{E}{\delta \mu^\alpha} \right)^2 \right) \tag{6.34}$$

In the regime $0 \leq \alpha < 1/2$ the decay length diverges as $\mu \to \infty$. This might indicate that the wave packet penetrated into the superconducting region, but we have shown that the width of the initial wave packet in the normal region also grows in the same manner due to the restriction of the energy bandwidth. In the regime $1/2 < \alpha \leq 1$ the decay length tends to zero as μ grows asymptotically which would suggest that the wave packet will be completely reflected at the boundary without entering the superconducting region. Only when $\alpha = 1/2$ is $L(E)$ finite.

In the normal region, retaining terms up to first order in E/μ the resulting integral has the general form

$$\int dE \, f(E) \exp \left[-\frac{E^2}{4\hbar\omega\mu} - \frac{i}{\hbar v_{\text{F}}} E \left((q_0 \mp q) + v_{\text{F}} t \right) \pm \frac{i}{\hbar} q p_{\text{F}} \right]. \tag{6.35}$$

Although there is no obvious large parameter on which to base a stationary phase approximation the remaining terms in the exponent are in a solvable quadratic form.

In practice, we can therefore consider dynamics for values of $0 \leq \alpha < 1$ by expanding up to first order in powers of E/μ and Δ_0/μ. The lowest order expansion is merely the plane wave solution with no resolution of the wave packet. For consistency the amplitude terms in the scattering wave functions also need to be expanded up to the same order. The first order approximations of the scattering amplitudes are given in Section 4.2. The

159

first order expansion in the normal region then requires solving the integral

$$\Phi_N^e(q,t) \approx N^{-1}\frac{\sqrt{2}}{p_{\text{F}}} \int \left(1 - \frac{E}{2\mu}\right) \exp\left[-\frac{\lambda'}{2}E^2 - \frac{iE}{\hbar v_{\text{F}}}z_{\text{N}}(-q,t) + \frac{i}{\hbar}qp_{\text{F}}\right]$$
$$+ \frac{E}{\mu}\nu^{*2}(E) \exp\left[-\frac{\lambda'}{2}E^2 - \frac{iE}{\hbar v_{\text{F}}}z_{\text{N}}(q,t) - \frac{i}{\hbar}qp_{\text{F}}\right]dE.$$

$$(6.36)$$

where $\lambda' = 1/2\hbar\omega\mu$ and

$$z_{\text{N}}(q,t) = (q_0 + q) + v_{\text{F}}t. \tag{6.37}$$

Although the Gaussian integral by itself is readily solvable, Equation (6.36) also requires a means of solving the integrals with E dependent amplitudes. The linear term in E can be removed from under the integral using differentiation under the integral sign. If the amplitude term of the reflected electron is rewritten as

$$E\nu^{*2}(E) = \frac{\Delta_0}{2}\left(\frac{E}{\Delta} - i\sqrt{1 - \left(\frac{E}{\Delta_0}\right)^2}\right) \tag{6.38}$$

the identity

$$x - i\sqrt{1 - x^2} = \exp\left(-i\arccos(x)\right) \tag{6.39}$$

can then be used to absorb this terms into the exponent as an additional energy dependent phase. Altogether this gives

$$\Phi_N^e(q,t) \approx \frac{\sqrt{2}}{Np_{\text{F}}} \int dE \left(1 - \frac{i\hbar}{2\mu}\frac{d}{dt}\right)\exp\left(-\frac{\lambda'}{2}E^2 - \frac{iE}{\hbar v_{\text{F}}}z_{\text{N}}(-q,t) + \frac{i}{\hbar}qp_{\text{F}}\right)$$
$$+ \frac{\Delta_0}{2\mu}\exp\left(-\frac{\lambda'}{2}E^2 - \frac{iE}{\hbar v_{\text{F}}}z_{\text{N}}(q,t) - i\arccos\left(\frac{E}{\Delta_0}\right) - \frac{i}{\hbar}qp_{\text{F}}\right).$$

$$(6.40)$$

The regimes $0 \leq \alpha \leq 1/2$ and $1/2 < \alpha < 1$ now have to be considered separately here. First considering $1/2 < \alpha < 1$ terms can be consistently expand in powers of E/Δ_0. Expanding $\arccos(E/\Delta_0)$ up to first order the resulting integral has a simple closed solution. The resulting electron component of the wave function, in the normal region is then given by

$$\Phi_N^e(q,t) \approx \frac{2}{Np_{\text{F}}}\sqrt{\frac{\pi}{\lambda'}}\left[\left(1 - \frac{i\hbar}{2\mu}\frac{d}{dt}\right)\exp\left(-\frac{m\omega}{2\hbar}z_N(-q,t)^2 + \frac{iq}{\hbar}p_{\text{F}}\right)\right.$$
$$\left. - \frac{i\Delta_0}{2\mu}\exp\left(-\frac{m\omega}{2\hbar}\left(z_N(q,t) - \frac{\hbar}{\Delta_0}v_{\text{F}}\right)^2 - \frac{i}{\hbar}qp_{\text{F}}\right)\right]$$

$$(6.41)$$

The first term fits the description of the incident electron wave packet, propagating at the Fermi velocity, locating the peak inside the normal region until it meets the boundary at $t = q_0/v_\text{F}$. Referring back to section 4.2, the additional term in the location of the reflected wave packet is equal to $\hbar v_\text{F}/\Delta_0 = 2L(0)$, the decay length at $E = 0$. The second term describing the reflected electron, is centred at

$$q(t) = -(q_0 - 2L(0)) - v_\text{F}t \qquad (6.42)$$

The incident wave packet meets the boundary at $t = q_0/v_\text{F}$, the peak of the reflected wave packet does not emerge from the boundary until $t = (q_0 - L(0))/v_\text{F}$, indicating a delay between the incident wave packet meeting the boundary and being reflected due to the time taken for the incident wave packet to penetrate into the superconductor. It can also be seen that taking the absolute value of this wave function will generate not only the incident and reflected Gaussian wave packets, but also oscillations where the incident and reflected overlap (i.e. only at times when both components of the wave packet are close to the boundary).

A similar delay effect can be observed both during the total internal reflection of electromagnetic waves at an interface, and the scattering of wave packets. Named after and first measured by Goos and Hänchen [75], the *Goos-Hänchen shift* is evidenced as a lateral shift of the reflected wave. This shift can be viewed as a time delay associated with the scattering of a radiation pulse incident on the interface. The lateral shift results from the pulse propagating parallel to the interface during the time delay. The Goos-Hänchen shift is a coherence effect, and therefore also has an analogue for wave packets incident on a potential step, as derived by Carter and Hora [76].

The corresponding Andreev reflected hole component is given by

$$\Phi_N^h(q,t) \approx -\frac{2i}{Np_\text{F}}\sqrt{\frac{\pi}{\lambda'}} \exp\left[-\frac{m\omega}{2\hbar}\big(z_N(q,t) - 2L(0)\big)^2 + \frac{iq}{\hbar}p_\text{F}\right]. \qquad (6.43)$$

It demonstrates a similar delay from leaving the N-S boundary as the reflected electron component.

It should also noted that this choice of approximation has resulted in a wave packet that does not disperse over time. Time dependence in the width of the wave packet will only enter if additional terms of order $(E/\mu)^2$ in the expansion of $\alpha_+(E)$ in $\mathbf{\Phi}_N(q,t)$ were included.

Considering the regime $0 \le \alpha \le 1/2$; in this regime we cannot reliably discard terms of $(E/\Delta_0)^2$. Consideration would need to be given to how the

additional higher order terms in $\arccos(E/\Delta)$ enter the solution. Though these terms will always be in some sense "small" as we are still restricting the energy bandwidth inside Δ_0. As the next term in the expansion of $\arccos(E/\Delta)$ is of the order $(E/\Delta_0)^3$, these additional terms would enter the solution as deviations from the wave packets Gaussian profile.

So far we have only discussed the form of the reflected electron and hole components. Now let us consider the wave function inside the superconducting region where the value of α has a stronger effect. The electron-like component of the spinor in the superconducting region is given in integral form as

$$\Phi_S^e(q,t) \approx \frac{1}{\sqrt{2}Np_{\text{F}}} \int \left[\left(2 - \frac{E}{\mu}\nu^2(E)\right) \exp\left(\frac{i}{\hbar}qp_{\text{F}}\right) + \frac{E}{\mu}\nu^{*2}(E) \exp\left(-\frac{i}{\hbar}qp_{\text{F}}\right) \right]$$
$$\times \exp\left(-\frac{\lambda'}{2}E^2 - \frac{iE}{\hbar v_{\text{F}}}z_S(t) - \frac{q}{\hbar v_{\text{F}}}\sqrt{\Delta_0^2 - E^2} \right) dE$$

(6.44)

where $z_S(t) = q_0 + tv_{\text{F}}$. Rather than just attempting to solve this directly, this integral can be rearranged to include terms that occurred in the corresponding integral in the normal region

$$\Phi_S^e(q,t) \approx \frac{\sqrt{2}}{Np_{\text{F}}} \int dE \, \exp\left(-\frac{\lambda'}{2}E^2 - \frac{iE}{\hbar v_{\text{F}}}z_S(t) - \frac{q}{\hbar v_{\text{F}}}\sqrt{\Delta_0^2 - E^2} \right)$$
$$\times \left[\left(1 - \frac{E}{2\mu}\right) \exp\left(\frac{iqp_{\text{F}}}{\hbar}\right) + \frac{E}{\mu}\nu^{*2} \exp\left(-\frac{iqp_{\text{F}}}{\hbar}\right) + \frac{iE}{\mu}\nu^{*2} \sin\left(\frac{qp_{\text{F}}}{\hbar}\right) \right].$$

(6.45)

Moreover we note that there is an additional oscillating term due to the rotation between electron and hole components. If the same techniques to absorb the amplitude terms into the exponent are applied, the choice of short wavelength regime again informs the order of approximation. Only retaining terms up to second order in E/Δ_0 in the regime $1/2 < \alpha < 1$ (including the expansion of $\kappa_\pm(E)$) the solution is given by

$$\Phi_S^e(q,t) \approx \frac{2}{Np_{\text{F}}}\sqrt{\frac{\pi}{\zeta(q)}} \exp\left[-\frac{q}{2L(0)}\right] \times$$
$$\left[\left(1 - \frac{i\hbar}{2\mu}\frac{d}{dt}\right) \exp\left(-\frac{1}{2\zeta(q)}z_S(t)^2 + \frac{iqp_{\text{F}}}{\hbar}\right) \right.$$
$$-\frac{i\Delta_0}{2\mu} \exp\left(-\frac{1}{2\zeta(q)}(z_S(t) - 2L(0))^2 - \frac{iqp_{\text{F}}}{\hbar}\right)$$
$$\left. +\frac{\Delta_0}{2\mu}\sin\left(\frac{qp_{\text{F}}}{\hbar}\right) \exp\left(-\frac{1}{2\zeta(q)}(z_S(t) - 2L(0))^2\right) \right].$$

(6.46)

The hole component is likewise given by

$$\Phi_S^h(q,t) \approx -\frac{2i}{Np_{\text{F}}} \sqrt{\frac{\pi}{\zeta(q)}} \exp\left(-\frac{q}{2L(0)}\right) \times$$
$$\left[\exp\left(-\frac{1}{2\zeta(q)}\left(z_S(t) - 2L(0)\right)^2 + \frac{iqp_{\text{F}}}{\hbar}\right)\right.$$
$$\left.+\frac{\Delta_0}{2\mu}\sin\left(\frac{qp_{\text{F}}}{\hbar}\right)\exp\left(-\frac{1}{2\zeta(q)}z_S(t)^2\right)\right].$$
(6.47)

Here the width parameter is given by $\zeta(q) = \hbar(1/m\omega - qv_{\text{F}}/\Delta_0)$ and the time dependence is contained in

$$z_S(t) = q_0 + tv_{\text{F}}. \tag{6.48}$$

It's clear from the form of $z_S(t)$ that the wave packet does not fully enter the superconducting region as the spatial dependence only enters as terms in $\zeta(q)$ and in the oscillations contained in both components. The incident and reflected components each generate a corresponding component in the superconducting region, but there is also an additional oscillating term over both components.

If we consider higher powers of E/Δ_0 in the regime $0 \le \alpha < 1/2$ the next term in the expansion of $\arccos(E/\Delta)$ is of order $(E/\Delta_0)^3$ and next contribution from $\kappa_{\pm}(E)$ is of order $(E/\Delta_0)^4$. These terms will also represent deviations of the wave packet from the Gaussian distribution.

In the limiting case $\alpha = 1$, although the energy bandwidth is still naturally narrower than Δ_0, as Δ_0 scales as $\sim \mu$, we cannot consistently ignore terms of order Δ_0/μ in the expansion. We also expect that the form of wave function when $\alpha = 1$ should coincide with the limit $\hbar \to 0$ (up to time scaling). If we consider the ratio of Δ_0 and the approximate energy bandwidth δ_E

$$\frac{\Delta_0}{\delta_E} = \frac{\delta}{\sqrt{2\omega\hbar}}\mu^{\alpha-1/2} \tag{6.49}$$

when $\alpha = 1$ the ratio is proportional to $\sim \sqrt{\mu/\hbar}$. In this special case both short wavelength limits scale this ratio in an identical manner. Effectively in this regime, the limit $\hbar \to 0$ or $\mu \to \infty$ both correspond to the choice of either holding μ constant and shrinking the width of the energy contributions, or choosing to scale μ (and consequently Δ_0) faster than the energy width grows. In either case $\delta_E \ll \mu, \Delta_0$ and an expansion can still be made in powers of the small parameters E/μ and E/Δ_0.

If we first consider the normal region this expansion can be performed in the exponent of the integral. The amplitude terms have no simple expansion since terms of the form Δ_0/μ must be retained. This leaves

$$\Phi_N^e(q,t) \approx \frac{N^{-1}}{\alpha_+(E)}\sqrt{2}\int \exp\left(-\frac{\lambda'}{2}E^2 - \frac{iE}{\hbar v_{\mathrm{F}}}z_{\mathrm{N}}(-q,t) + \frac{i}{\hbar}qp_{\mathrm{F}}\right)$$
$$+ S_{ee}(E)\exp\left(-\frac{\lambda'}{2}E^2 - \frac{iE}{\hbar v_{\mathrm{F}}}z_{\mathrm{N}}(q,t) - \frac{i}{\hbar}qp_{\mathrm{F}}\right)dE. \quad (6.50)$$

In the limit $\hbar \to 0$ there is a stationary phase point on the closed contour made by the translation to $E \to E - iz_{\mathrm{N}}\omega p_{\mathrm{F}}$, with the assumption that we can close the contour with no contributions at $E = \pm\infty$. The limit $\hbar \to 0$ therefore creates a peak at $E' = 0$ giving the approximation

$$\Phi_N^e(q,t) \approx \frac{2N^{-1}}{\sqrt{\lambda'}}\alpha_+^{-1}(iz_{\mathrm{N}}\omega p_{\mathrm{F}})\left[\exp\left(-\frac{m\omega}{2\hbar}z_n(-q,t)^2 + \frac{i}{\hbar}qp_{\mathrm{F}}\right)\right.$$
$$\left.+ S_{ee}(iz_{\mathrm{N}}\omega p_{\mathrm{F}})\exp\left(-\frac{m\omega}{2\hbar}z_n(q,t)^2 - \frac{i}{\hbar}qp_{\mathrm{F}}\right)\right]. \quad (6.51)$$

The corresponding hole component is then given by

$$\Phi_N^h(q,t) \approx \frac{2N^{-1}}{\sqrt{\lambda'}}S_{he}(iz_{\mathrm{N}}\omega p_{\mathrm{F}})\exp\left(-\frac{m\omega}{2\hbar}z_n(q,t)^2 - \frac{i}{\hbar}qp_{\mathrm{F}}\right) \quad (6.52)$$

In the superconducting region if we consider that in this regime $\kappa_\pm \approx p_{\mathrm{F}}\sqrt{1 \pm i\delta}$ then the corresponding wave function consists of terms of the general form

$$\int dE\, f(E)\exp\left(-\frac{\lambda'}{2}E^2 - \frac{iE}{\hbar v_{\mathrm{F}}}z_{\mathrm{S}}(q,t) \pm \frac{i}{\hbar}qp_{\mathrm{F}}\sqrt{1 \pm i\delta}\right)$$
$$\approx f(iz_{\mathrm{S}}\omega p_{\mathrm{F}})\exp\left(-\frac{m\omega}{2\hbar}z_{\mathrm{S}}^2 \pm \frac{i}{\hbar}qp_{\mathrm{F}}\sqrt{1 \pm i\delta}\right) \quad (6.53)$$

Figure 6.4: Detail at the N-S boundary of the Andreev reflection of a Gaussian wavepacket as shown in Figure 6.3. The initial wave packet centred on $E = 0$, with $x = 0.1$, $y = 2$, $\Delta_0 = 0.05$. The time steps are in units $T = m|q_0|/p_\mathrm{F}$ (the approximate time for the centre of the wave packet to meet the boundary). Electron component is shown in red and the hole in blue. $L(0)$ is the typical decay length given by Equation (4.18).

(a) $t = 0.9 \times T$

(b) $t = 0.95 \times T$

(c) $t = 1 \times T$

(d) $t = 1.05 \times T$

(e) $t = 1.1 \times T$

(f) $t = 1.15 \times T$
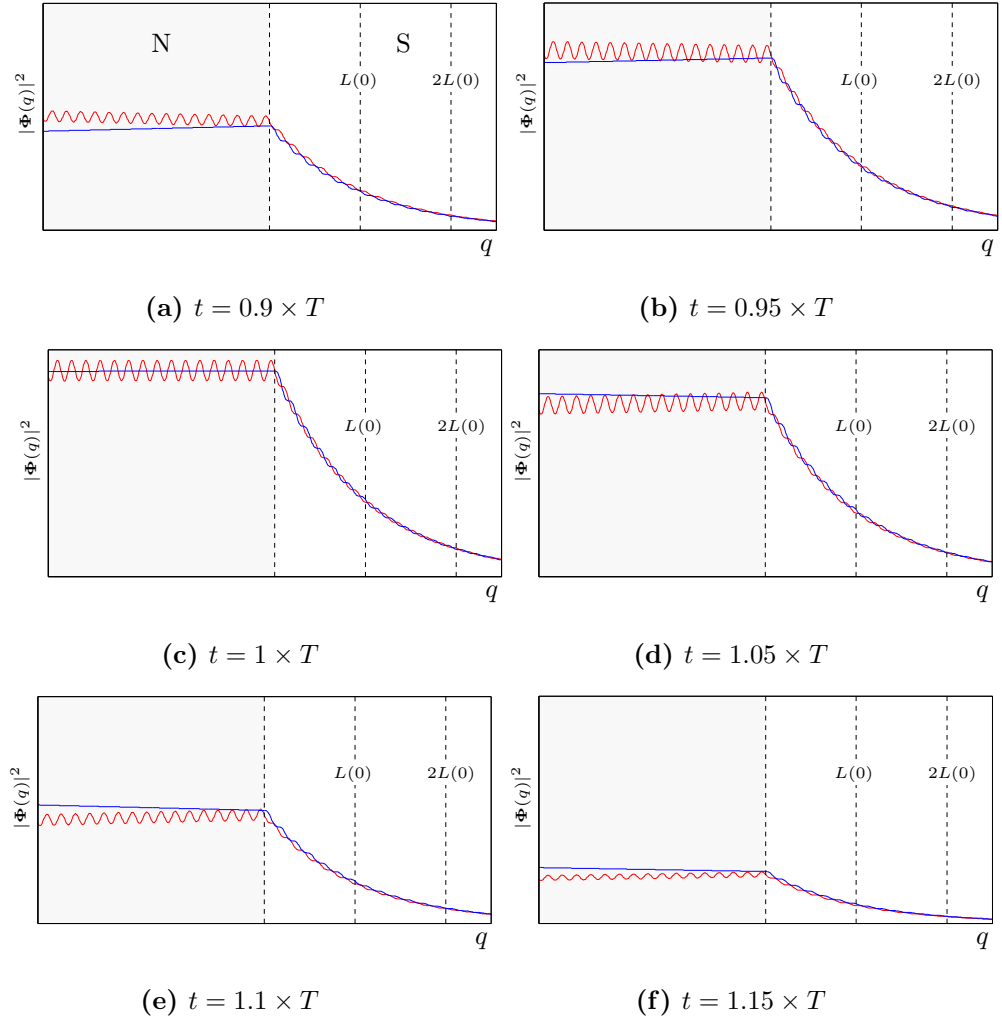
Chapter 7

Conclusions

We have shown that the E-H coherent states have better spatial localisation compared to product coherent states when attempting to describe the dynamics of BdG excitations. In some cases they demonstrate spreading analogous to the scalar SGS coherent states. At the same time they also lack some of the desirable analytic properties of SGS coherent states.

E-H coherent states retain the property of being minimum uncertainty states, albeit on position-pseudo-velocity phase space. They also have a identity of resolution that is analogous to the scalar SGS coherent states. This can be used to represent quantum states on position-pseudo-velocity phase space. However as the group action that defines the E-H coherent state is neither linear or anti-linear, the lack of a well defined adjoint means that the group formalism must be utilised carefully. The electron-hole Q-function lacks many of the analytic features demonstrated by the product and scalar Q-functions. In particular the electron-hole Q-function does not give a complete description of the state. Visually the reduced electron-hole Q-function does allow for additional details of the component trajectories to be shown.

The analysis of the wave packet dynamics in the normal and homogeneous superconductor indicate that E-H coherent states show the same dynamics independent of the amplitude of the initial components. In the normal case this means that the wave packet will follow the corresponding decoupled classical trajectories, and the coherent state wave packet spreads in an analogous manner to the free scalar SGS coherent state. This example although illustrative is somewhat trivial considering how the BdG equations decouple in this regime.

In the case of a homogeneous superconductor the dynamics are more

complex. Our analysis indicates that there are three main contributing factors to the dynamics due to the decomposition of the wave packet in positive and negative energy (with respect to the Fermi-energy) momentum eigenstates. These are the central momentum of the wave packet, the momentum bandwidth of the wave packet and interference effects between the positive and negative energy momentum eigenstates.

For wave packets located on $V_0 = 0$ or $V_0 \gg p_{\mathrm{F}}$ the contributing positive and negative energy plane waves are predominantly electron-like or hole-like respectively. This results in wave packets that behave like the decoupled solutions in the normal conductor due the lack of interference as there is little overlap between the two energy branches. Close to the Fermi momentum the contributing plane wave solutions are equal superposition of electron and hole components, as such the wave packet will then contain strong interference between the two energy branches.

Analysis of the BdG dispersion relation indicates that the group velocity of states on the band gap is zero. Putting aside the effects of the width of the wave packet this is true for the individual wave packets on the positive and negative branches of the dispersion relation. The initial velocity of the wave packet then depends on the initial value of β. For the product state, choosing $\beta = \pm 1$ is then closest to the picture provided by the dispersion relation; as it gives equal weighting to both branches with no additional phase between them, any interference effects are also symmetric between branches producing the symmetric product wave packet shown in Figures 5.16 and 5.17. Any other choice of $\beta \neq 1$ introduces interference between branches that produce the possible range of initial velocities between $\pm v_{\mathrm{F}}$ despite their individual zero velocity. Interference effects then also account for the rotation in quasi-spin, and consequently the oscillations of the wave packet around the origin. We have shown that the E-H coherent state propagate like an initial state with only an electron component for arbitrary values of β. The interference effects are still present, but their effect is to produce the dynamics consistent with the $\beta = 0$ case.

The effects of the momentum bandwidth of the wave packet are encompassed in the parameter $x = \delta_q / d_\sigma(p_{\mathrm{F}})$ the ratio of the width of the wave packet to the distance the free wave packet would travel after one full revolution in quasi-spin. A small value of $x \ll 1$ means the components of the wave packet move quickly outside the initial wave packet before any rotation in quasi-spin can invert the overall velocity of the wave packet. As

$x \to 0$ an electron wave packet will propagate like a free wave packet. For large values of x the fast rotation between components means any effects caused by oscillations in quasi-spin occur before the components can move outside the initial envelope. The wave packet will then remain localised close to origin, oscillating around the origin. In the limiting case $x \to \infty$ the product state will behave as indicated by the zero group velocity derived from the BdG dispersion relationship, though the components of the wave packet still propagate the rate of quasi-spin oscillations contain the wave packet on the origin.

In general either of the short wavelength regimes $\hbar \to 0$ or $\mu \to \infty$ will either result in a value $x \to 0$ or $x \to \infty$, or a wave packet that has no spatial or momentum resolution. We can retain oscillatory dynamics if we allow Δ_0 to scale as $\Delta_0 = \delta \mu^{\frac{1}{2}}$ as $\mu \to \infty$. As $\hbar \to 0$, the standard semiclassical choice of letting the widths in both momentum and position tend to zero will produce a value $x \to \infty$. Only the specific choice of squeezing the state such that the momentum width of the wave packet remains finite will the wave packet demonstrate oscillations.

Analysis of the long time behaviour of wave packets on the Fermi momentum would indicate that any asymmetry shown in the propagation of the wave packet is due to an asymmetry in the energy of the plane wave contributions away from the band gap. A sufficiently narrow momentum bandwidth will effectively not see this asymmetry, resulting in a spatially symmetric wave packet.

The product coherent state demonstrates symmetry dependent on the magnitude and phase of β. If $\beta = \pm 1$ the two components of the wave packet will be both symmetric and the same magnitude, meaning the wave packet will be spatially symmetric. The value x will then indicate how the wave packet disperses. Otherwise, as the momentum width of the wave packet increases, this asymmetry means contributions to the wave packet will quickly move outside the initial wave packet causing the wave packet to quickly dissipate.

In the case of a Gaussian wave packet incident on a discontinuous N-S interface, the restriction of the wave packet's energy bandwidth inside the superconducting band gap will preclude the wave packet from fully entering the superconducting region. As the allowed states inside the superconducting region are decaying, the resulting wave packet will decay in the same manner. The restriction to the band gap also means that the wave packet

will be much broader than the penetration depth into the superconducting region.

In the short wavelength regime we again considered the scaling of Δ_0 as $\Delta_0 = \delta\mu^\alpha$. An analysis of the penetration depth in the short wavelength regime shows that if $0 \leq \alpha < 1/2$ the penetration depth will diverge, but the restriction of the energy bandwidth inside the superconducting gap means that the width of the initial wave packet will also grow. Only when $\alpha = 1/2$ will the penetration depth remain finite, disappearing otherwise when $1/2 < \alpha \leq 1$.

When $1/2 < \alpha < 1$ we have shown that omitting small terms of the order E/μ, Δ/μ and E/Δ_0 means the wave packet is predominantly Andreev reflected, with little dispersion of the incident electron or reflected hole. The reflected components also demonstrate a delay from the incident wave packet proportional to the decay length of states in the superconducting region. Outside of this regime additional terms in the will contribute to deviations of the wave packet from the Gaussian profile during the reflection process.

7.1 Outlook

There are a number of obvious extensions to the work contained in this thesis (a number of which were omitted due to time constraints). Firstly we have mainly considered the simplest case of a superconducting system with no external potentials or magnetic field, so an obvious extension is considering the dynamics produced by these additional terms in the BdG equation. We have given some consideration to external potentials in the Heisenberg equations of motion. Except for a constant external potential the additional spatial dependence would complicate the solutions to the Heisenberg equations of motion, and also the calculation of the action of the Schrödinger equation. This would most likely require the consideration of slowly varying external potential compared to the size of and rate of oscillations of the wave packet.

Another interesting extension would be to analyse wave packet dynamics in an inhomogeneous superconductor. Although there are not simple analytic solutions to the BdG equations for arbitrary functions $\Delta(q)$ we might consider a slowly varying pair potential. We have seen that in certain cases wave packets located on the Fermi momentum oscillate about a

Figure 7.1: Reduced Q-function representations of the Andreev reflection of an electron incident from a normal conductor onto linearly varying band gap $\Delta(q) = 10 \times q\theta(q)$. $E = 50$, $\mu = 100$, $\hbar, m = 1$. q_T denotes the classical turning point where $E = \Delta(q)$.

(a) $Q_\otimes^{\mathtt{red}}(z)$ (b) $Q_\bowtie^{\mathtt{red}}(z)$
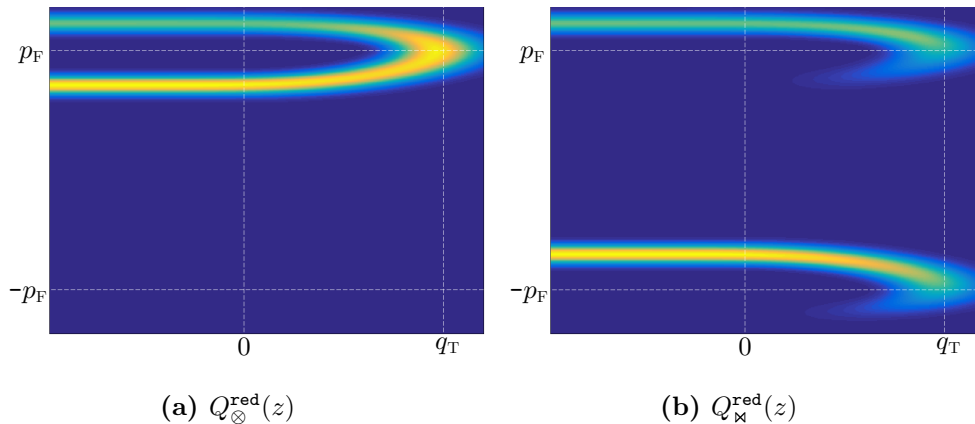
small region about the origin. In this case the wave packet would effectively not see any slow variations across this small region. In the case of Andreev reflection at a continuous boundary, we could consider applying the WKB style solutions as developed by Duncan and Györffy [27] (see Sub-section 2.1.4) in the construction of Gaussian wave packets.

A less trivial extension of this work would be the dynamics of wave packets in the presence of flux structures arising on the surface of a type II superconductor, where we have only really considered simplified type I superconductor models. We have considered the BdG equations under the restriction that $\Delta(q)$ is real and positive, but this extension would not only require the inclusion the external field potential in $\mathcal{H}_0$, but that we also consider the phase of a complex $\Delta(q)$, and the topological phase effects presented by the vortex cores.

We have left the question of whether it is possible to relate the dynamics of superconducting excitations to 'classical' phase space trajectories somewhat open. In the case of scattering of wave packets at a N-S boundary, analysis of the step potential would seem to indicate that there are no continuous trajectories as the wave packet does not fully enter the superconducting region. The work of Duncan and Györffy [27] and numerical plots (Figure 7.1) of the product and E-H Q-function would seem to indicate that such trajectories can occur if the boundary is smooth, containing classical turning points.

Appendix A

Detailed Calculations

This chapter contains any detailed calculations that have been omitted from the main body of the text. Calculations are arranged by the chapter, section (and sub-section) they refer to.

A.1 Chapter 4

A.1.1 Section 4.2

To calculate the transfer matrix relating electron and hole amplitudes at a discontinuous $\Delta(q)$ step located at $q = 0$, as shown in Figure 4.1, we satisfy the condition that the general solutions (4.13) and (4.19) and their first derivatives are continuous at the N-S boundary, hence

$$\mathbf{\Psi}_N(0) = \mathbf{\Psi}_S(0) \quad \text{and} \quad \mathbf{\Psi}'_N(0) = \mathbf{\Psi}'_S(0). \tag{A.1}$$

Written in terms of matrices acting on vectors in the amplitude basis these conditions are, for the electron wave function

$$\frac{1}{\sqrt{\alpha_+}} \begin{pmatrix} 1 & 1 \\ \frac{i}{\hbar}\alpha_+ & -\frac{i}{\hbar}\alpha_+ \end{pmatrix} \begin{pmatrix} A_I^e \\ A_R^e \end{pmatrix} = \begin{pmatrix} \nu/\sqrt{\kappa_+} & \nu^*/\sqrt{\kappa_-} \\ \frac{i}{\hbar}\nu\sqrt{\kappa_+} & -\frac{i}{\hbar}\nu^*\sqrt{\kappa_-} \end{pmatrix} \begin{pmatrix} F \\ G \end{pmatrix} \tag{A.2}$$

and similarly for the hole wave function

$$\frac{1}{\sqrt{\alpha_-}} \begin{pmatrix} 1 & 1 \\ \frac{i}{\hbar}\alpha_- & -\frac{i}{\hbar}\alpha_- \end{pmatrix} \begin{pmatrix} A_R^h \\ A_I^h \end{pmatrix} = \begin{pmatrix} \nu^*/\sqrt{\kappa_+} & \nu/\sqrt{\kappa_-} \\ \frac{i}{\hbar}\nu^*\sqrt{\kappa_+} & -\frac{i}{\hbar}\nu\sqrt{\kappa_-} \end{pmatrix} \begin{pmatrix} F \\ G \end{pmatrix}. \tag{A.3}$$

We will label the matrices, creating the simultaneous equations

$$\mathbf{a}\begin{pmatrix} A_e^I \\ B_e^R \end{pmatrix} = \mathbf{b}\begin{pmatrix} F \\ G \end{pmatrix} \quad \text{and} \quad \mathbf{c}\begin{pmatrix} A_h^R \\ A_h^I \end{pmatrix} = \mathbf{d}\begin{pmatrix} F \\ G \end{pmatrix}. \tag{A.4}$$

It is then straightforward to rearrange and substitute equations to form an equation that relates the electron and hole amplitudes

$$\begin{pmatrix} A_I^e \\ A_R^e \end{pmatrix} = \boldsymbol{a}^{-1}\boldsymbol{b}\boldsymbol{d}^{-1}\boldsymbol{c}\begin{pmatrix} A_R^h \\ A_I^h \end{pmatrix}. \tag{A.5}$$

We can then populate the scattering matrix $\boldsymbol{S}$ by imposing the condition that the incident state is either an electron ($A_I^e = 1$ and $A_I^h = 0$), or a hole ($A_I^h = 1$ and $A_I^e = 0$). With these conditions we can read the scattering matrix entries from (A.5). In principle this method can be used to estimate the scattering processes across an arbitrary potential or inhomogeneous band-gap by approximating the function as a series of potential steps and satisfying the continuity condition at each boundary successively, generating a total transfer matrix across the inhomogeneous region. Further details of this extension of the method, and the application of the transfer matrix method with reference to linear potentials can be found in [63].

A.1.2 Section 4.3

For an N-S interface modelled by a general continuous function of $\Delta(q)$ of length a bounded by homogeneous normal and superconducting regions it is necessary that we utilize a numerical ODE solver to generate the component wave functions across the varying region of $\Delta(q)$. From these solutions we can then satisfy the same continuity matching conditions. As with the discontinuous $\Delta(q)$ system we first look to find the transfer matrix, $\boldsymbol{T}$, that relates the amplitudes of states in the normal and spatially homogeneous region either side of the varying region.

The numerical ODE solver employed first requires that we reduce the order of the BdG equations, writing them as

$$\Psi^{e\prime}(q) = x(q) \qquad x'(q) = \frac{2m}{\hbar^2}[-\mu\Psi^e(q) + \Delta(q)\Psi^h(q) - E\Psi^e(q)] \tag{A.6}$$

$$\Psi^{h\prime}(q) = y(q) \qquad y'(q) = \frac{2m}{\hbar^2}[-\mu\Psi^h(q) - \Delta(q)\Psi^e(q) + E\Psi^h(q)]. \tag{A.7}$$

We also require 4 initial conditions at $q = 0$ and, we therefore work with vectors consisting of the wave functions and their derivatives at $q = 0$ and $q = a$

$$\bar{\Psi}_N(0) = \begin{pmatrix} \Psi_N^e(0) \\ \Psi_N^{e\prime}(0) \\ \Psi_N^h(0) \\ \Psi_N^{h\prime}(0) \end{pmatrix} \qquad \bar{\Psi}_S(a) = \begin{pmatrix} \Psi_S^e(a) \\ \Psi_S^{e\prime}(a) \\ \Psi_S^h(a) \\ \Psi_S^{h\prime}(a) \end{pmatrix}. \tag{A.8}$$

We can then relate the two boundaries by $\boldsymbol{T}\bar{\Psi}_N(0) = \bar{\Psi}_S(a)$ with $\boldsymbol{T}$ to be found. Since we cannot yet define an initial state with which to assign initial conditions, to generate the elements of $\boldsymbol{T}$, the algorithm first sets the first element of $\bar{\Psi}_N(0)$ to 1 and the remaining to 0 as

$$\bar{\Psi}_N(0) = \begin{pmatrix} 1 \\ 0 \\ 0 \\ 0 \end{pmatrix} \tag{A.9}$$

which is passed as the initial conditions to the ODE solver. We then generate corresponding values of $\bar{\Psi}_S(a)$ from this initial condition. This gives the first row of elements in $\boldsymbol{T}$ which are

$$\begin{pmatrix} T_{11} \\ T_{12} \\ T_{13} \\ T_{14} \end{pmatrix} = \begin{pmatrix} \Psi_S^e(a) \\ \Psi_S^{e\prime}(a) \\ \Psi_S^h(a) \\ \Psi_S^{h\prime}(a) \end{pmatrix}. \tag{A.10}$$

We can then repeat the process to generate all the elements of $\boldsymbol{T}$ by setting each component of $\bar{\Psi}_N(0)$ to 1 (and the remaining to 0) in turn. Once we know the full form of $\boldsymbol{T}$, inverting our initial equation $\bar{\Psi}_N(0) = \boldsymbol{T}^{-1}\bar{\Psi}_S(a)$ then gives us 4 equations that can then be reformulated in terms of transfer matrix elements acting on amplitudes. For example for

$$\Psi_N^e(0) = T_{11}^{-1}\Psi_S^e(a) + T_{12}^{-1}\Psi_S^{e\prime}(a) + T_{13}^{-1}\Psi_S^h(a) + T_{14}^{-1}\Psi_S^{h\prime}(a). \tag{A.11}$$

This can be written in full using the general solutions in the homogeneous regions as

$$\begin{aligned}
\frac{1}{\sqrt{\alpha_+}}\left[A_I^e + A_R^e\right] = & T_{11}^{-1}\left[\frac{F\nu}{\sqrt{\kappa_+}}\exp\left(\frac{ia}{\hbar}\kappa_+\right) + \frac{G\nu^*}{\sqrt{\kappa_-}}\exp\left(-\frac{ia}{\hbar}\kappa_-\right)\right] \\
& + T_{12}^{-1}\left[\frac{i\kappa_+F\nu}{\hbar\sqrt{\kappa_+}}\exp\left(\frac{ia}{\hbar}\kappa_+\right) - \frac{i\kappa_-G\nu^*}{\hbar\sqrt{\kappa_-}}\exp\left(-\frac{ia}{\hbar}\kappa_-\right)\right] \\
& + T_{13}^{-1}\left[\frac{F\nu^*}{\sqrt{\kappa_+}}\exp\left(\frac{ia}{\hbar}\kappa_+\right) + \frac{G\nu}{\sqrt{\kappa_-}}\nu\exp\left(-\frac{ia}{\hbar}\kappa_-\right)\right] \\
& + T_{14}^{-1}\left[\frac{i\kappa_+F\nu^*}{\hbar\sqrt{\kappa_+}}\exp\left(\frac{ia}{\hbar}\kappa_+\right) - \frac{i\kappa_-G\nu}{\hbar\sqrt{\kappa_-}}\nu\exp\left(-\frac{ia}{\hbar}\kappa_-\right)\right]
\end{aligned} \tag{A.12}$$

and likewise for the remaining rows of $\boldsymbol{T}^{-1}$. Gathering terms in F and G generates entries in the scattering matrix that relate the amplitudes at the

normal boundary, A_I^e and A_e^R, to F and G in the superconducting region

$$\frac{1}{\sqrt{\alpha_+}}\left[A_I^e + A_R^e\right] = \frac{F}{\sqrt{\kappa_+}} \exp\left(\frac{ia}{\hbar}\kappa_+\right)\left[\nu\left(T_{11} + \frac{i}{\hbar}T_{12}\kappa_+\right) + \nu^*\left(T_{13} + \frac{i}{\hbar}T_{14}\kappa_+\right)\right]$$
$$+ \frac{G}{\sqrt{\kappa_-}} \exp\left(-\frac{ia}{\hbar}\kappa_-\right)\left[\nu^*\left(T_{11} - \frac{i}{\hbar}T_{12}\kappa_-\right) + \nu\left(T_{13} - \frac{i}{\hbar}T_{14}\kappa_-\right)\right].$$

(A.13)

Working through all the components we can then write an equation that relates the electron and hole amplitudes, from which we can find the entries in the full scattering matrix, given the conditions on the incoming state. Once the correct amplitudes have been found, the wave functions for the region $\Delta(q)$ can be then be numerically generated from the initial conditions $\boldsymbol{\Psi}_l(0)$ and $\boldsymbol{\Psi}_l'(0)$.

A.2   Chapter 5

A.2.1   section 5.4

We look to solve the set of differential Heisenberg equations of motion given in section 5.3 to find the explicit form of the time dependent operators. The obvious starting point is the time indipendent momentum operator

$$\frac{d}{dt}\hat{p}(t) = 0 \implies \hat{p}(t) = \hat{p}.$$

(A.14)

We can insert this into the position operator equation giving

$$\frac{d}{dt}\hat{q}(t) = \frac{1}{m}\sigma_3(t)\hat{p}(t) = \frac{1}{m}\hat{p}\sigma_3(t).$$

(A.15)

We then also have the set of quasi-spin operators

$$\frac{d}{dt}\sigma_1(t) = -\frac{2}{\hbar}\hat{\mathcal{H}}_0\sigma_2(t)$$

(A.16)

$$\frac{d}{dt}\sigma_2(t) = \frac{2}{\hbar}\left[\hat{\mathcal{H}}_0\sigma_1(t) - \Delta_0\sigma_3(t)\right]$$

(A.17)

$$\frac{d}{dt}\sigma_3(t) = \frac{2}{\hbar}\Delta_0\sigma_2(t).$$

(A.18)

Noting that if we differentiate equation (A.17) again we can then substitute equations (A.16) and (A.18) into the right hand side, giving a second order ODE in $\sigma_2(t)$,

$$\frac{d^2}{dt^2}\sigma_2(t) = -\frac{4}{\hbar^2}[\hat{\mathcal{H}}_0^2 + \Delta_0^2]\sigma_2(t).$$

(A.19)

This has the general solution

$$\sigma_2(t) = A\exp\left[\frac{2it}{\hbar}\sqrt{\hat{\mathcal{H}}_0^2 + \Delta_0^2}\right] + B\exp\left[-\frac{2it}{\hbar}\sqrt{\hat{\mathcal{H}}_0^2 + \Delta_0^2}\right].$$

(A.20)

We also then have the initial conditions $\sigma_2(0) = A + B$ and

$$\frac{d}{dt}\sigma_2(0) = \frac{2i}{\hbar}(A - B)\sqrt{\hat{\mathcal{H}}_0^2 + \Delta_0^2}. \tag{A.21}$$

We can then insert this general solution and directly integrate the differential equations for $\sigma_1(t)$ (A.16) and $\sigma_3(t)$ (A.18) giving

$$\sigma_1(t) = -\frac{2\hat{\mathcal{H}}_0}{\hbar} \int \sigma_2(t)\, dt \tag{A.22}$$

$$= \frac{i\hat{\mathcal{H}}_0}{\sqrt{\hat{\mathcal{H}}_0^2 + \Delta_0^2}} \left[A \exp\left(\frac{2it}{\hbar}\sqrt{\hat{\mathcal{H}}_0^2 + \Delta_0^2}\right) - B \exp\left(-\frac{2it}{\hbar}\sqrt{\hat{\mathcal{H}}_0^2 + \Delta_0^2}\right) \right] + C_1 \tag{A.23}$$

where we have the initial condition

$$\sigma_1(0) = \frac{i\hat{\mathcal{H}}_0}{\sqrt{\hat{\mathcal{H}}_0^2 + \Delta_0^2}}(A - B) + C_1 \tag{A.24}$$

and

$$\sigma_3(t) = \frac{2\Delta_0}{\hbar} \int \sigma_2(t)\, dt \tag{A.25}$$

$$= \frac{-i\Delta_0}{\sqrt{\hat{\mathcal{H}}_0^2 + \Delta_0^2}} \left[A \exp\left(\frac{2it}{\hbar}\sqrt{\hat{\mathcal{H}}_0^2 + \Delta_0^2}\right) - B \exp\left(-\frac{2it}{\hbar}\sqrt{\hat{\mathcal{H}}_0^2 + \Delta_0^2}\right) \right] + C_3 \tag{A.26}$$

with the initial conditions

$$\sigma_3(0) = \frac{-i\Delta_0}{\sqrt{\hat{\mathcal{H}}_0^2 + \Delta_0^2}}(A - B) + C_3. \tag{A.27}$$

We can find the constants of integration by substituting these results back into the first order equation, for $\sigma_2(t)$ at $t = 0$

$$\frac{d}{dt}\sigma_2(0) = \frac{2}{\hbar}\left[\hat{\mathcal{H}}_0\sigma_1(0) - \Delta_0\sigma_3(0)\right] \tag{A.28}$$

$$= \frac{2}{\hbar}\left[i(A - B)\sqrt{\hat{\mathcal{H}}_0^2 + \Delta_0^2} + \hat{\mathcal{H}}_0 C_1 - \Delta_0 C_3\right] \tag{A.29}$$

$$\implies \hat{\mathcal{H}}_0 C_1 = \Delta_0 C_3. \tag{A.30}$$

Further algebraic manipulation then yields the two constants

$$C_3 = \frac{1}{\hat{\mathcal{H}}_0^2 + \Delta_0^2}\left[\hat{\mathcal{H}}_0^2\sigma_3(0) + \Delta_0\hat{\mathcal{H}}_0\sigma_1(0)\right] \tag{A.31}$$

$$C_1 = \frac{1}{\hat{\mathcal{H}}_0^2 + \Delta_0^2}\left[\Delta_0\hat{\mathcal{H}}_0\sigma_3(0) + \Delta_0^2\sigma_1(0)\right] \tag{A.32}$$

and the amplitudes

$$A = \frac{\sigma_2}{2} - \frac{1}{2}\frac{i}{\sqrt{\hat{\mathcal{H}}_0^2 + \Delta_0^2}}[\hat{\mathcal{H}}_0\sigma_1 - \Delta_0\sigma_3] \tag{A.33}$$

$$B = \frac{\sigma_2}{2} + \frac{1}{2}\frac{i}{\sqrt{\hat{\mathcal{H}}_0^2 + \Delta_0^2}}[\hat{\mathcal{H}}_0\sigma_1 - \Delta_0\sigma_3]. \tag{A.34}$$

In full the the time dependent spin operators are therefore

$$\sigma_1(t) = \frac{-\hat{\mathcal{H}}_0\sigma_2}{\sqrt{\hat{\mathcal{H}}_0^2 + \Delta_0^2}}\sin\left(\frac{2t}{\hbar}\sqrt{\hat{\mathcal{H}}_0^2 + \Delta_0^2}\right) + \frac{\hat{\mathcal{H}}_0^2\sigma_1 - \hat{\mathcal{H}}_0\Delta_0\sigma_3}{\hat{\mathcal{H}}_0^2 + \Delta_0^2}\cos\left(\frac{2t}{\hbar}\sqrt{\hat{\mathcal{H}}_0^2 + \Delta_0^2}\right)$$
$$+ \frac{1}{\hat{\mathcal{H}}_0^2 + \Delta_0^2}\left[\Delta_0\hat{\mathcal{H}}_0\sigma_3 + \Delta_0^2\sigma_1\right] \tag{A.35}$$

$$\sigma_2(t) = \sigma_2\cos\left(\frac{2t}{\hbar}\sqrt{\hat{\mathcal{H}}_0^2 + \Delta_0^2}\right) + \frac{\hat{\mathcal{H}}_0\sigma_1 - \Delta_0\sigma_3}{\sqrt{\hat{\mathcal{H}}_0^2 + \Delta_0^2}}\sin\left(\frac{2t}{\hbar}\sqrt{\hat{\mathcal{H}}_0^2 + \Delta_0^2}\right)$$

$$\tag{A.36}$$

$$\sigma_3(t) = \frac{\Delta_0\sigma_2}{\sqrt{\hat{\mathcal{H}}_0^2 + \Delta_0^2}}\sin\left(\frac{2t}{\hbar}\sqrt{\hat{\mathcal{H}}_0^2 + \Delta_0^2}\right) - \frac{\hat{\mathcal{H}}_0\Delta_0\sigma_1 - \Delta_0^2\sigma_3}{\hat{\mathcal{H}}_0^2 + \Delta_0^2}\cos\left(\frac{2t}{\hbar}\sqrt{\hat{\mathcal{H}}_0^2 + \Delta_0^2}\right)$$
$$+ \frac{1}{\hat{\mathcal{H}}_0^2 + \Delta_0^2}\left[\hat{\mathcal{H}}_0^2\sigma_3 + \Delta_0\hat{\mathcal{H}}_0\sigma_1\right]. \tag{A.37}$$

These time dependent operators satisfy the same unitary conditions as the Pauli matrices $\sigma_1(t)^2 = \sigma_2(t)^2 = \sigma_3(t)^2 = -i\sigma_1(t)\sigma_2(t)\sigma_3(t) = \mathbb{I}$.

The time dependent position operator is found by integrating the differential equation now that we know $\sigma_3(t)$, so that $\hat{q}(t) = \frac{\hat{p}}{m}\int \sigma_3(t)\,dt + C$ which gives us

$$\hat{q}(t) = \frac{\hbar\hat{p}}{2m}\left\{\frac{\Delta_0\sigma_2}{\hat{\mathcal{H}}_0^2 + \Delta_0^2}\left(1 - \cos\left[\frac{2t}{\hbar}\sqrt{\hat{\mathcal{H}}_0^2 + \Delta_0^2}\right]\right) + \frac{2t}{\hbar(\hat{\mathcal{H}}_0^2 + \Delta_0^2)}\left[\hat{\mathcal{H}}_0^2\sigma_3 + \Delta_0\hat{\mathcal{H}}_0\sigma_1\right]\right.$$
$$\left. - \frac{[\hat{\mathcal{H}}_0\Delta_0\sigma_1 - \Delta_0^2\sigma_3]}{(\hat{\mathcal{H}}_0^2 + \Delta_0^2)^{3/2}}\sin\left[\frac{2t}{\hbar}\sqrt{\hat{\mathcal{H}}_0^2 + \Delta_0^2}\right]\right\} + \hat{q}(0) \tag{A.38}$$

where we've fixed $q(0)$ at t=0 via the constant of integration. As the momentum operator is time independent the time dependent pseudo-velocity operator is simply $\hat{V}(t) = \hat{p}\sigma_3(t)$.

A.2.2   Section 5.4.5

The expectation values of the time dependent quasi-spin operators require that we find the convolution of terms of the form

$$\frac{\mathcal{H}_0}{\mathcal{H}_0^2 + \Delta_0^2} \quad \text{and} \quad \frac{\Delta_0}{\mathcal{H}_0^2 + \Delta_0^2} \tag{A.39}$$

and a Gaussian envelope we can express these terms as the real and complex parts of

$$\frac{\mathcal{H}_0 + i\Delta_0}{\mathcal{H}_0^2 + \Delta_0^2} = \frac{2m}{p^2 - 2m(\mu + i\Delta_0)} = \frac{2m}{p^2 - a^2}. \tag{A.40}$$

We have defined the complex term

$$a = \sqrt{2m(\mu + i\Delta_0)}. \tag{A.41}$$

We then have the identities

$$\frac{\mathcal{H}_0}{\mathcal{H}_0^2 + \Delta_0^2} = \mathrm{Re}\left[\frac{2m}{p^2 - a^2}\right] \quad \text{and} \quad \frac{\Delta_0}{\mathcal{H}_0^2 + \Delta_0^2} = \mathrm{Im}\left[\frac{2m}{p^2 - a^2}\right]. \tag{A.42}$$

We first consider the convolution of a Gaussian function and the real term

$$\int \frac{\mathcal{H}_0}{\mathcal{H}_0^2 + \Delta_0^2} e^{-\lambda(p-V_0)^2} dp = \int \mathrm{Re}\left[\frac{2m}{p^2 - a^2}\right] e^{-\lambda(p-V_0)^2} dp. \tag{A.43}$$

Since we are integrating along the real line, and over a real Gaussian we can therefore move the real operator outside the integral, and after rescaling and shifting p we have

$$\int \mathrm{Re}\left[\frac{2m}{p^2 - a^2}\right] e^{-\lambda(p-V_0)^2} dp = \mathrm{Re}\left[\int \left(\frac{m}{a}\left(\frac{1}{p-a} - \frac{1}{p+a}\right)\right) e^{-\lambda(p-V_0)^2} dp\right] \tag{A.44}$$

$$= \mathrm{Re}\left[\int \left(\frac{m}{a}\left(\frac{1}{p-z_-} - \frac{1}{p-z_+}\right)\right) e^{-p^2} dp\right] \tag{A.45}$$

where $z_\pm = -\sqrt{\lambda}(V_0 \pm a)$. These integrals are commonly referred to as the *plasma dispersion function*[73] $Z(z)$ the Hilbert transform of a Gaussian function and a scaled form of the Faddeeva function. It is defined as

$$Z(z) = \int dx \frac{e^{-x^2}}{x - z} = i\pi w(z), \qquad \mathrm{Im}(z) > 0. \tag{A.46}$$

Care has to be taken with the poles in the complex plane, as such this definition is valid for non-zero $\mathrm{Im}(z) > 0$, but the function can be defined for all z in the complex plane by analytic continuation. We will make use of the form that relates the solution for $\mathrm{Im}(z) < 0$ as

$$w^*(z) = -w(-z), \quad \mathrm{Im}(z) < 0. \tag{A.47}$$

We will only be required to use this integral where $\Delta_0 \neq 0$ and so will not require the analytic continuation when $\mathrm{Im}(z) = 0$. The final result we require is therefore

$$\int \frac{\mathcal{H}_0}{\mathcal{H}_0^2 + \Delta_0^2} e^{-\lambda(p-V_0)^2} dp = \mathrm{Re}\left[\frac{im\pi}{a}\left(w(z_-) + w(-z_+)\right)\right] \tag{A.48}$$

and likewise for

$$\int \frac{\Delta_0}{\mathcal{H}_0^2 + \Delta_0^2} e^{-\lambda(p-V_0)^2} dp = \text{Im} \left[\frac{im\pi}{a} \left(w(z_-) + w(-z_+) \right) \right]. \qquad \text{(A.49)}$$

For the expectation value of the pseudo-velocity operator we require the solution to to a similar integral

$$\sqrt{\frac{\lambda}{\pi}} \Delta_0^2 \int \frac{p}{E^2(p)} e^{-\lambda(p-V_0)^2} dp = \sqrt{\lambda\pi} m \Delta_0 \int \text{Im} \left[\frac{1}{p+a} + \frac{1}{p-a} \right] e^{-\lambda(p-V_0)^2} dp$$

(A.50)

$$= \sqrt{\lambda\pi} m \Delta_0 \text{Im} \left[i \left(w(z_-) - w(-z_+) \right) \right] \qquad \text{(A.51)}$$

In this case we can analyse the behaviour of the Faddeeva function terms $\text{Im}[iw(\pm z_\mp)]$ by approximating a, when $\Delta_0 \ll \mu$, as

$$a \approx p_{\text{F}} \left[1 + \frac{i\Delta_0}{2\mu} \right]. \qquad \text{(A.52)}$$

We can then approximate the terms in Equation (A.50) as

$$\frac{1}{p \pm a} \approx \frac{(p \pm p_{\text{F}}) \mp i\Delta_0/v_{\text{F}}}{(p \pm p_{\text{F}})^2 + (\Delta_0/v_{\text{F}})^2} \qquad \text{(A.53)}$$

the imaginary part of this is recognisable as a Lorentz distribution of the form

$$f(x; x_0, \gamma) = \frac{1}{\pi\gamma} \left[\frac{\gamma^2}{(x - x_0)^2 + \gamma^2} \right]. \qquad \text{(A.54)}$$

The Lorentz distribution is parametrized by x_0, the location of the peak of the distribution, and the scale-parameter γ, the half-width half-max of the distribution. The height of the distribution at it's peak is given by $1/\pi\gamma$. This gives us the relation

$$\text{Im} \left(\frac{1}{p \pm a} \right) \approx \mp \pi f(p; \mp p_{\text{F}}, \Delta_0/v_{\text{F}}). \qquad \text{(A.55)}$$

Though this does not simplify the calculation, we can however consider the behaviour of the convolution, in particular when the peaks of the Lorentz and Gaussian functions coincide.

A.2.3   Sub-Section 5.5.3

$\mu \to \infty, \, \Delta_0 = \delta\mu^{1/2}$

Holding Δ_0 constant as $\mu \to \infty$ allowed us to expand the phase term, $E(p)$, in powers of $\Delta_0/\mathcal{H}_0$. But when Δ_0 is scaled by μ there is no discontinuity in

178

$E'(p)$ we can use to simplify the calculation. We instead look to apply the stationary phase approximation using Fermi energy as the large parameter. If we consider a wave packet centred on p_F, to see which terms dominate in this regime we first proceed by translating the integration variable to $p \to p + p_\text{F}$ centring the Gaussian term on the origin. Applying the scaling of $\Delta_0 = \delta\mu^{1/2}$ we have rewritten integral (5.234) as

$$I(q,t) = N e^{\frac{i}{\hbar}qp_\text{F}} \int f(p + p_\text{F}) \exp\left[-\frac{\lambda}{2}p^2 + \frac{i}{\hbar}pq \pm \frac{it}{\hbar}E(p + p_\text{F})\right] dp. \quad (A.56)$$

We can then approximate and relabel the rescaled phase term as

$$E(p + p_\text{F}) = \left[\left(\frac{p}{2m}\right)^2 (p + 2p_\text{F})^2 + \mu(\delta)^2\right]^{1/2} \quad (A.57)$$

$$\approx \mu^{1/2}\left[\frac{2}{m}p^2 + \delta^2\right]^{1/2} = \mu^{1/2}\varphi(p) \quad (A.58)$$

We have obtained the approximation on the second line by extracting the large term μ from inside $E(p + p_\text{F})$ under the condition that we are considering integrating over p close to the origin. Terms of order p/p_F will then be negligible in the limit $\mu \to \infty$. As was the case for long times we will therefore define an overall phase term in the exponent of $I(q,t)$

$$\theta_\pm(p) = \frac{pq}{\sqrt{\mu}} \pm t\left[\frac{2}{m}p^2 + \delta^2\right]^{1/2} \quad (A.59)$$

then Equation (A.56) can be written in a form suitable for the application of the stationary phase approximation when $\mu \to \infty$

$$I(q,t) = N e^{\frac{i}{\hbar}qp_\text{F}} \int f(p + p_\text{F}) \exp\left[-\frac{\lambda}{2}p^2 + \frac{i}{\hbar}\sqrt{\mu}\,\theta_\pm(p)\right] dp. \quad (A.60)$$

For this simplified phase term it is straightforward to find analytic solutions of stationary phase condition $\theta'_\pm(\mp p_\text{s}(q)) = 0$. $p_\text{s}(q)$ is

$$p_\text{s}(q) = \sqrt{\frac{m}{2}}\,\delta q\left[(tv_\text{F})^2 - q^2\right]^{-1/2}. \quad (A.61)$$

With this in hand the application of the stationary phase approximation gives the general solution

$$I(q,t) \approx N\sqrt{\frac{2\pi\hbar}{t\mu^{1/2}|\varphi''(p_\text{s}(q))|}}\, f\left(p_\text{F} \mp p_\text{s}(q)\right)$$

$$\times \exp\left[-\frac{\lambda}{2}p_\text{s}^2(q) + \frac{i}{\hbar}qp_\text{F} \pm \frac{i}{\hbar}\sqrt{\mu}\,\theta_+\left(-p_\text{s}(q)\right) \pm \frac{i\pi c}{4}\right]. \quad (A.62)$$

c again refers to the sign of $\varphi''(p_\text{s}(q))$.

$\hbar \to 0$, $\alpha = -1$

$\alpha = -1$ corresponds to a fixed momentum width indipendent of $\hbar$. The width is parametrized by $\lambda = 1/m\Omega$ (where $\Omega = (2\Delta_0/x\pi)^2/\mu$). We are therefore required to approximate the solution to the integral

$$I(q,t) = N \int A(p) \exp\left[-\frac{\lambda}{2}(p - V_0)^2 + \frac{i}{\hbar}pq \pm \frac{it}{\hbar}E(p)\right] dp. \qquad (A.63)$$

Since λ is constant indipendent of $\hbar$ we see that in this case the limit $\hbar \to 0$ is equivalent to the previously derived $t \to \infty$ approximation , except we do not need to explicitly take the large parameter outside the phase term. The appropriate phase term is

$$\theta_\pm(p) = pq \pm tE(p) \qquad (A.64)$$

but in effect the resultant stationary phase points are given by the same solutions. The stationary phase approximation therefore has the same form as for long times,

$$I(q,t) \approx N \sum_{p_i} A(p_i)\sqrt{\frac{2\pi\hbar}{t|E''(p_i)|}} \exp\left[-\frac{\lambda}{2}(p_i - V_0)^2 + \frac{i}{\hbar}\theta_\pm(p_i) \pm \frac{ic\pi}{4}\right] \qquad (A.65)$$

again summing over real stationary points. We can then again consider the contributing stationary points contained under the wave packets momentum distribution.

$\hbar \to 0$, $\alpha = 1$

Holding δq at a constant value ($\alpha = 1$), our integral then looks like

$$I(q,t) = \int A(p) \exp\left[\frac{1}{\hbar}\left(-\frac{\lambda'}{2}(p - V_0)^2 + i\theta_\pm(p)\right)\right] dp \qquad (A.66)$$

where λ' is the rescaled width $\lambda' = 1/m\Omega\hbar$. Then as $\hbar \to 0$ the real Gaussian term, with width proportional to $\hbar$, converges on a single value faster than the width of the stationary phase approximation which scales with $\sqrt{\hbar}$. If we thus apply the Laplace method (see appendix C.1 for details) by expanding the oscillating term around the centre of the Gaussian V_0 giving

$$I(q,t) \approx NA(V_0) \int \exp\left[-\frac{\lambda'}{2\hbar}(p - V_0)^2 + \frac{i}{\hbar}pq \right.$$
$$\left. \pm \frac{it}{\hbar}\left(E(V_0) + E'(V_0)(p - V_0) + \frac{1}{2}E''(V_0)(p - V_0)^2\right)\right] dp \qquad (A.67)$$

this is a standard complex Gaussian integral with the solution

$$= NA(V_0)\sqrt{\frac{2\pi\hbar}{a_{\mp}(t)}}\exp\left[-\frac{1}{2\hbar a_{\mp}(t)}(q \pm tE'(V_0))^2 + \frac{i}{\hbar}(qV_0 \pm tE(V_0))\right]$$

(A.68)

where the complex width parameter is defined as $a_{\pm}(t) = (\lambda' \pm itE''(V_0))$. If we apply this to an initial electron wave packet centred on the Fermi momentum

$$\psi_e(q,t) \approx \frac{N}{2}\sqrt{\frac{2\pi\hbar}{a_+(t)}}(|e\rangle - |h\rangle)\exp\left[-\frac{1}{2\hbar a_+(t)}q^2 + \frac{i}{\hbar}(qp_{\mathrm{F}} - t\Delta_0)\right]$$

$$+ \frac{N}{2}\sqrt{\frac{2\pi\hbar}{a_-(t)}}(|e\rangle + |h\rangle)\exp\left[-\frac{1}{2\hbar a_-(t)}q^2 + \frac{i}{\hbar}(qp_{\mathrm{F}} + t\Delta_0)\right]$$

(A.69)

as anticipated this wave packet remains centred on the origin, with a linear t dependent wave packet width.

$\hbar \to 0$, $\alpha = 1/2$

If we allow the width of the distribution in phase space to tend to 0 identically in both p and q as $\hbar \to 0$ when $\alpha = 1/2$, we see that where as in the previous two examples one of the terms in the exponent has clearly converged faster than the other, in this case the width of the contribution from the Gaussian term and the width of the stationary phase contributions both converge at approximately the same rate, $\sqrt{\hbar}$. Rather than finding the stationary points of the whole term in the exponential via the method of steepest descent, we can greatly simplify the calculation by expanding the phase term close to the stationary point but still consider the contributions from the Gaussian term rather than just evaluate it at the stationary phase points. This has the form

$$I(q,t) \approx N\int A(p)\exp\left[-\frac{\lambda}{2}(p - V_0)^2 + \frac{i}{\hbar}\left(\theta_{\pm}(p_i) + \frac{1}{2}\theta''_{\pm}(p_i)(p - p_i)^2\right)\right]dp.$$

(A.70)

The result is therefore just the convolution of the two largest Gaussian contributions, which is itself a Gaussian profile with a complex offset whose

width will also scale with $\sqrt{\hbar}$. Thus

$$I(q,t) \approx NA\left(z_{\mp}\right) \int \exp\left[-\frac{\lambda \gamma_{\mp}}{2}\left(p - z_{\mp}\right)^2 \pm \frac{itE''(p_i)}{2\hbar\gamma_{\mp}}\left(p_i - V_0\right)^2 + \frac{i}{\hbar}\theta_{\pm}(V_0)\right]dp$$

$$\text{(A.71)}$$

$$= NA\left(z_{\mp}\right)\sqrt{\frac{2\pi}{\lambda \gamma_{\mp}}}\exp\left[\pm\frac{itE''(p_i)}{2\hbar\gamma_{\mp}}\left(p_i - V_0\right)^2 + \frac{i}{\hbar}\theta_{\pm}(V_0)\right] \quad \text{(A.72)}$$

where the width of the resultant distribution is described by

$$\gamma_{\pm} = 1 \pm itm\omega E''(p_i). \tag{A.73}$$

where the p_i are same stationary points as derived for the long time case. The complex offset of the Gaussian integral is then given by

$$z_{\pm} = \gamma_{\pm}^{-1}\left(V_0 \pm itm\omega E''(p_i)p_i\right). \tag{A.74}$$

Both theses terms are indipendent of $\hbar$, $\hbar$ only entering the solution as $1/\hbar$ scaling in both the Gaussian and oscillating term, so in the limit $\hbar \to 0$ we will see both very fast oscillations but also the suppression of contributions when $p_0 \neq V_0$ (i.e. the largest contributions will be where $q/t \approx 0$).

It should be noted that the amplitude terms included here (i.e. $A(p)$) can contain poles in complex plane. Expanding $E^{-1}(p)$ (which also occurs in $A_{\pm}(p)$) as

$$E^{-1}(p) = [(p + a)(p - a)(p + a^*)(p - a^*)]^{-\frac{1}{2}} \tag{A.75}$$

where $a = \sqrt{\mu + i\Delta_0}$. The result given by Equation (A.72) is arrived at by shifting the contour of integration parallel to the real line to the complex offset $z_{\pm}$. The real and complex parts of $z_{\pm}$ are given by

$$z_{\pm} = |\gamma_{\pm}|^{-2}\left[V_0 + p_i\left(tm\omega E''(p_i)\right)^2 \pm itm\omega E''(p_i)\left(V_0 - p_i\right)\right]. \tag{A.76}$$

We have shown that any contributions when p_i is far from the peak of (A.72) at V_0 are suppressed. This means that though $z_{\pm}$ can take values that would requires consideration of the contributions from the poles of $E^{-1}(p)$, these contributions will become negligible as $\hbar \to 0$.

A.3 Chapter 6

A.3.1 Section 6.1

We would like to prove the orthogonality of the scattering states at energies $|E| < \Delta_0$, which in bra-ket notation we will denote as $|\boldsymbol{E}, e\rangle$ for the scattering state resulting from an incident electron with energy E above μ and

$|\boldsymbol{E}, h\rangle$ likewise an incident hole with energy E below μ. Thus $\langle q|E, e\rangle = \boldsymbol{\Psi}_e(q)$ and $\langle q|E, h\rangle = \boldsymbol{\Psi}_h(q)$ are the two component spinor with electron and hole wave function components as derive in section 4.2, equations (4.21) and (4.22) in the normal region, and (4.29) and (4.30) in the superconductor. The appropriate orthogonality condition we would like to prove is

$$\langle E', \sigma'|E, \sigma\rangle = \delta(E' - E)\delta_{\sigma'\sigma} \tag{A.77}$$

where $\sigma = \{e, h\}$ denotes the incident state. We will prove this by inserting the identity in the position basis and integrating over the normal and superconducting regions independently,

$$\int \langle E', \sigma'|q\rangle\langle q|\mathbb{I}|E, \sigma\rangle dq = \int_{-\infty}^{0} \boldsymbol{\Psi}_N^{\sigma'\dagger}(E')\boldsymbol{\Psi}_N^{\sigma}(E)dq + \int_{0}^{\infty} \boldsymbol{\Psi}_S^{\sigma'\dagger}(E')\boldsymbol{\Psi}_S^{\sigma}(E)dq. \tag{A.78}$$

We first prove the orthogonality condition where $\sigma' \neq \sigma$. In the superconducting region the integrals we require

$$\int_{0}^{\infty} \boldsymbol{\Psi}_S^{h\dagger}(E')\boldsymbol{\Psi}_S^{e}(E)dq =$$
$$\int_{0}^{\infty} \frac{2}{\Delta_0}\frac{\sqrt{\alpha_+\alpha_-'}}{\gamma^{*'}\gamma}\Big[(E'\nu'^2 + E\nu^2)(\kappa_+' - \alpha_+')(\kappa_- + \alpha_-)e^{-iq(\kappa_-' - \kappa_+)}$$
$$+ (E'\nu'^2 + E\nu^{*2})(\kappa_+' - \alpha_+')(\kappa_+ - \alpha_-)e^{-iq(\kappa_-' + \kappa_-)}$$
$$+ (E'\nu^{*'2} + E\nu^2)(\kappa_-' + \alpha_+')(\kappa_- + \alpha_-)e^{iq(\kappa_+' + \kappa_+)}$$
$$+ (E'\nu^{*'2} + E\nu^{*2})(\kappa_-' + \alpha_+')(\kappa_+ - \alpha_-)e^{iq(\kappa_+' - \kappa_-)}\Big] dq \tag{A.79}$$

The prime notation here is shorthand for an energy dependent function evaluated at E'. The convergence of the integrals in the superconducting region is ensured by the requirement that the wave functions decay as $q \to \infty$. With this condition the general solution for an integral of this form is simply

$$\int_{0}^{\infty} e^{iqX}dq = \frac{i}{X} \tag{A.80}$$

when $X \in \mathbb{Z}$ is chosen such that the integral converges. Applied to the integral this gives

$$\int_{0}^{\infty} \boldsymbol{\Psi}_S^{h\dagger}(E')\boldsymbol{\Psi}_S^{e}(E)dq =$$
$$\frac{2i\sqrt{\alpha_+\alpha_-'}}{\Delta_0\gamma^{*'}\gamma}\Big[\frac{(E'\nu'^2 + E\nu^2)}{(\kappa_+ - \kappa_-')}\kappa_+^{\alpha_+'}\kappa_-^{\alpha_-} - \frac{(E'\nu'^2 + E\nu^{*2})}{(\kappa_-' + \kappa_-)}\kappa_+^{\alpha_+'}\kappa_+^{\alpha_-}$$
$$+ \frac{(E'\nu^{*'2} + E\nu^2)}{(\kappa_+' + \kappa_+)}\kappa_-^{\alpha_+'}\kappa_-^{\alpha_-} + \frac{(E'\nu^{*'2} + E\nu^{*2})}{(\kappa_+' - \kappa_-)}\kappa_-^{\alpha_+'}\kappa_+^{\alpha_-}\Big] \tag{A.81}$$

where the notation $\kappa^x_\pm$ assigned here is shorthand for

$$\kappa^x_\pm = \kappa_\pm \mp x. \tag{A.82}$$

The terms in the superconducting region do not cancel themselves, we will show that these terms cancel with those in the normal region. For the normal region we need to integrate

$$\int_{-\infty}^{0} \Psi_N^{h\dagger}(E')\Psi_N^e(E)dq = \int_{-\infty}^{0} \frac{S^{*\prime}_{eh}}{\sqrt{\alpha_+\alpha'_+}}e^{i\alpha'_+ q}\left[e^{i\alpha_+ q} + S_{ee}e^{-i\alpha_+ q}\right]$$
$$+ \frac{S_{he}}{\sqrt{\alpha_-\alpha'_-}}e^{i\alpha_- q}\left[e^{i\alpha'_- q} + S^{*\prime}_{hh}e^{-i\alpha'_- q}\right]dq. \tag{A.83}$$

As these terms describe plane waves they do not naturally converge as $q \to -\infty$. We will therefore ensure convergence by inserting a term into the exponential of the form

$$\int_{-\infty}^{0} e^{iqX}dq = \lim_{\epsilon\to 0}\int_{-\infty}^{0} e^{iqX+\epsilon q}dq = \lim_{\epsilon\to 0}\frac{1}{iX+\epsilon} \tag{A.84}$$

such that in the limit $\epsilon \to 0$ we regain the original integral. Inserting this into the integral the solution in the limit $\epsilon \to 0$ is therefore

$$\int_{-\infty}^{0} \Psi_N^{h\dagger}(E')\Psi_N^e(E)dq = \lim_{\epsilon\to 0}\frac{S^{*\prime}_{eh}}{\sqrt{\alpha_+\alpha'_+}}\left[\frac{1}{\epsilon + i(\alpha'_+ + \alpha_+)} + \frac{S_{ee}}{\epsilon + i(\alpha'_+ - \alpha_+)}\right]$$
$$+ \frac{S_{he}}{\sqrt{\alpha_-\alpha'_-}}\left[\frac{1}{\epsilon + i(\alpha_- + \alpha'_-)} + \frac{S^{*\prime}_{hh}}{\epsilon + i(\alpha_- - \alpha'_-)}\right]. \tag{A.85}$$

This can be rewritten using the identity

$$\lim_{\epsilon\to 0}\frac{1}{\epsilon + iX} = \lim_{\epsilon\to 0}\frac{\epsilon - iX}{\epsilon^2 + X^2} = \pi\delta(X) - \lim_{\epsilon\to 0}\frac{iX}{\epsilon^2 + X^2} \tag{A.86}$$

as

$$\int_{-\infty}^{0} \Psi_N^{h\dagger}(E')\Psi_N^e(E)dq$$
$$= \lim_{\epsilon\to 0}\frac{S^{*\prime}_{eh}}{\sqrt{\alpha_+\alpha'_+}}\left[-\frac{i(\alpha_+ + \alpha'_+)}{\epsilon^2 + (\alpha_+ + \alpha'_+)^2} + S_{ee}\left[\pi\delta(\alpha'_+ - \alpha_+) - \frac{i(\alpha'_+ - \alpha_+)}{\epsilon^2 + (\alpha'_+ - \alpha_+)^2}\right]\right]$$
$$+ \frac{S_{he}}{\sqrt{\alpha_-\alpha'_-}}\left[-\frac{i(\alpha_- + \alpha'_-)}{\epsilon^2 + (\alpha_- + \alpha'_-)^2} + S^{*\prime}_{hh}\left[\pi\delta(\alpha_- - \alpha'_-) - \frac{i(\alpha_- - \alpha'_-)}{\epsilon^2 + (\alpha_- - \alpha'_-)^2}\right]\right]. \tag{A.87}$$

We've used the fact that $\delta(\alpha'_+ + \alpha_+) = 0$ and $\delta(\alpha'_- + \alpha_-) = 0$ for all E. The delta functions of $\alpha_\pm$ can be written in terms of delta functions in E using the identity

$$\delta(f(x)) = \frac{\delta(x - x_0)}{|f'(x_0)|} \tag{A.88}$$

where x_0 is a root of $f(x)$. Applied to the delta functions with $f(E) = \pm(\alpha'_\pm - \alpha_\pm)$ then

$$\delta(f(E)) = \frac{m}{\alpha'_\pm(E')}\delta(E - E'). \tag{A.89}$$

If we first assume that $E = E'$ then the delta function terms cancel due to the unitary condition $S_{ee}S^*_{eh} + S^*_{hh}S_{eh} = 0$. Then assuming $E \neq E'$ in the limit $\epsilon \to 0$ we are left with

$$\int_{-\infty}^0 \boldsymbol{\Psi}_N^{h\dagger}(E')\boldsymbol{\Psi}_N^e(E)dq$$
$$= \lim_{\epsilon \to 0}\frac{-iS^{*\prime}_{eh}}{\sqrt{\alpha'_+\alpha_+}}\left[\frac{1}{\alpha'_+ + \alpha_+} + \frac{S_{ee}}{\alpha'_+ - \alpha_+}\right] - \frac{iS_{he}}{\sqrt{\alpha'_-\alpha_-}}\left[\frac{1}{\alpha'_- + \alpha_-} + \frac{S^{*\prime}_{hh}}{\alpha_- - \alpha'_-}\right] \tag{A.90}$$

which now cancel with the terms in the superconducting region $q > 0$.

We now prove orthogonality for differing energies but $\sigma' = \sigma$. We consider the product of two incident electron states, on the left the integral is

$$\int \boldsymbol{\Psi}_N^{e\dagger}(E')\boldsymbol{\Psi}_N^e(E)dq = \int \frac{1}{\sqrt{\alpha_+\alpha'_+}}\left[e^{iq(\alpha_+ - \alpha'_+)} + S_{ee}e^{-iq(\alpha_+ + \alpha'_+)} + S^{*\prime}_{ee}e^{iq(\alpha_+ + \alpha'_+)}\right.$$
$$\left. + S^{*\prime}_{ee}S_{ee}e^{iq(\alpha'_+ - \alpha_+)}\right] + \frac{S^{*\prime}_{he}S_{he}}{\sqrt{\alpha_-\alpha'_-}}e^{iq(\alpha_- - \alpha'_-)}dq. \tag{A.91}$$

As before we need to make the integral converge by the addition of a term ϵ in the exponential, which gives the solution

$$= \lim_{\epsilon \to 0}\frac{1}{\sqrt{\alpha_+\alpha'_+}}\left[\pi\delta(\alpha_+ - \alpha'_+)(1 + S^{*\prime}_{ee}S_{ee}) + \frac{i(\alpha_+ - \alpha'_+)(S^{*\prime}_{ee}S_{ee} - 1)}{\epsilon^2 + (\alpha_+ - \alpha'_+)^2}\right.$$
$$\left. + \frac{i(\alpha_+ + \alpha'_+)(S_{ee} - S^{*\prime}_{ee})}{\epsilon^2 + (\alpha_+ + \alpha'_+)^2}\right] + \frac{S^{*\prime}_{he}S_{he}}{\sqrt{\alpha_-\alpha'_-}}\left[\pi\delta(\alpha_- - \alpha'_-) - \frac{i(\alpha_- - \alpha'_-)}{\epsilon^2 + (\alpha_- - \alpha'_-)^2}\right]. \tag{A.92}$$

We see that when $E = E'$ the remaining terms are

$$\frac{\pi}{m}\left(1 + |S_{ee}|^2 + |S_{he}|^2\right) = \frac{2\pi}{m} \tag{A.93}$$

due to the unitary condition $|S_{ee}|^2 + |S_{he}|^2 = 1$. When $E \neq E'$ the terms again cancel with those for $q > 0$.

Appendix B

Error Integrals

integrating a Gaussian function over a negative range, the solution is given by the error integral (see [66] p.297)

$$\int_{-\infty}^{0} \exp\left(-ax^2 + bx + c\right) \, dx = \frac{1}{2}\sqrt{\frac{\pi}{a}} \exp\left(\frac{b^2}{4a} + c\right) \operatorname{erfc}\left(\frac{b}{2\sqrt{a}}\right) \quad \text{(B.1)}$$

$$= \frac{1}{2}\sqrt{\frac{\pi}{a}} \exp\left(\frac{-(ib)^2}{4a} + c\right) \operatorname{erfc}\left(-i\left(\frac{ib}{2\sqrt{a}}\right)\right)$$
$$\text{(B.2)}$$

$$= \frac{1}{2}\sqrt{\frac{\pi}{a}} \exp(c)w\left(\frac{ib}{2\sqrt{a}}\right). \quad \text{(B.3)}$$

The last line has given the solution in terms of the *Faddeeva function* defined as

$$w(x) = e^{-x^2} \operatorname{erfc}(-ix). \quad \text{(B.4)}$$

The complementary error function, $\operatorname{erfc}(x)$, is defined as

$$\operatorname{erfc}(x) = \frac{2}{\sqrt{\pi}} \int_{x}^{\infty} e^{-t^2} dt. \quad \text{(B.5)}$$

The integral over a positive range has the similar solution

$$\int_{0}^{\infty} \exp\left(-ax^2 + bx + c\right) \, dx = \frac{1}{2}\sqrt{\frac{\pi}{a}} \exp(c)w\left(\frac{-ib}{2\sqrt{a}}\right) \quad \text{(B.6)}$$

(this can also be seen using the identities $\operatorname{erfc}(z) = 1 - \operatorname{erf}(z)$ and $\operatorname{erf}(-z) = -\operatorname{erf}(z)$).

Appendix C

Asymptotic Techniques

C.1 Laplace's Method

We consider the behaviour of the integral

$$I(\lambda) = \int_a^b dx\, f(x) \exp\big(-\lambda\phi(x)\big) \qquad (C.1)$$

(see [77]) as $\lambda \to \infty$. Here $f(x)$ and $\phi(x)$ are smooth functions, $\phi : \mathbb{R} \to \mathbb{R}$, $f : \mathbb{R} \to \mathbb{C}$ and the integral is taken over a real interval. Suppose that $\phi(x)$ has an absolute minimum in the interval $[a, b]$ at $x = x_0$. Here $a < x_0 < b$, $\phi'(x_0) = 0$ and $\phi''(x_0) > 0$. The largest contributions to the integral then come from an arbitrarily small neighbourhood of x_0 as $\lambda \to \infty$. Taylor expanding $f(x)$ and $\phi(x)$ about the minimum x_0

$$I(\lambda) \approx \int_a^b f(x_0) \exp\left[-\lambda\left(\phi(x_0) + \frac{1}{2}\phi''(x_0)(x - x_0)^2\right)\right] dx \qquad (C.2)$$

in the limit $\lambda \to \infty$ the strong decay of the integral away from x_0 means we can expand the limits of integration without introducing any significant errors

$$I(\lambda) \approx f(x_0) \exp\big(-\lambda\phi(x_0)\big) \int_{-\infty}^{\infty} \exp\left(-\frac{\lambda}{2}\phi''(x_0)(x - x_0)^2\right) dx. \qquad (C.3)$$

The solution is simply given by the Gaussian integral

$$I(\lambda) \approx \sqrt{\frac{2\pi}{\lambda\phi''(x_0)}}\, f(x_0) \exp\big(-\lambda\phi(x_0)\big). \qquad (C.4)$$

Equation (C.4) is sometimes also referred to as *Laplace's formula*. For a more rigorous derivation of the asymptotic nature of the Laplace method see [77].

C.2 Stationary Phase Method

We now consider integrals of the form

$$I(\lambda) = \int_a^b dx \, f(x) \exp\left(i\lambda\phi(x)\right) \tag{C.5}$$

in the limit $\lambda \to \infty$. The integral is taken over the real line and again $\phi : \mathbb{R} \to \mathbb{R}$ and $f : \mathbb{R} \to \mathbb{C}$. Large values of λ produce fast oscillations about zero except at stationary points $x = x_0$ satisfying $\phi'(x_0) = 0$ (hence the name *stationary phase*). These oscillations will generally cancel, lowering the value of the integral. We will then assume that there is a point of stationary phase in the interval $[a, b]$ and that $\phi''(x_0) \neq 0$. The *order* of a stationary point refers to the first non-zero term in the expansion, in this case this is a *first-order* or *simple* saddle point. We can then apply the same process used to arrive at Laplace's integral by expanding $\phi(x)$ around the point of stationary phase x_0

$$\phi(x) \approx \phi(x_0) + \frac{1}{2}\phi''(x_0)(x - x_0)^2 \tag{C.6}$$

which inserted into $I(\lambda)$ gives a complex Gaussian integral

$$I(\lambda) \approx \exp\left(i\lambda\phi(x_0)\right) \int_a^b dx \, f(x) \exp\left(\frac{i}{2}\lambda\phi''(x_0)(x - x_0)^2\right) \tag{C.7}$$

$$\approx f(x_0)\exp\left(i\lambda\phi(x_0)\right) \int_\infty^\infty dx \, \exp\left(\frac{i}{2}\lambda\phi''(x_0)(x - x_0)^2\right). \tag{C.8}$$

Again the expansion of the integration range introduces negligible errors. The stationary phase approximation of the integral is therefore

$$I(\lambda) \approx \sqrt{\frac{2\pi i}{\lambda\phi''(x_0)}} \, f(x_0) \exp[i\lambda\phi(x_0)] \tag{C.9}$$

$$= \sqrt{\frac{2\pi i}{\lambda|\phi''(x_0)|}} f(x_0) \exp\left(i\left(\lambda\phi(x_0) + \mathrm{sgn}(\phi''(x_0))\right)\right) \tag{C.10}$$

where $\mathrm{sgn}(a)$ is the sign function.

For both the Laplace and stationary phase methods if there are multiple but distinct minima or stationary points contained in the desired range of integration, the approximation is then made by the sum over distinct stationary points x_i

$$I(\lambda) \approx \sum_{x_i} \sqrt{\frac{2\pi i}{\lambda|\phi''(x_i)|}} f(x_0) \exp\left(i\left(\lambda\phi(x_i) + \mathrm{sgn}(\phi''(x_i))\right)\right). \tag{C.11}$$

Care must be taken using approximation if the location of the stationary points depend upon another variable, as stationary stationary points can coalesce. If two simple saddle points $x_i(y)$ approach each other before coalescing at some critical value y_0 (i.e. $x_i(y_0) = x_j(y_0)$) they produce a stationary point of order two. Techniques exist that can be applied in this case to produce a uniform approximation but as we will not utilize them fully in this thesis will omit the details, though we give a brief synopsis in sub-section 5.5.2 and additional details can be found in [77].

In both the stationary phase method and Lapace's method the approximation is valid under the assumption that $f(x)$ varies slowly compared to $\phi(x)$ in the limit $\lambda \to \infty$. To find the magnitude of λ at which the stationary phase contributions become dominant we consider the width of the stationary phase contributions. If we make the change of integration variable $x = ix'$ (we'll also set $x_0 = 0$ without loss of generalisation) the approximation of the exponent is

$$\exp\left(i\lambda\phi(x_0) + \frac{i}{2}\lambda\phi''(x_0)x^2\right) = \exp\left(i\lambda\phi(x_0)\right)\exp\left(-\frac{\lambda}{2}\phi''(x_0)x'^2\right).$$
(C.12)

The width of the contributing region close to the stationary point is proportional to $2/\lambda\phi''(x_0)$. The stationary phase contribution is then dominant when the contributing region is narrower that any significant variations in $f(x)$. In particular if $f(x)$ is Gaussian the stationary phase contributions are dominant when $2/\lambda\phi''(x_0)$ is much smaller than the Gaussian width.

Bibliography

1. P.-G. de Gennes, *Superconductivity of metals and alloys*, trans. by P.A.Pincus (W.A. Benjamin, 1966).

2. D. Vollhardt and P. Wölfle, *The superfluid phase of helium 3* (London : Taylor & Francis, 1990).

3. P. Pieri and G. C. Strinati, 'Derivation of the Gross-Pitaevskii equation for condensed bosons from the Bogoliubov-de Gennes equations for superfluid fermions', Phys. Rev. Lett. **91**, 030401 (2003).

4. J. Bardeen, L. N. Cooper and J. R. Schrieffer, 'Theory of superconductivity', Phys. Rev. **108**, 1175–1204 (1957).

5. A. J. Leggett, 'Interpretation of recent results on $\boldsymbol{He}^3$ below 3 mK: a new liquid phase?', Phys. Rev. Lett. **29**, 1227–1230 (1972).

6. B. V. Svistunov, E. S. Babaev and N. V. Prokof'ev, *Superfluid states of matter* (CRC Press, 2015).

7. N. Bogoliubov, 'On a new method in the theory of superconductivity', Il Nuovo Cimento (1955–1965) **7**, 794–805 (1958).

8. T. L. Curtright, D. B. Fairlie and C. K. Zachos, *Quantum mechanics in phase space: an overview with selected papers* (London: World Scientific, 2005).

9. E. Schrödinger, 'Der stetige übergang von der mikro– zur makromechanik', Naturwissenschaften **14**, 664–666 (1926).

10. R. G. Littlejohn, 'The semiclassical evolution of wave packets', Phys. Rep. **138**, 193–291 (1986).

11. M. J. Davis and E. J. Heller, 'Comparisons of classical and quantum dynamics for initially localized states', J. Chem. Phys. **80**, 5036–5048 (1984).

12. K. Hepp, 'The classical limit for quantum mechanical correlation functions', Comm. Math. Phys. **35**, 265–277 (1974).

13. E. J. Heller, 'Frozen gaussians: a very simple semiclassical approximation', J. Chem. Phys. **75**, 2923–2931 (1981).

14. J. R. Klauder, 'Continuous–representation theory. II. generalized relation between quantum and classical dynamics', J. Math. Phys. **4**, 1058–1073 (1963).

15. M. Cini and M. Serva, 'Phase space representation of quantum mechanics in terms of coherent states', Il Nuovo Cimento B (1971–1996) **107**, 825–833 (1992).

16. A. Perelomov, *Generalized coherent states and their applications* (Berlin: Springer–Verlag, 1986).

17. W.-M. Zhang, D. H. Feng and R. Gilmore, 'Coherent states: theory and some applications', Rev. Mod. Phys. **62**, 867–927 (1990).

18. J. M. Radcliffe, 'Some properties of coherent spin states', J. Phys. A: Gen. Phys. **4**, 313 (1971).

19. R. Gilmore, 'Geometry of symmetrized states', Ann. Phys. **74**, 391–463 (1972).

20. A. Perelomov, 'Coherent states for arbitrary lie group', Comm. Math. Phys. **26**, 222–236 (1972).

21. J. Bolte and R. Glaser, 'Semiclassical propagation of coherent states with spin–orbit interaction', Annales Henri Poincaré **6**, 625–656 (2005).

22. A. Andreev, 'The thermal conductivity of the intermediate state in superconductors', Sov. Phys. JETP **19**, 1228 (1964).

23. C. W. J. Beenakker, 'Quantum transport in semiconductor–superconductor microjunctions', Phys. Rev. B **46**, 12841–12844 (1992).

24. C. J. Lambert, 'Generalized Landauer formulae for quasi-particle transport in disordered superconductors', J. Phys. Condens. Matter **3**, 6579 (1991).

25. A. Andreev, 'Electron spectrum of the intermediate state of superconductors', Sov. Phys. JETP **22**, 455 (1966).

26. J. Bardeen, R. Kümmel, A. E. Jacobs and L. Tewordt, 'Structure of vortex lines in pure superconductors', Phys. Rev. **187**, 556–569 (1969).

27. K. Duncan and B. Györffy, 'Semiclassical theory of quasiparticles in the superconducting state', Annals of Physics **298**, 273–333 (2002).

28. E. J. Heller, 'Time–dependent approach to semiclassical dynamics', The Journal of Chemical Physics **62**, 1544–1555 (1975).

29. S. Gnutzmann, M. Kuś and J. Langham–Lopez, 'Electron-hole coherent states for the Bogoliubov–de Gennes equation', J. Phys. A: Math. Theor. **49**, 085302 (2016).

30. G. E. Blonder, M. Tinkham and T. M. Klapwijk, 'Transition from metallic to tunneling regimes in superconducting microconstrictions: excess current, charge imbalance, and supercurrent conversion', Phys. Rev. B **25**, 4515–4532 (1982).

31. M. Tinkham, *Introduction to superconductivity*, 2nd (McGraw–Hill, 1996).

32. H. Kamerlingh Onnes, Leiden Comm. **120b**, 124c (1911).

33. J. File and R. G. Mills, 'Observation of persistent current in a superconducting solenoid', Phys. Rev. Lett. **10**, 93–96 (1963).

34. W. Meissner and R. Ochsenfeld, 'Ein neuer effekt bei eintritt der supraleitfähigkeit', Naturwissenschaften **21**, 787–788 (1933).

35. F. London and H. London, 'The electromagnetic equations of the supraconductor', Proceedings of the Royal Society of London A: Mathematical, Physical and Engineering Sciences **149**, 71–88 (1935).

36. V. L. Ginzburg and L. D. Landau, 'On the theory of superconductivity', Zh. Eksp. Teor. Fiz. **20**, 1064–1082 (1950), English translation: L. D. Landau, *Collected papers* (Pergamon Press, Oxford, 1965).

37. L. Landau, 'The intermediate state of supraconductors', Nature **141**, 688 (1938).

38. L. Landau, 'On the theory of the intermediate state of superconductors', J. Phys. USSR **7**, 99 (1943).

39. W. H. Kleiner, L. M. Roth and S. H. Autler, 'Bulk solution of Ginzburg-Landau equations for type II superconductors: upper critical field region', Phys. Rev. **133**, A1226–A1227 (1964).

40. A. A. Abrikosov, 'On the magnetic properties of superconductors of the second group', Sov. Phys. JETP **5**, 1174–1182 (1957).

41. L. N. Cooper, 'Bound electron pairs in a degenerate fermi gas', Phys. Rev. **104**, 1189–1190 (1956).

42. H. Fröhlich, 'Theory of the superconducting state. I. the ground state at the absolute zero of temperature', Phys. Rev. **79**, 845–856 (1950).

43. E. Maxwell, 'Isotope effect in the superconductivity of mercury', Phys. Rev. **78**, 477–477 (1950).

44. B. Keimer, S. A. Kivelson, M. R. Norman, S. Uchida and J. Zaanen, 'From quantum matter to high–temperature superconductivity in copper oxides', Nature **518**, 179–186 (2015).

45. L. P. Gor'kov, 'Microscopic derivation of the Ginzburg–Landau equations in the theory of superconductivity', Sov. Phys. JETP **9**, 1364–1367 (1959).

46. N. N. Bogoliubov, 'On the theory of superfluidity', J. Phys. (USSR) **11**, 23–32 (1947).

47. B. D. Josephson, 'The discovery of tunnelling supercurrents', Rev. Mod. Phys. **46**, 251–254 (1974).

48. D. Saint–James, 'Excitations élémentaires au voisinage de la surface de séparation d'un métal normal et d'un métal supraconducteur', Journal de Physique **25**, 899 (1964).

49. I. Kulik, 'Macroscopic quantization and the proximity effect in S-N-S junctions', Sov. Phys. JETP **30**, 944 (1970).

50. M. Azbel, 'Resonance and oscillatory effects in superconductors', Sov. Phys. JETP **32**, 159 (1971).

51. R. Glauber, 'Photon correlations', Phys. Rev. Lett. **10**, 84–86 (1963).

52. R. Glauber, 'The quantum theory of optical coherence', Phys. Rev. **130**, 2529–2539 (1963).

53. R. Glauber, 'Coherent and incoherent states of the radiation field', Phys. Rev. **131**, 2766–2788 (1963).

54. E. Sudarshan, 'Equivalence of semiclassical and quantum mechanical descriptions of statistical light beams', Phys. Rev. Lett. **10**, 277–279 (1963).

55. J. R. Klauder, 'Continuous–representation theory. I. postulates of continuous–representation theory', J. Math. Phys. **4**, 1055–1058 (1963).

56. V. Bargmann, 'On a Hilbert space of analytic functions and an associated integral transform part I', Comm. Pure and Appl. Math. **14**, 187–214 (1961).

57. G. S. Agarwal and E. Wolf, 'Calculus for functions of noncommuting operators and general phase–space methods in quantum mechanics. II. quantum mechanics in phase space', Phys. Rev. D **2**, 2187–2205 (1970).

58. L. Cohen, 'Generalized phase–space distribution functions', J. Math. Phys. **7**, 781–786 (1966).

59. K. Husimi, 'Some formal properties of the density matrix', Proceedings of the Physico–Mathematical Society of Japan. 3rd Series **22**, 264–314 (1940).

60. P. Ehrenfest, 'Bemerkung über die angenäherte gültigkeit der klassischen mechanik innerhalb der quantenmechanik', Z. Phys. **45**, 455–457 (1927).

61. R. Schubert, R. O. Vallejos and F. Toscano, 'How do wave packets spread? time evolution on ehrenfest time scales', J. Phys. A: Math. Theor. **45**, 215307 (2012).

62. A. Perelomov, 'Generalized coherent states and some of their applications', Sov. Phys. Usp. **20**, 703 (1977).

63. W. W. Lui and M. Fukuma, 'Exact solution of the Schrödinger equation across an arbitrary one–dimensional piecewise–linear potential barrier', J. of Appl. Phys. **60**, 1555–1559 (1986).

64. J. Bardeen and J. L. Johnson, 'Josephson current flow in pure superconducting–normal–superconducting junctions', Phys. Rev. B **5**, 72–78 (1972).

65. R. Kümmel, 'Electronic structure of the intermediate state in type–I superconductors', Phys. Rev. B **3**, 784–793 (1971).

66. M. Abramowitz and I. Stegun, *Handbook of mathematical functions: with formulas, graphs, and mathematical tables*, Applied mathematics series (Dover Publications, 1964).

67. L. I. Schiff, *Quantum mechanics*, International series in pure and applied physics (McGraw–Hill, 1968).

68. M. Born and R. Oppenheimer, 'Zur quantentheorie der molekeln', Annalen der Physik **389**, 457–484 (1927).

69. G. A. Hagedorn, 'A time dependent Born–Oppenheimer approximation', Communications in Mathematical Physics **77**, 1–19 (1980).

70. H. Spohn and S. Teufel, 'Adiabatic decoupling and time–dependent Born–Oppenheimer theory', Communications in Mathematical Physics **224**, 113–132 (2001).

71. L. Landau, 'On the theory of transfer of energy at collisions II', Phys. Z. Sowjetunion **2**, 7 (1932).

72. C. Zener, 'Non–adiabatic crossing of energy levels', Proceedings of the Royal Society of London A: Mathematical, Physical and Engineering Sciences **137**, 696–702 (1932).

73. B. D. Fried and S. Conte, *The plasma dispersion function* (N.Y. : Academic Press, 1961).

74. C. Chester, B. Friedman and F. Ursell, 'An extension of the method of steepest descents', Mathematical Proceedings of the Cambridge Philosophical Society **53**, 599–611 (1957).

75. F. Goos and H. Hänchen, 'Ein neuer und fundamentaler versuch zur totalreflexion', Annalen der Physik **436**, 333–346 (1947).

76. J. L. Carter and H. Hora, 'Total reflection of matter waves: the Goos–Haenchen effect for grazing incidence', J. Opt. Soc. Am. **61**, 1640–1645 (1971).

77. N. Bleistein and R. Handelsman, *Asymptotic expansions of integrals*, Dover Books on Mathematics Series (Dover Publications, 1986).